Investigation of antiplasmodial compounds from various plant extracts : Argemone mexicana L. (Papaveraceae), Licania octandra (Hoffmanns. ex. Roem & Schult) Kuntze (Chrysobalanaceae) and Syzygium cumini (L.) Skeels (Myrtaceae)

Simoes Avello, Claudia

Investigation of antiplasmodial compounds from various plant extracts: *Argemone mexicana* L. (Papaveraceae), *Licania octandra* (Hoffmanns. ex. Roem & Schult) Kuntze (Chrysobalanaceae) and *Syzygium cumini* (L.) Skeels (Myrtaceae)

THESE de DOCTORAT

présentée à la Faculté des Sciences de l'Université de Genève
pour obtenir le grade de Docteur ès Sciences, mention sciences pharmaceutiques

par

Claudia AVELLO SIMOES PIRES

de

Bagé (Brésil)

Thèse N° 4129

Genève
Atelier de reproduction
2009

UNIVERSITÉ
DE GENÈVE

FACULTÉ DES SCIENCES

Doctorat ès sciences
mention sciences pharmaceutiques

Thèse de *Madame Claudia AVELLO SIMOES PIRES*

intitulée :

"Investigation of Antiplasmodial Compounds from Various Plant Extracts : *Argemone mexicana* L. (Papaveraceae), *Licania octandra* (Hoffmanns. ex. Roem & Schult) Kuntze (Chrysobalanaceae) and *Syzygium cumini* (L.) Skeels (Myrtaceae)"

La Faculté des sciences, sur le préavis de Messieurs K. HOSTETTMANN, professeur ordinaire et directeur de thèse, (Section des sciences pharmaceutiques, Laboratoire de pharmacognosie et phytochimie), X. CHILLIER, docteur (Département de chimie physique), L. DECOSTERD, docteur (Division de pharmacologie clinique, Centre Hospitalier Universitaire Vaudois, Lausanne, Suisse), R. VERPOORTE, professeur (Department of Plant Metabolomics/Pharmacognosie, University of Leiden, Leiden, The Netherlands) et J. FALQUET, docteur (Antenna Technologies, Genève, Suisse), autorise l'impression de la présente thèse, sans exprimer d'opinion sur les propositions qui y sont énoncées.

Genève, le 27 juillet 2009

Thèse - 4129 -

Le Doyen, Jean-Marc TRISCONE

N.B. - La thèse doit porter la déclaration précédente et remplir les conditions énumérées dans les "Informations relatives aux thèses de doctorat à l'Université de Genève".

Nombre d'exemplaires à livrer par colis séparé à la Faculté : - 4 -

La femme qui accomplit avec amour et abdication les tâches difficiles et inhérentes à sa condition de femme est une héroïne.

L'héroïne qui, consciente de sa condition, s'apprête à forger un autre avenir pour ses descendantes est une visionnaire.

A ma grand-mère...

SCIENTIFIC COMMUNICATIONS

The present work was carried out at the Laboratory of Pharmacognosy and Phytochemistry of the University of Geneva (March 2005 to July 2009), under the direction of Prof. Dr. Kurt Hostettmann. Some aspects of the present research have been published in scientific journals and presented in scientific events as posters.

Publications

Simões-Pires, C. A.; Varga, S.; Marston, A.; Ioset, J. R.; Paulo, M. Q.; Matheeussen, A.; Maes, L.; Hostettmann, K. Ellagic acid derivatives from *Syzygium cumini* stem bark: investigation of their antiplasmodial activity. *Natural Product Communications* 4: 1371-1376, 2009.

Simões-Pires, C. A.; Falquet, J.; Diop, E.H.A., Ioset, J. R.; Matheeussen, A.; Maes, L.; Hostettmann, K. Bioguided fractionation of the antimalarials plant *Argemone Mexicana*: isolation and quantification of active compounds from effective clinical batches. *Planta Medica* **75**: PD22, 2009.

Simões-Pires, C. A.; Marston, A.; Matheeussen, A.; Maes, L.; Hostettmann, K. Flavonoids from *Licania octandra* and their antiplasmodial activity. (Under elaboration).

Posters

Isolation of the antiplasmodial compounds of *Syzygium cumini*: an application of the assay for the inhibition of haematin polymerization. First Joint IOCD-ISDNP International Symposium on Natural Products. Kasane, Botswana, 2008.

Separation of ellagic acid and its derivatives from the aqueous extract of *Syzygium cumini* stem bark by centrifugal partition chromatography. 5th International Symposium on Chromatography of Natural Products. Lublin, Poland, 2006.

Isolation and on-line identification of antioxidant compounds from *Licania octandra* (Chrysobalanaceae). 4th International Conference on Natural Products. Leysin, Switzerland, 2006.

REMERCIEMENTS

J’exprime toute ma gratitude au Professeur Kurt Hostettmann pour m’avoir accueillie au sein du Laboratoire de Pharmacognosie et Phytochimie de l’Université de Genève afin d’effectuer ma thèse. Je le remercie également pour son soutien, pour tous les moyens techniques qu’il a mis à ma disposition, de m’avoir permis de participer à de nombreux congrès internationaux, ainsi que de m’avoir délégué l’encadrement de travaux de diplômes et de travaux pratiques à l’Ecole de Pharmacie.

Je remercie chaleureusement le Professeur Andrew Marston d’avoir supervisé mon projet de thèse et de m’avoir apporté de precieux conseils de sciences et de vie tout au long de ces quatre dernières années.

Je tiens à remercier les Docteurs Jacques Falquet, Jean-Robert Ioset et Bertrand Graz de m’avoir invité à participer au projet *Argemone mexicana*. Je les remercie pour les nombreuses discussions scientifiques ainsi que pour tous les conseils pratiques qu’ils ont pu partager.

Je remercie également le Dr. Yves Allenbach pour le travail fourni au début du projet *Argemone mexicana*, pour sa contribution au sein du LPP et pour son amitié.

Tous mes remerciements à l’équipe FIOCRUZ, ainsi qu’au Professeur Louis Maes de l’Université d’Anvers pour les tests d’activité antiparasitaire.

Je remercie sincèrement ma collègue, le Dr. Sandra Vargas, d’avoir mis au point le test d’inhibition de la β-hématin au sein de notre laboratoire et de m’avoir permis de l’effectuer pendant mon travail de thèse.

J’aimerai exprimer ma gratitude au Dr. Karine Ndjoko pour ses enseignements en spectrométrie de masses ainsi qu’en RMN.

Je remercie également le Dr. Gaëtan Glauser pour les analyses UPLC/TOF-MS.

J’adresse mes remerciements au Dr. Emerson Ferreira Queiroz qui m’a épaulé au début de ce travail.

Merci également au Professeur Marçal Queiroz Paulo pour les extraits de plantes fournis grâce au projet de collaboration entre le LPP et l’Université Fédérale de Paraiba, au Brésil.

Je remercie tous mes étudiants de travail de diplôme, et spécialement, Gaëlle Braichet, Assane Diop et Joëlle Christen.

Merci au Dr. Trixie Bartholomeuz et à Silke Walleser pour la correction du manuscrit en Anglais et pour les moments d’amitié que nous avons pu partager.

Merci également au Dr. Marc Goulette pour la correction des textes en Français, ainsi que pour son amitié et pour tous les tangos partagés.

Je remercie mes collègues du LPP pour tous les moments passés ensembles.

Merci à mes amis Diogo Pilger, Fabiane Farias et Renata Limberger qui ont toujours su être présents dans les bons et mauvais moments, malgré la distance qui nous sépare.

Merci également à mes amis Jean-Claude Bonnet, Sylvian Cretton, Fan Peihong, Karin Megzari, Raimana Ho, Philippe Eugster, Nadine Bohni, Bernadette Biloa et tant d'autres avec qui j'ai pu partager d'agréables moments pendant les années de thèse.

Un grand merci à toute ma famille, restée au Brésil, d'avoir compris mon absence et de m'avoir soutenue tout au long de ma formation académique.

J'aimerai encore exprimer ma gratitude à mon fils Arthur qui a accepté le défi d'un changement de pays et qui a su si bien s'adapter à une nouvelle culture. Merci aussi de sa compréhension lors de mon absence.

Un grand merci à Raphaël Cochet pour sa présence dans ma vie, pour tout ce qu'il m'a apporté, pour son amour, sa capacité d'écoute et de compréhension et pour toute l'aide apportée à la fin de mon travail de thèse.

Enfin, ma gratitude à tous ceux qui ont contribué à l'élaboration de ce travail et à ceux qui m'ont aidé à la réalisation de tâches scientifiques ou administratives.

ABBREVIATIONS, SYMBOLS AND CONVENTIONS

δ_C	^{13}C chemical shift (ppm)
δ_H	^{1}H chemical shift (ppm)
$[\alpha]_D$	specific rotation at the wavelength D of sodium
1D	one dimensional
2D	two dimensional
ACC	acetyl-CoA carboxylase
ACP	acyl carrier protein
ACT	artemisinin-based combination therapy
$AlCl_3$	aluminium chloride
brs	broad singlet
cAMP	cyclic adenosine monophosphate
CC	column chromatography
CD	circular dichroism spectroscopy
CD_3OD	deuterated methanol
cGMP	cyclic guanosine monophosphate
CH_2Cl_2	dichloromethane
CoA	coenzyme A
COSY	correlation spectroscopy
CPC	centrifugal partition chromatography
CPM	counts per minute
CV	coefficient of variation
d	doublet
D_2O	deuterated water
Da	Dalton
dd	double doublet (NMR)
DMSO-*d6*	deuterated dimethylsulfoxide
DPPH	2,2'-diphenylpicrylhydrazyl
DTM	Department of Traditional Medicine (Mali)
ECG	electrocardiogram
ED_{50}	effective dose in 50% test population
ESI	electrospray ionization (MS)
EtOH	ethanol
FabA	β-hydroxyacyl-ACP-dehydrase I
FabD	ACP transacyclase
FabF	β-ketoacyl-ACP synthase II

FabG	β-ketoacyl-ACP synthase I
FabH	β-ketoacyl-ACP synthase III
FabZ	β-hydroxyacyl-ACP-dehydrase II
FASI	type I fatty acid synthase
FASII	type II fatty acid synthase
FDA	American Food and Drug Administration
Fe(II)PPIX	heme
Fe(III)PPIX	hematin
H_3BO_3	boric acid
HCl	hydrochloric acid
HMBC	heteronuclear multiple bond correlation
HPLC	high performance liquid chromatography
HPLC/MS	high performance liquid chromatography coupled with mass spectrometry
HPLC/UV-DAD	high performance liquid chromatography coupled with ultraviolet photodiode array detector
HRMS	high resolution mass spectrometry
HRP-2	histidine rich protein-2
HSQC	heteronuclear single quantum coherence
Hz	hertz
i.d.	internal diameter
IC_{50}	50% inhibitory concentration
IR	infrared spectoscopy
ITM	improved traditional medicine
ITN	insecticide treated net
J	coupling constant
m	multiplet (NMR)
m/z	mass per electronic charge
MeCN	acetonitrile
MeOH	methanol
MHz	megahertz
MPLC	medium pressure liquid chromatography
MS	mass spectrometry
MS^n	multiple stage MS
MW	molecular weight
NAD^+	nicotinamide adenine dinucleotide
NADH	reduced nicotinamide adenine dinucleotide
$NADP^+$	nicotinamide adenine dinucleotide phosphate

NADPH	reduced nicotinamide adenine dinucleotide phosphate
NaOAc	sodium acetate
NaOH	sodium hydroxide
NaOMe	sodium methoxide
NCE	new chemical entity
NMR	nuclear magnetic resonance
NOESY	nuclear overhauser effect spectroscopy
O-CH_2-O	methylene dioxide
O-CH_3	methoxyl
o-diOH	ortho-related di-hydroxyl groups
Pf	*Plasmodium falciparum*
ppm	parts per million (NMR unity)
PW	pulse width
pyridine-$_{d5}$	deuterated pyridine
QNMR	quantitative nuclear magnetic resonance
QT interval	measure of the time between the start of the Q wave and the end of the T wave in the heart's electric cycle
RD	relaxation delay
RDT	rapid diagnostic test
R_f	retention factor
rpm	rotations per minute
s	singlet
SD	standard deviation
sp.	undefined species
SPHPLC	semi-preparative high performance liquid chromatography
spp.	several species of the same genus
t	triplet
TFA	trifluoroacetic acid
TIC	total ion chromatogram
TLC	thin-layer chromatography
TMS	tetramethylsilane
TOCSY	total correlation spectroscopy
TOF	time of flight
UPLC	ultra performance liquid chromatography
UV	ultraviolet
VLC	vacuum liquid chromatography
WHO	World Health Organization
λ_{max}	wavelength of absorption maxima (nm)

ABSTRACT

Malaria is one of the world's leading killer infectious diseases, with an estimated 300-500 million cases every year. It is caused by protozoan parasites of the genus *Plasmodium*, *P. falciparum* being the one responsible for the vast majority of deaths from malaria. The first part of this work consisted of the screening for antiplasmodial activity in various plant extracts which were selected through two different strategies: 1) selection of extracts from plants used in traditional medicine for treating malaria or with a reported antiplasmodial activity in the literature and 2) a random selection of available plant extracts. Three plant species were selected for phytochemical investigation: *Argemone mexicana* L. (Papaveraceae), *Licania octandra* (Hoffmanns. ex. Roem & Schult) Kuntze (Chrysobalanaceae) and *Syzygium cumini* (L.) Skeels (Myrtaceae). Following the preliminary antimalarial screening and extract fingerprints, the plant extracts presenting moderate to good antiplasmodial activity *in vitro* were selected for bioguided fractionation and isolation. Fractionation of extracts was conducted by means of different and consecutive separation techniques. Pure compounds had their structures elucidated through classical spectroscopic techniques, including high resolution mass spectroscopy (HR-MS) and nuclear magnetic resonance (NMR). The alkaloids allocryptopine, berberine and protopine were isolated from *A. mexicana* traditional preparation. All of them were highly active against *P. falciparum in vitro* and allocryptopine was able to inhibit β-hematin formation. A quantitative NMR method was successfully developed to determine the concentrations of isolated alkaloids in the traditional decoction. A simple semi-quantitative TLC method was suggested for the quality-control of an improved traditional medicine (ITM) in Mali. In the case of *L. octandra*, three flavonoids were isolated from the hydroalcoholic leaf extract: (2R,3R)-taxifolin 3-*O*-β-D-xylopyranoside, myricetin 3-*O*-α-L-rhamnopyranoside and quercetin 3-*O*-α-L-rhamnopyranoside. Myricetin and quercetin derivatives, as well as their aglycones were considered active against *P. falciparum in vitro*, while taxifolin and its derivative were not active. Three other compounds had their structure inferred by dereplication techniques. From *S. cumini* stem bark decoction, gallic acid, ellagic acid, 3-*O*-methylellagic acid 3'-*O*-α-L-rhamnopyranoside, ellagic acid 4-*O*-α-L-2''-acetylrhamnopyranoside and the new compound 3-*O*-methylellagic acid 3'-*O*-β-D-glucopyranoside were isolated. Only ellagic acid showed reduction of *in vitro* parasitaemia, while both gallic and ellagic acids were able to significantly inhibit β-hematin formation.

RESUME DE THESE EN FRANÇAIS

Introduction

Le paludisme est une parasitose issue de l'infection par des protozoaires du genre *Plasmodium*, transmise par la piqûre de la femelle du moustique *Anopheles ssp.* Plusieurs espèces de parasite sont capables d'infecter l'être humain (*Plasmodium falciparum*, *P. vivax*, *P. malariae* et *P. ovale*), *P. falciparum* étant l'espèce responsable de la plupart des décès liés à la maladie.

Malgré toutes les avancés scientifiques et tous les efforts impliqués dans la lutte contre le paludisme, la maladie est considérée mondialement parmi les plus mortelles, avec une estimation de 300 à 500 millions de cas chaque année. Plusieurs raisons peuvent expliquer ce phénomène, telles que la résistance du parasite à la chloroquine, la résistance des moustiques vecteurs aux insecticides, l'expansion démographique ainsi que la détérioration des conditions de vie dans les régions endémiques, notamment en Afrique. Selon les rapports de l'Organisation Mondiale de la Santé (OMS) au sujet du paludisme, les principaux problèmes observés dans de nombreux pays africains sont liés aux besoins et à l'accès des outils de prévention et aux thérapies à base d'artémisinine (ACTs, artemisinin-based combination therapies). Celles-ci s'avèrent efficaces dans les cas de paludisme non compliqué dus à *P. falciparum*, espèce présentant des souches résistantes aux traitements à base de chloroquine et sulfadoxine-pyriméthamine.

Le succès du traitement dépend de la vitesse du diagnostic, de l'emploi d'un antimalarique adéquat, de la gravité de la maladie, ainsi que de l'âge et les conditions immunologiques des patients. Une grande partie de la population affectée se situe dans des régions isolées, n'ayant comme accès immédiat que la médecine traditionnelle, souvent à base de préparations de plantes. La recherche des composés antimalariques à partir des plantes médicinales contribue d'une part à justifier leur utilisation et à évaluer leur niveau d'innocuité et d'autre part, à la découverte de nouvelles molécules potentiellement actives. L'investigation de composés antimalariques à partir de plantes est souvent réalisé par criblage biologique des extraits à l'aide de tests *in vitro* sur l'inhibition de la parasitémie. Des cibles associées à certains mécanismes d'action

peuvent aussi être prises en considération lors d'un criblage biologique. Une grande variété de cibles est en cours d'investigation à l'heure actuelle. De façon générale, les cibles se situent au niveau des différentes organelles du parasite, particulièrement la vacuole digestive (site de dégradation de l'hémoglobine) et l'apicoplaste (plastide provenant probablement d'une cyanobactérie symbiotique pendant le processus évolutif).

Pendant la digestion de l'hémoglobine provenant de la cellule hôte par *Plasmodium sp.*, une grande quantité d'hème s'accumule dans la vacuole digestive. Etant toxique pour le parasite, l'hème est détoxiqué par sa transformation en hématine puis en hémozoïne (dimère de l'hématine). L'hème est partiellement impliqué dans le mécanisme d'action de l'artémisinine par la formation des adduits radicalaires qui empêcheraient la détoxication de l'hème. L'hématine semble être la principale cible de la chloroquine et d'autres antimalariques du type quinoline. Ces drogues sont capables de complexer l'hématine, empêchant ainsi la formation d'hémozoïne.

L'apicoplaste renferme certaines fonctions essentielles à la survie du parasite, en étant le site où se déroule une série de réactions appartenant à plusieurs voies biosynthétiques. Ce sont, entre autres, des voies concernant la biosynthèse d'acides gras et d'isoprenoïdes, aussi présentes dans les bactéries, les plantes et d'autres parasites, mais fondamentalement différentes des voies biosynthétiques chez l'être humain. Par conséquent, les voies biosynthétiques de l'apicoplaste apparaissent comme des cibles potentiellement spécifiques dans le développement de nouveaux antimalariques.

Parmi les voies biosynthétiques connues chez le parasite, celle de la biosynthèse d'acides gras a été spécialement étudiée. La synthèse d'acides gras est réalisée à l'aide d'un système de synthétases du type I (FASI), tels que les enzymes FabB, FabG et FabI de *P. falciparum*. Certains produits naturels, comme de nombreux flavonoïdes, se sont montrés capables d'inhiber ces enzymes.

Le but principal de ce travail est l'étude des extraits et fractions actives des plantes pour leur activité antiplasmodiale afin d'isoler et d'identifier les composés responsables de cette activité. Les plantes ont été sélectionnées selon deux stratégies différentes : 1) sélection de plantes utilisées dans la médecine traditionnelle pour le

traitement du paludisme ou ayant une activité antiplasmodiale rapportée dans la littérature et 2) sélection aléatoire d'extraits disponibles. Des objectifs spécifiques ont ainsi été établis.

Dans le premier cas, *Argemone mexicana* L. (Papaveraceae) a été sélectionnée grâce à une étude collaborative entre l'organisation non gouvernementale Antenna Technologies (Genève) et le Département de Médecine Traditionnelle (Mali). L'objectif de l'étude implique l'identification des composés responsables de l'activité de la plante au sein d'une préparation traditionnelle, efficace dans le traitement du paludisme non compliqué dû à *P. falciparum*. Le but final étant de fournir des paramètres de contrôle de qualité pour le développement d'un Médicament Traditionnel Amélioré (MTA) au Mali.

Dans le deuxième cas, les espèces *Licania octandra* (Hoffmanns. ex. Roem & Schult.) Kuntze (Chrysobalanaceae) et *Syzygium cumini* (L.) Skeels (Myrtaceae) ont été sélectionnées pour l'activité antiplasmodiale de leurs fractions. L'objectif spécifique étant d'identifier les composés responsables de l'activité et des nouvelles molécules à travers l'isolement bioguidé par des tests *in vitro* et des techniques de déréplication.

A. mexicana est une plante utilisée dans la médecine traditionnelle pour traiter diverses affections, telles que les inflammations oculaires, les piqûres de scorpion et le paludisme. Une étude clinique menée à Missidougou, dans la région de Sikasso au Mali a montré l'efficacité de la décoction traditionnelle de cette plante pour le traitement du paludisme non compliqué dû à *P. falciparum*, avec une posologie de 2 prises par jour. Des doses plus élevées ont été associées à un risque potentiel de cardiotoxicité, indiqué par l'augmentation des intervalles QT dans les ECGs chez un petit nombre de patients. La présence de l'alcaloïde berbérine, connu par son activité antiplasmodiale *in vitro*, a été investigué dans la tisane et une méthode semi-quantitative de dosage par chromatographie sur couche mince (CCM) a révélé une concentration d'environ 20 mg/L de cet alcaloïde. Étant donné la faible absorption orale de la berbérine et la faible concentration dans la tisane, la recherche de la présence d'autres molécules actives est justifiée. Selon la littérature, d'autres alcaloïdes ont aussi été rapportés dans la plante, notamment des alcaloïdes des types protoberbérine, protopine et benzophénanthridine. Pour ce dernier type, la sanguinarine est connue pour sa toxicité. Elle est considérée comme responsable de l'intoxication due à la contamination des huiles alimentaires avec l'huile d'*Argemone*. Certains alcaloïdes du type protoberbérine et protopine ont

aussi été étudiés pour leurs effets cardiaques, responsables d'une augmentation des potentiels d'action des myocytes.

Des espèces du genre *Licania* sont traditionnellement employées dans les régions de l'Amazonie et du nord-est du Brésil, particulièrement pour leur bois résistant, mais aussi dans la médecine populaire comme anti-inflammatoires et dans le traitement de diverses maladies. *Licania octandra* n'a jamais été étudiée du point de vue phytochimique. Toutefois, d'autres espèces du même genre ont été étudiées, notamment *L. densiflora*, *L. heteromorpha*, *L. licaniiflora*, *L. michauxii* et *L. tomentosa*. Les principales classes de composés retrouvées dans le genre sont les flavonoïdes et les terpènes.

S. cumini est une Myrtacée largement utilisée en médecine traditionnelle, principalement dans le traitement du diabète, mais aussi en tant que digestif, astringent, antihelminthique, dans le traitement des bronchites, des dysenteries et des ulcères. La composition chimique et certaines activités biologiques ont déjà été investiguée dans l'écorce de cette plante. La présence de dérivés de l'acide gallique et de l'acide ellagique a été démontrée. Cependant, les structures des dérivés de l'acide ellagique n'ont pas été élucidées.

Résultats

Lors du criblage biologique initial des diverses plantes, une activité antiplasmodiale intéressante a été associée à trois espèces sélectionnées pour cette étude, *A. mexicana*, *L. octandra* et *S. cumini*.

Les échantillons ont été testés pour leur activité antiparasitaire *in vitro* contre *P. falciparum*, *T. cruzi*, *T. b. brucei* ainsi que pour leur cytotoxicité. Le but de cette étude étant la recherche des composés ayant une activité antiplasmodiale. L'activité sur d'autres parasites ainsi que la cytotoxicité ont été prises en considération afin d'établir le degré de spécificité de l'activité. De la même façon, les résultats de cytotoxicité ont été utilisés pour éliminer les échantillons potentiellement toxiques.

Argemone mexicana

Différents lots de feuilles de *A. mexicana* ont été extraits selon la préparation traditionnelle. Les décoctions obtenues ont été lyophilisées et analysées par chromatographie liquide à haute performance couplée à un détecteur UV et à la spectrométrie de masse (CLHP/UV/SM). Les lots AM 1 à 12 ont présenté un profil chromatographique semblable et l'alcaloïde berbérine a été détecté dans tous les lots analysés. Le lot clinique AM 8 a été choisi pour le fractionnement. Son extrait lyophilisé (26 g) a été initialement fractionné par une extraction liquide-solide dans du méthanol donnant une fraction insoluble dans le méthanol (AM 8_A) et une autre soluble (AM 8_B). La fraction AM8_B a présenté lors de l'analyse CLHP/UV un pic correspondant à la berbérine, composé qui a été concentré avec d'autres alcaloïdes à l'aide d'une extraction liquide-liquide avec du CH_2Cl_2. L'analyse CLHP/SM en mode positif de la fraction CH_2Cl_2 a mis en évidence 4 composés avec des ions pseudo-moléculaires à *m/z* 354 $[M+H]^+$, 370 $[M+H]^+$, 354 $[M+H]^+$ et 336 $[M]^+$. L'un des pics à m/z 354 $[M+H]^+$ a été identifié comme étant la protopine par comparaison avec un témoin. Une analyse par chromatographie liquide à haute performance couplée à la spectrométrie de masse de haute résolution (CLHP/SMHR) de la fraction a démontré que le pic du composé non identifié à *m/z* 354,1711 $[M+H]^+$ possédait la même formule moléculaire que la protopine, d'où la possibilité d'un isomère. Le composé à m/z 370,1654 $[M+H]^+$

correspond à la formule moléculaire $C_{21}H_{24}NO_5$. Celle-ci correspond à différents alcaloïdes tels que la cryptopine, l'allocryptopine et les argemexicaïnes A et B. La fraction CH_2Cl_2 a été très active contre *P. falciparum in vitro*. Afin d'identifier les composés actifs, cette fraction a été purifiée par colonne de gel de Sephadex LH-20 suivi d'une HPLC semi-préparative. Les composés **A1**, **A2** et **A3** ont pu être isolés et caractérisés par des méthodes spectroscopiques classiques telles que la SMHR, la RMN à une dimension (^1H et ^{13}C) et à deux dimensions (HSQC, HMBC et COSY). Les composés isolés ont été identifiés comme étant la protopine (**A1**), l'allocryptopine (**A2**) et la berbérine (**A3**). Toutes les trois molécules ainsi que le témoin sanguinarine ont été testés pour leur activité antiparasitaire. La berbérine s'est avérée très active contre *P. falciparum* (IC_{50}=0,32 µg/mL). Toutefois, comme dans le cas de la sanguinarine, l'activité n'a pas été spécifique et ces deux composés se sont révélés cytotoxiques. En contrepartie, les deux alcaloïdes du type protopine, **A1** et **A2** ont présenté une activité antiplasmodiale de façon spécifique avec des IC_{50} de 0,32 et 1,46 µg/mL, respectivement. Les composés isolés ont été testés pour leur activité inhibitrice de la formation de β-hématine, seule l'allocryptopine a été capable d'inhiber significativement cette réaction physico-chimique. Une méthode d'analyse quantitative par RMN (QNMR) a été développée pour déterminer les concentrations des alcaloïdes actifs dans la tisane traditionnelle. Pour ce faire, la tisane a été extraite à l'aide d'un partage avec du CH_2Cl_2, évaporée à sec et solubilisée dans la pyridine-$_{d5}$. Deux lots cliniques (AM 8 et AM 11) ont ainsi été quantifiés et les résultats obtenus sont résumés dans le Tableau I.

Une méthode d'analyse semi-quantitative par CCM a été appliquée aux échantillons obtenus par la même méthode d'extraction pour la quantification de berbérine dont les résultats ont affiché des concentrations plus faibles, probablement dues à la saturation de l'image correspondant à la tâche de la berbérine.

Tableau I. Concentrations calculées d'allocryptopine, protopine et berberine dans la décoction de lots cliniques de feuilles d'*A. mexicana* par la méthode QNMR.

Lot	Composé	Concentration dans la tisane (mg/mL)*	% dans la plante (m/m)*	CV (%)
AM 8	Allocryptopine	0,11 ± 0,01	0,47 ± 0,03	5,63
	Protopine	0,12 ± 0,02	0,51 ± 0,02	3,84
	Berberine	0,11 ± 0,01	0,48 ± 0,03	5,99
AM 11	Allocryptopine	0,18 ± 0,01	1,10 ± 0,07	6,57
	Protopine	0,06 ± 0,00	0,39 ± 0,01	3,86
	Berberine	0,07 ± 0,01	0,43 ± 0,04	8,37

* Moyenne ± écart-type

Licania octandra

L'extrait hydroalcoolique de feuilles de *L. octandra* a été analysé par CLHP/UV indiquant la présence de flavonoïdes. Pour le criblage biologique, les principales fractions obtenues par des extractions liquide-liquide successives avec de l'hexane (fraction HF), de l'acétate d'éthyle (fraction AcF), et du butanol (fraction BF) ont été investiguées pour leur activité antiparasitaire. Les fractions HF et AcF se sont révélées actives contre *P. falciparum* avec des IC_{50} de 12.11 et 9.86 µg/mL, respectivement. En outre, la fraction AcF a présenté une activité antiradicalaire lors du test de détection avec le radical DPPH sur plaque CCM. Un fractionnement de cette fraction par CPC a fourni quatre fractions majoritaires, AcF-A à AcF-D. L'isolement de composés a été effectué à partir des fractions AcF-A et AcF-C, tandis que la fraction AcF-B a été soumise à des techniques de déréplication afin de permettre l'identification en ligne des flavonoïdes présents.

Les composés (2R,3R)-taxifoline 3-*O*-β-D-xylopyranoside (**L2**), myricétine 3-*O*-α-L-rhamnopyranoside (**L4**) et quercétine 3-*O*-α-L-rhamnopyranoside (**L6**) ont été isolés et identifiés à l'aide des techniques spectroscopiques classiques telles que l'UV avec des réactifs de déplacement chimique, SMHR, la RMN à une dimension (^{1}H et ^{13}C) et à deux dimensions (HSQC, HMBC et COSY). L'étude de l'activité antiparasitaire a été réalisée pour les trois composés isolés ainsi que pour leurs aglycones, obtenus par hydrolyse acide. Les IC_{50} sont présentées dans le Tableau II.

A l'aide d'analyses par CLHP/SM et CLHP/UV avec addition post-colonne de réactifs de déplacement UV, trois flavonoïdes ont pu être partiellement identifiés dans la fraction AcF-B : le xyloside ou l'arabinoside de taxifoline, le glucoside ou le galactoside de quercétine et la quercétine.

Tableau II. Activités antiparasitaires et cytotoxicité des composés isolés de *L. octandra* et leurs aglycones.

Activité / Composé	Anti-*P. falciparum*	Anti-*T. cruzi*	Anti-*T. b. brucei*	Cytotoxicité
	IC_{50} (µg/mL)			
L2	>32,00	>32,00	>32,00	>32,00
L2 aglycone	>32,00	>32,00	>32,00	>32,00
L4	17,37	11,34	11,57	>32,00
L4 aglycone	10,38	12,81	12,02	>32,00
L6	11,62	>32,00	>32,00	>32,00
L6 aglycone	3,94	8,00	16,00	8,00

Syzygium cumini

L'analyse CLHP/UV/SM de la décoction de l'écorce du tronc de *S. cumini* a indiqué la présence d'une série de dérivés de l'acide ellagique. Les fractions majoritaires obtenues par chromatographie de partage centrifuge (CPC) (fractions A à D) ont été testées pour leur activité antiparasitaire. La fraction C s'est montrée très active contre *P. falciparum* avec une IC_{50} de 0,25 µg/mL et dépourvue de cytotoxicité. Les fractions A et B ont été considérées inactives contre *P. falciparum*. Néanmoins, l'IC_{50} de la fraction D montre une valeur d'activité modérée. En plus, cette fraction a aussi une cytotoxicité modérée. Les fractions C et D ont donc été choisies pour l'isolement à l'aide de la MPLC et de la CLHP semi-préparative.

Une précipitation observée dans la fraction B a abouti à l'isolement du composé **S1**, identifié comme étant l'acide gallique. Les composés **S4** et **S5** sont isolés à partir de la fraction C, l'un étant identifié comme un nouveau composé, l'acide 3-*O*-méthyl-ellagique-3-*O*-β-D-glucopyranoside, et l'autre comme l'acide ellagique, respectivement. Les composés **S7** et **S8** ont été isolés de la fraction D et identifiés respectivement comme l'acide 3-*O*-méthyl-ellagique-3'-*O*-α-L-rhamnopyranoside et l'acide ellagique 4-

O-α-L-2''-acetylrhamnopyranoside. Parmi les composés isolés, seul l'acide ellagique a présenté une activité *in vitro* contre *P. falciparum* avec une IC_{50} de 2.78 µM. Lors de l'essai d'inhibition de la formation de la β-hématine, l'acide gallique et l'acide ellagique ont montré une capacité d'inhibition significative de cette réaction physico-chimique.

Conclusions et perspectives

Argemone mexicana

Les techniques de déréplication utilisées pour l'analyse de *A. mexicana* ont permis l'identification de la berbérine et de la protopine dans la tisane des lots cliniques de la plante. Les techniques d'isolement appliquées à la fraction active de la plante (CH_2Cl_2) ont permis d'isoler l'allocryptopine, la berbérine et la protopine. Les trois molécules sont très actives contre *P. falciparum in vitro*, celles du type protopine (allocryptopine et protopine) étant sélectivement actives. La méthode de dosage par RMN réalisée sur deux lots cliniques a démontré que les deux alcaloïdes du type protopine ensemble sont plus concentrés que la berbérine. Selon la littérature, l'activité antimalarique *in vivo* de la berbérine est controversée. Néanmoins, l'activité *in vivo* de la protopine et de l'allocryptopine n'a pas été investiguée jusqu'à présent. De ce fait, l'étude de l'activité antimalarique de ces deux molécules, à l'aide de modèles *in vivo*, est prometteuse. L'allocryptopine a été la seule capable d'inhiber la formation de β-hématine et l'étude de cette molécule ainsi que de la protopine vis-à-vis d'autres mécanismes d'action est recommandée. En outre, la présence de ces alcaloïdes dans la tisane d'*Argemone* pourrait expliquer les effets cardiaques observés lors de l'étude clinique, ce qui indique l'importance d'étudier la corrélation entre activité cardiaque et antimalarique dans le futur. La méthode semi-quantitative sur CCM semble être utile dans la quantification de la berbérine dans la tisane, à condition qu'une méthode d'extraction adéquate soit utilisée et que la limite supérieure de détection soit respectée. Néanmoins, la berbérine ne semble pas être la seule molécule responsable de l'activité et une quantification des protopines est envisageable pour le contrôle de qualité du MTA.

Licania octandra

Le fractionnement bioguidé de l'extrait hydroalcoolique de feuilles de *L. octandra* a abouti à l'isolement de trois flavonoïdes, le (2R,3R)-taxifoline 3-*O*-β-D-xylopyranoside (**L2**), le myricétine 3-*O*-α-L-rhamnopyranoside (**L4**) et le quercétine 3-*O*-α-L-rhamnopyranoside (**L6**). L'activité antiparasitaire a été établie pour tous les flavonoïdes isolés ainsi que pour leurs aglycones. La quercétine a présenté la meilleure activité antiplasmodiale avec une IC_{50} de 3,94 µg/mL. La substitution de l'hydroxyle du flavonoïde en C-3 (comme pour **L6**) a diminué son activité antiplasmodiale. La myricétine et son dérivé 3-OH substitué (**L4**) ont présenté une activité antiplasmodiale modérée et dans ce cas, la substitution de l'hydroxyle en C-3 n'a pas abouti à un changement de l'activité. La taxifoline et son dérivé (**L2**) se sont avérés inactifs contre *P. falciparum* et la différence principale de ces alcaloïdes par rapport aux précédents est la saturation entre C-2 et C-3. La recherche de l'activité antiplasmodiale de flavonoïdes de structures diverses est utile pour évaluer les relations entre structure et activité de cette classe de composés.

Syzygium cumini

Le fractionnement bioguidé de la décoction de l'écorce de tronc de *S. cumini* a conduit à l'isolement de l'acide gallique (**S1**), de l'acide 3-*O*-méthyl-ellagique-3'-*O*-β-D-glucopyranoside (**S4**), de l'acide ellagique (**S5**), de l'acide 3-*O*-methyl-ellagique-3'-*O*-α-L-rhamnopyranoside (**S7**) et de l'acide ellagique 4-O-α-L-2''-acetylrhamnopyranoside (**S8**). Le composé **S4** étant élucidé comme un nouveau produit naturel. Seul l'acide ellagique a présenté une activité antiplasmodiale *in vitro* liée à sa capacité d'inhibition de la formation de β-hématine. L'activité antimalarique *in vivo* de celui-ci par voie intrapéritonéale a déjà été rapportée dans la littérature, par contre l'activité n'a pas été observée par voie orale, probablement liée à une mauvaise absorption de la drogue. Donc, l'étude de l'activité antimalarique *in vivo* de ces dérivés est envisageable afin de vérifier leur potentiel d'action comme pro-drogues.

TABLE OF CONTENTS

Chapter I

Aim of work

Despite important scientific advances and considerable efforts in the campaign against malaria, the illness is one of the world's leading killer infectious diseases, with an estimated 300-500 million cases every year, giving rise to an estimated 1.5 – 2.7 million yearly deaths (WHO, 2008). There are many possible reasons for this situation, including: the emergence of resistance to chloroquine and other known antimalarial drugs (Hyde, 2007), resistance of parasite vectors to insecticides, demographic growth with subsequent worsening of living and infrastructure standards in endemic areas. "Malaria is both a disease of poverty and a cause of poverty" (Bourdy *et al.*, 2008). Most affected populations have little access to western medicine and therefore turn towards the use of traditional medicinal plants for their primary healthcare. However, few clinical studies have been conducted to evaluate plant safety and efficacy in the treatment of malaria (Willcox *et al.*, 2007). The search for new antimalarial compounds from plants is a contribution to the safety and efficacy evaluation of plant extracts used in traditional medicine; it may provide quality control parameters for the production of traditional phytomedicines and also a source of lead compounds to be developed into new drugs against resistant *Plasmodium falciparum* infection.

The main goal of this work is to study plant extracts and fractions active against the human malaria parasite *P. falciparum* by conducting a bioguided fractionation in order to identify and isolate natural products responsible for the antiplasmodial activity.

Considering that plant extracts are selected for screening of antiplasmodial activity through two different strategies: 1) selection of extracts from plants used in traditional medicine for treating malaria or with a reported antiplasmodial activity in the literature and 2) a random selection of available plant extracts, specific objectives were outlined for each case.

In the first case, the specific objective is to identify compounds responsible for the activity in a traditional preparation known for its clinical efficacy in the treatment of uncomplicated malaria. The final goal in this case is to provide quality control parameters for the development of an improved traditional medicine (ITM).

In the second case, the specific objective is to identify molecules responsible for the activity in extracts and to guide the isolation towards active pure compounds and new molecules, using hits obtained from dereplication methods.

Chapter II
Introduction

Natural products of plant and microorganism origin have been of great importance for the development of drugs and lead compounds. Some classical examples are the alkaloid morphine (**1**) from *Papaver somniferum*, a potent analgesic; quinine (**2**), an antimalarial drug isolated from *Cinchona spp.*; penicillin (**3**), an antibiotic isolated from the microorganism *Penicillium notatum*; and lovastatine (**4**), a hypolipidemic drug isolated from *Aspergillus terreus* under the name of mevinolin (Grabley and Thiericke, 1999).

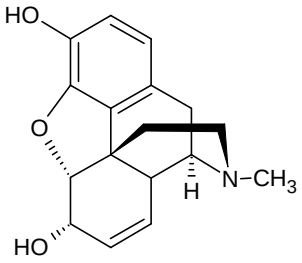

1

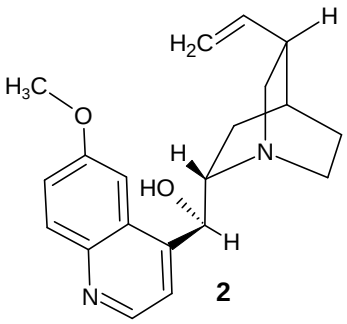

2

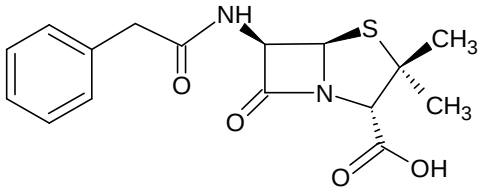

3

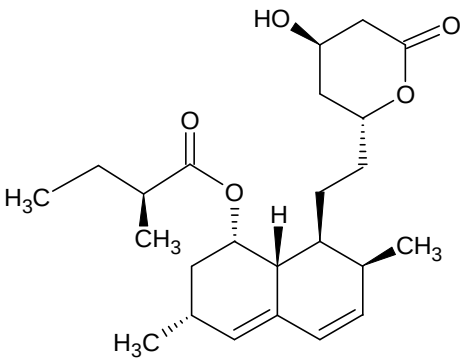

4

Although nature has been considered the main source of drug lead compounds for a long time, researchers in the field of medicinal chemistry have tried to increase the number of new molecules by means of combinatorial and computational chemistry. These techniques allow the synthesis of a great diversity of compounds to be tested in high throughput screening assays. Despite the wide use of combinatorial chemistry in the search for new drugs within the past 25 years, only one new chemical entity (NCE) has arisen as a drug obtained entirely from this discovery process. It is the antitumor molecule

sorafenib (Nexavar®, **5**), approved in 2005 by the Food and Drug Administration (FDA) (Newman and Cragg, 2007).

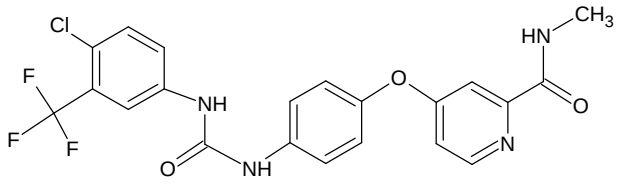

5

As a consequence of the difficulties in providing new drugs from such a randomized and high throughput strategy, the large combinatorial chemical libraries have been replaced by small collections of molecules (100 to 3000) presenting structure characteristics close to those of natural products. These libraries are then used to develop so-called Diversity Oriented Synthesis or Natural Product-like Synthesis (Newman and Cragg, 2007).

In other words, molecules of natural origin are still the main source of diversity leading to bioactivity and to the development of new drugs. This diversity has been developed by nature through millions of years of evolution and reflects a unique process of natural combinatorial chemistry (Yunes and Cechinel-Filho, 2001).

Given these observations, many researchers pursue the search for natural products with diverse biological activities. This thesis work concerns the search for antimalarial natural products. Specific points on the disease and the studied plants are detailed in the subsequent topics.

II.1. Malaria

Malaria is an infectious disease caused by unicellular, protozoan parasites of the genus *Plasmodium*. Four species of plasmodia are infectious to humans: *Plasmodium falciparum*, *P. vivax*, *P. malariae* and *P. ovale*. *P. falciparum* is the one which is responsible for the vast majority of deaths from malaria (Snow *et al.*, 2005). Human malaria is probably as old as mankind and the earliest report of human disease suggestive of malaria comes from ancient Egypt as published in the Edwin Smith Surgical Papyrus

(Figure 2.1), 1600 B.C. (Breasted, 1930) which describes measures to be taken against the entry of “fever-provoking vapors into houses”. The first accurate clinical description of malarial fevers were given by Hippocrates in 400 B.C., who mentioned the classic triad of chills, fever and sweating, and analyzed the characteristic periodicity of various forms of malaria and associated splenomegaly with the endemicity of malaria and its topographic aspects (Wernsdorfer, 1980).

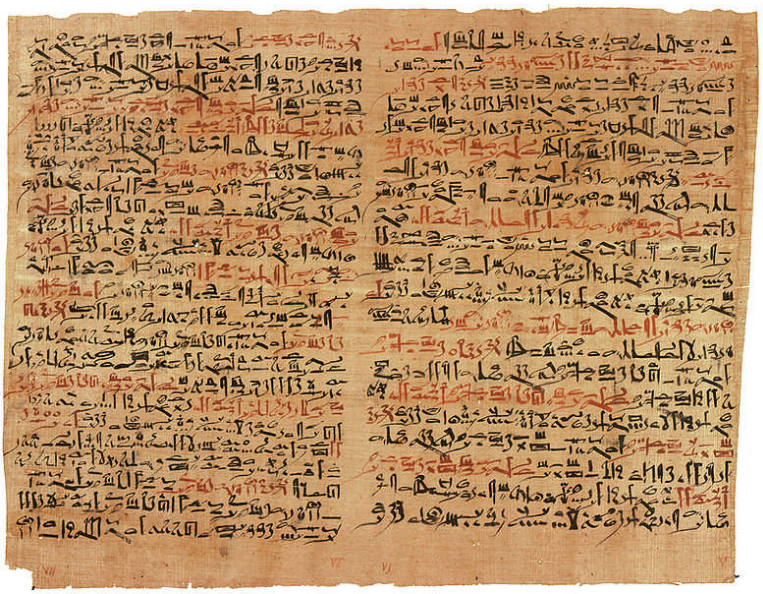

Figure 2.1. Digital image of the Edwin Smith Surgical Papyrus, 1600 B.C. (Source: http://en.wikipedia.org/wiki/File:Edwin_Smith_Papyrus_v2.jpg)

The first attempt to treat malaria came in the middle of the seventeenth century, with the introduction of the bark of a Peruvian tree with which the Countess of Chinchón was successfully treated for her febrile condition. An illustration depicting Peruvian natives counseling Europeans to use the tree is shown in Figure 2.2. The botanical description of the tree providing the Peruvian bark became known only 100 years after its introduction into Europe. Linné, in memory of the Countess of Chinchón’s recovery, named the new genus of the bark-yielding tree *Cinchona*. Subsequently, the bark was generally called cinchona (Wernsdorfer, 1980).

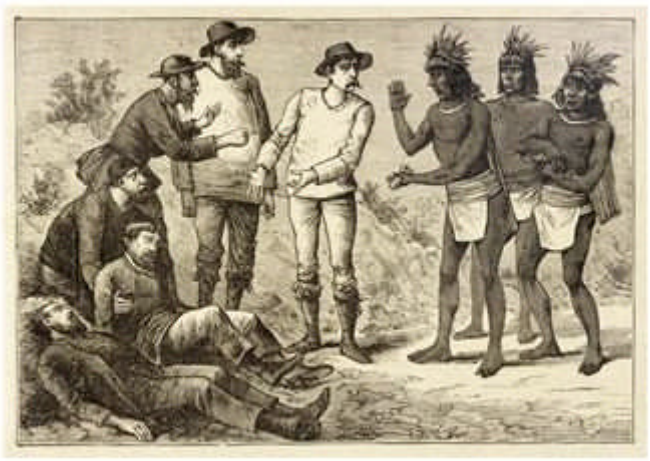

Figure 2.2. Illustration title: Peruvian natives explain to Europeans that quinine is what their sick companions need. Author: unknown.
(Source: http://www.killerplants.com/plants-that-changed-history/20020430.asp)

Since then, different therapeutic approaches have been established for the treatment of malaria (cf. section II.1.3), and the combination of approaches to fight malaria now includes long-lasting insecticidal nets, artemisinin-based combination therapy, supported by indoor residual spraying of insecticide, and intermittent preventive treatment in pregnancy. Nevertheless, malaria is estimated as an immense and persistent burden. The illness is one of the world's leading killer infectious diseases, causing nearly 1 million deaths per year, mostly of children under 5 years age. According to the World Malaria Report 2008 (WHO, 2008), half of the world's population is at risk of malaria, and an estimated 250 million cases led to nearly 1 million deaths in 2006. The 1.2 billion people at high risk live in Africa and Southeast Asia. It has been estimated that *P. falciparum* is responsible for ca. 91% of cases, 86 % of these occurring in the African region. Eighty percent of the cases in Africa were concentrated in 13 countries and over half were in Nigeria, Democratic Republic of the Congo, Ethiopia, United Republic of Tanzania and Kenya (WHO, 2008). Figure 2.3 depicts the estimated worldwide incidence of malaria.

There are many possible reasons for this situation, including the emergence of resistance to chloroquine and other known antimalarial drugs, resistance of parasite vectors to insecticides, environmental deterioration, and demographic growth with subsequent worsening of living and infrastructure standards in endemic areas, especially

in Africa (Hyde, 2007). According to surveillance data reported by the World Health Organization, the main problems observed in several African countries are associated with the gap observed between access and need in terms of prevention tools and artemisinin-based treatment. A survey conducted in 18 African countries found that 34% of households owned an insecticide treated net (ITN), 23% of children and 27% of pregnant women slept under an ITN. 38% of children with fever were treated with antimalarial drugs, but only 3% with artemisinin-based combination therapy, and 18% of women used preventive treatment during pregnancy (WHO, 2008).

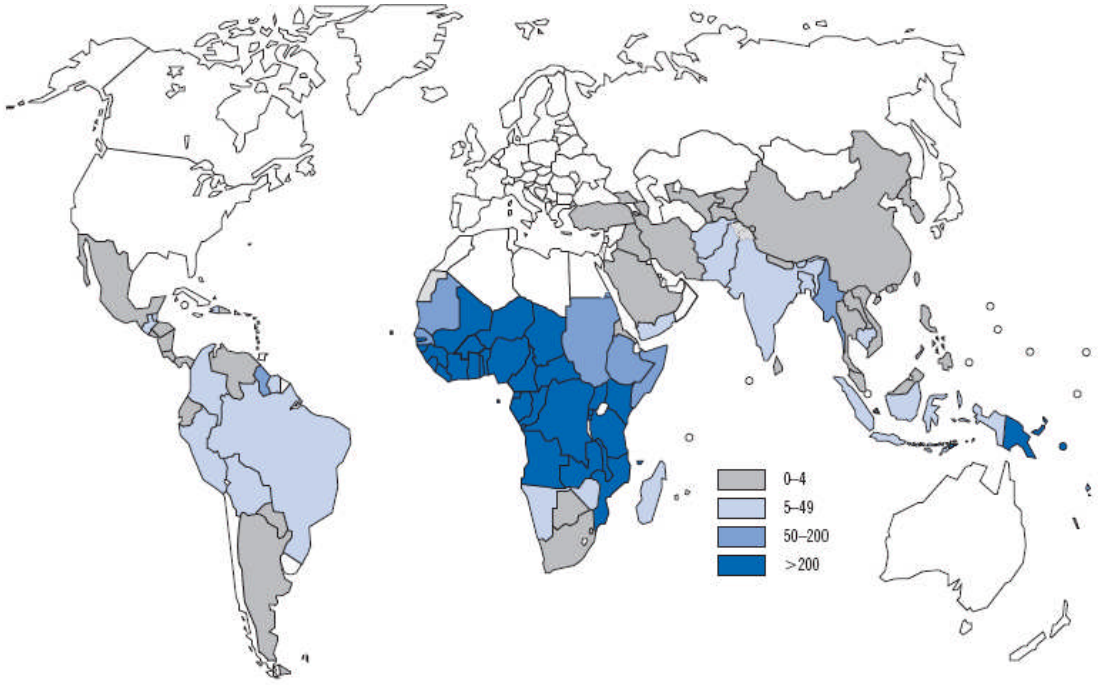

Figure 2.3. Estimated incidence of malaria per 1000 population, 2006. Source: World Malaria Report 2008 (WHO, 2008).

II.1.1. *Plasmodium* parasite cycle

Malaria parasites undergo a complex life cycle alternating between vertebrate and arthropod hosts. The transmission to man starts after the inoculation of sporozoites into blood circulation by an infected mosquito. In the case of human malaria, only female

mosquitoes of the genus *Anopheles* (Figure 2.4) are potential vectors, since male anophelines do not feed on blood (Kreier, 1980).

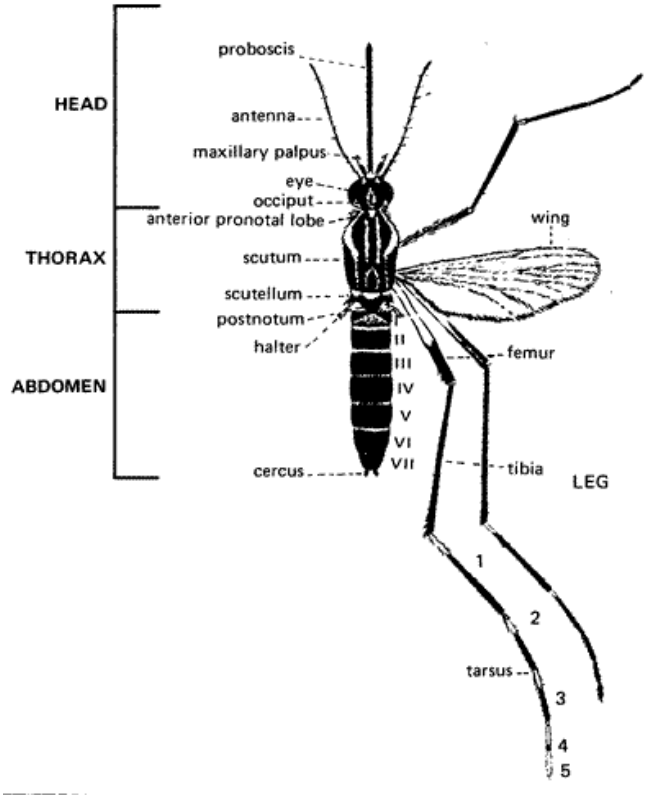

Figure 2.4. Diagram of a female adult *Anopheles* mosquito.
(Source: http://www.cdc.gov/malaria/biology/mosquito/female_diagram.htm).

Possibly guided by chemotaxis and recognizing its targets, sporozoites leave the capillary lumen and enter hepatocytes (in the case of mammalian plasmodia). At this moment, parasites undergo a drastic morphological change. They appear round or oval and contain a chromatin nucleus surrounded by a cytoplasm. During the tissue (exoerythrocytic) schyzogony, the nucleus divides and the cytoplasmatic mass grows. The number of nuclear divisions and their intervals vary among different species (Kreier, 1980).

By the end of nuclear division stage, the cytoplasm segregates and merozoites are formed, consisting of a single nucleus and cytoplasm. The number of merozoites produced by one hepatic schizont is estimated to be ca. 2000 in *P. malariae*, 10000 in *P. vivax*, 15000 in *P. ovale* and more than 30000 in *P. falciparum*. Hepatic merozoites are then delivered into the blood circulation to infect erythrocytes that will invaginate to form the

parasitophorous vacuole. The erythrocytic merozoites are ovoid or elongated structures and species-specific in size (Kreier, 1980).

Once within the parasitophorous vacuole, the parasite rapidly transforms into an immature trophozoite (ring stage). Hemoglobin is ingested and digested to produce the typical malaria pigment (hemozoin). During this process, the parasite grows and the nuclear material of the mature trophozoite increases and undergoes several nuclear divisions to form a schizont. The mature schizont finally bursts to liberate individual erythrocytic merozoites. The latter differ from the hepatic form, mainly by the presence of malaria pigment. Erythrocytic merozoites can now infect other erythrocytes. The duration of blood schyzogony is generally a multiple of 24 h, usually 24, 42 or 72 hours and is related to the clinical manifestation of the disease (Kreier, 1980).

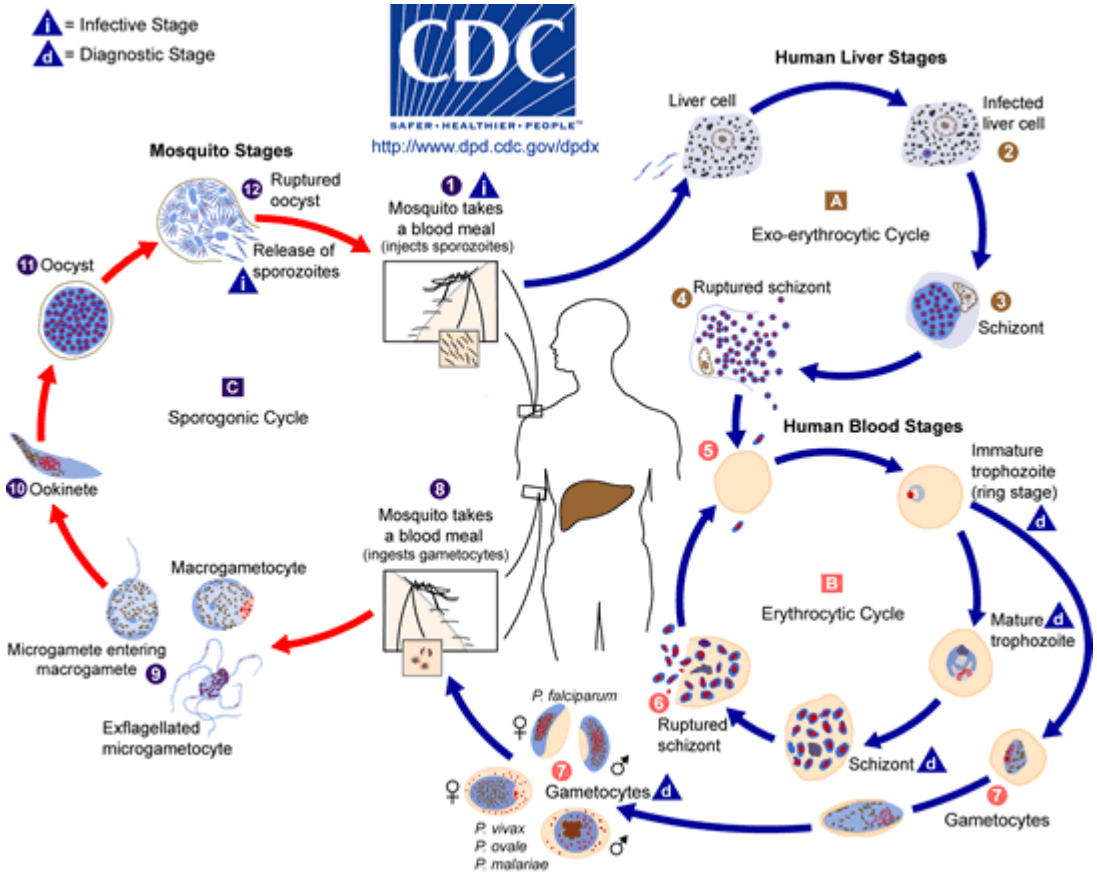

Figure 2.5. Scheme of *Plasmodium* parasite cycle.
(Source: http://www.cdc.gov/malaria/biology/life_cycle.htm)

Upon invading a new erythrocyte the merozoites can either initiate renewed blood schyzogony or develop into a gametocyte from the ring stage trophozoite (Kreier, 1980).

Gametocytes can be ingested by the female *Anopheles* mosquito during a blood meal. The parasites' multiplication in the mosquito is known as the sporogonic cycle. Once in the mosquito's stomach, the microgametes (male gametes) penetrate the macrogametes (female gametes) generating zygotes. The zygotes in turn become motile and elongated (ookinetes) which invade the intestinal wall of the mosquito where they develop into oocysts. The oocysts grow, rupture, and release sporozoites, which migrate to the mosquito's salivary glands. Inoculation of the sporozoites into a new human host perpetuates the life cycle (Kreier, 1980). The *Plasmodium* life cycle is summarized in Figure 2.5.

II.1.2. General clinical manifestations of malaria

More than 80% of non-immune patient with malaria present with fever, rigor, malaise and headache. Afebrile patients usually give a history of chills and sweat. Fever is usually irregular initially, when symptoms may be non-specific and difficult to distinguish from those caused by other infections, such as influenza, dengue and typhoid-fever. Vomiting occurs in up to 34% and diarrhea in about 16% of patients. Classic periodic fever (every second day in tertian parasites *P. falciparum*, *P. vivax* and *P. ovale*, and every third day in quartan parasite *P. malariae*) is uncommon initially, although if present is highly suggestive of malaria. However, periodic fever is neither necessary nor sufficient for the diagnosis of malaria. Splenomegaly and splenic tenderness are the most common physical findings. Tachycardia, tachypnoea, icterus, hepatomegaly and hypotension also occur (Gillespie and Pearson, 2001).

The incubation period is the time between the infective bite by the *Anopheles* mosquito and the first symptoms. Shorter periods are observed in general with *P. falciparum*, and longer with *P. malariae*. *P. vivax* and *P. ovale* can produce dormant liver stage parasites (hypnozoites), thus the liver stages may reactivate and cause disease several months after the infective mosquito bite. This is called a relapse (Kreier, 1980).

Malaria disease can be categorized as 1) uncomplicated or 2) severe (complicated). Severe malaria occurs when *P. falciparum* infections are complicated by serious organ failures or abnormalities in the patient's blood or metabolism. Severe malaria often develops very rapidly with specific complications, including cerebral malaria, severe anaemia, pulmonary oedema, acute black water fever, and renal failure. The clinical features of severe malaria depend on age and the immune status of the host. In endemic areas, most cases occur in young children (under five years old) and pregnant women (Gillespie and Pearson, 2001).

The diagnosis of malaria may be obtained either by the observation of parasites on a blood smear microscopic analysis or by rapid diagnostic tests (RDTs). Light microscopy has the advantage of low cost and high sensitivity and specificity when used by well-trained staff. RDTs are based on the detection of parasite antigens and are generally more expensive. In *P. falciparum* malaria, further laboratory results can be found, such as mild anaemia, mild thrombocytopenia, elevation of bilirubin and others (Gillespie and Pearson, 2001; WHO, 2006).

II.1.3. Current chemotherapy in the management of malaria

Malaria control requires an integrated approach comprising prevention targeted at vector control and treatment with effective antimalarials. The successful management of malaria depends on prompt diagnosis, an accurate clinical assessment and instituting suitable chemotherapy as soon as possible. Treatment depends not only on the parasite species but also the susceptibility to antimalarial drugs, the severity of the illness, and the age and background immunity of the patient (Gillespie and Pearson, 2001).

The affordable and widely available antimalarial drug chloroquine that was in the past the main treatment in malaria control is now ineffective in most *falciparum* malaria endemic areas and resistance to sulfadoxine–pyrimethamine is increasing rapidly. The discovery and development of the artemisinin derivatives in China, and their evaluation in Southeast Asia and other regions, have provided a new class of highly effective antimalarials, and have already transformed the chemotherapy of malaria. Artemisinin-based combination therapies (ACTs) are now generally considered as the best current

treatment for uncomplicated *falciparum* malaria. The recommended ACTs are: artemether-lumefantrine, artesunate + amodiaquine, artesunate + mefloquine, artesunate + sulfadoxine–pyrimethamine. As second-line treatment for uncomplicated *falciparum* malaria, the following combinations are used: artesunate + tetracycline, or doxycycline or clindamycin; and quinine + tetracycline, or doxycycline or clindamycin. In the case of severe *falciparum* malaria, quinine and artemisinin derivatives (artesunate, artemether, artemotil, dihydroartemisinin) are basically used (WHO, 2006).

II.1.4. Targets in the search for new antimalarial compounds

Many antimalarial targets can be related to the functions of distinct organellar structures within the parasite, mainly the lysossomal food vacuole (the site of extensive hemoglobin degradation), the apicoplast (a plastid organelle thought to originate from a cyanobacterium symbiont) and the acrystate mitochondrion and its electron transport system (Sahu *et al.*, 2008). Some of these targets have been considered so far in the investigation of natural products as antimalarials. Two out of these are detailed in the following topics and comprise the heme detoxification process and apicoplast targets.

II.1.4.1. Heme, hematin or hemozoin as targets

During the digestion of its host cell hemoglobin, large amounts of heme (Fe(II)PPIX) are released in the food vacuole of the intraerythrocytic malaria parasite. This ferriprotoporphyrin is toxic for the parasite and its detoxification occurs via the formation of hematin (Fe(III)PPIX) and finally hemozoin, which is a dimer of Fe(III)PPIX, also known as malaria pigment (Egan, 2008). A schematic representation of the mechanism of heme detoxification by hemozoin formation is presented in Figure 2.6.

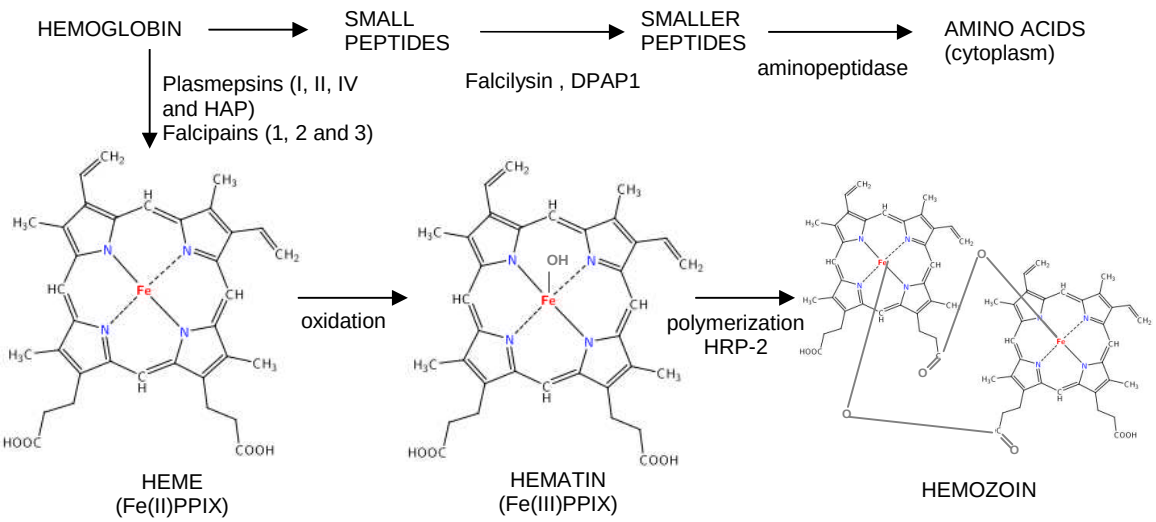

Figure 2.6. Schematic representation of the mechanism of heme detoxification by hemozoin formation in *P. falciparum* food vacuole (Sahu *et al.*, 2008).

Heme has been partially implicated in the mode of action of endoperoxide antimalarials, such as artemisinin, which specifically enters infected blood cells to form radical adducts with heme (Robert *et al.*, 2006). Hematin is believed to be the target of chloroquine and other quinoline antimalarials, and there is evidence suggesting that these drugs act by complexing with hematin, thus preventing its detoxification by blocking the formation of hemozoin (Ginsburg and Krugliak, 1999). The mechanism of hemozoin formation in the parasite is not completely elucidated, but histidine-rich protein-2 (HRP-2) has been implicated as an enzyme in the process and could be considered as a new target in the search for antimalarial drugs (Sahu *et al.*, 2008).

II.1.4.2. Apicoplast targets

The apicoplast has been discovered as a relict chloroplast organelle in malarial parasites and other apicomplexan parasites. The apicoplast apparently resulted from endosymbiosis with cyanobacteria and – although no longer photosynthetic – is essential to parasites. The organelle maintains certain specific functions and more than 500 proteins were identified. Apicoplast function includes several biochemical pathways such as fatty

acid, isoprenoid, and heme synthesis, which are present in bacteria, plants, and apicomplexan parasites, but are fundamentally different to the analogous pathways in the human host. Hence, these parasite-specific metabolic pathways are potentially good targets for drug development (Ralph *et al.*, 2004).

One of the new approaches involving these metabolic pathways is fatty acid synthesis in the intra-erythrocytic parasite, which is crucial for the synthesis of cell and organellar membranes. Higher eukaryotes normally use a type I fatty acid synthase (FASI) system, while in the apicoplast a type II fatty acid synthase (FASII) system takes place. In the FASII system, each fatty acid biosynthetic pathway is carried out by an enzyme encoded by a different gene.

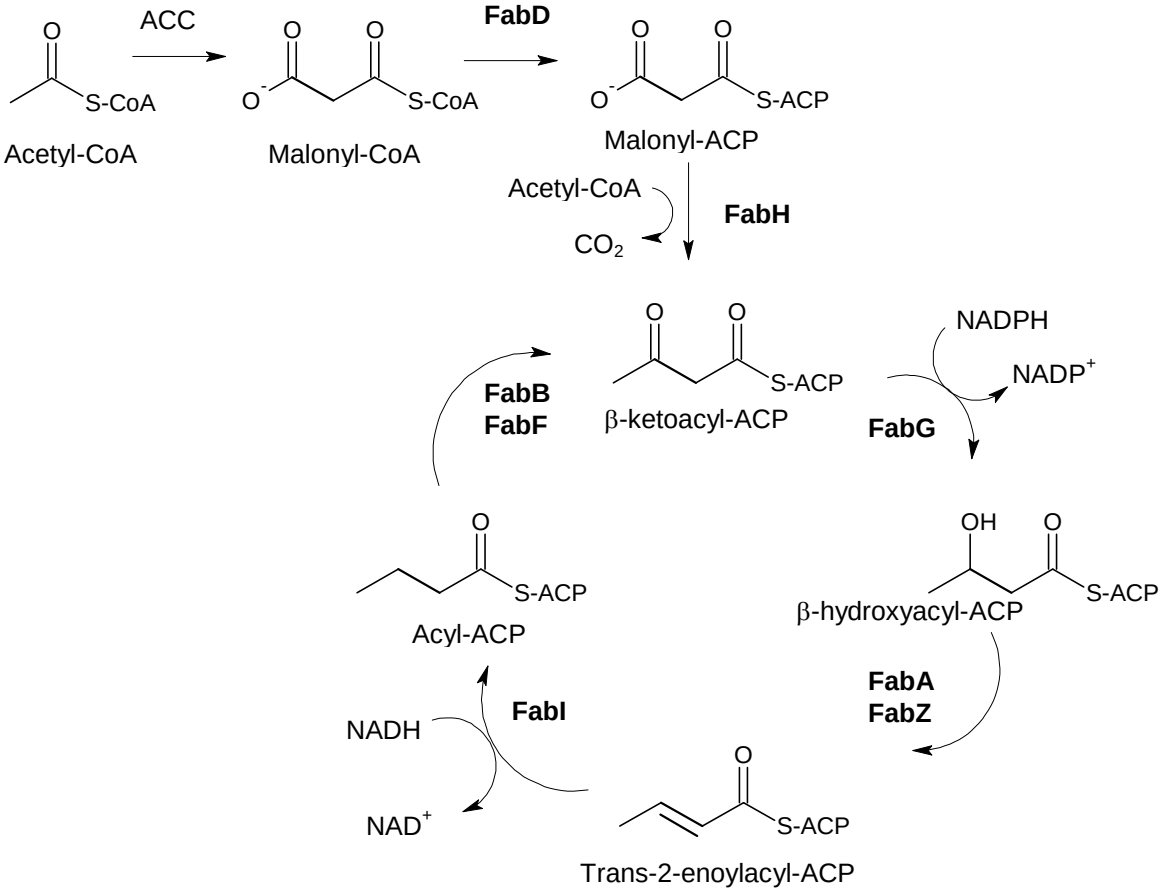

Figure 2.7. Type II fatty acid biosynthetic pathway and key enzymes in the process. ACC: acetyl-CoA carboxylase, ACP: acyl carrier protein, FabD: ACP transacyclase, FabH: β-ketoacyl-ACP synthase III, FabG: β-ketoacyl-ACP synthase I, FabA: β-hydroxyacyl-ACP-dehydrase I, FabZ: β-hydroxyacyl-ACP-dehydrase II, FabF: β-ketoacyl-ACP synthase II.

In *P. falciparum*, this biosynthetic pathway incorporates several enzymes susceptible to inhibition by drugs (Figure 2.7). Some examples of FASII inhibitors are isoniazide and triclosan (FabI inhibitors), as well as thiolactomycin and derivatives (FabB and FabG inhibitors). Among these enzymes, the *P. falciparum* enoyl-ACP reductase (*Pf*FabI) has been particularly investigated for inhibition, since its active site is known and a crystal structure of the enzyme is available incorporating the inhibitor triclosan and the cofactor NADH in the active site. Triclosan binding traps the *Pf*FabI enzyme in the nonproductive NAD^+ cofactor state and prevents the binding of NADH (Carballeira, 2008; Sahu *et al.*, 2008). Some natural products, such as flavonoids, have been demonstrated to inhibit FabG, FabZ and FabI (Tasdemir *et al.*, 2006).

II.2. Studied plants

II.2.1. *Argemone mexicana* L. (Papaveraceae)

II.2.1.1. Botanical description

Family

The Papaveraceae belongs to the order Papaverales within the Angiosperms classification. The family comprises ca. 250 species distributed within ca. 26 genera, most of them native to the northern temperate zone. Species are mainly herbaceous annuals or perennials but with some shrubs, all of which produce latex (Heywood, 1993).

Leaves are alternate, without stipules. Stems, leaves and other parts of the plant contain a well-developed system of secretory canals which produce yellow, milky or watery latex. The flowers are large and conspicuous, either solitary or arranged in cymose or racemose inflorescences (Heywood, 1993).

Economically the most important species in this family is *Papaver somniferum* (opium poppy) which yields opium. Seeds are used in baking and yield an important drying oil. Likewise, the seeds of *Glaucium flavum* and *Argemone mexicana* yield oils which are

important in the manufacturing of soaps. Many species are cultivated as garden ornamental plants (Heywood, 1993). The world distribution of Papaveraceae is shown in Figure 2.8.

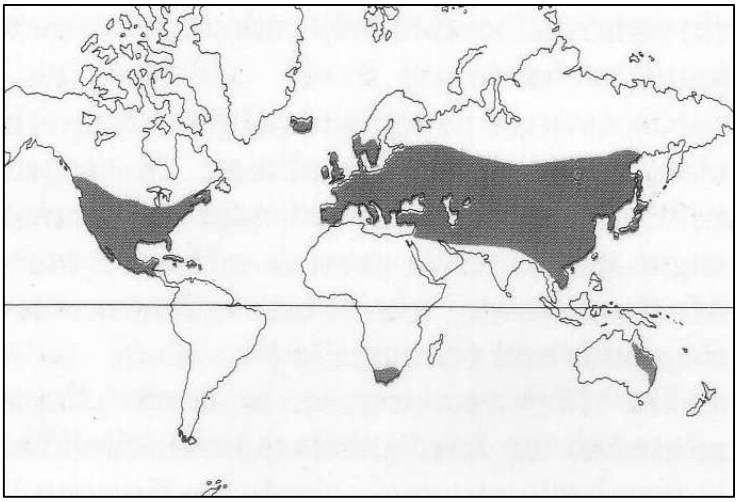

Figure 2.8. World distribution of the botanical family Papaveraceae (Heywood, 1993).

Genus

The genus *Argemone* L. is closely allied to the genus *Papaver* L. and is mainly distributed in America (10 species). Species have white or yellow flowers similar to those of the genus *Papaver*, although the leaves of some *Argemone* species are prickly (Heywood, 1993).

Species

Argemone mexicana L. has different vernacular names, such as Mexican pricklypoppy, Mexican poppy, devil's fig, golden thistle of Peru (English), "Cardo Santo" (Spanish), and "èqún arìgbò" (Yoruba language). The species originates from Mexico but is now a worldwide distributed tropical weed, especially in coastal regions, and widely naturalized in the Old World (Scott, 1996).

A. mexicana counts fourteen synonyms: *Echtrus trivialis* Lour., *Echtrus mexicanus* (L.) Nieuwl., *Argemone vulgaris* Spach, *Argemone versicolor* Salisb., *Argemone spinosa* Moench, *Argemone sexvalis* Stokes, *Argemone ochroleuca* Sweet, *Argemone mucronata* Dum. Cours. ex Steud., *Argemone mexicana* var. *typica* Prain[1], *Argemone mexicana* var. *parviflora* Kuntze, *Argemone mexicana* var. *ochroleuca* (Sweet) Lindl., *Argemone mexicana* var. *lutea* Kuntze, *Argemone mexicana* fo. *leiocarpa* (Greene) G.B. Ownbey, *Argemone leiocarpa* Greene (MBG, 2009).

This annual plant can usually reach 60 – 90 cm in height. Stems are often branching at 2.5 – 8 dm from the base and branches are sparingly prickly, presenting bright yellow latex. Leaves are sessile, spiny, sinuate-pinnate, variegated with white. Flowers are large (4 – 7 cm of diameter), subtended by 1-2 foliaceous bracts; petals are bright yellow. Stamens are in number of 30 – 50. Fruits are presented as prickly oblong-ovoid capsules, opening by 4 – 6 valves, containing numerous spheric seeds of 1.6 – 2 mm (Eichler, 1865). Figure 2.9 illustrates flowers and leaves of *A. mexicana* as well as the stem containing a bright yellow latex.

A **B**

Figure 2.9. *Argemone mexicana* L. (Papaveraceae). A: Yellow flower and prickly leaves. B: Cross section of the prickly stem bark showing a bright yellow latex. Source: (http://www.genevainternational.org/navigate.php?kind=1&id=307&lang=en&last=87&lastsub=117).

[1] Considered invalid/illegitimate by Missouri Botanical Garden (http://www.tropicos.org).

II.2.1.2. Pharmacological and chemical aspects

A. mexicana has been used for more than 100 years in Indian traditional medicine to treat several diseases. A paste prepared from the roots is used for treating scorpion bite, the latex is used for eye inflammation, and the juice of leaves as well as the latex with lemon juice is used for treating malaria (Kosalge and Fursule, 2009; Poonam and Singh, 2009). An ethnobotanical and retrospective treatment-outcome clinical study conducted in the Sikasso and Bandiagara regions of Mali showed that *A. mexicana* was one of the most effective plants used traditionally to treat non-complicated and severe malaria in that country (Diallo *et al.*, 2006).

An entire research project has been developed by the non-governmental organization Antenna Technologies (Geneva) and the Department of Traditional Medicine (DTM) of Mali to establish the safety and efficacy of the traditional preparation of *A. mexicana* in order to develop an improved traditional medicine (ITM) or “medicament traditionnel amélioré” (MTA). In Mali, the DTM, as part or the Ministry of Health, is responsible for the production of ITMs to be included in the National Formulary. As a preliminary result of this study, the decoction of *A. mexicana* was demonstrated to be active when taken twice a day. Higher doses (four times a day) were associated with a risk of cardiac toxicity, demonstrated by the prolongation of QT intervals obtained in the ECGs of patients. TLC/densitometry and HPLC/UV analyses of the decoction showed the presence of berberine at 20 mg/L, which would be able to explain the *in vitro* antiplasmodial activity but not the clinical results, since berberine is poorly absorbed orally. This suggested the presence of other active compounds. The search for other active compounds in the decoction was then included as part of the objectives in this thesis project (Willcox *et al.*, 2007).

From the chemical point of view, several isoquinoline alkaloids have been isolated from *A. mexicana* extracts. Isoquinoline alkaloids are a large family of alkaloids derived mostly from the amino acid tyrosine. In the case of *A. mexicana* alkaloids, three main types of isoquinoline derivatives are found: 1) the protoberberine type: berberine (**6**), scoulerine (**7**) and cheilanthifoline (**8**); 2) the protopine type: allocryptopine (**9**), argemexicaine A (**10**) and B (**11**), and protopine (**12**); 3) the benzo[c]phenanthridine type:

norchelerythrine (**13**), norsanguinarine (**14**) pancorine(**15**), and sanguinarine (**16**) (Bentley, 1998; Chang *et al.*, 2003a; Chang *et al.*, 2003b; Israilov and Yunusov, 1986).

Protoberberine alkaloids are one of the most widely distributed among the isoquinoline alkaloids groups. The classic biosynthetic route for the formation of protoberberines involves the same fundamental units as those for the formation of benzylisoquinoline alkaloids. Two molecules of tyrosine are involved, one yielding dopamine via DOPA, and the second proceeding to 3,4-dihydroxy-phenyl pyruvic acid. These molecules afford norlaudanosoline by Mannich condensation followed by decarboxylation. A selective methylation of norlaudanosoline provides reticuline, which is a precursor of many isoquinoline alkaloids (Cordell, 1981). A representative scheme of the formation of reticuline from the two molecules of tyrosine is shown in Figure 2.10.

It is well known that (+)-isomer of reticuline is the true biosynthetic precursor of several alkaloids, including berberine. The so-called berberine bridge carbon at C-8 of the protoberberine alkaloids has been shown to be derived from the S-methyl group of methionine. The oxidation of the N-methyl group and subsequent ring closure is thought to proceed via an iminium species to give either 9,10- (pathway I) or 10,11- substituted (pathway II) series of compounds (Figure 2.11) (Cordell, 1981).

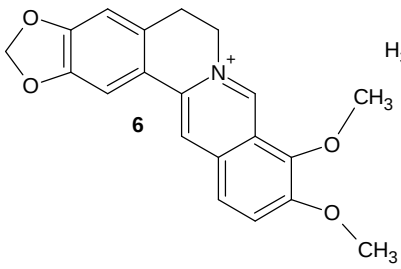

6

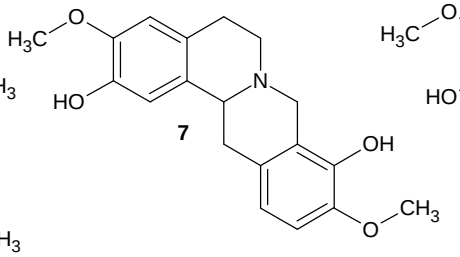

7

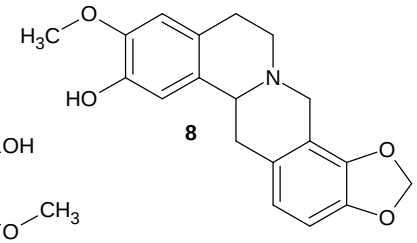

8

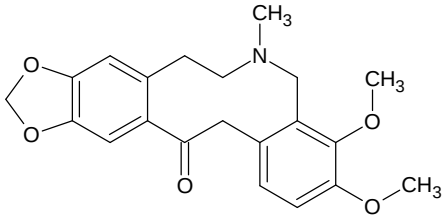

9

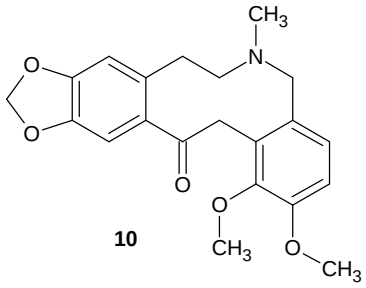

10

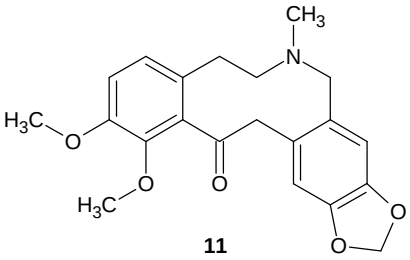

11

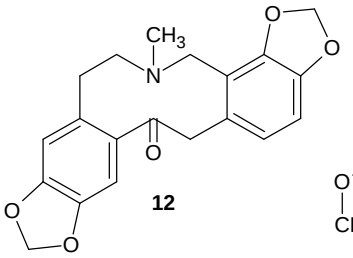

12

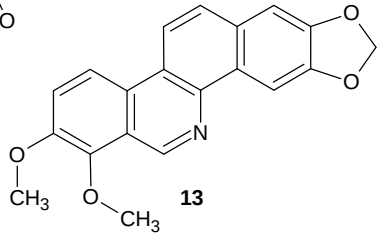

13

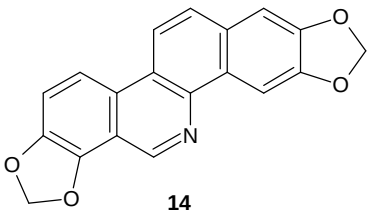

14

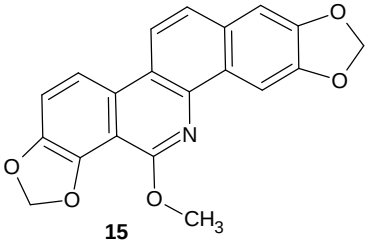

15

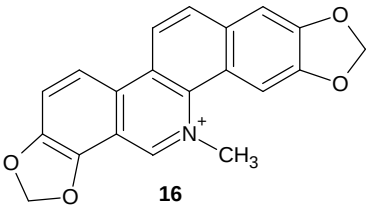

16

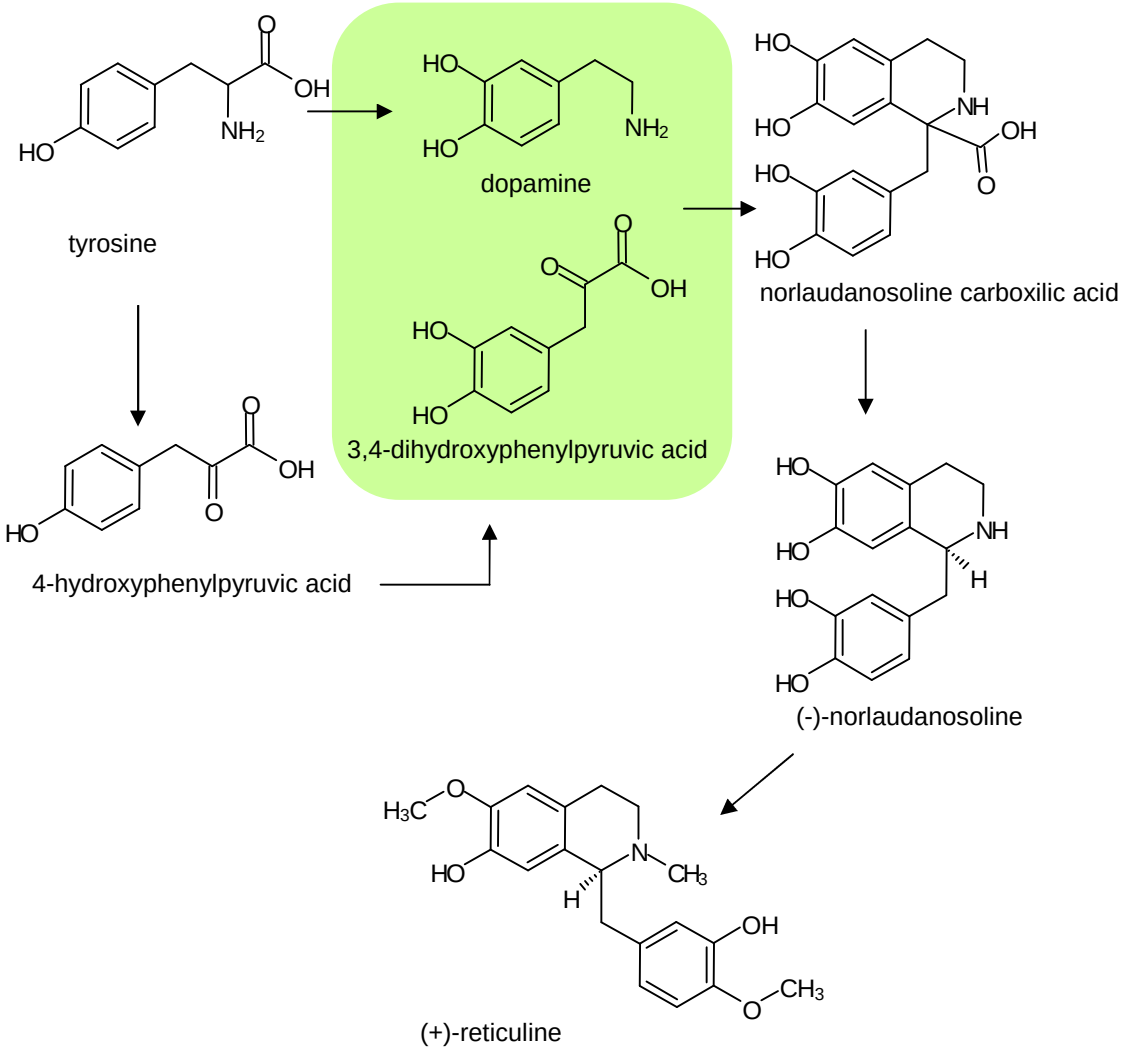

Figure 2.10. Biosynthesis of (+)-reticuline, a precursor of several isoquinoline alkaloids.

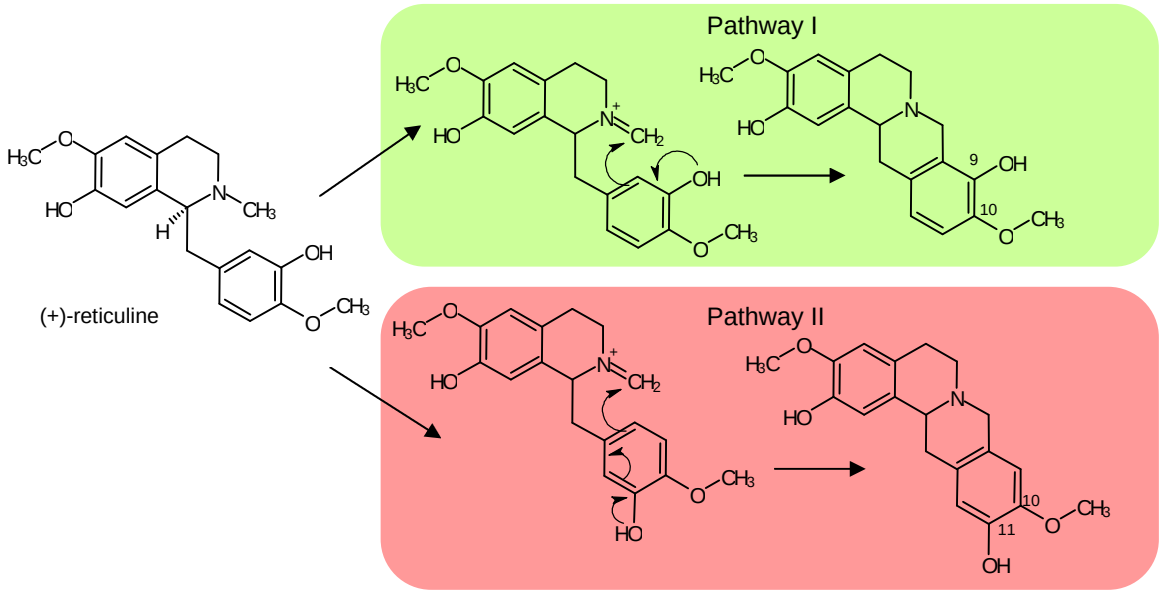

Figure 2.11. Formation of 9,10- or 10,11-substituted intermediates from (+)-reticuline in the biosynthesis of protoberberine alkaloids.

Protoberberine alkaloids are also considered the precursors of other skeletal structures, particularly the protopine and benzophenanthridine alkaloids.

In the case of protopine alkaloids, reticuline was shown to proceed to scoulerine (**7**) and then isocorypalmine to give allocryptopine (**9**). Scoulerine (**7**) has also been demonstrated to be an intermediate in the biosynthesis of protopine (**12**) via the formation of the protoberberine alkaloid cheilanthifoline (**8**) (Cordell, 1981).

Benzophenanthridine biosynthesis also involves reticuline as a common precursor. It has been suggested that these alkaloids are derived by fission of the 6,7-bond of protoberberines with subsequent bond formation between C-6 and C-13. One example is the formation of chelidonine and sanguinarine from reticuline. The latter cyclizes into scoulerine which will undergo the formation of two methylendioxy groups to produce stylopine. The intermediate **17**, which is believed to originate from stylopine metho salt, would undergo a cleavage to the enamine aldehyde **18**, providing either chelidonine by the reduction of the imino species **19** or sanguinarine by oxidative dehydration (Figure 2.12) (Cordell, 1981).

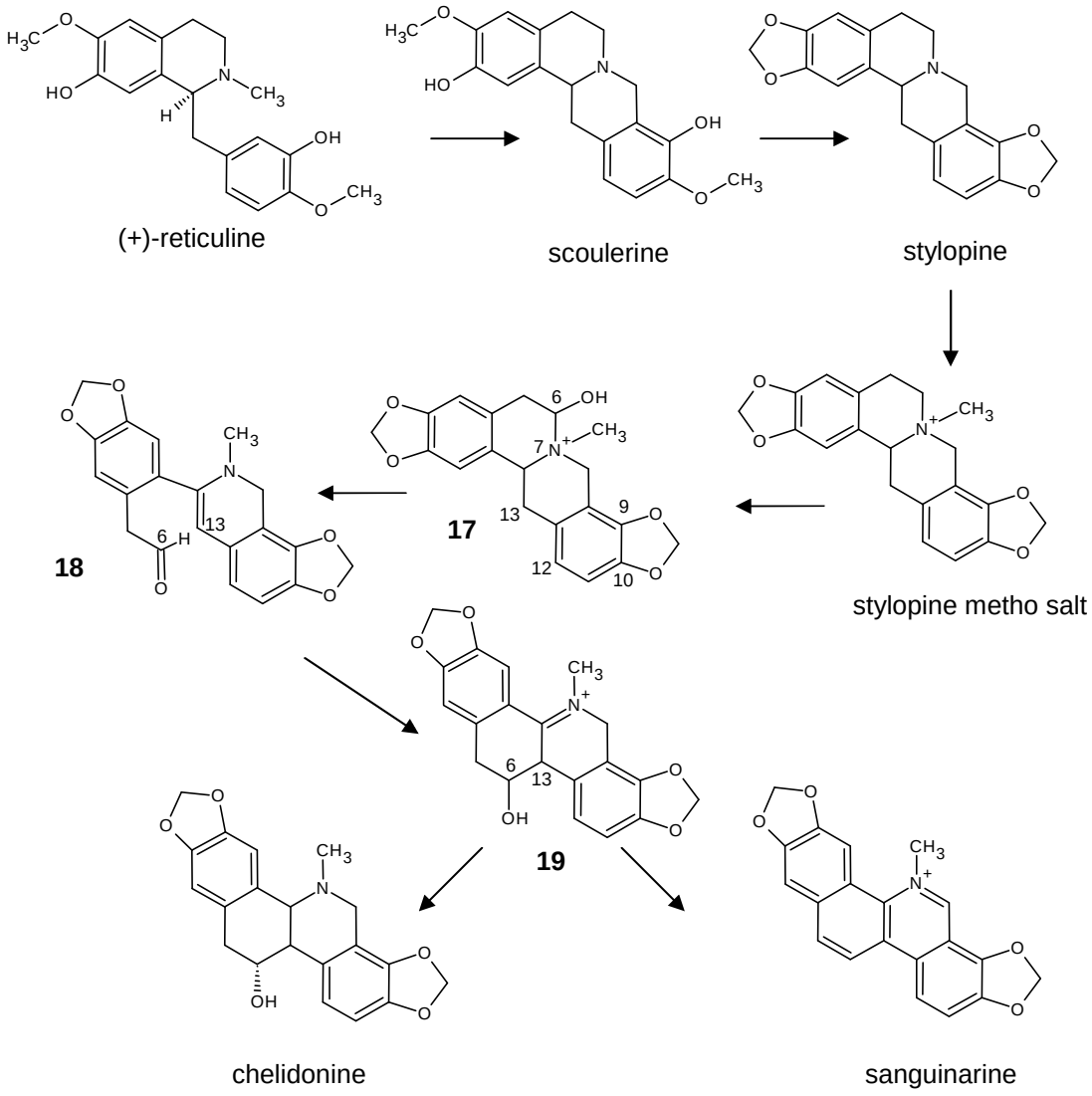

Figure 2.12. Biosynthesis of the benzophenanthridine alkaloids chelidonine and sanguinarine from the common precursor (+)-reticuline.

From the pharmacological point of view, protoberberine and protopine alkaloids have presented a series of different *in vitro* and *in vivo* activities. Berberine and its derivatives have been particularly studied and have demonstrated important antimicrobial activity, covering a range of organisms from fungi and protozoa to bacteria. Berberine sulphate shows inhibitory activity against *Corynebacterium diphteriae*, *Staphylococcus aureus*, *Xanthomonas citri* and *Candida tropicalis* (Cordell, 1981). Berberine is able to increase membrane permeablility in bacteria and intercalate into DNA (Lewis and Ausubel,

2006) and has demonstrated a good antiprotozoal activity against several species of *Leishmania*. In fact, this alkaloid has been used clinically for the treatment of leishmaniasis for over 50 years (Osorio *et al.*, 2008). Among the different types of isoquinoline alkaloids, the protoberberines showed to have the most potent antiplasmodial activity against *P. falciparum* (strain K1). Dehydrodiscretine and berberine were the most active with IC_{50} values lower than 1 µM, while the protopine-type alkaloids protopine and allocryptopine had IC_{50} values of 34.0 and 5.1 µM, respectively (Wright *et al.*, 2000). Studies on the structure-activity relationships of protoberberine alkaloids having an antimalarial activity shows that the presence of a quaternary nitrogen in this series of alkaloids seems to increase the antimalarial activity (Osorio *et al.*, 2008). Moreover, the activity can also be increased by the aromatization of ring C due to the quaternization of the nitrogen in ring B, and by the type of oxygen functions in rings A, C, and D (Iwasa *et al.*, 1998; Iwasa *et al.*, 1999; Osorio *et al.*, 2008). It has been demonstrated that berberine is a potent *in vitro* inhibitor of both nucleic acid and protein synthesis in *P. falciparum* (Elford, 1986). While the mechanism of action and pharmacological activities of berberine have been extensively studied, very little is known about the other protoberberine alkaloids.

Another important feature of protoberberine and protopine alkaloids are their cardiac effects observed *in vitro* and *in vivo*. Berberine salt has been used in China to treat arrhythmia and heart failure for years. The capacity of the alkaloid to prolong the duration of cardiac action potentials is well known and this effect is mainly attributed to the inhibition of slowly activating components (IKs) and increase of L-type Ca^{2+} currents in myocytes (Rodriguez-Menchaca *et al.*, 2006; Wang and Zheng, 1997; Wang *et al.*, 1996). In the same way, allocryptopine has also been studied for its anti-arrhythmic properties. This alkaloid was demonstrated to prolong the refractory phase of the heart muscle, abolishing fibrillations, in the same way as quinine and quinidine (Benthe, 1956). Possible mechanisms of action for the anti-arrhythmic effect of allocryptopine have been investigated showing that the alkaloid was able to produce a blocking effect on the transient outward potassium current in rabbit left-ventricular myocytes (Li *et al.*, 2008). The alkaloid protopine has been studied especially in China for its cardiac effects. An anti-arrhythmic activity has also been demonstrated by the prolongation of the functional refractory period. An inhibition of spontaneous beat and contractive force were also observed (Yu *et al.*, 1999). Some mechanisms of action could be demonstrated for protopine, such as the promotion of the translocation of protein kinase C from the cytosol

to the membrane in the presence of noradrenaline, the decrease of the intracellular Ca^{2+} and the increasing effect on cAMP and cGMP (Li *et al.*, 2005).

Benzophenanthridine alkaloids present in *A. mexicana* are known to be responsible for the toxicity of *Argemone* oil, whose ingestion is the cause of the disease called epidemic dropsy. A great number of poisoning cases (over 3000) was reported in India during August-September 1998 due to the consumption of mustard oil adultered with *Argemone* seed oil. The disease is characterized by pathological accumulation of diluted lymph in body tissues and cavities (Verma *et al.*, 2001). Sanguinarine and dihydro-sanguinarine are the main alkaloids in the *Argemone* oil, and they are present mostly in the seeds and roots of the plant. A few mechanisms have been associated with the toxicity of sanguinarine, such as the increase of peroxidation and changes in enzyme activity of serum in the liver. The hepatotoxicity of the alkaloid seems to be associated with oxidation of protein thiols and disturbance of mitochondrial respiration (Choy *et al.*, 2008). It is important to notice that sanguinarine has been reported as a trypanocidal agent against *T. brucei* with an IC_{50} value of 1.9 µM. However, the activity was not specific, since the alkaloid showed high cytotoxicity (Osorio *et al.*, 2008).

II.2.2. *Licania octandra* (Hoffmanns. ex. Roem & Schult.) Kuntze (Chrysobalanaceae)

II.2.2.1. Botanical description

Family

The Chrysobalanaceae belongs to the order Malpighiales within the Angiosperms classification. The family comprises ca. 400 species distributed within ca. 17 genera, most of them native tropical and subtropical lowlands. Species are mainly trees and shrubs, some of which are locally important in the tropics as fruit trees. The family is closely allied to the Rosaceae and was formerly included in it, but differs especially in its erect ovules.

Leaves are simple, alternate and with stipules. Flowers are bisexual, less commonly unisexual, more or less irregular and markedly perigynous, with five sepals, up

to five petals and two to 300 stamens. The anthers dehisce introrsely. The ovary is superior and has three carpels, but only one develops, usually with two erect basal ovules. Style is simple, with a simple stigma. Fruit is a dry or fleshy drupe with a bony endocarp. Seeds have no endosperm.

Economically, some species are useful in construction under water and underground for its hard, silica-enriched wood (Letouzey and White, 1978). Exemples are *Licania ternatensis* and *L. octandra*. Several species are cultivated for their fruit, coco plum (*Chrysobalanus icaco*) being the most important. Oil may be extracted from the seeds of many species; *Licania rigida* (oiticica) is grown for this purpose in Brazil, the oil being used as a substitute for tung oil, while the oil of *L. arborea* is used in candle and soap making (Heywood, 1993). The world distribution of Chrysobalanaceae is shown in Figure 2.13.

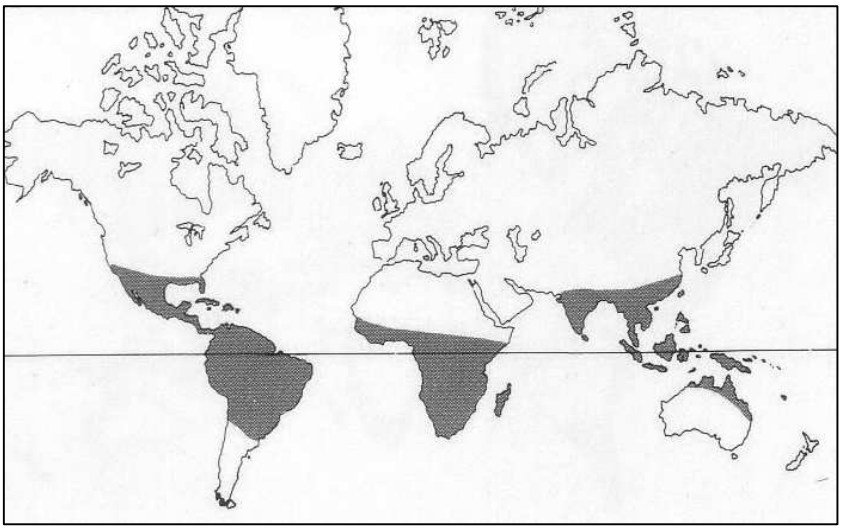

Figure 2.13. World distribution of the botanical family Chrysobalanaceae (Heywood, 1993).

Genus

The genus *Licania* Aubl. comprises about 185 species of trees that can reach up to 35 m. Species are mostly distributed in Amazonian Forest and Western Africa. Some species can also be found in Malaysia, Southern USA and different regions of Brazil - from Roraima to Rio de Janeiro (Prance, 1972b). Figure 2.14 depicts typical fruit and leaves of the genus.

Figure 2.14. Typical fruit and leaves of genus *Licania* Aubl. Source: (http://www.tropicos.org/Image/32344).

Species

Licania octandra (Hoffmanns. ex. Roem & Schult.) Kuntze occurs in northern Venezuela, the Guianas, eastern Amazonian and southeastern Brazil. Some of its vernacular names are hoogboskwepi, kwepi (in Suriname) and Caripé (in Brazil) (Prance, 1972b).

L. octandra counts four synonyms: *Hirtella octandra* Hoffmanns. ex Roem. & Schult., *Licania octandra* (Hoffmanns. ex Roem. & Schult.) Pilg. ex J.F. Macbr., *Moquilea pallida* Hook. f., and *Moquilea turiuva* (Cham. & Schltdl.) Hook. f. (MBG, 2009).

The plant is a small to medium-sized tree with glabrous young branches. Stipules are linear, up to 5 mm long, membraneous, hirsutulous, subpersistent, on young branches only. Petioles are up to 7 mm long, tomentose, becoming less so with age, terete or rarely shallowly canaliculated, with two sessile glands at or near junction with lower surface of lamina, the glands often obscured by pubescence. Blades are broadly ovate to oblong (3-12 x 2-4 cm), obtuse to acuminate at apex, with acument 1-5 mm long, rounded to subcuneate at base, glabrous and shining above, with well-developed stomatal cavities beneath, with venation flattened around small slit-like apertures to the cavities, the mouth of the cavities glabrous to lanate. Inflorescences are disposed in racemose panicles, the rachis and branches are sparsely grey-brown-tomentose. Bracts and bracteoles are 1 – 4 mm long, persistent, tomentose outside, often serrate, with stipitate glands. Flowers are 2 – 3 mm long, sessile or nearly so in primary branches of inflorescence, solitary or in small groups. Receptacle is campanulate, tomentose outside, densely villous within. Calyx lobes are acute, tomentose on both surfaces. Petals are absent. Stamens are in number of 8 – 12, inserted in a complete circle, filaments far exceeding calyx lobes, free to base and glabrous. Ovary is inserted at the base of receptacle, villous; style is villous at the base only, with a glabrous upper portion and equaling filaments. Fruit is globose to elongate-lanceolate, up to 2.5 cm long. Epicarp is glabrous or with a light brown appressed pubescence, mesocarp thin and fleshy, endocarp hard, thin, fibrous, glabrous or sparsely hirsute when young.

II.2.2.2. Pharmacological and chemical aspects

Some species of the genus *Licania* are traditionally employed in Amazonia and northeastern Brazil, especially for its timber and dry oils, oititica (*L. rigida*) being the most used in these regions. Amazonian Indian tribes employ the bark ashes of *L. octandra* (Caripé) as a hardening agent for ceramics (Prance, 1972a). The leaves and fruits of several *Licania* species have also been used in Brazilian and Venezuelan traditional medicine as anti-inflammatory, and for the treatment of diarrhea and leucorrhea (Castilho *et al.*, 2005).

There are no reports on the chemical composition of *Licania octandra* in the literature. However, other species of the genus have been studied, particularly *L. densiflora* Kleinhoonte, *L. heteromorpha* Benth., *L. licaniiflora* (Sagot) S.F. Blake, *L. michauxii* Prance, and *L. tomentosa* (Benth.) Fritsch. The main classes of compounds found in the genus are flavonoids and terpenoids.

From the biosynthetic perspective, flavonoids are phenolic compounds originating from the condensation of a triacetate (ring A) and a cinnamic acid (ring B), followed by a cyclization step to form the central pyranic ring. Thus, the B-ring and part of the heterocyclic ring of the flavonoid skeleton are provided by a suitable hydroxycinnamic acid CoA ester (4-coumaroyl-CoA), whereas the A-ring originates from three acetate units via malonyl-CoA. Both precursors are derived from carbohydrates. Malonyl-CoA is formed from acetyl-CoA and CO_2 catalysed by acetyl-CoA carboxylase, while 4-coumaryl-CoA and related hydroxycinnamic acid esters are supplied by the first steps of the general phenylpropanoid pathway. The latter starts from the aromatic amino acid phenylalanine, which is synthesized via the shikimate/arogenate pathway. Flavonoids can be classified as flavones, flavonols, flavanones, dihydroflavonols, flavan-3-ols, flavan-3,4-diols, chalcones, aurones and antocyanidins, as shown in Figure 2.15 (Heller and Forkmann, 1994).

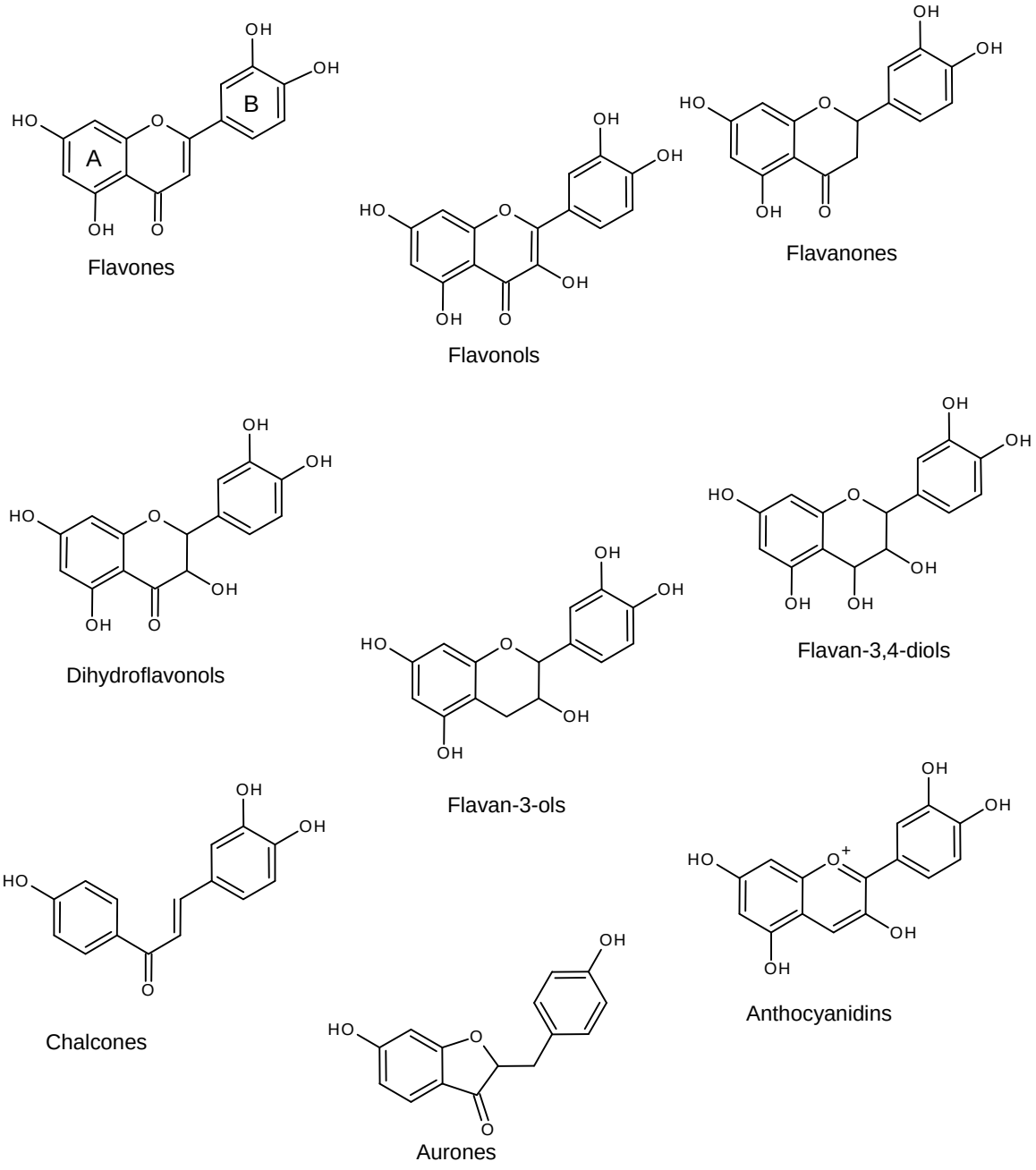

Figure 2.15. General structures of flavonoids according to their classification.

From *L. densiflora* leaves, used as an anti-inflammatory remedy in Venezuela, a series of myricetin glycosides could be isolated: myricetin 3'-methylether 3-*O*-glucoside (**20**); myricetin 3'-methylether 3-*O*-galactoside (**21**); myricetin 4'-methylether 3-*O*-rhamnoside (**22**); myricetin 3',5'-dimethylether 3-*O*-glucoside (**23**); myricetin 3',5'-dimethylether 3-*O*-rhamnoside (**24**) (Braca *et al.*, 2001a). Naringenin, apigenine, quercetine and kaempherol derivatives were also reported in the species (Braca *et al.*, 1999b).

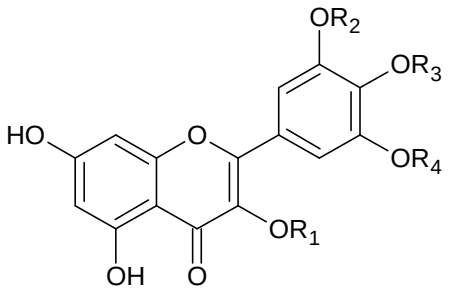

20	R_1=glucose	R_2=CH_3 R_3=R_4=H	
21	R_1=galactose	R_2=CH_3 R_3=R_4=H	
22	R_1=rhamnose	R_2=R_4=H	R_3=CH_3
23	R_1=glucose	R_2=R_4=CH_3	R_3=H
24	R_1=rhamnose	R_2=R_4=CH_3	R_3=H
25	R_1=glucose	R_2=H	R_3=R_4=CH_3
26	R_1=2''-*O*-rhamnosyl-rhamnose	R_2=R_3=R_4=H	
28	R_1=R_3= rhamnose	R_2=R_4=H	
29	R_1=galactose	R_2=R_4=H	R_3=CH_3
30	R_1=galactose	R_2=R_3=R_4=H	
31	R_1=rhamnose	R_2=R_3=R_4=H	
32	R_1=glucose	R_2=R_4=H	R_3=CH_3
33	R_1=arabinose	R_2=R_3=R_4=H	

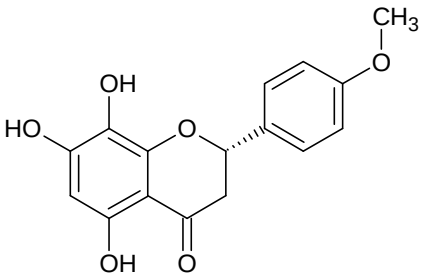

27

Other flavonoids were also reported in the leaves of *L. densiflora*, namely myricetin 3',4'-dimethylether 3-*O*-β-D-glucopyranoside (**25**), myricetin 3-*O*-α-L-(2''-*O*-α-L-rhamnopyranosyl)-rhamnopyranoside (**26**), and 8-hydroxy-naringenin 4'-methylether (**27**) (Braca *et al.*, 1999a).

L. heteromorpha leaf extract presented a similar profile concerning its myricetin derivative flavonoid composition. Some of the myricetin derivatives found for these species are myricetin 3,4'-di-O-rhamnoside (**28**), myricetin 4'-methylether 3-*O*-galactoside (**29**), myricetin 3-*O*-galactoside (**30**), myricetin 3-*O*-rhamnoside (**31**), myricetin 4'-methylether 3-*O*-glucoside (**32**), and myricetin 4'-methylether 3-*O*-rhamnoside (**22**). From the non-polar fractions of *L. heteromorpha*, eight triterpenoids could be isolated: betulinic acid, alphitolic acid (I), 3β-*O*-trans-*p*-coumaroyl maslinic acid (II), 3β-*O*-cis-*p*-coumaroyl maslinic acid (III), 3β-*O*-trans-*p*-coumaroyl alphitolic acid (IV), 3β-*O*-cis-*p*-coumaroyl alphitolic acid, 3β-*O*-trans-*p*-coumaroyl-2α-hydroxy-urs-12-en-28-oic acid, and 3β-*O*-cis-*p*-coumaroyl-2α-hydroxy-urs-12-en-28-oic acid (Braca *et al.*, 1999b). Compounds I-IV have demonstrated an antimicrobial activity against Gram-positive bacteria and yeasts, but no activity against Gram-negative organisms (Braca *et al.*, 2000).

From the species *L. licaniiflora*, myricetin derivatives have also been isolated. Some examples are myricetin-3-*O*-galactoside (**30**) and myricetin 3-*O*-arabinoside (**33**).

Moreover, some quercetin and kaempherol derivatives, as well as taxifolin 3-*O*-rhamnoside could be isolated (Braca *et al.*, 2002a). The presence of flavonoids in *L. licaniiflora* has been associated with its radical scavenging activity measured with the DPPH spectrophotometric assay (Braca *et al.*, 2002b). The species also presented the triterpenoids, such as oleanolic acid, maslinic acid, oleanolic acid-3-O-arabinoside, betulinic acid, arjunetin, tormentic acid glucosyl ester, pomolic acid and olean-12-en-2α,3β-diol (Braca *et al.*, 2001b).

The root extracts of *L. maichauxii* have demonstrated a cytotoxic activity against human hepatoma and colon carcinoma cell lines (Badisa *et al.*, 2000). Following a bioassay-guided fractionation of a root extract of this plant, two new ent-kaurene diterpenes could be isolated, licamichauxiioic acids A (**34**) and B (**35**) (Chaudhuri *et al.*, 2002).

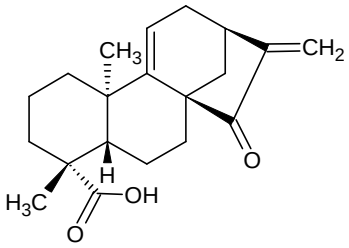

34

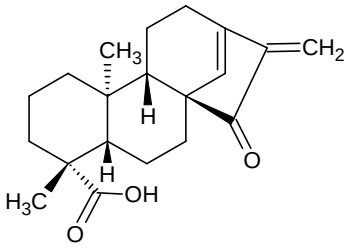

35

The seed extract from *L. tomentosa* has been investigated for its anti-herpes simplex virus activity. The incubation of the extract, at non-cytotoxic concentrations, with the acyclovir-resistant herpes simplex virus type 1 impaired the productive replication of this virus in a concentration-dependent way and had virucidal effect (Miranda *et al.*, 2002). Although authors did not identify the compound(s) responsible for activity, another research group has isolated from the fresh fruits of the plant the new triterpene lactone licanolide (**36**), together with the well-known compounds betulinic acid, oleanolic acid, lupeol, palmitoeic and hexadecanoic acids, sitosterol, tormentic and ursolic acids (Castilho *et al.*, 2005; Castilho and Kaplan, 2008).

In terms of antiplasmodial or antiparasitic activity, no reports were found in the literature for the genus *Licania*. Within the Chrysobalanaceae family, there is one report on

the traditional use of *Parinari curatellifolia* Planch. ex Benth. bark to treat malaria or fever in Zimbabwe. However, the extracts obtained with leaves and stems of this species have not shown any *in vitro* activity against *P. falciparum* (Kraft *et al.*, 2003).

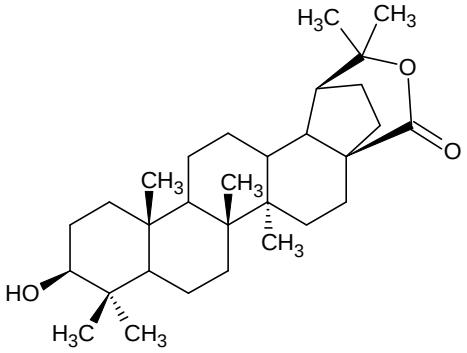

36

II.2.3. *Syzygium cumini* (L.) Skeels (Myrtaceae)

II.2.3.1. Botanical description

Family

The Myrtaceae belongs to order Myrtales within the Angiosperms classification. This large family comprises ca. 3000 species distributed in about 100 genera. The habit ranges from straggling and small shrubs to the lofty *Eucalyptus* trees and the Myrtaceae species are distributed mostly in tropical and subtropical regions, concentrated in America and eastern and southwestern Australia. The family is divided into two subfamilies: Myrtoideae and Leptospermoideae (Heywood, 1993).

As general features, the species from the family Myrtaceae are woody plants, mostly shrubs to large trees. Leaves are usually opposite (less often alternate), leathery, evergreen and typically entire, without stipules, and characteristically pellucid-dotted with subepidermal glands (also found on the young stem, floral organ and fruit) containing volatile oils. The flowers are regular and bisexual, most frequently in cymose, less of the in racemose inflorescences, rarely solitary. The stamens are numerous (rarely few), sometimes in tufts opposite the petals, typically free and with versatile anthers. The ovary is commonly inferior with one to many (2-5) locules. The style is long and simple with a simple capitate stigma. The fruit is usually a fleshy berry (rarely drupe) or dry (then, a capsule or nut). There is little or no endosperm (Heywood, 1993).

Economically the most important genus is *Eucalyptus*, especially for its timber, but also for its essential oil. The family also yields valuable spices, such as cloves (*Eugenia caryophyllata*) and pimento (*Pimenta dioica*). Among the edible fruits are the tropical American and West Indian guava (*Psidium guajava*) and jaboticaba (*Myrciaria cauliflora*) (Heywood, 1993). The world distribution of Myrtaceae is shown in Figure 2.16.

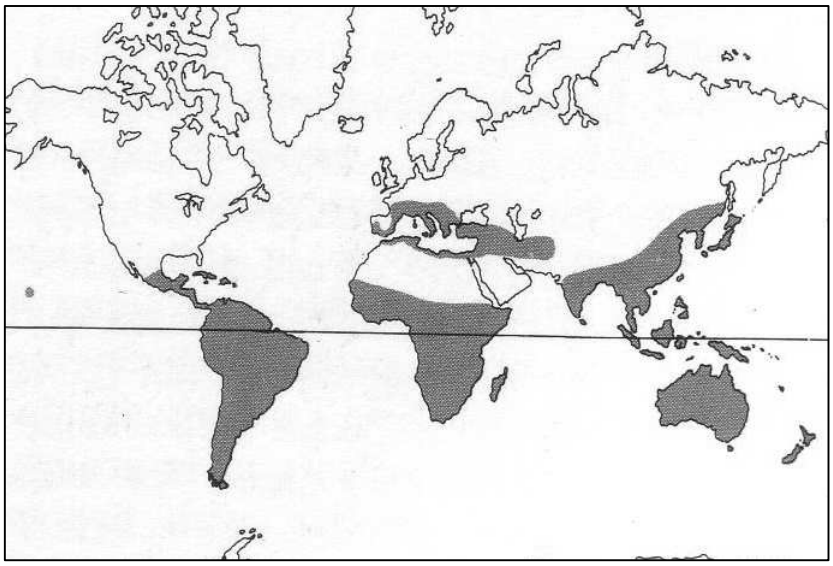

Figure 2.16. World distribution of the botanical family Myrtaceae (Heywood, 1993).

Genus

Syzygium Gaertn. is a large genus of over 500 species of trees and shrubs found throughout the warm areas of the world. Leaves are opposite with entire margins. Flowers are in dense clusters in axils of leaves or at the end of branches. Fruit is a fleshy berry (Schmidt *et al.*, 2002).

Species

Syzygium cumini (L.) Skeels is thought to be native to India but can also be found in Thailand, the Philippines, Madagascar, as well as in tropical and subtropical regions of America. Some of the vernacular names of the species are Jam, Jaman (in India), Luk wa (in Thailand), Madan (in Japan), Rotra (in Madagascar), Jambo, and Jambolão (in Brazil) (Ross, 2003).

The species counts five synonyms: *Syzygium jambolanum* (Lam.) DC., *Myrtus cumini* L., *Eugenia jambolana* Lam., *Eugenia cumini* (L.) Druce, *Calyptranthes oneillii* Lundell (MBG, 2009).

The plant is a tree of 4 – 15 m in height. Leaves are leathery, oblong-ovate to elliptic to obovate, 6 – 12 cm long, opposite, decussate, exstipulate, petiolate, acute, glaucous, and unicostate reticulate. Panicles are borne mostly from the branchlets below the leaves, often being axillary or terminal and are 4 – 6 cm long. Flowers are numerous, clustered in cyme, ebracetate, sub-sessile, complete, actinomporphic, hermaphrodite, pentamerous, epigynous and cyclic. Calyx, containing 5 sepals, is gamesopalous, valvate, forming a funnel-shaped tube which is adnate to the ovary. Corolla, containing 4 petals, is polypetalous, imbricate and caducous. Stamens are numerous, inserted at the brim of the calyx tube, dithecous, dorsifixed and introrse. Ovary is inferior, bilocular, with axile placentation. Style and stygmate are simple. Fruit is oval to elliptic, 1.5 – 3.5 cm long, dark purple or nearly black, luscious, fleshy and edible, containing a single large seed. Stem is woody, aerial, erect, cylindrical, branched, solid, smooth (Ross, 2003). Figure 2.17 illustrates the fruits, leaves and stem of *S. cumini*.

Figure 2.17. Fruits, leaves and stem of *Syzygium cumini* (L.) Skeels.

II.2.3.2. Pharmacological and chemical aspects

S. cumini has been used for years in Indian traditional medicine, especially for the treatment of diabetes, but also as a digestive, astringent, anthelmintic, in the treatment of bronchitis, dysentery and ulcers (Sagrawat *et al.*, 2006).

Several studies were conducted with leaf, seed and bark extracts of *S. cumini* in order to demonstrate an antidiabetic activity *in vivo*. This activity has been demonstrated by several research groups and attributed to different natural products, such as flavonoids (Sharma *et al.*, 2008), ferulic acid (Mandal *et al.*, 2008), androstane derivatives (Shankar *et al.*, 2007), and sapogenins (Damasceno *et al.*, 2002). The inhibition of α-glucosidase, usually associated with the treatment of type 2 diabetes, has been pointed out as one of the possible mechanisms of action for the antidiabetic activity of *S. cumini* seed extract (Shinde *et al.*, 2008). The aqueous extract of the seeds has inhibited porcine pancreatic α-amylase and the bioassay guided fractionation has led to the isolation of betulinic acid and 3,5,7,4'-tetrahydroxy flavone as the active principles (Karthic *et al.*, 2008).

Various extracts of the plant have also presented antioxidant activity, which has been associated with the flavonoids (kaempferol, quercetin and myricetin), isolated from

the bark (Sultana *et al.*, 2007), and anthocyanidins usually present in the fruit pulp (Veigas *et al.*, 2007). Ferulic acid and catechins have also been considered as responsible for the antioxidant activity of the leaf extract (Ruan *et al.*, 2008).

An anti-inflammatory activity has been found for the leaf extract of the plant and could be attributed to its phenolic content (Lima *et al.*, 2007). Furthermore, a flavonoid containing fraction from the seed extract has shown *in vitro* efficacy against multi-drug resistant enteric bacteria (Jamine *et al.*, 2007). The leaf essential oil, rich in monoterpenes (ocimene, α- and β-pinenes), has also demonstrated anti-inflammatory properties (Ramos *et al.*, 2006), and good antibacterial activity against *Salmonella typhimurium* and *Pseudomonas aeruginosa* (Shafi *et al.*, 2002).

Some extracts of *S. cumini* are claimed to have a protective effect, particularly fruit extracts which exert protection on the tetrachloride induced toxicity in isolated rat hepatocytes (Veigas *et al.*, 2008), the gastroprotective effect of tannins extracted from bark on HCl/ethanol induced gastric mucosal injury in rats (Ramirez and Roa, 2003) and a reduction of radiation-induced DNA damage in cultured human lymphocytes by the leaf extract (Jagetia and Baliga, 2002).

A few other activities have been reported for *S. cumini* extracts, such as larvicidal against *Culex quinquefasciatus* and *Anopheles stephensi* (Pushpalatha and Muthukrishnan, 1995), antileishmanial and antifungal activities (Braga *et al.*, 2007), the increase of the uterine alkaline phosphatase in mice induced by the leaf extract (Sanwal *et al.*, 1973), and the antihistaminic effect of the aqueous leaf extract (Brito *et al.*, 2007).

From the stem bark of *S. cumini*, which is the object of this thesis, several compounds from different classes have previously been isolated. Vibriocidal activity has been demonstrated for the ethanol bark extract against *Vibrio cholerae*, and the activity has been attributed to the isolated compounds gallic acid (**37**) and non-identified tannins (Sharma *et al.*, 2009). The non-identified tannins of the barks have also exerted a gastroprotective effect on HCl/ethanol-induced gastric mucosal injury in rats (Ramirez and Roa, 2003). Other identified compounds in *S. cumini* bark are the gallic tannins: 3-galloyl glucose (**38**), 6-galloyl glucose (**39**), 1-galloyl glucose (**40**), corilagin (**41**); the ellagitannins: ellagic acid (**42**), 3,3'-di-*O*-methylellagic acid (**43**), 3,3',4-tri-*O*-methylellagic acid and five other non-identified ellagitannins (Bhatia and Bajaj, 1975); the triterpenes: betulinic acid,

friedelin, 3-friedelanol, β-sitosterol, β-sitosterol-glucoside; and the flavonoids: kaempferol, kaempferol 3-glucoside, quercetin (Bhargava *et al.*, 1974) and bergenin (Kopanski and Schnelle, 1988).

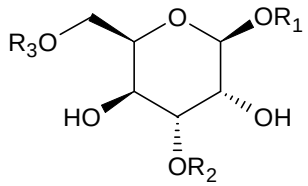

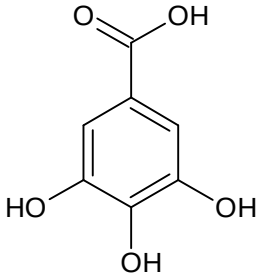

37

38	R_1=R_3=H	R_2= galloyl
39	R_1=R_2=H	R_3=galloyl
40	R_1= galloyl	R_2=R_3=H
41	R_1= R_2=R_3=galloyl	

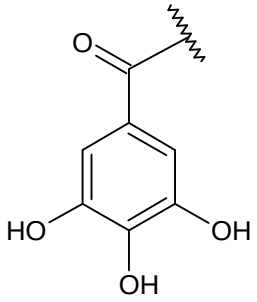

galloyl

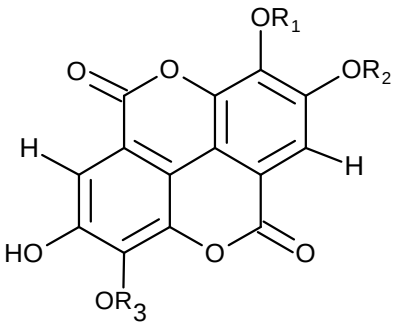

42	R_1=R_2=R_3=H		
43	R_1=R_3=CH_3	R_2=H	
44	R_1=R_2=R_3=CH_3		

From the biosynthetic point of view, gallic and ellagitannins are subclasses of hydrolysable plant tannins characterized by 3,4,5,3',4',5'-hexahydroxydiphenic (HHDP) acid residues that occur in nature in the form of various glucose esters and which, after

hydrolytic release, spontaneously rearrange into the dilactone ellagic acid. Recent studies using [*U*-^{14}C] labeled substrates demonstrated that the HHHDP acid unit and gallic acid originate from the hydrolysis of tellimagrandin II, which was enzymaticaly formed from 1,2,3,4,6-penta-O-galloyl β-D-glucose (Figure 2.18) (Niemetz and Gross, 2005).

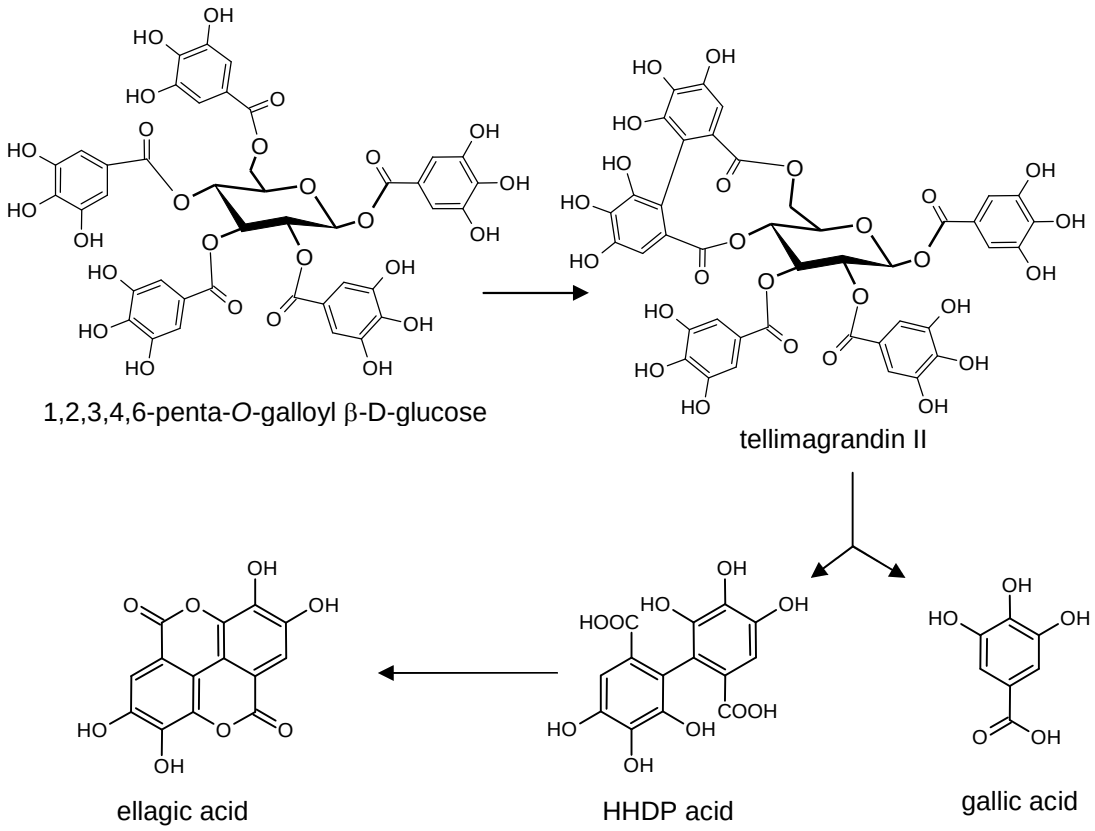

Figure 2.18. Biosynthesis of ellagic and gallic acid units from the common precursor 1,2,3,4,6-penta-*O*-galloyl β-D-glucose.

Chapter III

Results and discussion

III.1. Biological activity screening

Plant extracts were selected for the screening of antiplasmodial activity through two different strategies: 1) selection of extracts from plants used in traditional medicine for treating malaria or with a reported antiplasmodial activity in the literature and 2) a random selection of available plant extracts. In order to obtain further information on the biological activities of the extracts, all samples were tested against *P. falciparum* and for their *in vitro* cytotoxicity on human fibroblasts or mice splenocytes. Whenever possible, samples were also screened for activity against other parasites such as *Trypanosoma cruzi*, *T. b. brucei*, *Leishmania infantum*, and *L. amazonensis*. Even though the aim of this project was the search for antimalarial compounds, the investigation of activity against other parasites was also considered as part of a general investigation approach to detect whether an activity is specific or not. In the same way, the cytotoxicity assay results were used to discard samples which were potentially toxic in an unspecific way.

It is also important to highlight that the investigation of crude extracts in screening tests may lead to false-positive or false-negative results, due to the presence of interfering molecules, especially tannins. These are secondary metabolites widely distributed in the plant kingdom. The reactivity of such polyphenolic compounds to proteins has been associated with bioassay interference, particularly in assays involving enzymes (Wall *et al.*, 1996). As a matter of fact, a pre-purification step is usually recommended to remove tannins from complex plant matrices. Some of the techniques used in this way are the precipitation with skin powder or lead acetate, and polyamide column chromatography (Hostettmann *et al.*, 1998). The disadvantage of such techniques is that they are not specific and may completely remove other polyphenols together with tannins. The complete removal of polyphenols is controversial and some authors claim they may play an important role in specific activities (Phillipson *et al.*, 1998). Accordingly, the extracts considered in the present work were not pre-purified for tannin removal before screening assays. As an alternative approach, major fractions of extracts were co-screened in order to increase chances of finding an activity by concentration of active principles and/or removal of interfering compounds.

A primary sample selection was based on the in-house availability of plant species from the family Asteraceae. The antiparasitic activity and toxicity of their extracts are presented in Table 3.1.

A secondary sample selection included three plant extracts and their fractions from a collaboration project between the University of Geneva (Switzerland) and the Federal University of Paraíba (João Pessoa, Brazil). The decoction of *Argemone mexicana* L. was also considered for secondary screening based on ethnopharmacological data and its previously published clinical results (Willcox *et al.*, 2007) in collaboration with Antenna Technologies (Geneva, Switzerland). The antiparasitic activity and toxicity of these samples are shown in Table 3.2.

Considering the results of the primary and the secondary screenings, the following species were selected for phytochemical investigation: *Syzygium cumini* (L.) Skeels (Myrtaceae), *Licania octandra* (Hoffmanns. ex Roem. & Schult.) Kuntze (Chrysobalanaceae) and *Argemone mexicana* L. (Papaveraceae).

Table 3.1. Antiparasitic activity and cytotoxicity of primary selected MeOH extracts of plants from the family Asteraceae.

Plant information / Activity			Anti-*P. falciparum* [a]	Anti-*T. cruzi* [a]	Anti-*L. amazonensis* [a]	Cytotoxicity [a,b]
Species	Organ	Country	%			
Achillea erba-rotta All.	leaves	Italy	5.36	NA	NA	37.60
Artemisia borealis Pall.	leaves	Italy	NA	NA	NA	34.50
Blumea sessiliflora Decne.	aerial parts	Indonesia	NA	NA	NA	2.80
Centaurea vallesiaca (DC.) Jord.	aerial parts	Switzerland	NA	NA	NA	36.30
	roots	Switzerland	NA	NA	NA	40.50
Eupatorium inulifolium Kunth	aerial parts	Indonesia	NA	NA	NA	0.00
	roots	Indonesia	NA	NA	NA	2.10
Hieracium alpinum L.	aerial parts	Italy	NA	NA	NA	8.30
Melanthera aspera (Jacq.) Steud. ex Small	leaves	Panama	NA	NA	NA	0.90
	stems	Panama	NA	NA	NA	3.20
Mikania leiostachya Benth.	twigs	Panama	NA	NA	NA	18.50
Rolandra fruticosa (L.) Kuntze	aerial parts	Panama	18.39	NA	NA	0.00
Spilanthes iabadicensis A.H. Moore	aerial parts	Indonesia	NA	NA	NA	14.00
Vernonia cinerea (L.) Less.	aerial parts	Indonesia	NA	NA	NA	7.10
Vernonia patens Kunth	leaves	Panama	37.45	NA	NA	5.70
	flowers	Panama	45.88	NA	NA	0.30
	stems	Panama	NA	NA	NA	6.20

NA = not active; [a]cf Experimental section (V.6.1) for experimental assay description; [b]tested on mouse splenocytes.

Table 3.2. Antiparasitic activity and cytotoxicity of secondary selected extracts and fractions of plants from different botanical families.

Plant information / Activity					Anti-*P. falciparum* [a,b]	Anti-*T. cruzi* [a,c]	Anti-*T. b. brucei* [a,d]	Cytotoxicity [a,e]
Species	Family	Organ	Extract/ Fraction	Country	IC_{50} (µg/ml)			
Argemone mexicana L.	Papaveraceae	aerial parts	Decoction	Mali	>64.00	39.24	0.57	>64.00
			AM 8_A		>64.00	<0.25	>64.00	>64.00
			AM 8_B		>64.00	51.42	10.08	>64.00
			AM 8_C		>64.00	>64.00	1.32	>64.00
			AM 8_D		1.71	0.25	0.25	24.98
Licania octandra (Hoffmanns. ex Roem. & Schult.) Kuntze	Chrysobalanaceae	leaves	EtOH 80% extract	Brazil	29.84	>32.00	13.74	>32.00
			HF		12.11	32.00	32.00	32.00
			AcF		9.86	24.78	16.19	>32.00
			BF		18.80	>32.00	13.26	>32.00
			AqF		>32.00	>32.00	>32.00	>32.00
Syzygium cumini (L.) Skeels	Myrtaceae	stem bark	decoction	Brazil	32.00	34.56	4.31	>64.00
			CPC A		>64.00	34.56	2.69	>64.00
			CPC B		27.07	33.99	5.55	>64.00
			CPC C		<0.25	34.56	2.05	>64.00
			CPC D		19.80	7.50	1.86	26.44

[a]cf Experimental section (IV.6.2) for experimental assay description;
[b]IC_{50} >16 µg/ml: inactive; IC_{50} between 2 and 16 µg/ml: moderately active; IC_{50} <2 µg/ml: highly active;
[c]IC_{50} >30 µg/ml: inactive; IC_{50} between 2 and 30 µg/ml: moderately active; IC_{50} <2 µg/ml: highly active;
[d]IC_{50} >5 µg/ml: inactive; IC_{50} between 1 and 5 µg/ml: moderately active; IC_{50} <1 µg/ml: highly active;
[e]tested on human fibroblasts (MRC-5 cell line); IC_{50} >30 µg/ml: not toxic; IC_{50} between 10 and 30 µg/ml: moderately toxic; IC_{50} <10 µg/ml: highly toxic.

III.2. Bioguided phytochemical investigation of *Argemone mexicana*

The available batches of *A. mexicana* leaves were first extracted to get a decoction similar to that used in Malian traditional medicine. The decoctions were freeze-dried and their HPLC/UV profile compared under the same analysis conditions. The profile of 12 different batches is found in Appendix 1. Figure 3.1 illustrates the analysis of the extract AM 8, from a clinical batch provided by Antenna Technologies (Willcox *et al.*, 2007), which was chosen for fractionation procedures. The HPLC/UV chromatograms of AM 1 to 12 are representative of the complexity of the plant decoction, with a pronounced matrix effect from retention time 10 to 25 min. A large peak at 20.15 min could be detected and identified as berberine on the basis of its UV spectrum (λ_{max} 420, 345, 263, 228 nm) and co-injection with a standard compound.

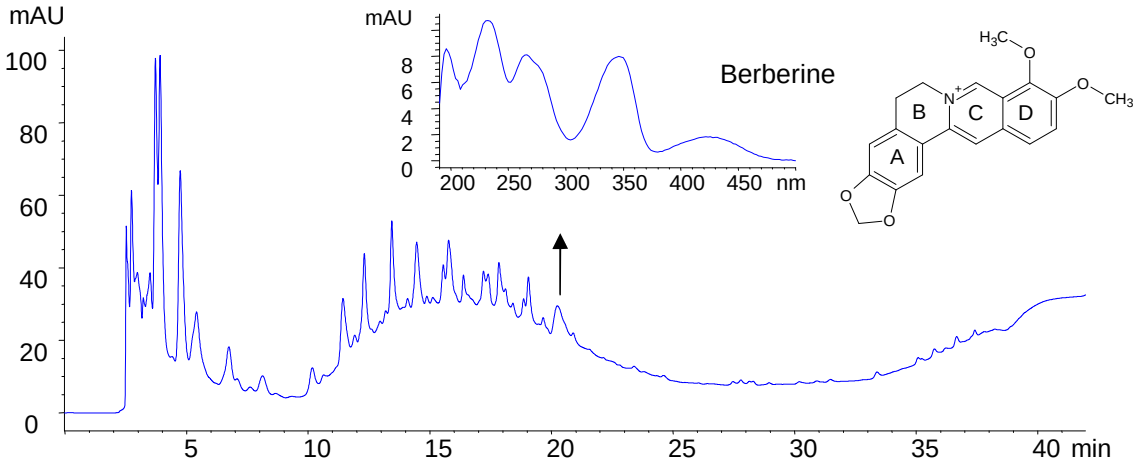

Figure 3.1. HPLC/UV at 254 nm of the decoction of *Argemone mexicana* leaves (batch AM 8). Column: Symmetry C_{18} (4.6 x 250 mm). Chromatographic conditions described in Experimental section V.2.2, Table 4.2.

III.2.1. Fractionation and isolation of active compounds from *A. mexicana* traditional decoction

In order to establish which compounds could be implicated in the clinical results of *A. mexicana* in Mali, a bioguided fractionation procedure was developed for the clinical batch AM 8. Since the extract was of polar nature, a first partition step was considered to provide fractions from different polarity without loss of possibly active compounds. However, in the specific case of *A. mexicana* decoction, a thick and persistent emulsion was obtained and the liquid-liquid extraction was solvent consuming.

Another fractionation approach was then considered and the general fractionation scheme is presented in Figure 3.2. The freeze-dried aqueous extract obtained from leaves of *A. mexicana* (26 g) was fractionated by liquid-solid extraction in methanol providing a MeOH insoluble fraction (AM 8_A) and a MeOH soluble fraction (AM 8_B).

The MeOH insoluble fraction AM 8_A presented an important matrix effect in HPLC/UV chromatogram. Thus, a vacuum liquid chromatography (VLC) on C_{18} silica gel was conducted providing two major fractions: one from the aqueous elution and another one from the methanol elution. This procedure resulted in a simplified fraction (AM 8 A_2) without the matrix effect previously observed (Figure 3.3). An HPLC/UV/MS analysis in APCI and ESI modes was conducted to provide dereplication data for this fraction. Unfortunately, a suitable ionization method in HPLC/MS analysis could not be established, even after several modifications on different MS parameters. The only on-line data available for the compounds in AM 8_A_2 are their UV spectra, which were very similar and characteristic of phenolic compounds. The possibility of phenolic compounds was also demonstrated by the radical scavenging activity observed in the DPPH TLC assay (Figure 3.3).

Subsequent isolation steps resulted in degradation of the compounds observed in the chromatogram of AM 8_A_2 and the identification of compounds was not possible.

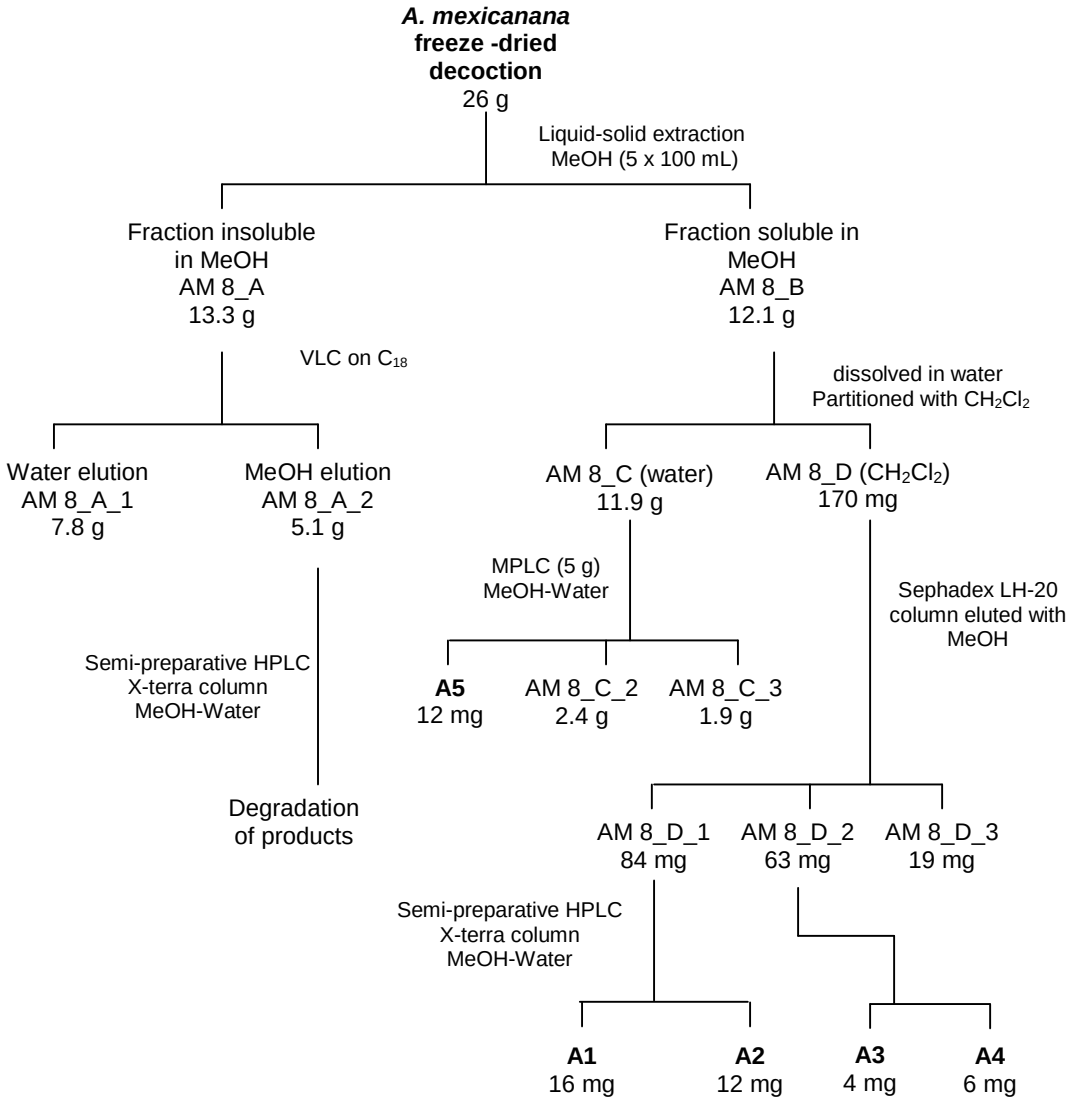

Figure 3.2. General fractionation scheme for *A. mexicana* decoction.

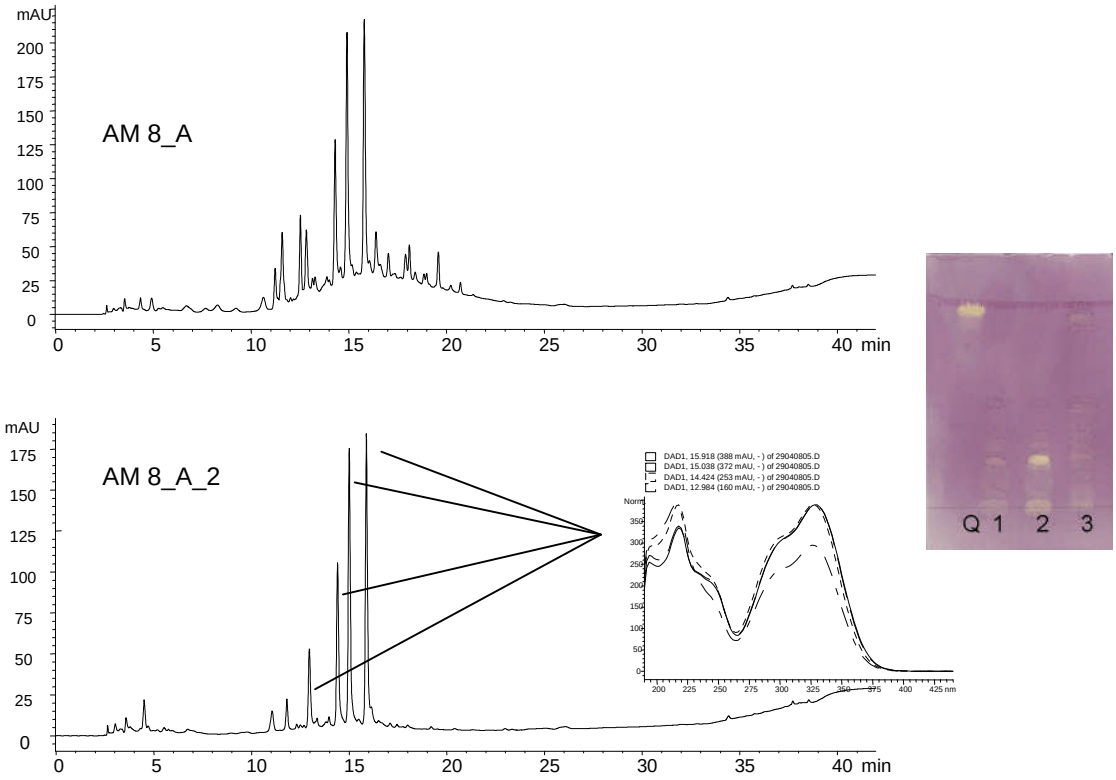

Figure 3.3. HPLC/UV of fractions AM 8_A and AM 8_A_2 at 254 nm. Column: Symmetry C_{18} (4.6 x 250 mm). HPLC conditions described in Experimental section V.2.2, Table 5.2. DPPH assay on TLC: Q=quercetin; 1 = AM 8_A; 2 = AM 8_A_2; and 3 = AM 8_A_1). Chromatographic system: ethyl acetate/ acetic acid/formic acid/H_2O (10:1:1:3).

The MeOH soluble fraction (AM 8_B) presented a peak corresponding to berberine in the HPLC/UV analysis, and it was then inferred that other alkaloids could be present. The dried fraction was then evaporated to dryness and recovered in water to be partitioned with CH_2Cl_2. The alkaloid enriched CH_2Cl_2 fraction (AM 8_D) was the only fraction considered active against the chloroquine resistant strain of *P. falciparum in vitro*, with an IC_{50} value of 1.71 µg/mL (Table 3.2). The HPLC/MS analysis using electrospray ionization (ESI) in positive mode showed four major compounds at retention times 17.86, 18.38, 19.48 and 20.71. Their mass spectra provided base peaks at *m/z* 354 [M + H]+, 370 [M + H]+, 354 [M + H]+ and 336 [M]+, respectively (Figure 3.4).

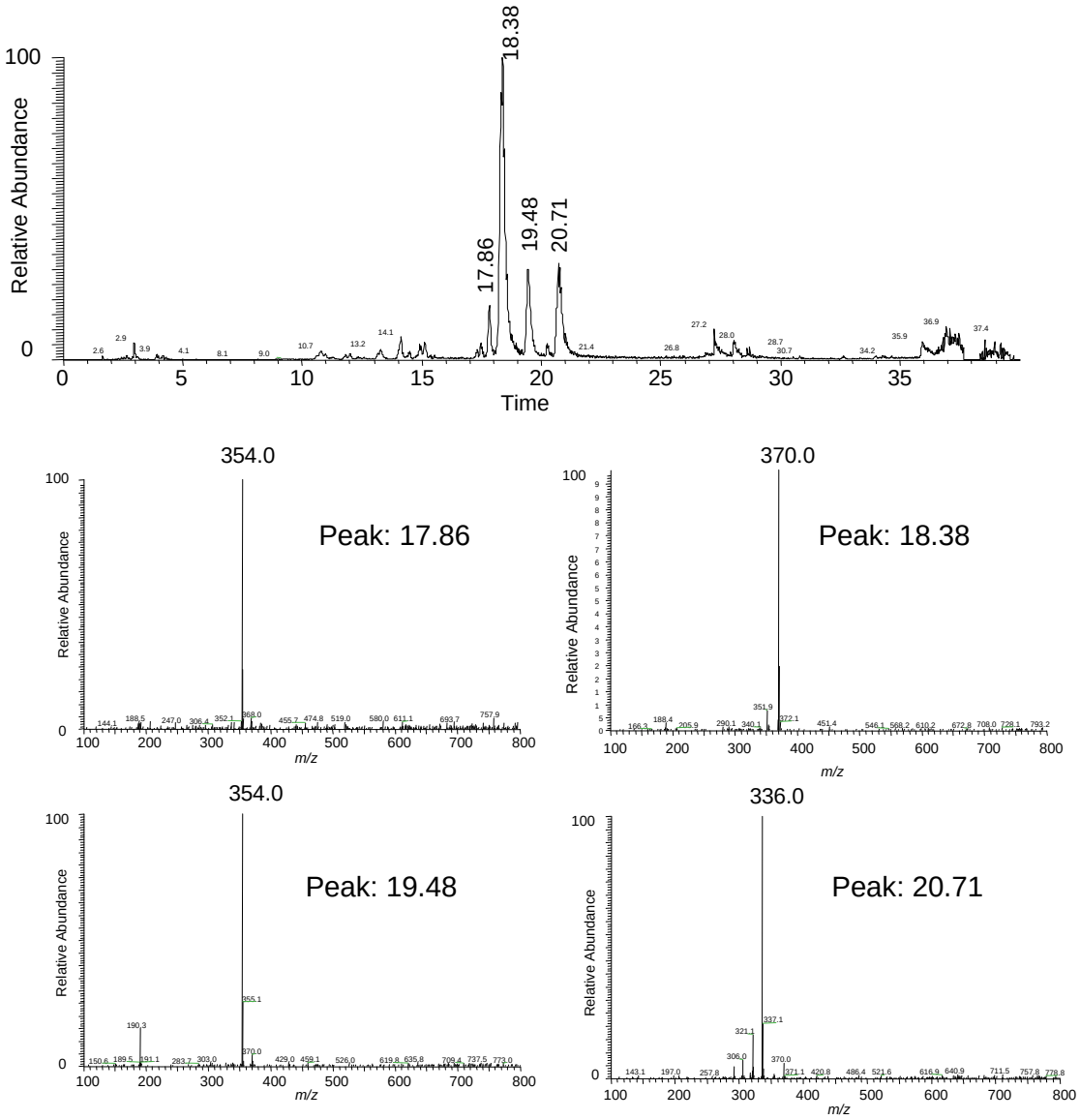

Figure 3.4. HPLC/ESI-MS chromatogram in positive mode of fraction AM 8_D and mass spectra of major detected compounds. Column: Symmetry C_{18} (4.6 x 250 mm). Chromatographic conditions described in Experimental sections V.2.2 and V.2.3, Tables 5.2 and 5.3.

The peak at 20.71 min corresponded to berberine, while the one at 17.86 min corresponded to protopine. Both compounds were confirmed by co-injection with standard compounds under the same conditions. The peak at 19.48 min displayed the same MS spectrum as protopine and it was considered as a possible isomer. An ultra performance liquid chromatography analysis coupled to a TOF high resolution mass spectrometer (UPLC/TOF-HRMS) was then performed for fraction AM 8_D in order to obtain further information from high resolution mass spectrum of the protopine isomer (Figure 3.5).

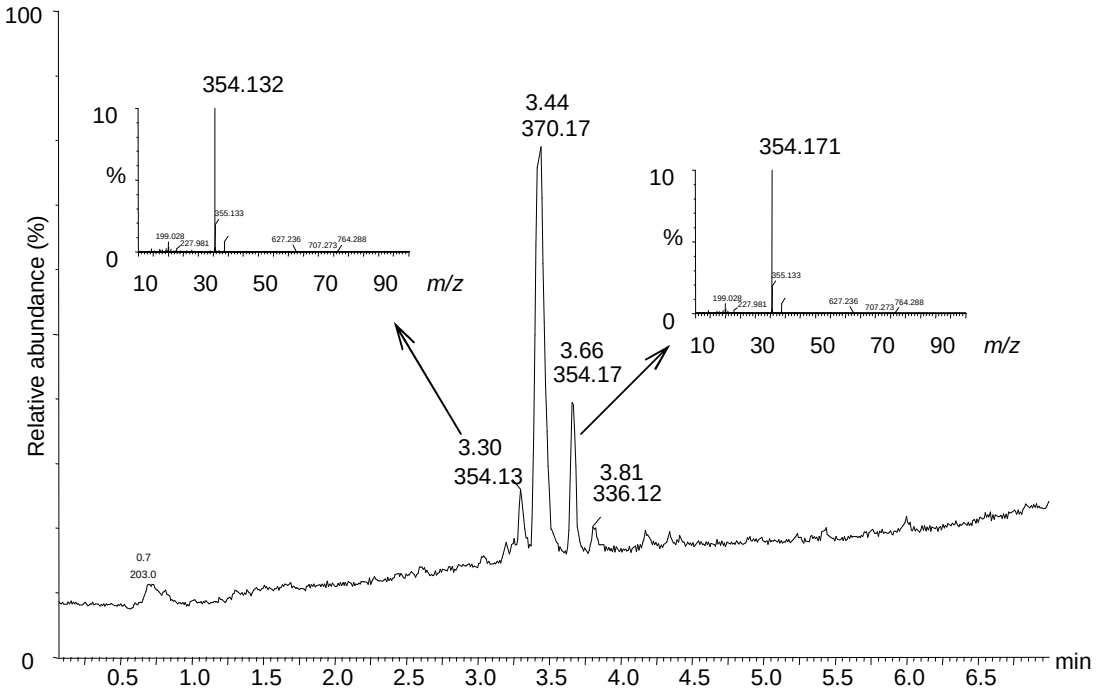

Figure 3.5. UPLC/TOF-HRMS chromatogram of fraction AM 8_D. Column: Acquity BEH C_{18} (2.1 x 150 mm, 17 µm). Chromatographic conditions described in Experimental section V.2.5.

The high resolution MS spectrum of the compound at 3.30 min in the UPLC/MS provided a pseudo-molecular ion at *m/z* 354.1320, calculated for $C_{20}H_{20}NO_5$ $[M+H]^+$ (354.1341), corresponding to protopine. On the other hand, the pseudo-molecular ion of the compound at 3.66 min was at *m/z* 354.1711, calculated for $C_{21}H_{24}NO_4$ $[M]^+$ or $[M+H]^+$ (354.1705). The molecular formula $C_{21}H_{24}NO_4^+$ matches that of a series of quaternary alkaloids, such as N-methyl-canadine, N-methyl, eschscholtzidine, N-methyl nantenine, N-methyl-reframine, N-methyl-sinactine, N-methyl-papaverine and takatonine. On the other hand, the molecular formula $C_{21}H_{23}NO_4$ matches that of other alkaloids such as cavidine, dehydroglaucine, thalictuberine and thalictricavine (CRC, 2009).

The pseudo-molecular ion of compound at 3.44 min was at *m/z* 370.1654, calculated for $C_{21}H_{24}NO_5$ $[M+H]^+$ (370.1654). The molecular formula $C_{21}H_{23}NO_5$ matches an extensive list of alkaloids (CRC, 2009), some of which have previously been isolated from *A. mexicana*. That is the case of cryptopine, allocryptopine (Haisova and Slavik, 1975), and argemexicaines A and B (Chang *et al.*, 2003b).

In order to correctly identify the compounds, subsequent isolation procedures were undertaken, including Sephadex LH-20 column separation and semi-preparative HPLC. As a result, three compounds were purified from the active fraction AM8_D to be tested *in vitro* against *P. falciparum*: **A1**, **A2**, and **A3**. The fraction **A4** was a mixture of berberine and other compounds. The major compound of this mixture corresponded to the one with molecular formula $C_{21}H_{24}NO_4^+$ or $C_{21}H_{23}NO_4$. Another compound, **A5**, was isolated from fraction AM_8_C, and was identified as the nucleoside adenosine.

Isolated compounds had their structure elucidated by means of classical spectroscopic methods, such as high resolution mass spectrometry (HRMS) and nuclear magnetic resonance (NMR) experiments: ^1H and ^{13}C NMR, HSQC, HMBC, COSY and NOESY.

III.2.1.1. Structure determination of compound A1

Compound **A1** was obtained as a white amorphous powder from the Sephadex fraction AM 8_D_1. The high resolution mass spectrum ESI-TOF-MS in positive mode provided a pseudo-molecular ion at *m/z* 354.1360 $[M+H]^+$ (Figure 3.6), calculated for $C_{20}H_{20}NO_5$, 354.1341. The deduced molecular formula $C_{20}H_{19}NO_5$ matches that of protopine and further spectral data was used to confirm its identity.

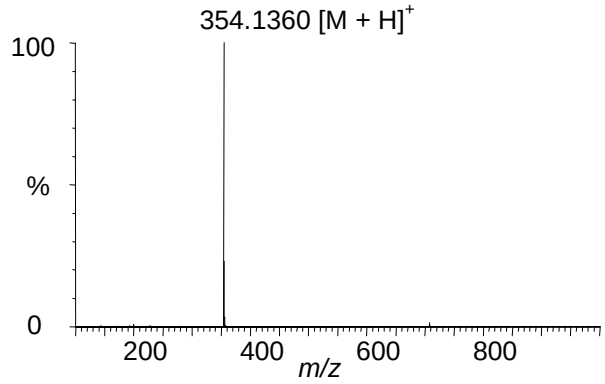

Figure 3.6. High resolution ESI-TOF-MS spectrum in positive mode of compound **A1**.

The ^{1}H NMR spectrum of **A1** in $CDCl_3$ presented a set of broad signals, which is a well known behavior of protopine. The ten-membered ring of the molecule inverts rapidly at room temperature giving rise to broad methylene signals. One of the solutions to get sharp signals is to use temperature modulated NMR experiments (Chang *et al.*, 2003b).

The ^{1}H NMR spectrum of **A1** at 70 °C in pyridine-d_5 is shown in Figure 3.7. The structure of the compound and its main HMBC correlations are presented in Figure 3.8 with the HMBC spectrum depicted in Appendix 2.

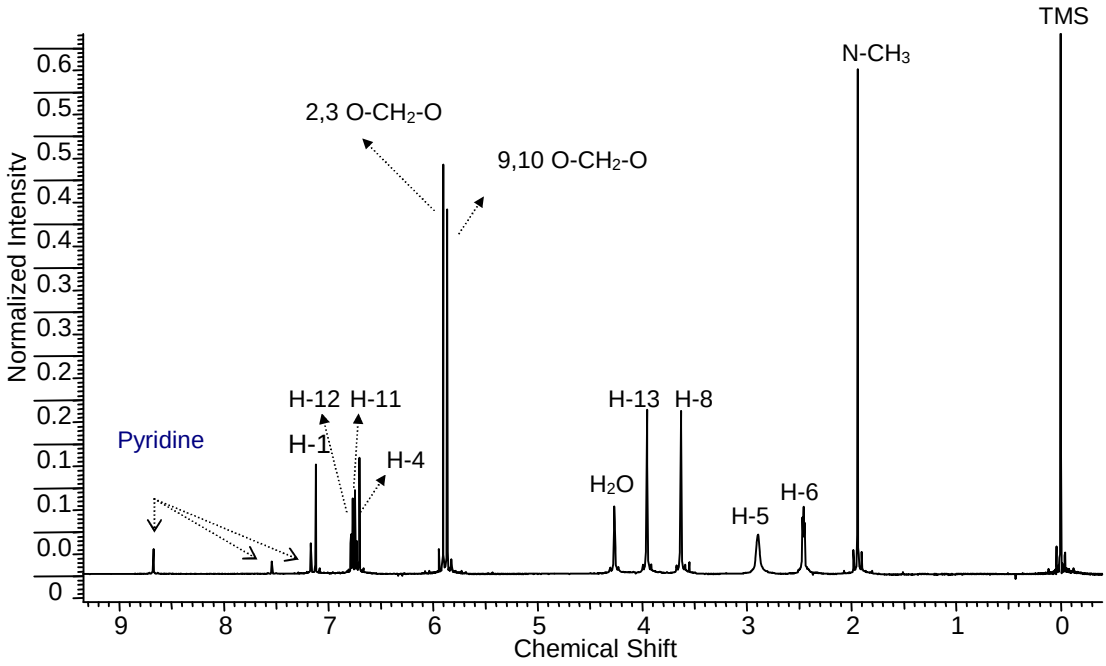

Figure 3.7. ^{1}H NMR spectrum of compound **A1** (500 MHz, 70 °C, pyridine-d_5).

Both the aromatic proton at δ_H 6.71 (H-4) and the methylene protons at δ_H 5.90 correlated with the carbon at δ_C 146.9 (C-2) in the HMBC spectrum, determining that the ^{1}H signal at 5.90 ppm corresponded to the methylene dioxy group between C-2 and C-3. The aromatic proton at δ_H 7.12 coupled with the carbon at δ_C 148.7 (C-3) and the carbonyl at δ_C 194.8 indicating that the carbonyl group was in position 14.

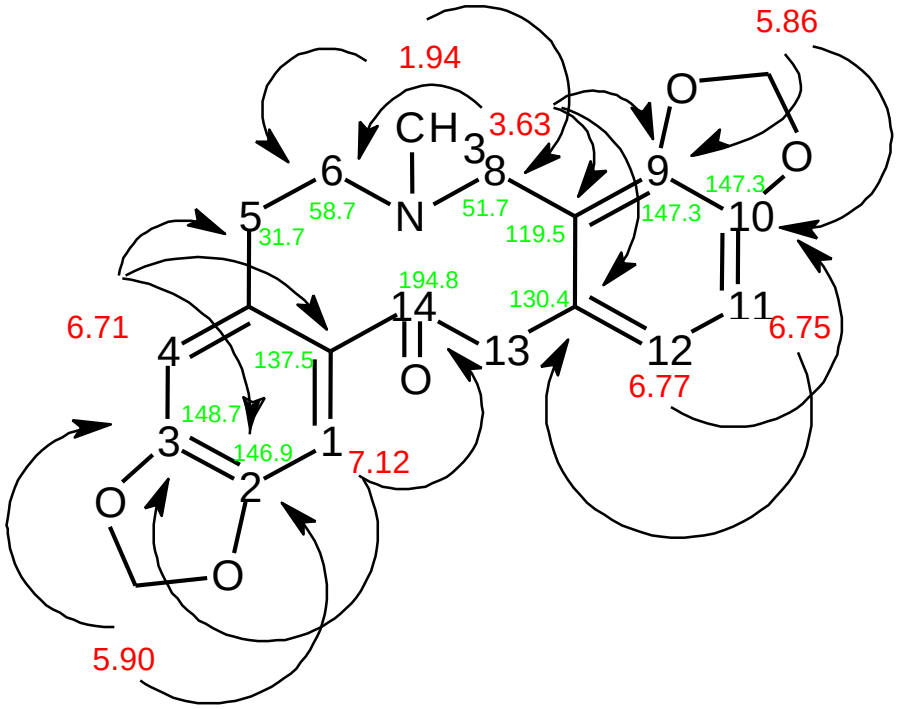

Figure 3.8. Structure and main HMBC correlations for compound **A1**. Chemical shifts are presented in ppm (green: ^{13}C, red: ^{1}H).

Although the coupling between protons at δ_H 2.89 and 2.46 (H-5 and H-6, respectively) could not be seen in the ^{1}H NMR spectrum, their coupling clearly appeared in the COSY spectrum (Figure 3.9).

Compound **A1** was confirmed to be protopine, a protopine-type alkaloid already isolated from *A. mexicana* extracts (Tripathi *et al.*, 1999). This is the first report of the isolation of protopine directly from the traditional decoction of the plant.

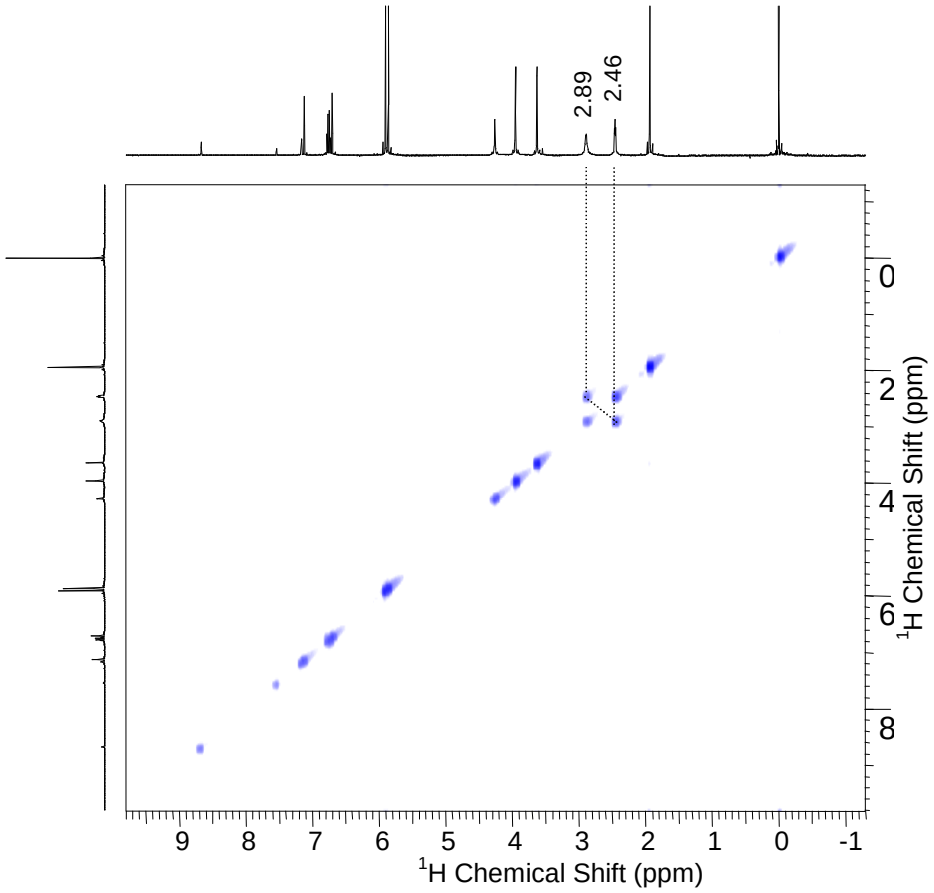

Figure 3.9. COSY spectrum of **A1** (500 MHz, 70 °C, pyridine-d_5).

III.2.1.2. Structure determination of compound A2

Compound **A2** was obtained as a white amorphous powder from the Sephadex fraction AM 8_D_1. The high resolution mass spectrum ESI-TOF-MS in positive mode provided a pseudo-molecular ion at *m/z* 370.1635 $[M+H]^+$(Figure 3.10), calculated for $C_{21}H_{24}NO_5$, 370.1654.

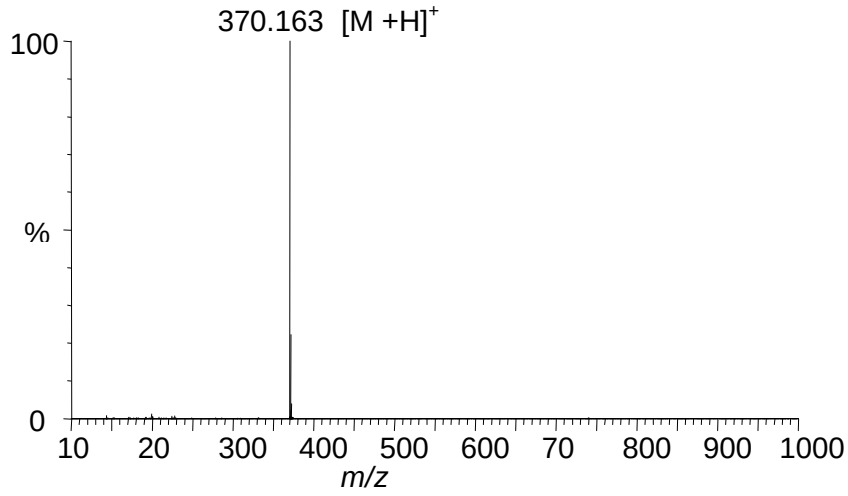

Figure 3.10. High resolution ESI-TOF-MS spectrum in positive mode of compound **A2**.

The ^{1}H NMR spectrum of **A2** was conducted in $CDCl_3$, where broad singlets could be observed at δ_H 2.54, 3.00, 3.18, 3.39 and 4.25 (Figure 3.11). The coupling constants of these signals were not visible and the observation of coupling in the 2D spectra was not possible for some of these signals. These effects have previously been observed for protopine-type alkaloids, due to the various conformations generated by different transannular interactions (Chang *et al.*, 2003b). In the case of argemexicaines A and B, these authors used thermo-modulated NMR at 70 °C in pyridine-d_5 . These conditions were thus considered for the NMR experiments of **A2**.

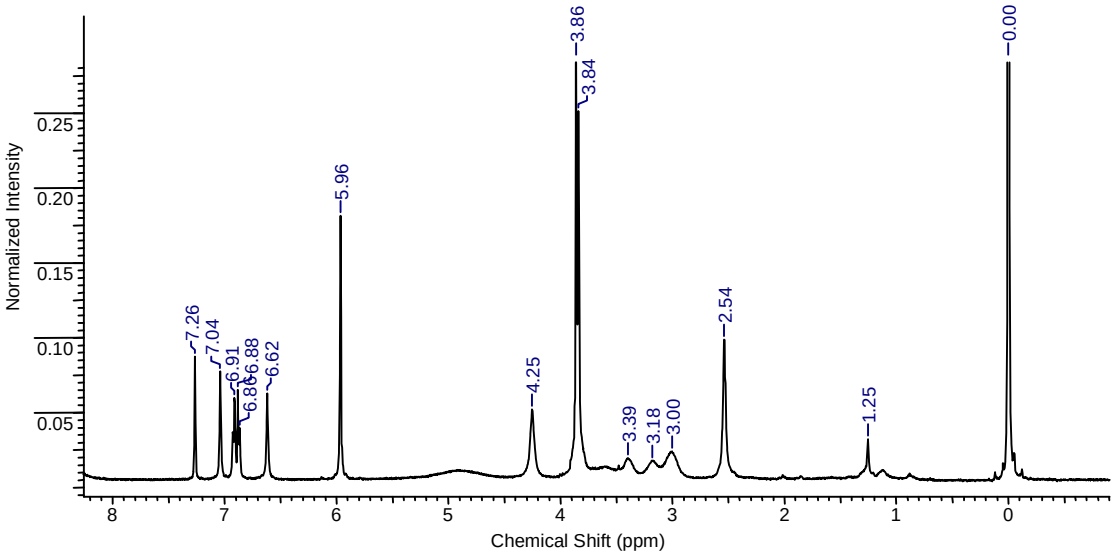

Figure 3.11. ^{1}H NMR spectrum of compound **A2** (500 MHz, 25 °C, $CDCl_3$).

The NMR spectrum of compound **A2** in pyridine-d_5 is presented in Figure 3.12, where an amelioration of resolution could be observed.

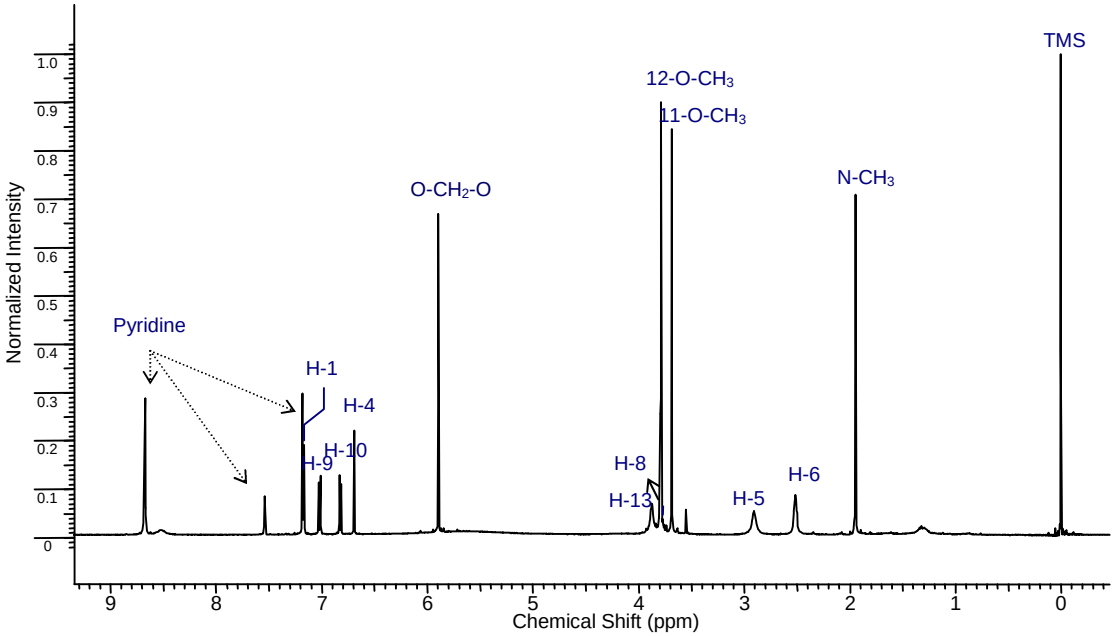

Figure 3.12. ^{1}H NMR spectrum of compound **A2** (500 MHz, 70 °C, pyridine-d_5).

The ^{1}H NMR shifts observed for **A2** were very similar to those of argemexicaines A and B previously published (Chang *et al.*, 2003). Considering that both of these protopine alkaloids have the same exact mass, the determination of compound **A2** was not possible on the basis of its ^{1}H NMR signals, only. Moreover, a comparison of the ^{1}H shifts of **A2** and argemexicaines A and B shows that all three compounds have signals slightly different from each other. (Table 3.3). The structures of argemexicaines A and B are presented in Figure 3.13.

The analysis of the 2D NMR spectra of **A2** showed that its structure differed from that of argemexicaine A on the position of methoxyl groups. In **A2** the methoxyl groups are at C-9 and C-10, instead of C-11 and C-12. The structure and main HMBC correlations for compound **A2** are presented in Figure 3.14, while its HMBC spectrum is shown in Appendix 3.

Table 3.3. ^{1}H NMR assignments of compound **A2** compared to argemexicaines A and B of the literature.

	δ_H (multiplicity, *J* in Hz)		
N*	**A2**[a]	Argemexicaine A[b]	Argemexicaine B[b]
1	7.17 (s)	7.20 (s)	
3			6.86 (d, 8.0)
4	6.69 (s)	6.72 (s)	6.79 (d, 8.0)
5	2.91 (brs)	3.01 (brs)	3.05 (brs)
6	2.52 (brs)	2.80 (brs)	2.73 (brs)
8	3.80 (s)	3.93 (s)	3.86 (s)
9		6.91 (d, 8.2)	6.87 (s)
10		7.03 (d, 8.2)	
11	6.83 (d, 8.3)		
12	7.03 (d, 8.3)		7.39 (s)
13	3.87 (s)	3.99 (s)	3.72 (s)
O-CH_3	3.68 (s)	3.79 (s)	3.83 (s)
O-CH_3	3.79 (s)	3.87 (s)	3.85 (s)
N-CH_3	1.95 (s)	2.18 (s)	2.14 (s)
O-CH_2-O	5.90 (s)	5.93 (s)	5.92 (s)

[a]500 MHz, 70 °C, pyridine-d_5; [b]400 MHz, 70 °C, pyridine-d_5 (Chang *et al.*, 2003). *Carbon numbering according to cited literature.

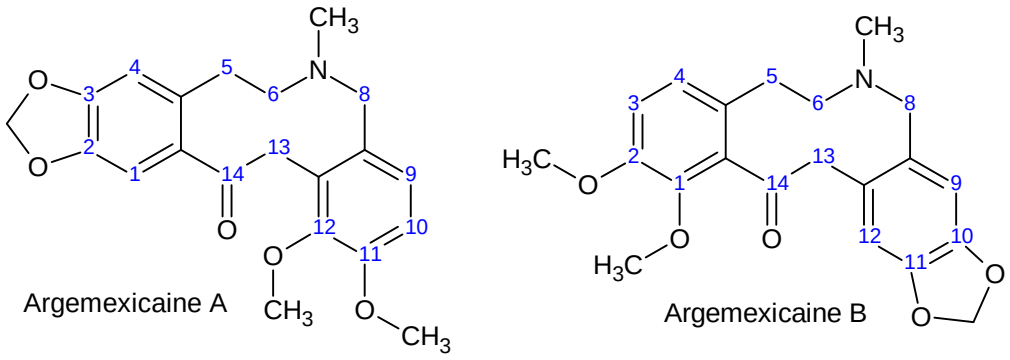

Figure 3.13. Structures of the protopine-type alkaloids: argemexicaines A and B.

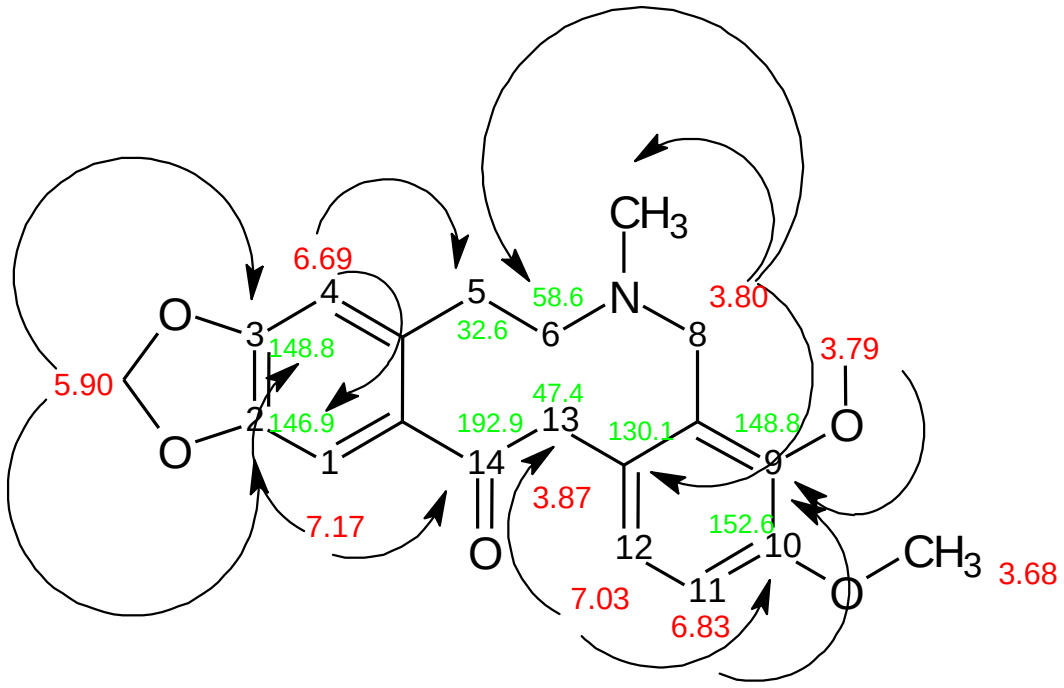

Figure 3.14. Structure and main HMBC correlations for compound **A2**. Chemical shifts are presented in ppm (green: ^{13}C, red: ^{1}H).

Both the aromatic proton at δ_H 6.69 (H-4) and the methylene protons at δ_H 5.90 correlated with the carbon at δ_C 146.9 (C-2) in the HMBC spectrum, determining that the ^{1}H signal at 5.90 ppm corresponded to the methylene dioxy group between C-2 and C-3. The aromatic proton at δ_H 7.17 coupled with the carbon at δ_C 148.8 (C-3) and the carbonyl at δ_C 192.9 indicating that the carbonyl group was in position 14. The methoxylation at C-9 and C-10 differentiated this molecule from argemexicaine A (Figure 3.13). It is interesting to notice that the in the case of **A2**, proton signals at δ_H 3.80 (H-8) and 2.52 (H-6) were highfield shifted from the values obtained for argemexicaine A at δ_H 3.93 (H-8) and 2.80 (H-6) (Table 3.3).

Although the coupling between protons at δ_H 2.91 and 2.52 (H-5 and H-6, respectively) could not be seen in the ^{1}H NMR spectrum, their coupling clearly appeared in the COSY spectrum (Figure 3.15).

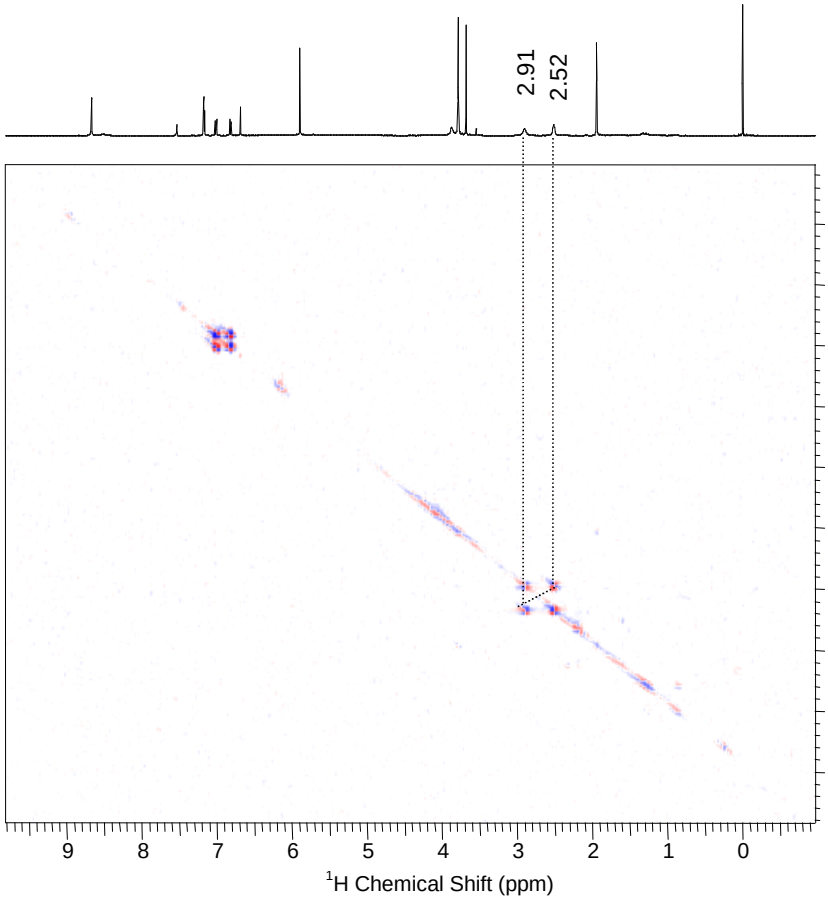

Figure 3.15. COSY spectrum of **A2** (500 MHz, 70 °C, pyridine-d_5).

Based on its spectral data, compound **A2** was identified as allocryptopine. This alkaloid has already been isolated from *A. mexicana* (Haisova and Slavik, 1975) and this is the first report of the isolation of this alkaloid from the traditional decoction.

III.2.1.3. Structure determination of compound A3

Compound **A3** was obtained as a yellow amorphous powder from the Sephadex fraction AM 8_D_2. The high resolution mass spectrum ESI-TOF-MS in positive mode provided a pseudo-molecular ion at *m/z* 336.1222 $[M+H]^+$ (Figure 3.16), calculated for $C_{20}H_{18}NO_4$, 336.1236. This molecular formula corresponds to that of berberine, as well as the color and the UV spectrum of the compound. The identity of **A3** was further confirmed by 1D and 2D NMR analyses.

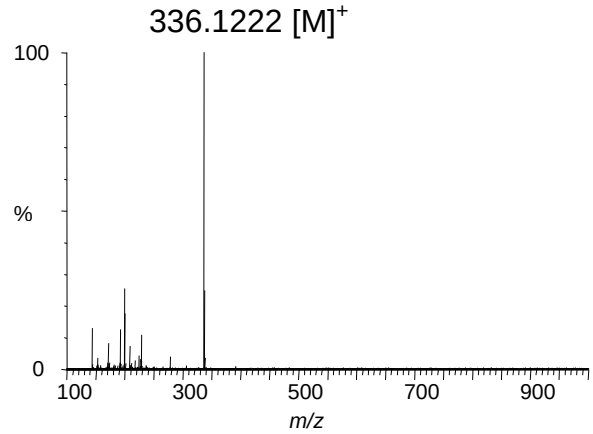

Figure 3.16. High resolution ESI-TOF-MS spectrum in positive mode of compound **A3**.

The ^{1}H NMR spectrum of **A3** in DMSO-d_6 is shown in Figure 3.17. The structure of the compound and its main HMBC correlations are presented in Figure 3.18 with the HMBC spectrum depicted in Appendix 4.

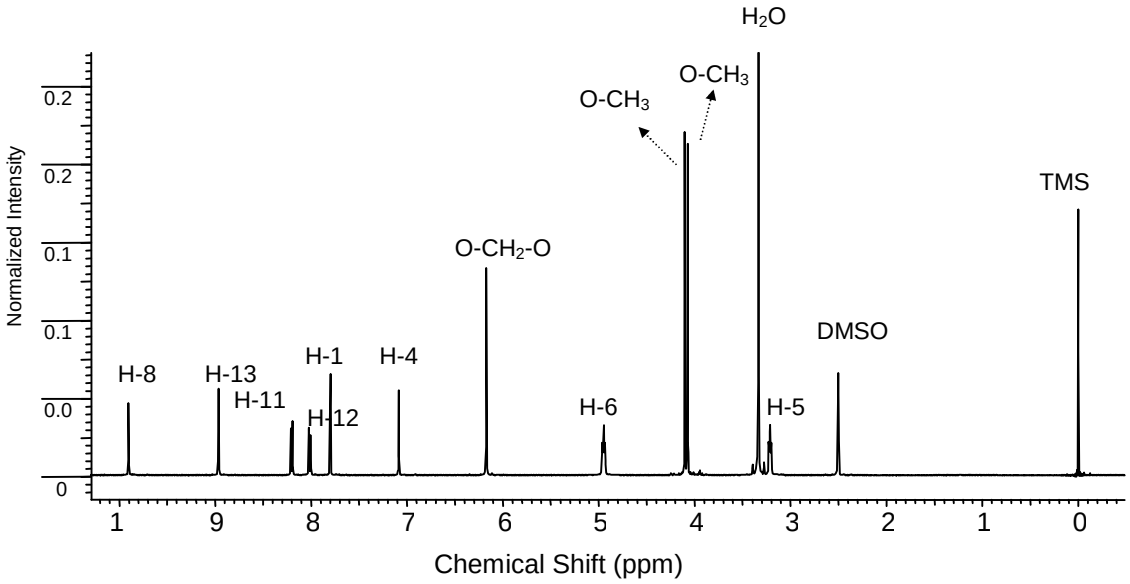

Figure 3.17. ^{1}H NMR spectrum of compound **A3** (500 MHz, 70 °C, DMSO-d_6).

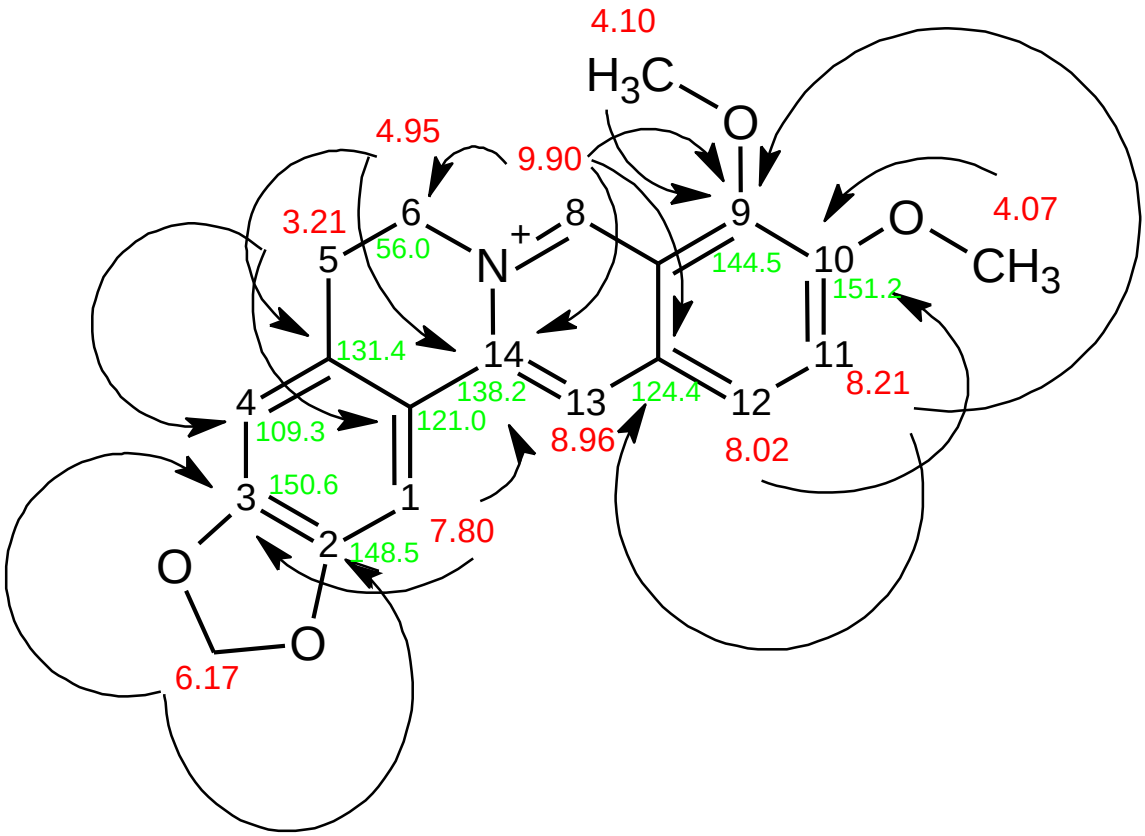

Figure 3.18. Structure and main HMBC correlations for compound **A3**. Chemical shifts are presented in ppm (green: ^{13}C, red: ^{1}H).

Compound **A3** was confirmed to be the alkaloid berberine. This alkaloid has previously been isolated from *A. mexicana* (Haisova and Slavik, 1975) and its presence in the decoction was demonstrated in active clinical batches of the plant (Willcox *et al.*, 2007).

III.2.2. Antiplasmodial activity of isolated compounds

The compounds isolated from the active fraction of *A. mexicana* decoction were tested *in vitro* against *P. falciparum*, and for their *in vitro* cytotoxicity on human fibroblasts and mouse macrophages. Samples were also screened against other parasites such as *Trypanosoma cruzi* and *T. b. brucei*. Results are presented in Table 3.4. The alkaloid sanguinarine, known to be present in *A. mexicana* seeds, but not found in the traditional decoction, was also tested.

Table 3.4. Antiparasitic activity and cytotoxicity of compounds isolated from *A. mexicana* and sanguinarine.

Activity / Compound	Anti-*P. falciparum*[a,b]	Anti-*T. cruzi*[a,c]	Anti-*T. b. brucei*[a,d]	Cytotoxicity[a,e]
	IC_{50} (µg/mL)			
protopine (**A1**)	0.32	>32.00	10.75	>32.00
allocryptopine (**A2**)	1.46	>32.00	10.49	>32.00
berberine (**A3**)	0.32	0.32	1.66	3.20
A4	8.58	7.85	>32.00	24.78
sanguinarine	7.02	7.42	>32.00	16.26

[a]cf Experimental section (V.6.2) for experimental assay description;
[b]IC_{50} >16 µg/mL: inactive; IC_{50} between 2 and 16 µg/mL: moderately active; IC_{50} <2 µg/mL: highly active;
[c]IC_{50} >30 µg/mL: inactive; IC_{50} between 2 and 30 µg/mL: moderately active; IC_{50} <2 µg/mL: highly active;
[d]IC_{50} >5 µg/mL: inactive; IC_{50} between 1 and 5 µg/mL: moderately active; IC_{50} <1 µg/mL: highly active;
[e]tested on human fibroblasts (MRC-5 cell line); IC_{50} >30 µg/mL: not toxic; IC_{50} between 10 and 30 µg/mL: moderately toxic; IC_{50} <10 µg/mL: highly toxic.

All isolated alkaloids were considered highly active against *P. falciparum* and were further investigated for the inhibition of β-hematin formation. These results are presented in Figure 3.19. Interestingly, only allocryptopine was able to significantly inhibit the β-hematin formation reaction *in vitro*. However, these qualitative results presented high standard deviation values and should be carefully considered.

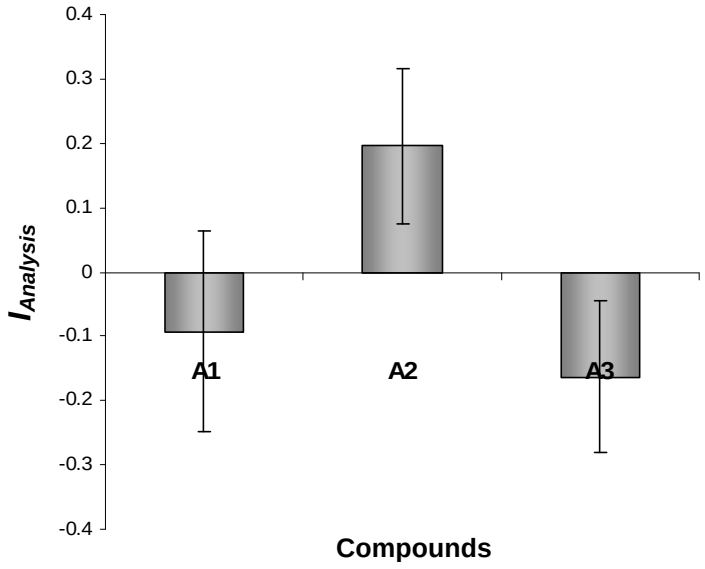

Figure 3.19. Inhibition of β-hematin formation by isolated compounds. Significant inhibition is denoted by positive values for $I_{Analysis}$.

At the beginning of this research project, the first hypothesis raised was that the presence of berberine in the decoction would be the main factor responsible for its clinical effects (Willcox *et al.*, 2007).

As a matter of fact, berberine is a quaternary alkaloid from the group of protoberberines, widely distributed in nature and well known for its antiparasitic activity (Osorio *et al.*, 2008), including activity against the malaria parasite *in vitro* (Iwasa *et al.*, 1998). An extensive review publication on quaternary protoberberine alkaloids highlights that berberine was shown to be a potent *in vitro* inhibitor of both nucleic acid and protein synthesis in *P. falciparum* FCR-3. Furthermore, it has been demonstrated that berberine was able to inhibit *P. falciparum* telomerase (Grycova *et al.*, 2007).

Despite the potent *in vitro* activity of berberine comparable to that of quinine, a study conducted with ten protoberberine alkaloids *in vivo* concluded that none of the studied molecules was able to decrease parasitaemia in *P. berghei*-infected mice (Vennerstrom and Klayman, 1988). In contrast, berberine significantly reduced parasitaemia in *P. chabaudi*-infected mice (McCall *et al.*, 1994).

The poor bioavailability of berberine could be one reason for the difficulties encountered in finding *in vivo* activity. A few studies have been conducted on berberine chloride pharmacokinetics. The salt is used in China for the treatment of heart failure and arrhythmia at doses of 300 mg. It has been demonstrated that a single dose of 300 mg will generate plasma concentrations with clinical efficacy. However, the amount of berberine in plasma is a very small part of that administered (Bao *et al.*, 1997).

Considering the poor bioavailability after oral administration of berberine chloride, it was important to check the concentration of the alkaloid in the traditional decoction of *A. mexicana*. Two analytical methods have been developed and validated in our laboratory for the analysis of the extract: an HPLC/UV method and a TLC semi-quantitative one. Both methods presented coherent results, demonstrating that the simple TLC analytical method could be useful for the quality control in the case of an improved traditional medicine (ITM) in Mali. The found concentrations ranged from 0.018 to 0.023 % among different powdered plant batches (Diop, 2006).

Nevertheless, the concentration of berberine in the traditional preparation seemed to be too low to explain its clinical effects. If one considers that patients were self-administered an average volume of decoction corresponding to 100 g of plant in 1 L decoction, the amount of berberine consumed would be ca. 20 mg.

According to the results presented in Table 3.4, protopine and allocryptopine would be better candidates as the compounds responsible for the clinical antimalarial activity of *A. mexicana* traditional preparation. They did not present any cytotoxicity on human fibroblasts and were shown to be highly specifically active against the malaria parasite when compared to other parasites.

Thus, a rapid quantitative NMR method was developed in order to check the amount of allocryptopine and protopine in clinical batches of the plant extracted as described for the traditional preparation.

III.2.3. Quantitative NMR analysis of active alkaloids in *A. mexicana* decoction

An NMR method was chosen to rapidly access information on the amount of active alkaloids in the traditional decoction. By this means, the three alkaloids allocryptopine, berberine and protopine could be quantified in the same spectrum. This

is possible because the NMR response can be made the same for all components, contrary to HPLC/UV or MS methods. In fact, the strength of the NMR signal is proportional to the number of nuclei, thus the number of molecules, present in the analyzed sample. Moreover, in quantitative NMR analysis, a universal reference standard can be used for the analysis of most materials. As a consequence, a quantitative determination of a specific compound does not require pure samples for calibration, which is of great interest for the determination of natural products not always available as standard compounds (Maniara *et al.*, 1998).

Preliminary analyses were conducted to find the best ^{1}H NMR conditions (solvent and temperature) for allocryptopine, protopine and berberine. Allocryptopine and protopine are alkaloids of the protopine-type, presenting bad resolution in the region of the methylene protons of the ten-membered ring, especially at room temperature. For this reason, the chosen signals were those corresponding to the methylene dioxide protons of each molecule.

A comparison of spectra for the three alkaloids in pyridine-d_5 at 42 °C is shown in Figure 3.20. Under this conditions, one of the methylene dioxide signals of protopine overlaps with that of allocryptopine (δ_H 5.95). Since protopine has a second methylene dioxide signal at δ_H 5.90, this one could be considered for quantification and its integral value was subtracted from that at δ_H 5.95, for the quantification of allocryptopine.

The second step of the method development was to check the spectrum of the sample prepared from the traditional decoction. Two different extraction methods were analyzed: 1) liquid-solid extraction, using methanol and the freeze-dried decoction, and 2) CH_2Cl_2 partition from the filtered decoction at room temperature. The first extraction method was the same used in the HPLC/UV determination of berberine previously cited (Diop, 2006). However, when sample was recovered in 0.6 mL pyridine-d_5, solubility problems arose. On the other hand, the second method provided a spectrum where all signals could be observed at a signal/noise ratio higher than 20 (Figure 3.21). The second extraction method was then chosen for the ^{1}H NMR quantification of the alkaloids in the decoction.

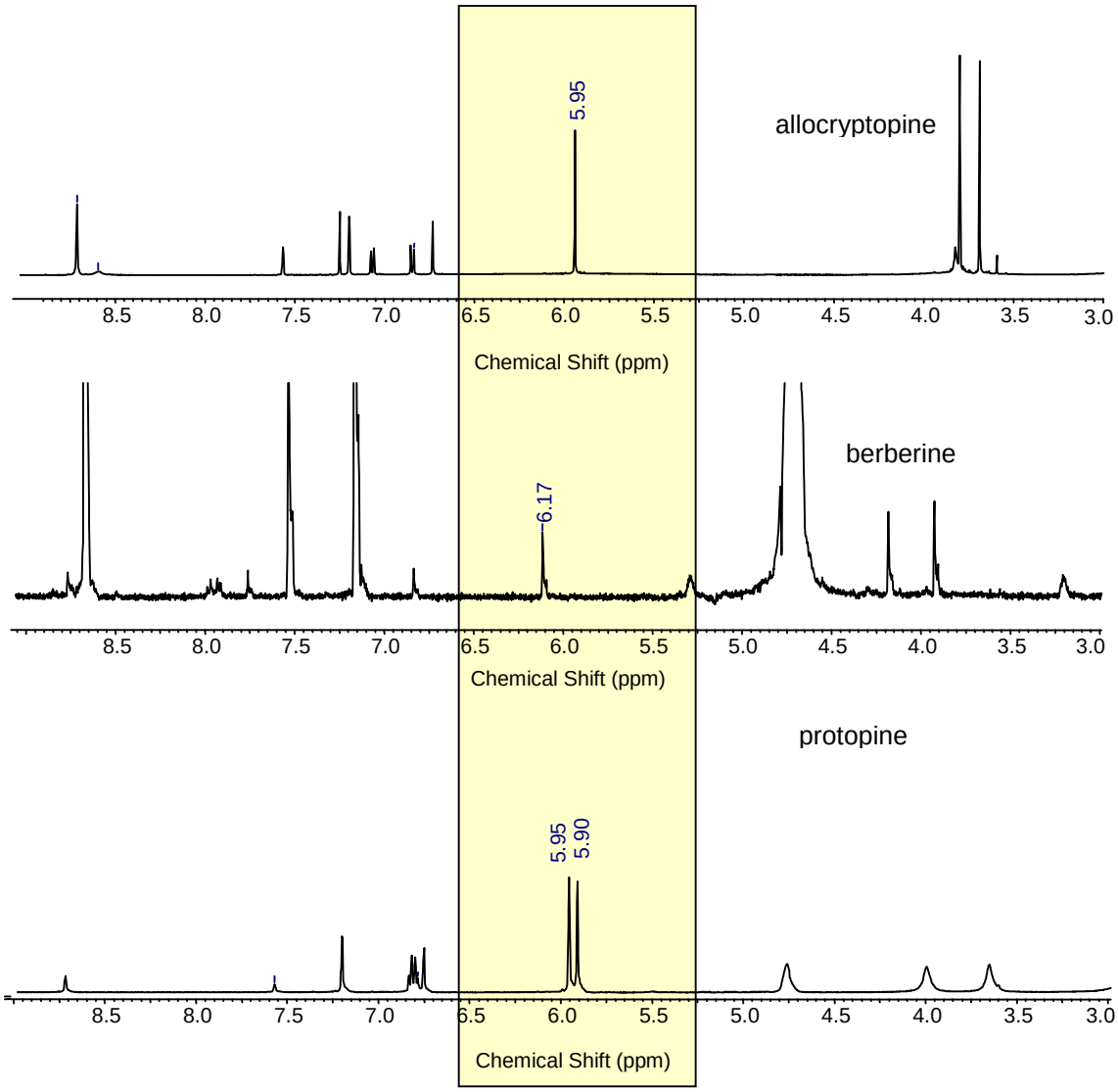

Figure 3.20. Comparative ^{1}H NMR spectra of allocryptopine, berberine and protopine (500 MHz, 42 °C, pyridine-d_5).

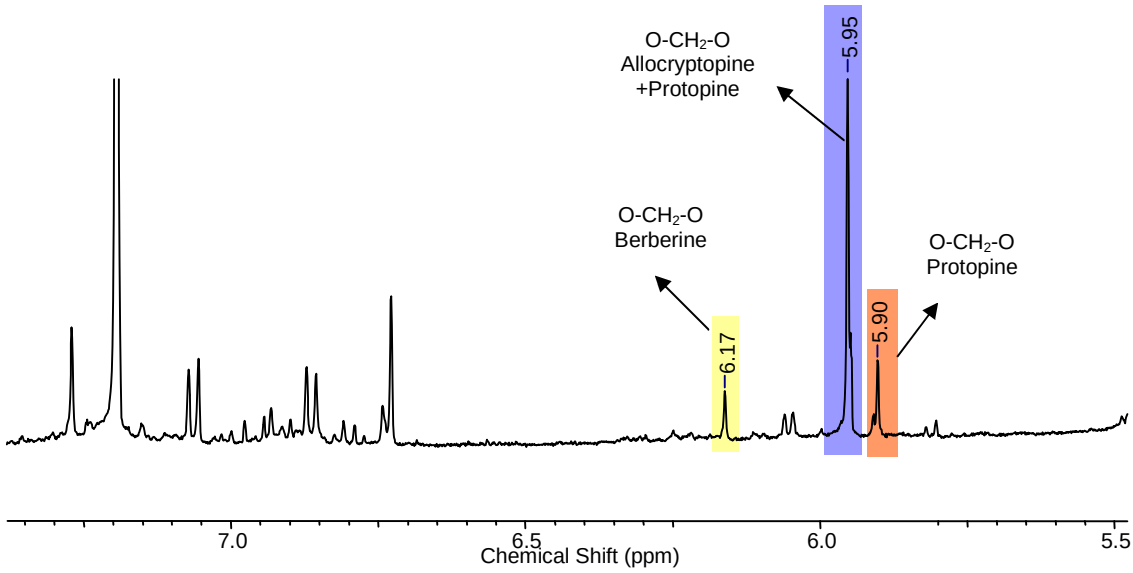

Figure 3.21. ^{1}H NMR spectrum of an analytical sample obtained using the extraction method 2 for the *A. mexicana* decoction (500 MHz, 70 °C, pyridine-d_5).

The third step in the method development was to demonstrate the linearity and accuracy of the method through a calibration curve established for allocryptopine. The calibration curve was obtained from the ratio between the area under the signal selected for the compound and that for anthracene (internal standard) corrected by their MW ratio. A calibration curve for allocryptopine was obtained in the range of 0.6 – 5.5 mg/mL in triplicate. The values of integrals and calculated concentrations are presented in Table 3.5, and the calibration curve is presented in Figure 3.22. The R^2 value was as high as 0.9999.

Table 3.5. Integrals and calculated concentration values in triplicate for the calibration curve of allocryptoine.

		Concentration (mg/mL)	Absolute integral	Calculated concentration (mg/mL)
Curve 1	Anthracene	5.3	14.4597	
		2.4	9.48637	
		1.6	6.31743	
		0.8	9.27064	
		0.5	4.62616	
	Allocryptopine	5.5	7.23496	5.49
		2.5	4.73448	2.48
		1.7	3.18654	1.67
		0.85	4.57808	0.82
		0.6	2.29315	0.51
Curve 2	Anthracene	5.3	9.512961	
		2.4	6.241033	
		1.6	4.156204	
		0.8	6.099105	
		0.5	3.043526	
	Allocryptopine	5.5	4.823307	5.57
		2.5	3.15632	2.51
		1.7	2.12436	1.69
		0.85	3.052053	0.83
		0.6	1.528767	0.52
Curve 3	Anthracene	5.3	6.384537	
		2.4	4.188613	
		1.6	2.789399	
		0.8	4.093359	
		0.5	2.042635	
	Allocryptopine	5.5	3.215538	5.53
		2.5	2.104213	2.50
		1.7	1.41624	1.68
		0.85	2.034702	0.82
		0.6	1.019178	0.52

		Average	SD
Average curve	**Calculated concentration (mg/mL)**	5.53	0.0366
		2.50	0.0165
		1.68	0.0111
		0.82	0.0054
		0.52	0.0034

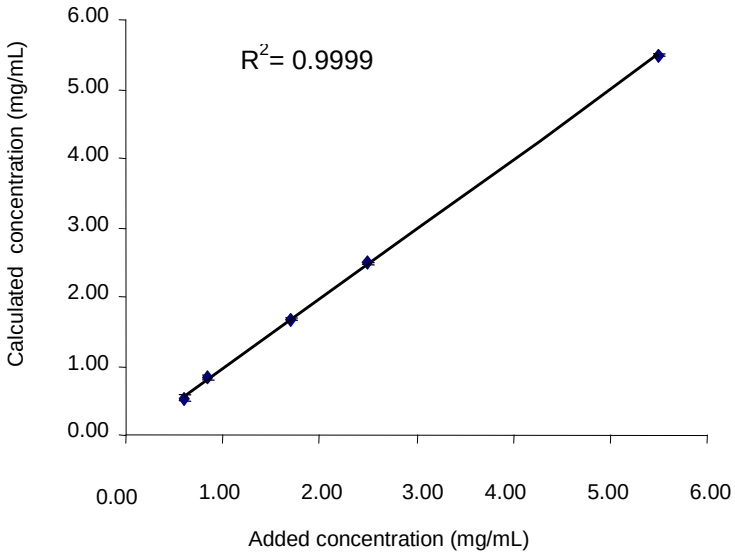

Figure 3.22. Calibration curve of allocryptopine.

In fact, calibration curves are not necessary in the quantitative NMR determination of compounds because the absolute integral under a peak is always proportional to the number of nuclei responsible for the signal. Thus, the area of a specific signal can be used to establish the concentration of a compound provided that the signal area of an internal standard is obtained at known concentrations.

The concentrations of allocryptopine, protopine and berberine were finally measured in two available clinical batches of *A. mexicana*. A CH_2Cl_2 partition was conducted in triplicate aliquots of 10.00 mL of decoction and the concentrations in the traditional preparation (mg/mL) were calculated from the absolute integral values of signal selected for each alkaloid and that of the internal standard. Table 3.6 presents the results expressed in terms of concentration (mg/mL) in tea as well as % (w/w) in the plant, which was calculated by using the initial mass of plant weighed and the total volume of decoction obtained.

The concentration of berberine was demonstrated to be similar between both batches when assessed by QNMR. The concentration of allocryptopine and protopine varied between both clinical batches. But the concentration of these protopine-type alkaloids together was higher than that of berberine in both clinical batches, which

corroborates the hypothesis that they are the main alkaloids responsible for the activity, as discussed before.

Table 3.6. Calculated concentrations of allocryptopine, protopine and berberine in the decoction of clinical batches of *A. mexicana* leaves obtained by the QNMR method.

Batch	Compound	Concentration in tea (mg/mL)*	% in plant (w/w)*	CV (%)
AM 8	Allocryptopine	0.11 ± 0.01	0.47 ± 0.03	5.63
	Protopine	0.12 ± 0.02	0.51 ± 0.02	3.84
	Berberine	0.11 ±0.01	0.48 ± 0.03	5.99
AM 11	Allocryptopine	0.18 ± 0.01	1.10 ± 0.07	6.57
	Protopine	0.06 ± 0.00	0.39 ± 0.01	3.86
	Berberine	0.07 ± 0.01	0.43 ± 0.04	8.37

* Average ± SD

The HPLC/UV and TLC methods previously developed for the quantification of berberine in the Mexican poppy decoction had demonstrated that the amount of this alkaloid in a non-clinical batch of *A. mexicana* leaves (batch AM 3) was 8.9 ± 0.3 µg/mL in the decoction. In this specific case, the analyzed sample was a solution of the freeze-dried decoction in methanol at 20 mg/L (Diop, 2006). This result is lower than that found by QNMR in clinical batches AM 8 and AM 11.

One possible explanation is the difference in the extraction method. In the HPLC/UV and TLC methods, the decoction was freeze-dried and the resulting powder diluted in MeOH at 20 mg/mL and centrifuged at 13000 rpm prior to analysis. It is important to notice that a precipitate was formed and not considered in quantification. When the same extraction method was applied to the QNMR method, the freeze-dried extract was not soluble at 20 mg/mL in the suitable solvent (pyridine-d_5) and at 0.5 mg/mL the ^{1}H NMR signals of interest could not be detected at a good signal/noise ratio. It was then important to develop an extraction method to get an alkaloid-enriched fraction. This could be achieved by CH_2Cl_2 partition directly from the decoction followed by centrifugation at 5000 rpm. The fact that the decoction was immediately cooled to room temperature and partitioned in the organic solvent, without a freeze-drying step, may have increased the recovery of alkaloids. Nevertheless, recovery data were

obtained neither for the previous method HPLC/UV and TLC methods nor in the QNMR method.

Since one of the specific goals related to *A. mexicana* investigation was to find a simple and low-cost semi-quantitative method for the quality control of an ITM in Mali, the semi-quantitative TLC method previously developed was applied to batches AM 8 and AM 11 and to an additional clinical batch AM 9, using the same extraction method as the one for the QNMR method. The results of different methods are critically compared and discussed in the next topic.

III.2.4. Semi-quantitative TLC analysis of berberine in *A. mexicana* decoction

The semi-quantitative TLC method for the determination of berberine relies on the fluorescence of this alkaloid at 366 nm. The fluorescent spot of berberine at this wavelength can be detected at low concentrations and can have its density measured by software assisted image treatment (Diop, 2006). The method was applied to the analysis of clinical batches AM 8, AM 9 and AM 11, using the same extraction method as in the QNMR method. It is important to notice that a calibration was necessary for each analyzed plate. Density of spots was calculated with the public domain software ImageJ®[1]. Plate images and calibration curves are presented in the annexes. Sample concentrations were calculated using the linear equation provided by the calibration curve. The results obtained for each clinical batch is summarized in Table 3.7.

Table 3.7. Calculated concentrations of berberine in the decoction of clinical batches of *A. mexicana* leaves obtained by the semi-quantitative TLC method.

Batch	Concentration in tea (µg/mL)*	% in plant (w/w)*	CV (%)
AM 8	18.85 ± 0.83	0.02 ± 0.002	4.39
AM 9	17.57 ± 1.12	0.03 ± 0.002	6.37
AM 11	19.54 ± 0.88	0.03 ± 0.001	4.48

* Average ± SD

[1] Available on-line at: http://rsb.info.nih.gov.ij/download.html.

Using the semi-quantitative TLC method, the encountered concentration in clinical batches ranged from 17.57 µg/mL to 19.54 µg/mL which was very similar to the value previously obtained for the non-clinical batch AM 3 (Diop, 2006). However, the compoarison of NMR and TLC techniques using the same extraction method resulted in much higher concentration using the quantitative NMR method. Hence, it was important to determine the recovery of the TLC method in order to determine if it is high enough to be considered as a useful quality control tool.

A recovery assay for the semi-quantitative TLC method was designed by spiking the AM 8 decoction with berberine at three concentration levels in triplicate. It is important to notice that calibration solutions, original (not spiked) sample in triplicate, and spiked samples in triplicate had to be spotted on the same plate for recovery calculations. Plate images and calibration curves are presented in the annexes. The results obtained in the recovery assay are summarized in Table 3.8.

Table 3.8. Recovery of the semi-quantitative TLC method for the determination of berberine using spiked decoction of *A. mexicana* leaves (batch AM 8) at three concentration levels.

Added berberine concentration (µg/mL)	Concentration in not spiked AM 8 decoction (mg/mL)*	Concentration in spiked AM 8 decoction (mg/mL)*	Recovered concentration (µg/mL)**	Recovery (%)
10	18.85 ± 0.83	19.13 ± 1.22	0.28	2.8
20	20.42 ± 0.77	21.28 ± 1.12	0.86	4.3
30	23.98 ± 0.39	24.66 ± 0.34	0.68	2.3

* Average ± SD; ** Difference between average values.

Surprisingly, the recovery was extremely low (2.3 – 2.8%) and the calculated concentrations in spiked samples were not significantly different from those in the not spiked sample. This may indicate that the method achieved its superior limit of detection and that concentrations higher than ca. 20 µg/mL would not be detected. This superior limit is probably determined by the saturation of berberine spot detected by image treatment. In fact, Diop (2006) had demonstrated that when berberine was spotted at amounts higher than 500 ng on the plate, the quantification was not trustful due to image saturation events. This may explain the similar concentration values obtained for all clinical batches using the TLC method. The amount of berberine present in the spotted sample was probably much higher with the CH_2Cl_2 extraction

method than with the previously tested liquid-solid extraction method in methanol. Hence, the CH_2Cl_2 extraction is recommended for the recovery and concentration of alkaloids from the decoction prior to quantitative analyses. Nevertheless, the obtained extract must be successively diluted and the superior limit for the spotted amount of extract must be determined to validate this method.

The semi-quantitative TLC method for the determination of berberine in decoctions of *A. mexicana* seems to be a good choice as a quality control method for the development of an effective ITM in Mali and further validation of the method is worthwhile. However, the concentration of berberine does not seem to be the parameter responsible for clinical efficacy as discussed before. An alternative parameter would be the determination of protopine.

Protopine showed very weak fluorescence on TLC plates observed at 366 nm as well as an R_f value distinct from that of berberine as shown in Figure 3.23. On the other hand, allocryptopine presented an R_f value too close to berberine, overlapping to berberine in the CH_2Cl_2 fraction of *A. mexicana* decoction. Therefore, the development and validation of a semi-quantitative TLC method for the quantification of protopine in *A. mexicana* decoctions is a promising option for the quality control of this traditional preparation.

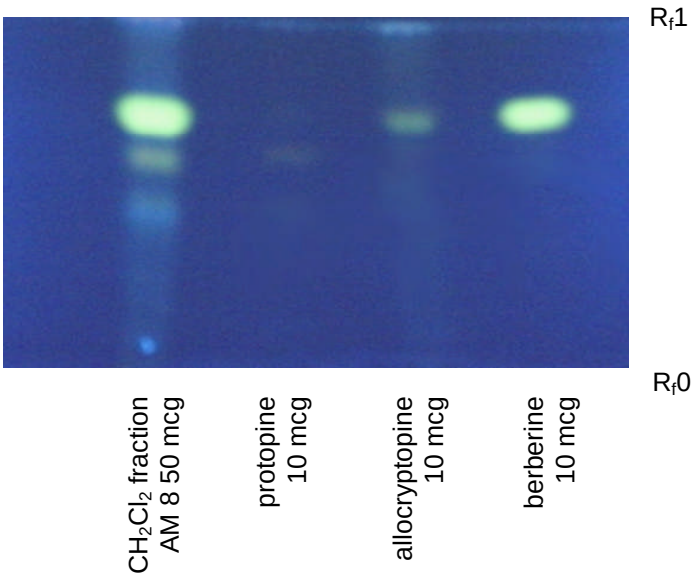

Figure 3.23. TLC of the CH_2Cl_2 fraction of the clinical batch AM 8 of *A. mexicana*, allocryptopine, protopine and berberine. UV detection at 366 nm. TLC system: formic acid/water/ethyl acetate (1:2:7).

III.3. Bioguided phytochemical investigation of *Licania octandra*

The dried hydroalcoholic extract of *L. octandra* leaves was first analyzed by HPLC/UV/MS using electrospray ionization in the negative mode. This preliminary analysis was able to detect only two compounds with clear UV spectra. However other compounds could be detected in the total ion chromatogram (TIC). The spectral data suggested the presence of flavonoids. Thus, a liquid-liquid extraction (LLE) was used in an attempt to concentrate these compounds and get useful on-line data for dereplication of flavonoids. Successive partition provided four major fractions: hexane fraction (HF), ethyl acetate fraction (AcF), buthanol fraction (BF), and a residual aqueous fraction (AqF). All fractions as well as the crude extract were tested against *P. falciparum* in vitro and a moderate activity was observed for HF and AcF with IC_{50} values of 12.11 and 9.86 µg/mL, respectively (Table 3.2). Moreover, fraction AcF presented a radical-scavenging activity on TLC plate using the stable free radical diphenylpicrylhydrazyl (DPPH) detection (Cavin *et al.*, 1999). This fraction was then fractionated using CPC to provide 3 flavonoid containing fractions (AcF-A, AcF-B and AcF-C) and a chlorophyll containing fraction recovered after phase inversion (AcF-D). This bioguided fractionation is summarized in Figure 3.24.

III.3.1. Isolation and identification of compounds from the ethyl acetate fraction (AcF) of the hydroalcoholic extract

Three major compounds could be isolated from CPC fractions AcF-A and AcF-C. Fraction AcF-C provided the pure compound **L6**, while fraction AcF-A was purified by semi-preparative HPLC providing compounds **L2** and **L4**. Fraction AcF-B was used for the on-line identification of flavonoids by means of HPLC/UV/MS analysis and post-column derivatization with UV shift reagents. The general fractionation scheme is presented in Figure 3.25.

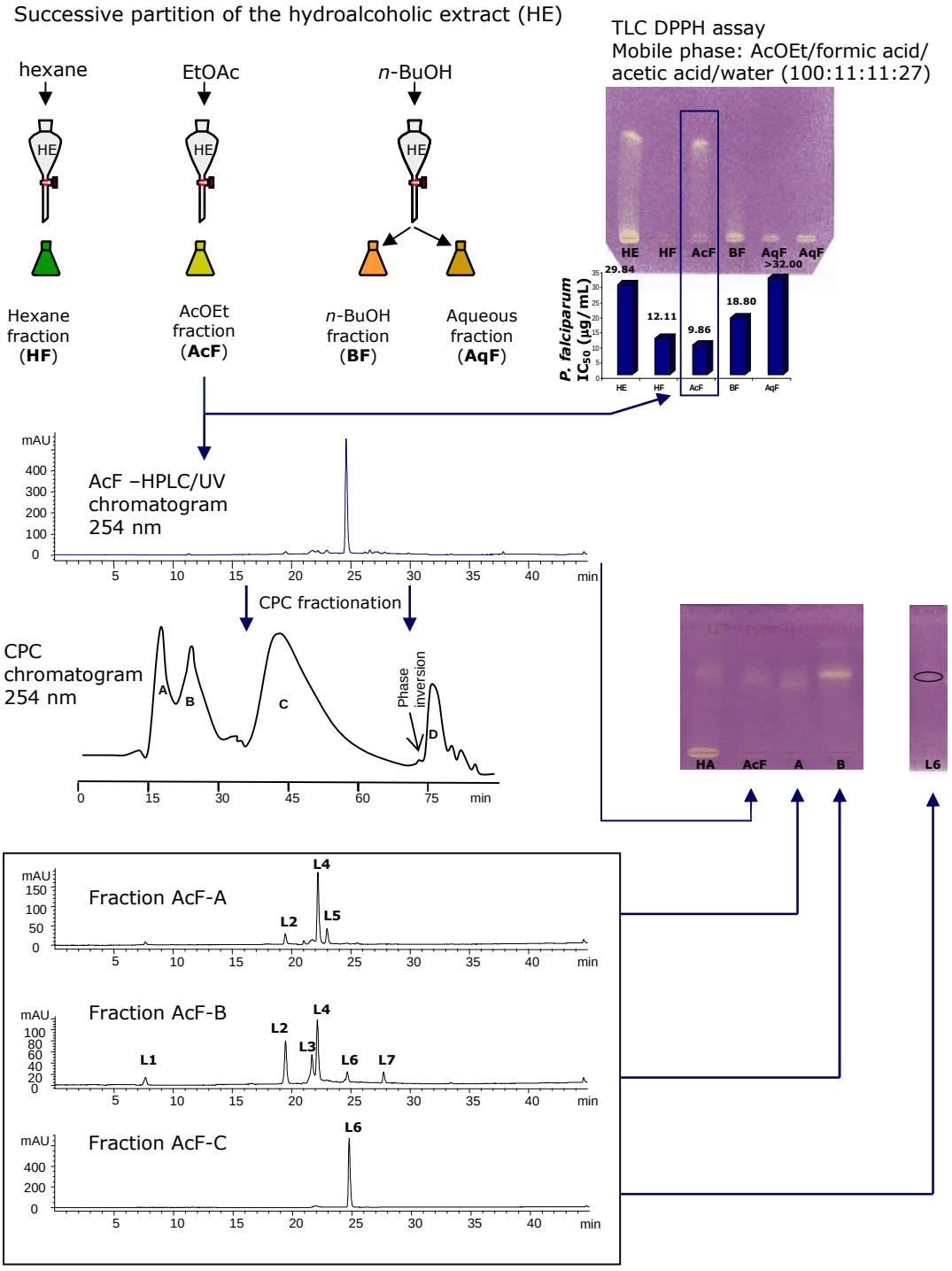

HPLC-UV conditions: MeOH-water (with 0.05% TFA) as mobile phase in gradient mode; C-18 column (4.6 x 250 mm, 5 μm); UV detection at 254 nm. Gradient: from 2% to 100% MeOH in 45 min.

Figure 3.24. Bioguided fractionation of the hydroalcoholic extract of *L. octandra* leaves.

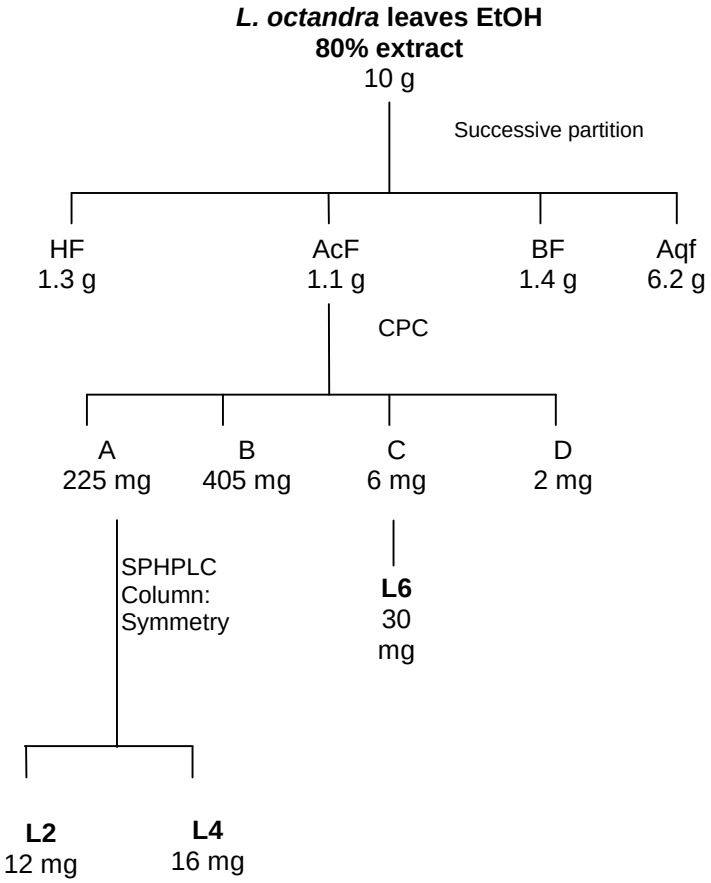

Figure. 3.25. General fractionation scheme of *L. octandra* hydroalcoholic extract.

III.3.1.1. Structure determination of compound L2

Compound **L2** was obtained as a pale green amorphous powder. The high resolution mass spectrum ESI-TOF-MS in negative mode provided a pseudo-molecular ion at *m/z* 435.0914 $[M-H]^-$ (Figure 3.26), calculated for $C_{20}H_{19}O_{11}$, 435.0927.

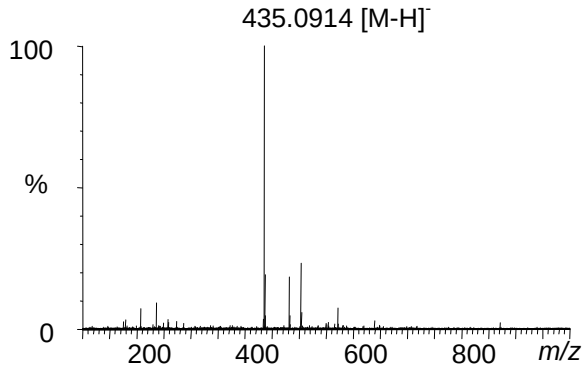

Figure 3.26. High resolution ESI-TOF-MS spectrum in negative mode of compound **L2**.

The UV spectrum of the compound **L2** showed a band II at λ 290 nm and a band I with relative low intensity, appearing as a shoulder at 330 nm, which is characteristic of dihydroflavonols or flavanones (Markham, 1982). The predicted molecular weight of 436 Da corresponds to a heteroside, thus an acid hydrolysis was performed in order to evaluate the UV spectra of the flavonoid and its aglycone before and after addition of UV shift reagents. These results were observed for band II and are described in Table 3.9.

Table 3.9. UV shifts observed for flavonoid **L2** and its aglycone in MeOH and after the addition of shift reagents.

	L2	**L2 aglycone**
Solvent	Band II (nm)	Band II (nm)
MeOH	290	290
Reagent		
NaOMe	+40	+35
NaOAc	+40	+35
$NaOAc/H_3BO_3$	-	-
$AlCl_3/HCl$	+10	+20
$AlCl_3$[a]	-	-

[a]In comparison to $AlCl_3/HCl$; + = bathochromic shift; - = no shift observed

The bathochromic shift observed after addition of NaOAc suggests, in the case of flavanones and dihydroflavonols, the presence of free hydroxyl groups at C-5 and C-7 and the absence of shift after addition of $NaOAc/H_3BO_3$ suggests the absence of *o*-

diOH in ring A (cf general structure of flavonoids, Figure 3.27). However, the position of the sugar substitution could not be determined by the UV spectral analysis and the sugar could be attached to one of the hydroxyl groups in ring B or even at C-3 in the case of a dihydroflavonol.

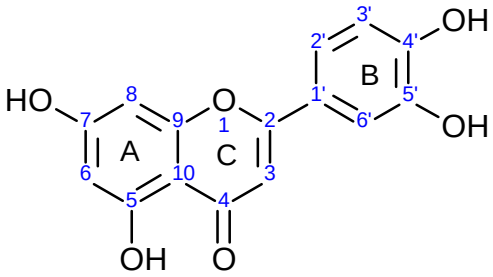

Figure 3.27. General structure for flavonoids.

The mass spectrum ESI-TOF-MS in negative mode of the aglycone provided a pseudo-molecular ion at *m/z* 303.05 $[M-H]^-$. By the difference of molecular weight between the aglycone and the original flavonoid (a loss of ca. 132 Da) the sugar could probably be inferred either as xylose or arabinose. A TLC was then performed with the residual sugar obtained after hydrolysis of the flavonoid and standard sugars arabinose, glucose, rhamnose, xylose, galactose and galacturonic acid. The sugar moiety of **L2** presented a spot at the same retention factor (R_f) as xylose (Figure 3.28).

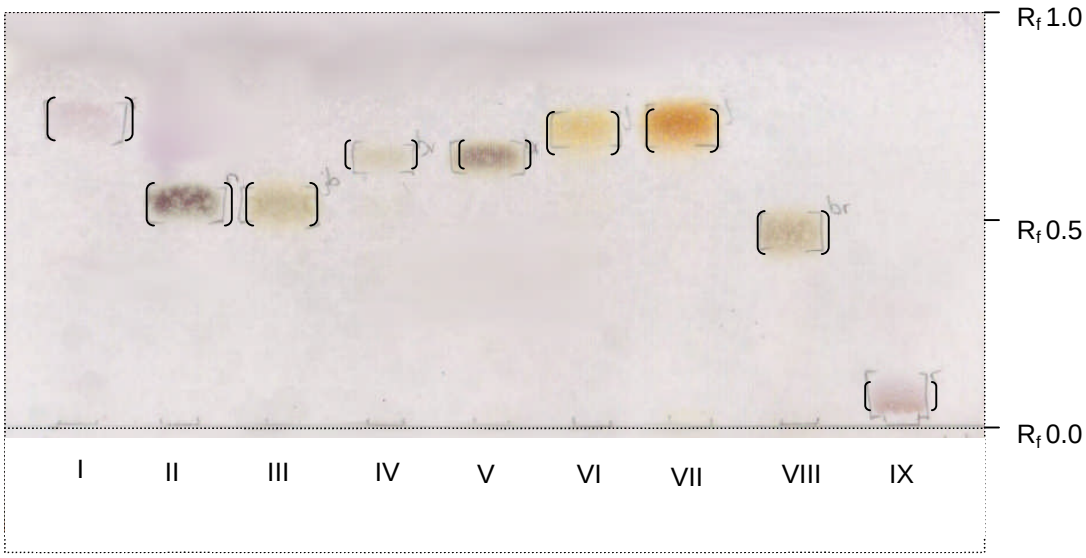

Figure 3.28. TLC for sugar identification using the system isopropanol/water (85 : 15) and Godin reagent for detection, 30 µg of sample were spotted. I: glucuronic acid; II: glucose; III: arabinose; IV: **L2** sugar; V: xylose; VI: **L4** sugar; VII: rhamnose; VIII: galactose; IX: galacturonic acid; R_f: retention factor.

The structure of compound **L2** was determined by the analysis of its ^{1}H, ^{13}C (Table 3.12), COSY, HSQC and HMBC spectral data.

Signals at δ_H 5.91 (d, J=2.5 Hz) and 5.90 (d, J=2.2 Hz) were attributed to H-6 and H-8, respectively. Their coupling constants correspond to the meta-coupling observed in ring A. Signals at δ_H 6.94 (s), 6.81 (d, J=8.4 Hz) and 6.79 (d, J=8.0 Hz) were attributed to H-6', H-2' and H-3', respectively, which corresponds to the ABX system in ring B. Two additional doublets at δ_H 5.19 (d, J=9.8 Hz) and 4.73 (d, J=10.2 Hz) confirmed the dihydroflavonol skeleton and were attributed to H-2 and H-3, respectively. According to data published in the literature (Gao *et al.*, 1990), a coupling constant of 10.3 Hz corresponds to the trans conformation of these protons, which means that there are two possible configurations, either the (+)-trans form (2R,3R) or the (-)-trans form (2S,3S). The configuration was determined to be 2R,3R by the optical rotation measurement obtained for the aglycone after hydrolysis, $[\alpha]_D^{20\,°C}$ = +11.55°.

The connectivity of protons from the sugar moiety could be determined by the correlations observed in the COSY spectrum and the attachment of the sugar to the hydroxyl at C-3 was determined by the correlation observed in the HMBC spectrum between the anomeric proton at δ_H 3.87 and the C-3 at δ_C 76.5 (Figure 3.29). The anomeric proton doublet had a coupling constant of 5.7 Hz characteristic of a β-D-xyloside.

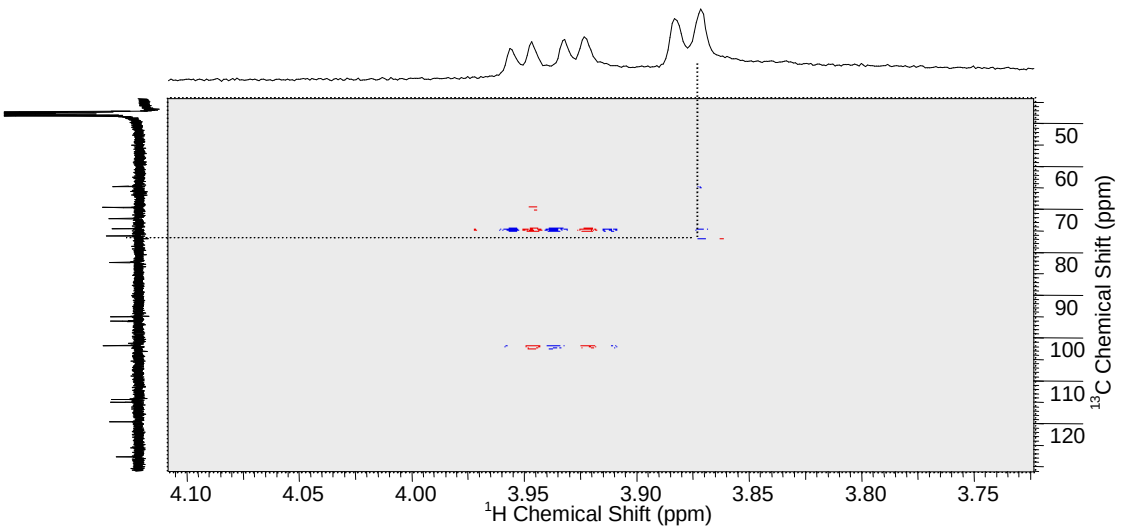

Figure 3.29. HMBC spectrum of compound **L2** (zoom in ^{1}H chemical shift scale from 3.7 to 4.1 ppm; zoom in ^{13}C chemical shift scale from 45 to 130 ppm).

Compound **L2** was identified as (2R,3R)-taxifolin 3-*O*-β-D-xylopyranoside (Figure 3.30).

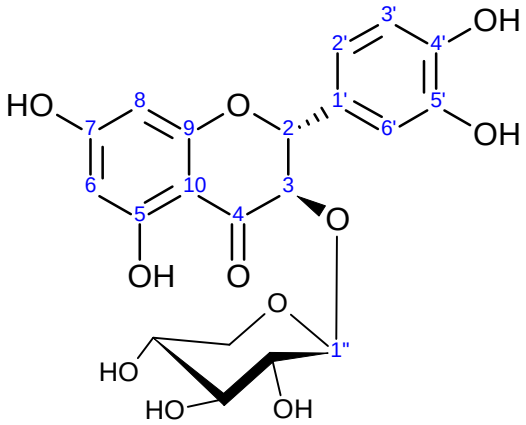

Figure 3.30. Chemical structure of compound **L2**.

III.3.1.2. Structure determination of compound L4

Compound **L4** was obtained as a yellow amorphous powder. The high resolution mass spectrum ESI-TOF-MS in negative mode provided a pseudo-molecular ion at *m/z* 463.0852 $[M-H]^-$ (Figure 3.31), calculated for $C_{21}H_{19}O_{12}$, 463.0877.

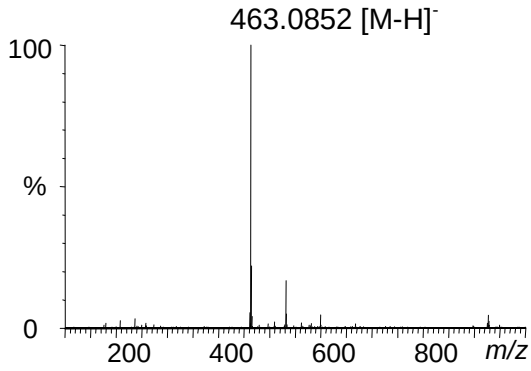

Figure 3.31. High resolution ESI-TOF-MS spectrum in negative mode of compound **L4**.

The UV spectrum of the compound **L4** showed a band II at λ 260 nm and a band I at 355 nm, characteristic of flavonols (Markham, 1982). The predicted molecular weight of 464 Da corresponds to a heteroside, thus an acid hydrolysis was performed

in order to evaluate the UV spectra of the flavonoid and its aglycone before and after addition of UV shift reagents. These results were observed for band II and are described in Table 3.10.

The continually reducing intensity observed for band I after addition of NaOMe is in agreement with the presence of 3 free adjacent hydroxyl groups in ring B. And the presence of a new band at 320 nm for the aglycone corresponds to a free hydroxyl group at C-7. Since this new band was not detected for the original flavonoid, the possibility that the sugar moiety is attached to the hydroxyl group at C-7 is raised. However, conclusions are not taken on non-observed shifts. On the other hand, the bathochromic shift of 10 nm in band II after addition of NaOAc for the original flavonoid is indicative of a free hydroxyl group at C-7.

The bathochromic shift of 50 nm in band I after addition of $AlCl_3$/HCl for the flavonoid suggests the presence of a free hydroxyl group at C-5 and the increase of this shift to 80 nm in the aglycone, suggests a free 3-OH, corroborating the attachment of the sugar moiety to the 3-OH.

Table 3.10. UV shifts observed for flavonoid **L4** and its aglycone in MeOH and after the addition of shift reagents.

	L4		**L4 aglycone**	
Solvent	Band I (nm)	Band II (nm)	Band I (nm)	Band II (nm)
MeOH	355	260	375	250
Reagent				
NaOMe	nd	-	Decreasing intensity	New band at 320
NaOAc	+35	+10 and a new band at 325	+25	+20 and a new band at 330
NaOAc/H_3BO_3	+25	-	+15	new band at 290
$AlCl_3$/HCl	+50	+10 and a new band at 310	+80	+20
$AlCl_3$[a]	+35	-	+40	-

[a]In comparison to $AlCl_3$/HCl; + = bathochromic shift; - = no shift observed; nd= not detected

A TLC was performed with the residual sugar obtained after hydrolysis of the flavonoid as well as standard sugars arabinose, glucose, rhamnose, xylose, galactose and galacturonic acid. The sugar moiety of **L4** presented a spot at the same retention factor (R_f) as rhamnose (Figure 3.28).

The structure of **L4** was confirmed as that of myricetin 3-O-α-L-rhamnopyranoside (Figure 3.32) by the analysis of ^{1}H, ^{13}C (Table 3.12), COSY, HSQC and HMBC spectra.

The attachment of the sugar moiety to the hydroxyl group at C-3 was confirmed by the correlation observed between the anomeric proton at δ_H 5.31 and C-3 at δ_C 135.0 in the HMBC spectrum (Appendix 5).

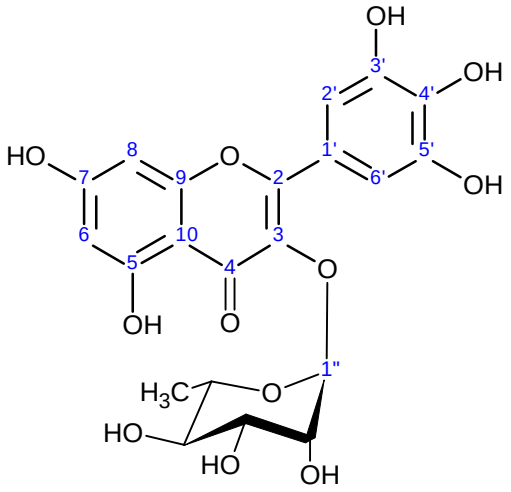

Figure 3.32. Structure of compound **L4**.

III.3.1.3. Structure determination of compound L6

Compound **L6** was obtained as a pale yellow amorphous powder. The high resolution mass spectrum ESI-TOF-MS in negative mode provided a pseudo-molecular ion at *m/z* 477.0929 $[M-H]^-$ (Figure 3.33), calculated for $C_{21}H_{20}O_{11}$, 447.0927.

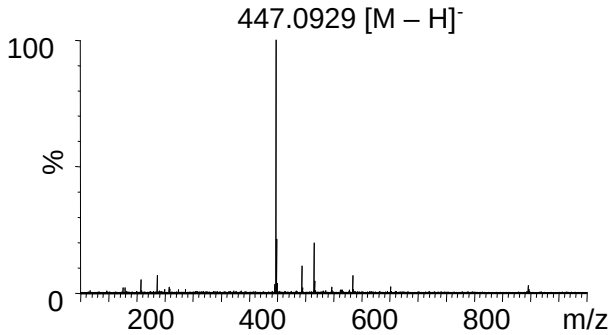

Figure 3.33. High resolution ESI-TOF-MS spectrum in negative mode of compound **L6**.

The UV analysis in methanol of the pure compound provided two bands at λ 350 and 260 nm characteristic of flavones and flavonols. (Markham, 1982). The predicted molecular weight of 448 Da corresponds to a heteroside, thus an acid hydrolysis was performed and both the flavonoid **L6** and its aglycone had their UV shifts compared before and after shift reagent addition. The shifts observed for the flavonoid and the aglycone are presented in Table 3.11.

Table 3.11. UV shifts observed for flavonoid **L6** and its aglycone in MeOH and after the addition of shift reagents.

	L6		**L6 aglycone**	
Solvent	Band I (nm)	Band II (nm)	Band I (nm)	Band II (nm)
MeOH	350	260	375	260
Reagent				
NaOMe	+50	+30	-55	nd
NaOAc	+35	+20	+25	+20
$NaOAc/H_3BO_3$	+25	-	+15	+5
$AlCl_3/HCl$	+50	-	+80	+15
$AlCl_3$[a]	+40	+5	+40	+15

[a]In comparison to $AlCl_3$/HCl; + = bathochromic shift; - = no shift observed; nd= not detected.

Considering the general structure of flavonoids (Figure 3.27), the main shifts obtained for the flavonoid **L6** suggest the presence of free hydroxyl groups in both rings A and B. The bathochromic shift of 25 nm observed for band I in the presence of $NaOAc/H_3BO_3$ suggested the presence of *o*-diOH in ring B, which was also confirmed by the bathochromic shift of 40 nm obtained with $AlCl_3$ compared to $AlCl_3$/HCl. The bathochromic shift of 50 nm observed in band I after addition of $AlCl_3$/HCl corresponds to an acid-stable complex formed between the free hydroxyl group at C-5 and its neighboring ketone at C-4. Thus, the sugar substitution could be at 7-OH or 3-OH in the case of a flavonol. The bathochromic shift of band II observed in the NaOAc spectrum corresponds to the ionization of OH groups in the most acidic position C-7. Hence, the flavonoid is probably a 3-OH substituted flavonol.

The UV spectrum of the aglycone was then analyzed. The wavelength of band I at 375 nm for the aglycone corroborates the hypothesis of a flavonol which has now a free 3-OH group compared to the 3-OH substituted original flavonoid (band I = 350 nm). The aglycone was then inferred to be the flavonol quercetin and its mass spectrum ESI-TOF-MS in negative mode provided a pseudo-molecular ion at *m/z*

301.03 [M – H]$^-$. By the difference of molecular weight between the aglycone and the original flavonoid (a loss of c.a. 146 Da) the sugar is probably a rhamnopyranoside. The compound was finally identified as quercetin 3-*O*-L-α-rhamnopyranoside after the analysis of the ^{1}H NMR spectrum together with HSQC, HMBC and COSY spectra.

The ^{1}H NMR spectrum of **L6** is shown in Figure 3.34.

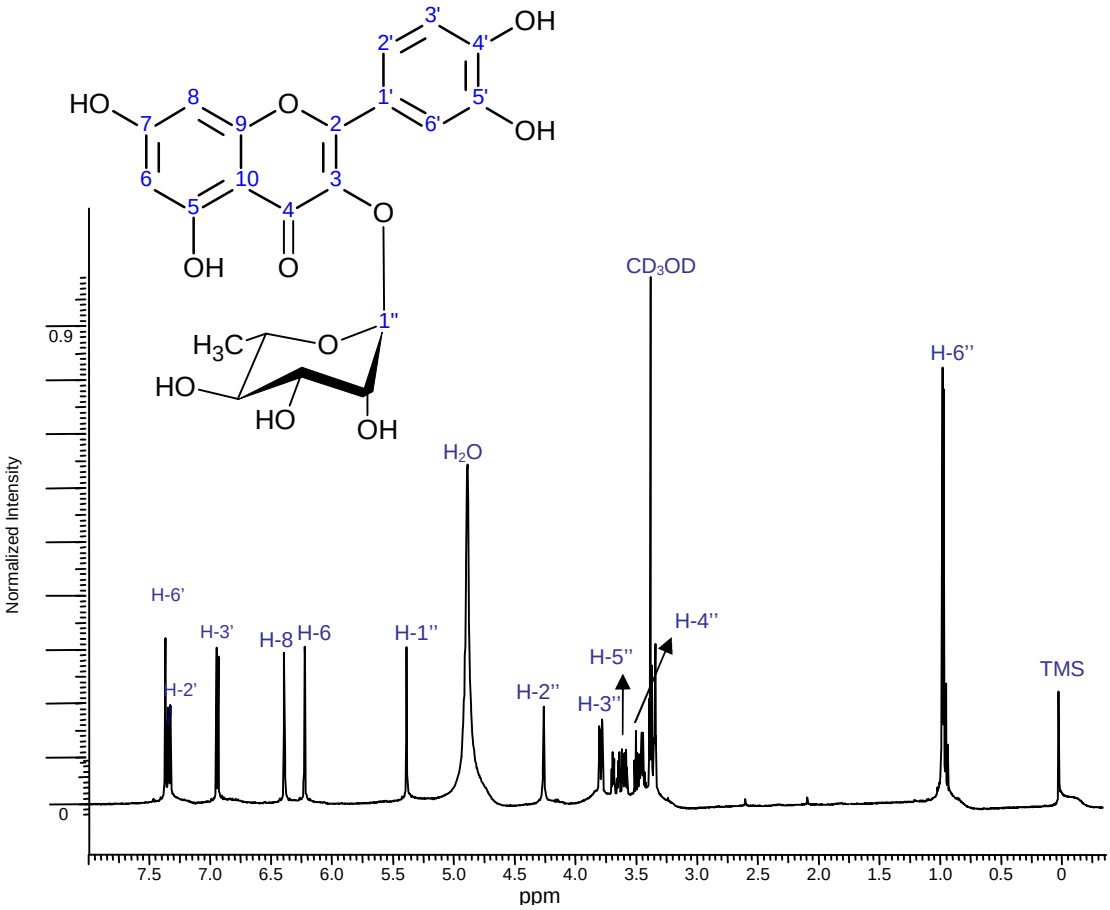

Figure 3.34. Structure and ^{1}H NMR spectrum of **L6** in CD_3OD (δ in ppm relative to TMS).

The *O*-rhamnoside substitution was further confirmed to be at C-3 by the correlation observed between the anomeric proton at δ_H 5.36 and C-3 at δ_C 135.5 in the HMBC spectrum (Figure 3.35). The connectivity between protons of the sugar moiety was determined by the correlations observed in the COSY spectrum, and it was demonstrated to be an α-L-rhamnopyranoside due to the value of the coupling constant of the anomeric proton (d, *J*=1.46 Hz). A TLC was also performed with the sugar recovered after hydrolysis and standard sugars arabinose, glucose, rhamnose, xylose, galactose and galacturonic acid, confirming the hypothesis of a rhamnoside.

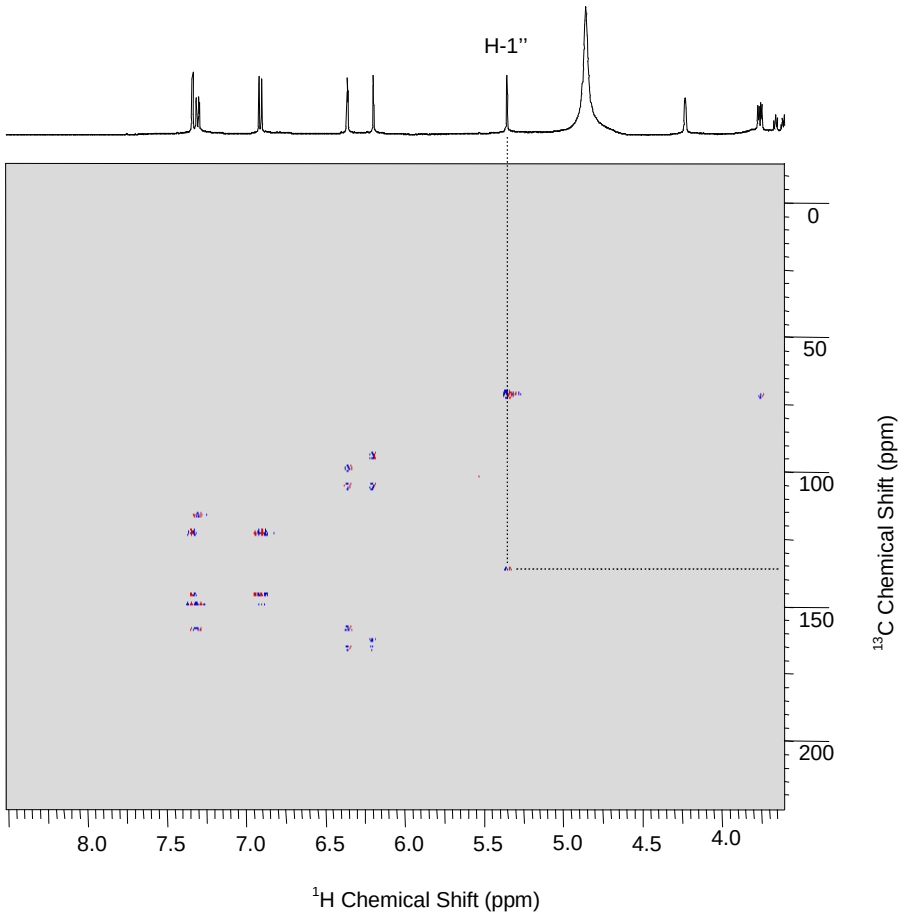

Figure 3.35. HMBC spectrum for compound **L6** (zoom in ^{1}H chemical shift scale from 3.2 to 9.0 ppm).

Table 3.12. ^{1}H and ^{13}C shifts in ppm (δ relative to TMS) of compounds **L2**, **L4**, and. **L6**.

	L2		**L4**		**L6**	
C	δ_H*	δ_C	δ_H*	δ_C	δ_H*	δ_C
2	5.19 (d, 9.7)	81.3		158.0		157.4
3	4.73 (d, 10.2)	76.5		135.0		134.5
4		195.6				
5		164.5		162.0		161.4
6	5.91 (d, 2.5)	96.3	6.20 (s)	98.7	6.20 (d, 1.9)	98.6
7		167.9		164.0		163.9
8	5.90 (d, 2.2)	95.3	6.36 (s)	93.6	6.36 (d, 1.9)	93.6
9		163.1		157.0		156.6
10		101.1		105.0		104.3
1’		127.9		121.0		122.4
2’	6.81 (d, 8.4)	119.8	6.95 (s)	108.5	7.30 (dd, 8.3, 2.4)	122.0
3’	6.79 (d, 8.1)	115.2		146.0	6.90 (d, 8.3)	115.2
4’		146.3		136.0		144.5
5’		145.5		146.0		147.8
6’	6.94 (s)	114.5	6.95 (s)	108.5	7.34 (d, 1.9)	115.8
1’’	3.87 (d, 5.7)	101.9	5.31 (d, 1.5)	102.3	5.36 (d, 1.5)	102.3
2’’	3.23 (dd, 12.4, 4.4)	74.7	4.22 (m)	70.8	4.23 (m)	70.4
3’’	3.30 (m)	72.4	3.77 (m)	71.0	3.75 (dd, 9.3, 3.4)	70.7
4’’	3.48 (m)	69.8	3.35 (m)	72.3	3.34 (m)	71.7
5’’a	3.06 (dd, 11.7, 4.1)	64.9	3.50 (m)	71.0	3.40 (m)	70.5
5’’b	3.93 (dd, 11.6, 4.7)	64.9				
6’’			0.96 (m)	16.6	0.94 (d, 6.5)	16.5

*Multiplicity and coupling constants (Hz) in parentheses.

III.3.2. On-line identification of compounds from the ethyl acetate fraction B (AcF-B)

Fraction AcF-B was used for the on-line identification of flavonoids by means of LC-UV-MS analysis and post-column derivatization with UV shift reagents. The shifts obtained on-line as well as the MS data are presented in Table 3.13.

Table 3.13. UV and MS on-line data for compounds detected in fraction AcF-B of the *Licania octandra* extract.

Compound	**L2**	**L3**	**L4**	**L5**	**L6**	**L7**
UV (nm)	**290**	**290**	**330, 240**	**365, 260**	**350, 260**	**360, 255**
UV shift 1	320	315	430, 270	430, 270	415, 270	425, 275
UV shift 2	310	310	410, 260	410, 265	400, 265	410, 270
UV shift 3	330	340	370*, 260	400*, 275	400, 270	400, 270
UV shift 4	330	340	335*, 255	370*, 265	355*, 265	360, 255
UV shift 5	330	340	370*, 260	380, 265	380*, 270	380, 260
ESI-MS (-)						
BP (*m/z*)	**435.13**	**435.00**	**462.98**	**463.00**	**447.26**	**302.43**
MS^2 (*m/z*)[a]	303.35	303.36	316.95	301.02	301.20	NA

*UV shift in the HPLC mobile phase (water + 0.1% formic acid (A) - MeOH + 0.1% formic acid (B); gradient mode from 2% to 100% of B in 40 min). UV shift 1: after addition of $AlCl_3$. UV shift 2: after addition of $AlCl_3$/HCl. UV shift 3: after addition of KOH. UV shift 4: after addition of NaOAc. UV shift 5: after addition of NaOAc/H_3BO_3. *shoulder at 320 nm. BP: base peak $[M - H]^-$. [a]Most intense ion. NA: not acquired.

Compounds **L2**, **L4** and **L6** have been identified after isolation (III.3.3.1 to III.3.1.3). Additionally, their UV on-line data are discussed here in order to demonstrate the application of UV shift reagent derivatization on the identification of flavonoids. The results obtained for these previously determined compounds allowed the correct interpretation of on-line data for the structure determination of **L3**, **L5** and **L7**.

In the case of compound **L2** the UV spectrum of the isolated compound in MeOH provides the same λ_{max} (290 nm) for band II as the one generated during the HPLC/UV/MS analysis. The bathochromic shift observed after addition of NaOAc is identical for the compound in the mobile phase (Table 3.13) and in MeOH (Table 3.9). However, when NaOAc/H_3BO_3 were added on-line, a bathochromic shift of 40 nm was produced which was not observed for the compound in methanol, and was the same shift observed for the single addition of NaOAc. One possible explanation is that the NaOH solution used to neutralize the acidic mobile phase (c.f. Experimental section) was strong enough to neutralize the weak acid H_3BO_3. Thus, the results obtained after addition of NaOAc/H_3BO_3 were circumspectly considered in the interpretation of on-line data. Another difference of results was observed for $AlCl_3$ and $AlCl_3$/HCl addition, after which the bathochromic shifts were higher in the mobile phase than in methanol. The difference did not influence the interpretation, though. This change may be due to the composition of the mobile phase which contained water and trifluoroacetic acid (TFA). It is also important to notice that the TFA containing mobile phase had its pH adjusted to 7 by the post-column addition of NaOH 0.01 M together with shift reagents, according to a previously published method (Simoes-Pires *et al.*, 2005). For the post-column derivatization, a KOH solution was used in the place of NaOMe, as the strong base, providing very similar results.

When the on-line and the MeOH UV spectra were compared for compounds **L4** and **L6**, one can observe the same kind of differences as for **L2**. Moreover, the decreasing band intensity effect after NaOMe addition (compound **L4**, table 3.10) was not observed following the on-line addition of KOH.

Compound **L3** presented a base peak at *m/z* 435.00 and an MS^2 fragment at *m/z* 303.36 suggesting a taxifolin xyloside or arabinoside. The UV spectrum of the compound corroborates the hypothesis of a dihydroflavonol due to the presence of only one band at 290 nm similar to (2R,3R)-taxifolin 3-O-β-D-xylopyranoside (**L2**). **L3** and **L2** presented very similar UV shifts under on-line addition of shift reagents indicating that the attachment of the sugar moiety in **L3** is most probably at C-3 hydroxyl group.

However, the difference between **L2** and **L3** could not be exactly determined by the analysis of the on-line data, depicting the limitations of dereplication methods.

Compound **L5** presented a base peak at *m/z* 463.00 and an MS^2 fragment at *m/z* 301.02 suggesting a quercetin glucoside or galactoside. The shifts obtained after addition of reagents suggest the presence of free hydroxyl groups at C-4', C-5' and C-5 (cf. $AlCl_3$ and $AlCl_3$/HCl shifts, Table 3.13). The shoulder observed at 320 nm after addition of NaOAc is typical of the presence of a free hydroxyl group at C-7. Therefore, the sugar substitution is most possibly at the C-3 hydroxyl group of quercetin. However, there is no reagent capable of determining the presence/absence of free hydroxyl groups at C-3 of flavonoids, hence the determination of C-3 substituted flavonoids must be carefully considered when using dereplication techniques.

Compound **L7** presented a base peak at *m/z* 302.43, and two UV bands at 360 and 255 nm, suggesting a flavonol aglycone. The hydroxylation pattern could be determined by the analysis of the on-line UV shifts. The bathochromic shift observed after addition of $AlCl_3$ suggests the presence of *o*-diOH in ring B (C-4' and C-5'). The shift observed with $AlCl_3$ followed by the addition of HCl suggests a further free hydroxyl group at C-5. The compound was then identified as quercetin.

The proposed structures for **L3**, **L5** and **L7** are presented in Figure 3.36.

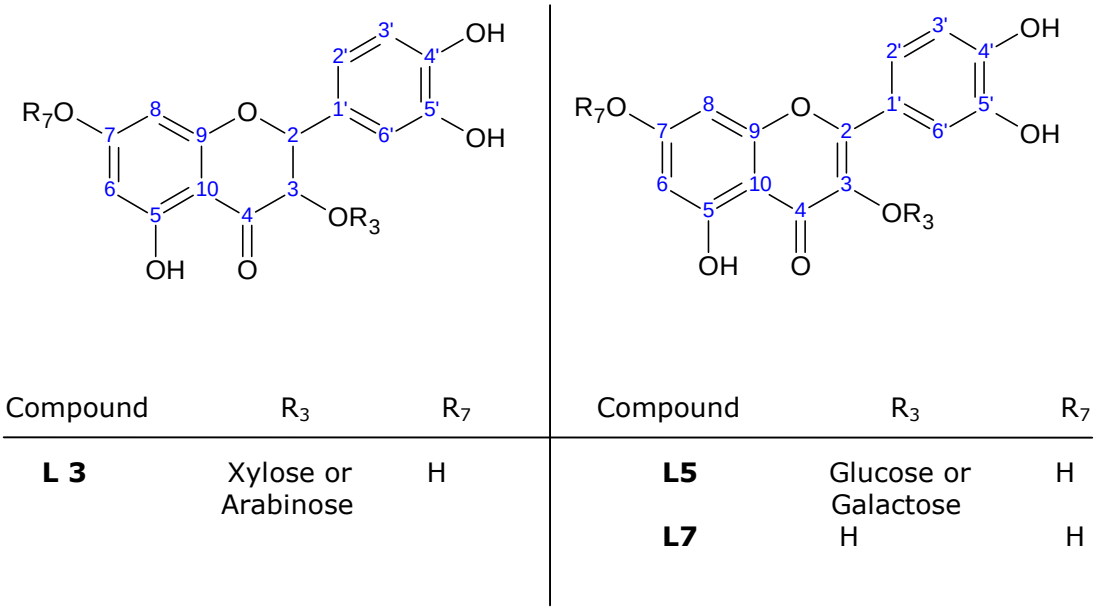

Compound	R_3	R_7	Compound	R_3	R_7
L 3	Xylose or Arabinose	H	**L5**	Glucose or Galactose	H
			L7	H	H

Figure 3.36. Proposed structures for compounds **L3**, **L5** and **L7** based on UV and MS on-line data.

On-line dereplication can be considered as a very useful and time-saving technique in the analysis of flavonoid enriched plant extracts and fractions. They are especially useful in determining the nature of the aglycone based on the hydroxylation pattern and MS^n results. Nevertheless, in most cases, the complete structure determination can only be achieved after 1D and 2D NMR analyses. The nature of the sugar moiety can be determined by the analysis of ^1H NMR, where the coupling constant of the anomeric proton plays an important role in the differentiation between α and β anomers. Thus, an on-line HPLC/NMR method would be useful. In the specific case of taxifolin derivatives, the configuration around C-2 and C-3 could only be determined after hydrolysis of heterosides and analysis of the optical rotation properties of the aglycone. One possible solution for the on-line analysis of such compounds would be high performance liquid chromatography coupled to a circular dichroism spectrometer (HPLC/CD) (Bringmann *et al.*, 2008).

III.3.3. Antiplasmodial activity of isolated compounds

The compounds isolated from *Licania octandra* by semi-preparative HPLC were all tested *in vitro* against *P. falciparum*, and for their *in vitro* cytotoxicity on human fibroblasts and mouse macrophages (Table 3.14). Samples were also screened against other parasites such as *Trypanosoma cruzi* and *T. b. brucei*.

Table 3.14. Antiparasitic activity and cytotoxicity of compounds isolated from *L. octandra* and their aglycones.

Activity / Compound	Anti-*P. falciparum*[a,b]	Anti-*T. cruzi*[a,c]	Anti-*T. b. brucei*[a,d]	Cytotoxicity[a,e]
	IC_{50} (µg/mL)			
L2	>32.00	>32.00	>32.00	>32.00
L2 aglycone	>32.00	>32.00	>32.00	>32.00
L4	17.37	11.34	11.57	>32.00
L4 aglycone	10.38	12.81	12.02	>32.00
L6	11.62	>32.00	>32.00	>32.00
L6 aglycone	3.94	8.00	16.00	8.00*

[a]cf Experimental section V.6.2 for experimental assay description;
[b]IC_{50} >16 µg/mL: inactive; IC_{50} between 2 and 16 µg/mL: moderately active; IC_{50} <2µg/mL: highly active;
[c]IC_{50} >30 µg/mL: inactive; IC_{50} between 2 and 30 µg/mL: moderately active; IC_{50} <2 µg/mL: highly active;
[d]IC_{50} >5 µg/mL: inactive; IC_{50} between 1 and 5 µg/mL: moderately active; IC_{50} <1 µg/mL: highly active;
[e] tested on human fibroblasts (MRC-5 cell line); IC_{50} >30 µg/mL: not toxic; IC_{50} between 10 and 30 µg/mL: moderately toxic; IC_{50} <10 µg/mL: highly toxic. *Not toxic on mouse macrophages.

The most active compound against *P. falciparum* was the **L6** aglycone quercetin with an IC_{50} value of 3.94 µg/mL (i.e. 13.05 µM). Moreover, quercetin showed a moderate anti-*T. cruzi* activity (IC_{50} = 8.00 µg/mL or 26.49 µM) and was considered toxic for human fibroblasts. The original flavonoid **L6**, quercetin-3-*O*-L-α-rhamnopyranoside was also considered moderately active against *P. falciparum* (IC_{50} = 11.62 µg/mL or 25.93 µM) but not active against the other tested parasites and not cytotoxic. The antiplasmodial activity of quercetin has previously been demonstrated and associated to its inhibition activity on β-ketoacyl-ACP-reductase (FabG), β-hydroxacyl-ACP-dehydratase (FabZ), and enoyl-ACP-reductase (FabI), which are enzymes involved in type II fatty acid biosynthesis (FAS-II) pathway of *P. falciparum* (Tasdemir et al., 2006). In the cited study, the aim was to establish structure-activity relationships among several commercially available flavonoids in terms of antiplasmodial activity and FAS-II enzymes inhibition. Although flavonoid heterosides were not tested, the authors realized that the presence of free hydroxyl groups in ring B was important for activity of flavanones and dihydroflavonols, while the absence of a hydroxyl group at C-3 did not play an important role for activity, as observed in the comparison between luteolin and quercetin IC_{50} values (Table 3.14).

The antiplasmodial activity of quercetin 3-*O*-L-α-rhamnopyranoside (**L6**) demonstrated in the present study shows that 3-OH substitution of quercetin does not interfere with the activity and moreover can reduce its cytotoxicity in vitro. Thus, the study of 3-OH substituted flavonols as antimalarial agents is worthwhile.

The myricetin derivative **L4** was considered as moderately active against *T. cruzi* and presented an IC_{50} value of 17.37 µg/mL against *P. falciparum*, which is not very different from that of its aglycone (IC_{50} = 10.38 µg/mL). The aglycone of **L4**, myricetin, was then considered moderately active against the chloroquine-resistant malaria parasite (*Pf* K1). Tasdemir *et al.* (2006) also demonstrated a similar activity for myricetin against *Pf* K1 (Table 3.15). Interestingly, as in the case of **L6**, the 3-OH substitution of myricetin by a sugar moiety doesn't seem to change the antiplasmodial activity of this class of flavonoid.

The taxifolin derivative **L2** and its aglycone did not present any antiparasitic activity or toxicity. A previous study showed some activity of taxifolin against two different strains of *P. falciparum,* PoW and Dd2 with IC_{50} values of 15.8 µM and 38.4 µM, respectively (Kraft *et al.*, 2001). However, in the screening conditions presented here, neither **L2** nor its aglycone was considered active against *Pf* K1. Among the

isolated flavonoids, **L2** and its aglycone presented the highest IC_{50} values and its main structural difference from the other active compounds is the saturation between C-2 and C-3. This result is in agreement with the study published by Tasdemir *et al.* (2006), where a flavanone (naringenin) was much less active than its corresponding flavonol (kaempferol) (Table 3.15). However, the authors did not include dihydroflavonols in their study.

Table 3.15. Antiplasmodial activity of some flavonoids against chloroquine-sensitive (*Pf* NF54) and –resistant (*Pf* K1) *Plasmodium falciparum*.[a]

Compound name	Structure	IC_{50} (µM) *Pf* NF54	IC_{50} (µM) *Pf* K1
Fisetin	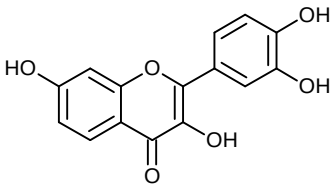	8.2	6.5
Kaempferol	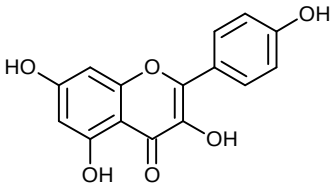	30.4	n.d.
Luteolin	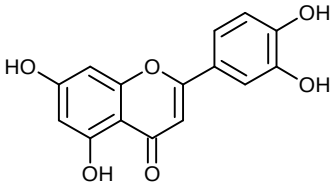	10.7	9.6
Myricetin	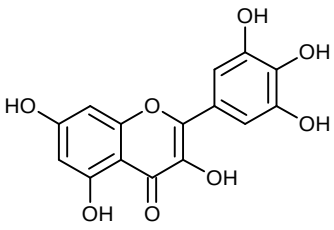	57.3	12.9
Naringenin	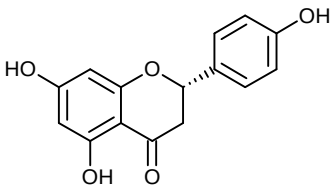	141.1	n.d.
Quercetin	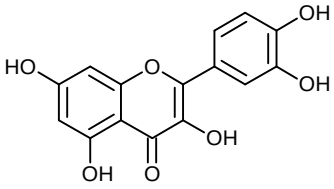	10.0	8.9

[a]Adapted from Tasdemir *et al.* (2006); n.d.= not determined.

III.4. Bioguided phytochemical investigation of *Syzygium cumini*

The freeze dried decoction of *S. cumini* stem bark was first analyzed by HPLC/UV/MS using electrospray ionization in negative mode. A series of compounds presenting similar UV spectra could be detected in the extract (**S2**-**S8**, Figure 3.37). Compound **S5** presented a UV spectrum with two bands at 254 and 370 nm. These absorbance maxima correspond to those of flavonoids, especially 3-OH free flavonols and chalcones. At the same time, the MS spectrum of **S5** provided a molecular ion of 301 $[M - H]^-$, corresponding to 302 Da, the same molecular weight (MW) as that of the flavonol quercetin. However, UV band I (370 nm) was less intense than expected for flavonoids in general (Markham, 1982). According to previous works published on the chemical composition of *S. cumini*, the bark of this plant contains ellagic acid (302 Da) and some methylated derivatives. The possibility that the compound **S5** was ellagic acid and that other ellagic acid derivatives were present in the extract was then taken into consideration. In fact, some of the detected molecular ions corresponded to known ellagic acid derivatives which are summarized in Table 3.16. It was not possible though, to establish the position of the substituents by means of the on-line techniques. Thus, fractionation and isolation procedures were developed for the complete structural determination of the compounds.

Table 3.16. Possible kinds of ellagic acid derivatives in *S. cumini* stem bark aqueous extract according to its HPLC/UV/MS analysis.

$[M - H]^-$	Ellagic acid derivative	MW (Da)
433	ellagic acid xylopyranoside[1]	434
447	ellagic acid rhamnopyranoside [2] *O*-methylellagic acid arabinofuranoside[3] *O*-methylellagic acid xylopyranoside[3]	448
461	*O*-methylellagic acid rhamnopyranoside[4] di-*O*-methylellagic acid xylopyranoside[1] di-*O*-methylellagic acid arabinofuranoside[5]	462
463	ellagic acid glucopyranoside[6]	464
489	tri-*O*-methylellagic acid rhamnopyranoside [2] ellagic acid acetyl-rhamnopyranoside[7] *O*-methyl-methylenedioxyellagic acid glucopyranoside[8]	490
503	*O*-methylellagic acid *O*-acetyl-rhamnopyranoside[4]	504

[1](Fogliani *et al.*, 2005); [2](Yang *et al.*, 1998), (Tabopda *et al.*, 2008); [3](Ye and Yang, 1996);[4](Elkhateeb *et al.*, 2005); [5](Tanaka *et al.*, 2001); [6](Lee *et al.*, 2005); [7](Gallo *et al.*, 2006); [8](Li *et al.*, 1999).

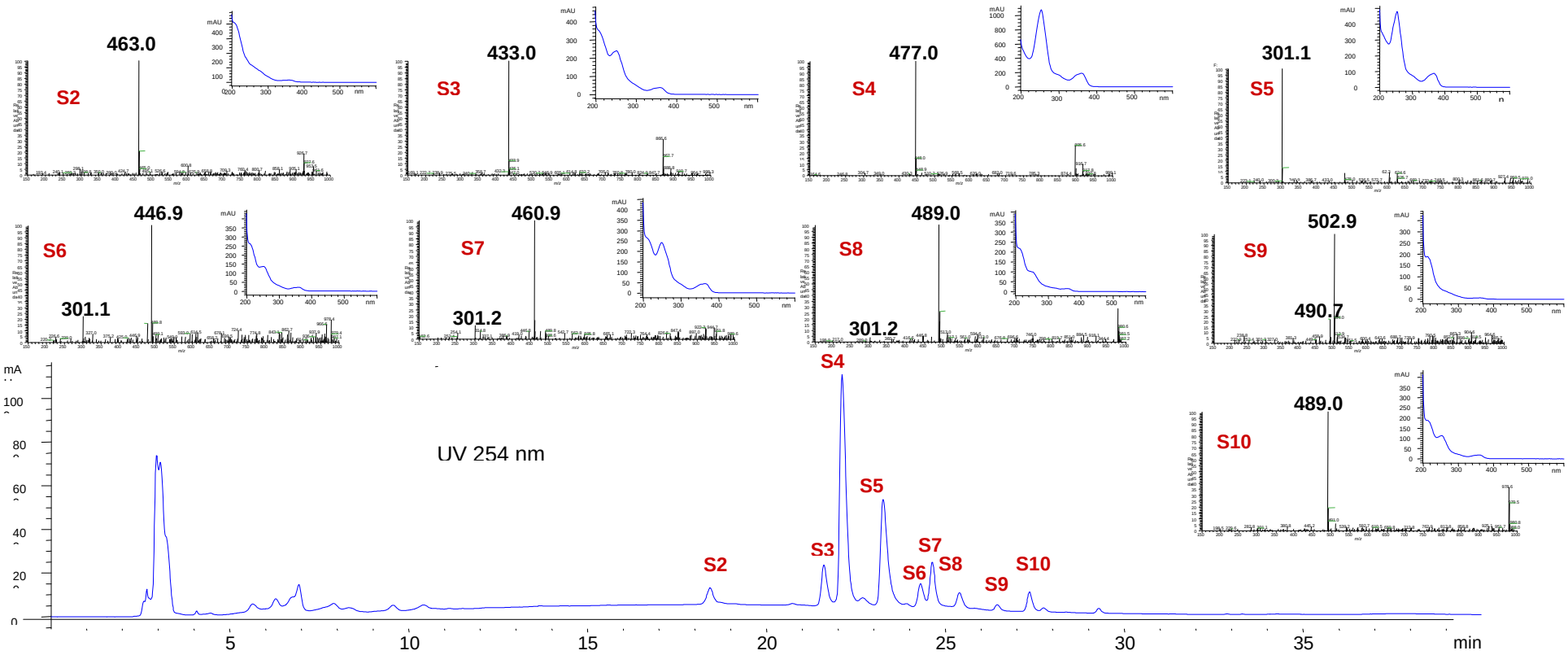

Figure 3.37. HPLC chromatogram of *S. cumini* aqueous extract at 254 nm (injection volume: 20 µL; sample concentration: 10 mg/mL in mobile phase). Mass spectra were obtained by HPLC/MS with electrospray ionization (ESI) in negative mode. Zorbax Extend C_{18} column (250 x 4 mm, i.d.); MeOH-H_2O + formic acid 0.1% in gradient mode as mobile phase.

III.4.1. Fractionation and isolation of active compounds from the stem bark aqueous extract

The freeze-dried aqueous extract obtained from the stem bark of *S. cumini* (20 g) was first fractionated by centrifugal partition chromatography (CPC) providing 160 fractions which were grouped into four major fractions (A – D), according to their TLC profile. The CPC chromatogram is depicted in Figure 3.38. The major fractions together with the crude extract were considered for the screening of activity against *P. falciparum*, *T. cruzi*, *T. b. brucei* and for their cytotoxicity (Table 3.2).

Fraction C was highly active against *P. falciparum*, with an IC_{50} value lower than 0.25 µg/mL with no toxicity on human fibroblasts (IC_{50} > 64.0 µg/mL). It also showed a moderate activity against the sleeping sickness parasite, *T. b. brucei* (IC_{50} = 2.05 µg/mL). For these reasons, fraction C was the main target for further isolation procedures. Fractions B and D were considered inactive against the malaria parasite. However, fraction D presented an IC_{50} of 19.80 µg/mL against *P. falciparum*, a value that is close to that of a moderate activity, but it was also considered moderately toxic (IC_{50} = 26.54 µg/mL). In order to determine which compounds were responsible for toxicity, fraction D was also considered for the subsequent isolation procedures.

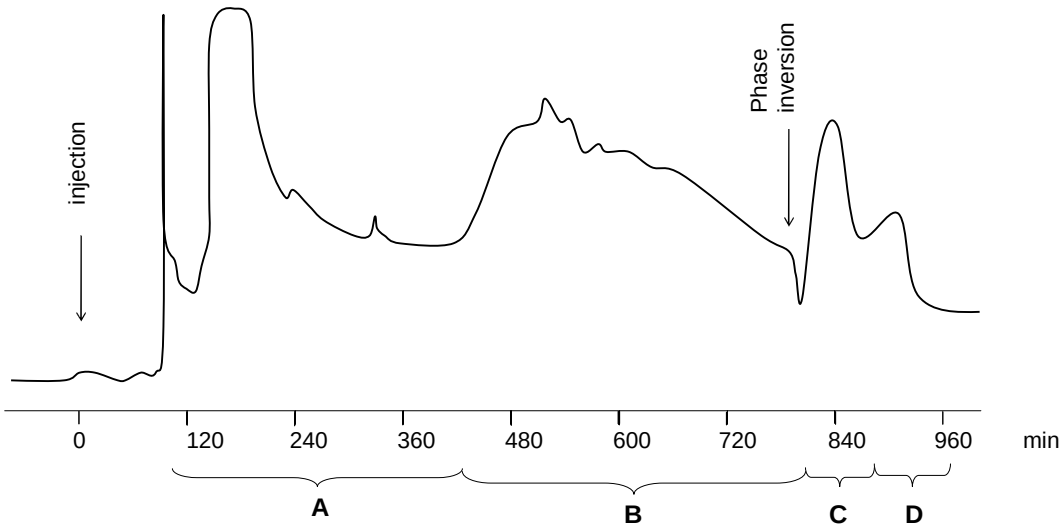

Figure 3.38. CPC/UV chromatogram at 254 nm of the aqueous extract of *S. cumini*. Solvent system: *tert*-butyl-methyl-ether, *n*-butanol, acetonitrile, water (2:2:1:5) with 0.05% TFA. The lower phase was used as the initial mobile phase and the elution was conducted at 3 mL/min.

Fractions C and D were finally fractionated by semi-preparative HPLC (SPHPLC) and the isolated compounds had their structure elucidated by means of classical spectroscopic methods, such as UV spectroscopy, mass spectrometry (MS) and nuclear magnetic resonance (NMR) experiments (^{1}H and ^{13}C NMR, HSQC, HMBC, COSY, NOESY). A general fractionation scheme is presented in Figure 3.39.

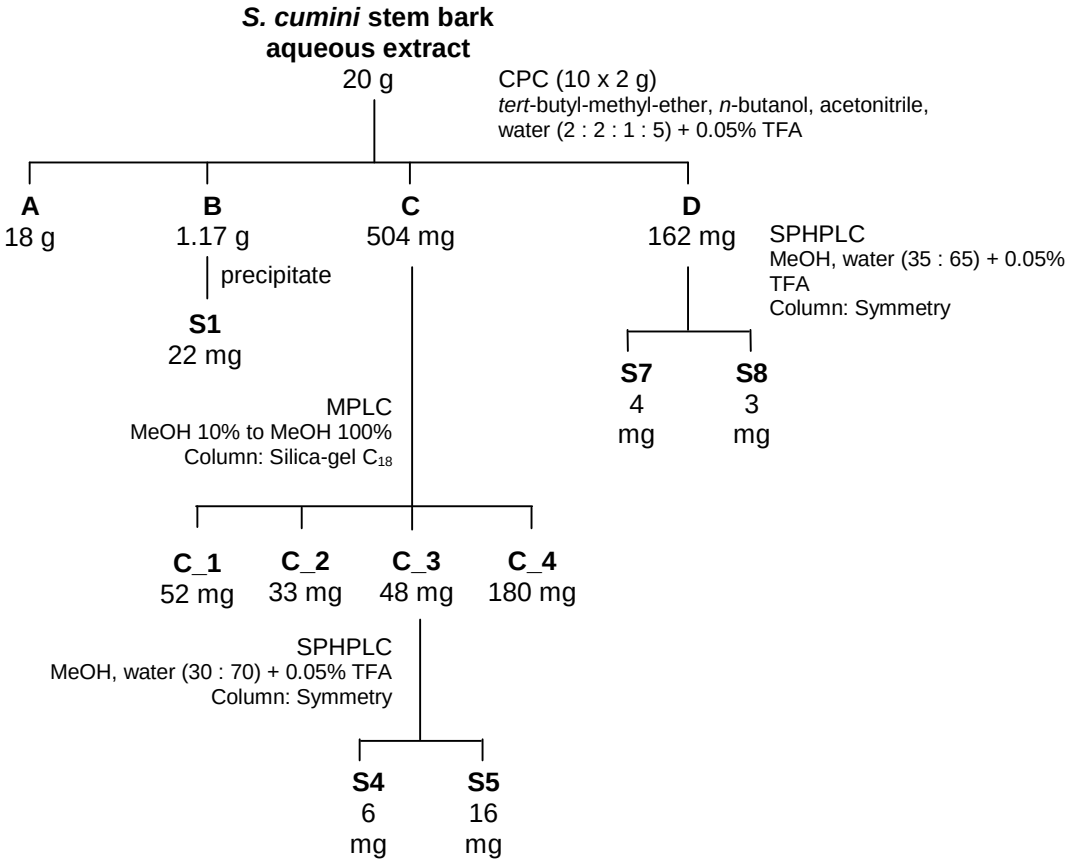

Figure 3.39. General fractionation and isolation scheme for *S. cumini* stem bark aqueous extract.

III.4.1.1. Structure determination of compound S1

Compound **S1** was recovered as a yellowish-white powder by filtration after precipitation in fraction B. The ESI-MS spectrum of **S1** detected a pseudo-molecular ion at *m/z* 169 $[M-H]^-$, which corresponds to 170 Da (Figure 3.40).

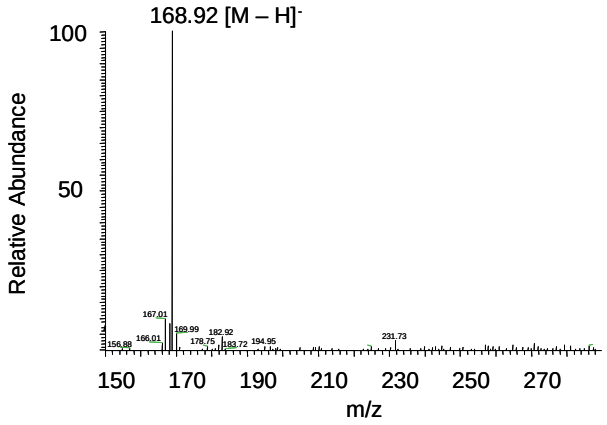

Figure 3.40. ESI-MS spectrum in negative mode of compound **S1**.

The ^{1}H NMR spectrum of **S1** (Figure 3.41) in CD_3OD presented only one singlet at δ_H 7.08, indicating the presence of one or two symmetric aromatic protons in the molecule.

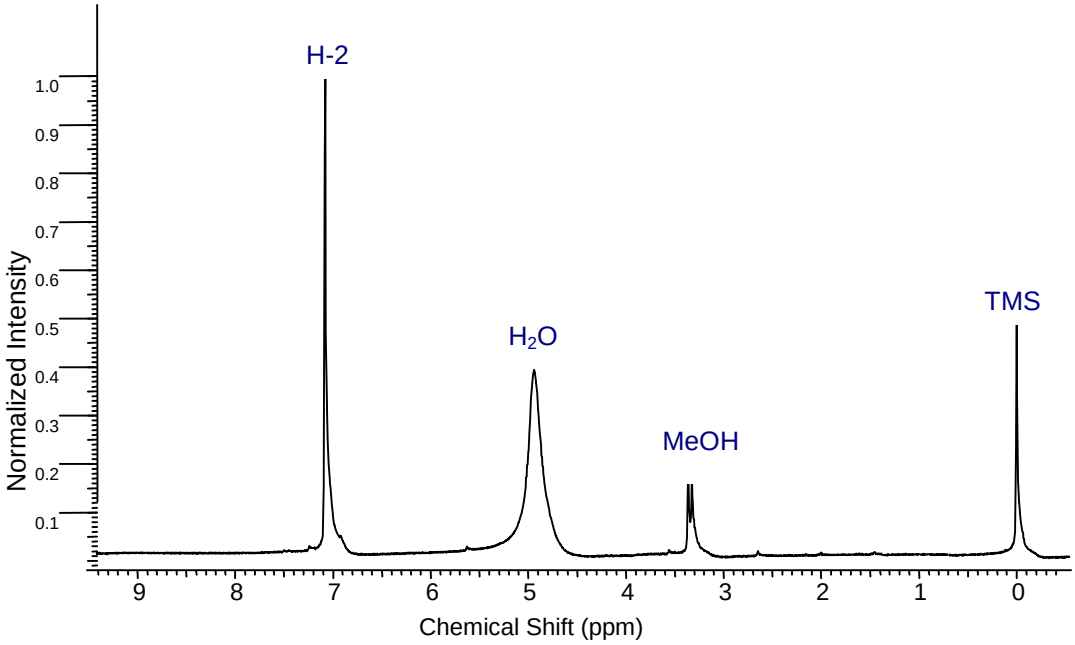

Figure 3.41. ^{1}H NMR spectrum of compound **S1** (CD_3OD, 500 MHz).

The correlations observed in the HMBC spectrum (Appendix 6) and represented in Figure 3.42 confirmed the identity of compound **S1** as gallic acid.

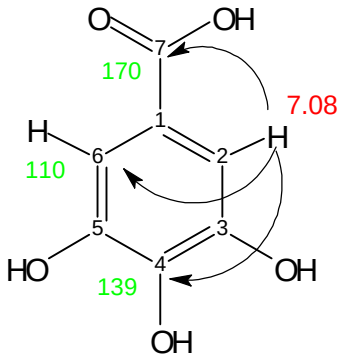

Figure 3.42. Structure of compound **S1**, gallic acid, and its mains HMBC correlations. Chemical shifts are presented in ppm (green: ^{13}C, red: ^{1}H).

III.4.1.2. Structure determination of compound S4

Compound **S4** was isolated from the MPLC fraction C_3 by semi-preparative HPLC as a yellow brownish amorphous powder. The high resolution mass spectrum ESI-TOF-MS in negative mode provided a pseudo-molecular ion at *m/z* 477.0633 $[M-H]^-$ (Figure 3.43), calculated for $C_{21}H_{17}O_{13}$, 477.0669. The deduced molecular formula ($C_{21}H_{18}O_{13}$) corresponds to three previously reported ellagic acid derivatives: 3-*O*-methylellagic acid 4'-*O*-β-D-glucopyranoside (Yan and Guo, 2004), 3-*O*-methylellagic acid 4-*O*-β-D-glucopyranoside (Khallouki *et al.*, 2007) and 4-*O*-methylellagic acid 4'-*O*-β-D-glucopyranoside (Wu *et al.*, 2008).

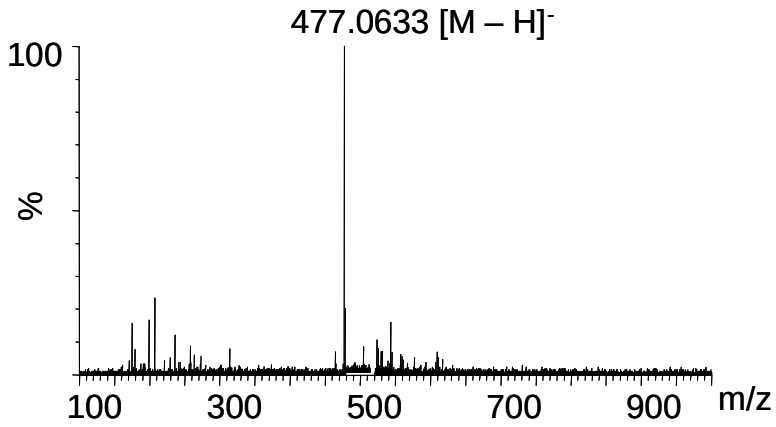

Figure 3.43. ESI-TOF-MS spectrum in negative mode of compound **S4**.

The ^{1}H NMR spectrum for **S4** showed a singlet at δ_H 4.05 ppm suggesting the presence of one *O*-methyl substituent. Moreover, signals corresponding to five protons of a sugar moiety could be directly observed in the spectrum (δ_H 5.06, 4.10, 3.51, 3.73, and 3.48). Unfortunately, it was not possible to achieve a sharp signal spectrum for this ellagic acid derivative, and the coupling constant could not be established for the anomeric proton. The HSQC spectrum revealed the presence of an additional proton belonging to the sugar moiety, δ_H 3.51 couplied with δ_C 69.5, characteristic of the methylene of a glucose.

The connectivity between protons of the sugar moiety was established by the COSY spectrum, corroborating the hypothesis of a glucoside. However, the precise determination of the sugar moiety was difficult based only on spectral data, due to solubility problems and overlapping signals. In order to confirm the hypothesis of a glucoside, an enzymatic hydrolysis was conducted using β-D-glucosidase, and the hydrolysis product was analyzed by HPLC/UV together with the original compound. The chromatograms are presented in Figure 3.44.

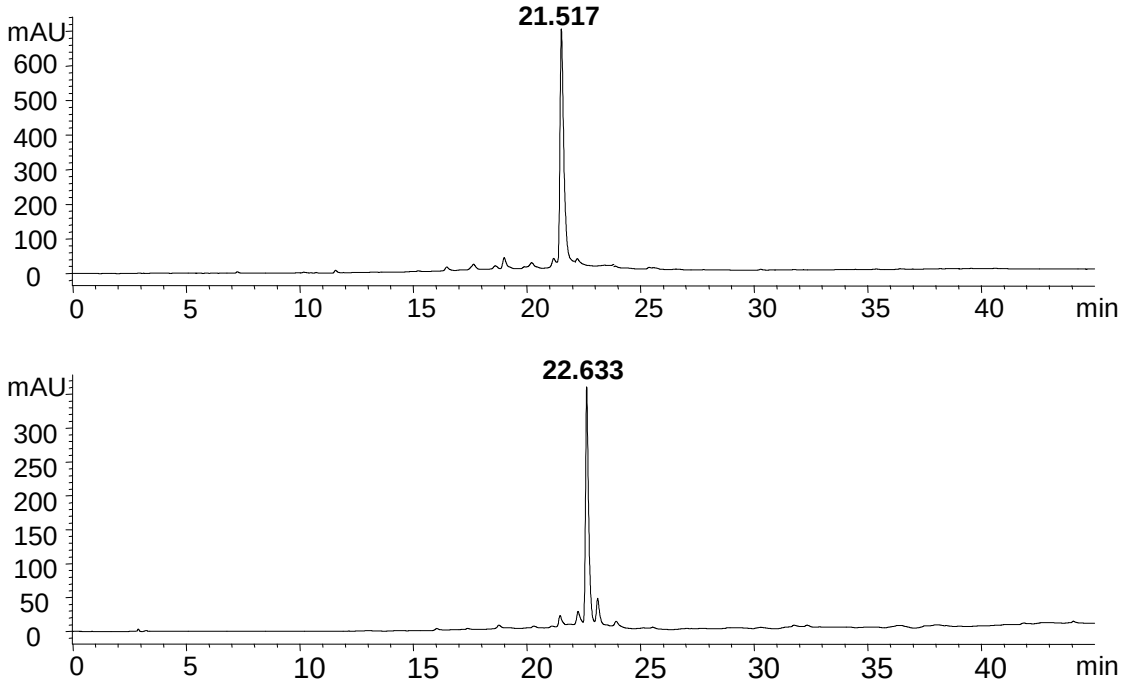

Figure 3.44. HPLC/UV (254 nm) chromatogram of compound **S4** and its β-glucosidase enzymatic hydrolysis product (injection volume: 30 µL; Zorbax Extend C-18 column (250 x 4 mm, i.d.); MeOH-H_2O + TFA 0.05% in gradient mode as mobile phase.

The attachment of the sugar moiety could be established at position 3' by the correlations observed in the HMBC spectrum (Appendix 7) and represented in Figure 3.45, as well as the upfield shift of H-5' (δ_H 7.71 instead of 7.80) compared to an *O*-glucoside substitution at position 4' (Li *et al.*, 1999). The methoxyl substitution at C-3 could be determined by the ^{13}C shift of ca. 64 ppm, instead of 57 ppm typical value of an *O*-methyl substitution at C-4 of ellagic acid (Khallouki *et al.*, 2007). In addition, no correlation could be seen between the *O*-methyl and H-5 signals in the NOESY spectrum. It was also interesting to notice that both compounds **S7** and **S4,** having a sugar substitution at C-3', showed a ^{13}C shift of ca. 115 ppm for C-1', rather than 112 ppm in ellagic acid (**S5**) and its analog with a sugar moiety at C-4' (**S8**) (Table 3.17). This substitution pattern is original, allowing the elucidation of the new ellagic acid derivative, 3-*O*-methylellagic acid 3'-*O*-β-D-glucopyranoside.

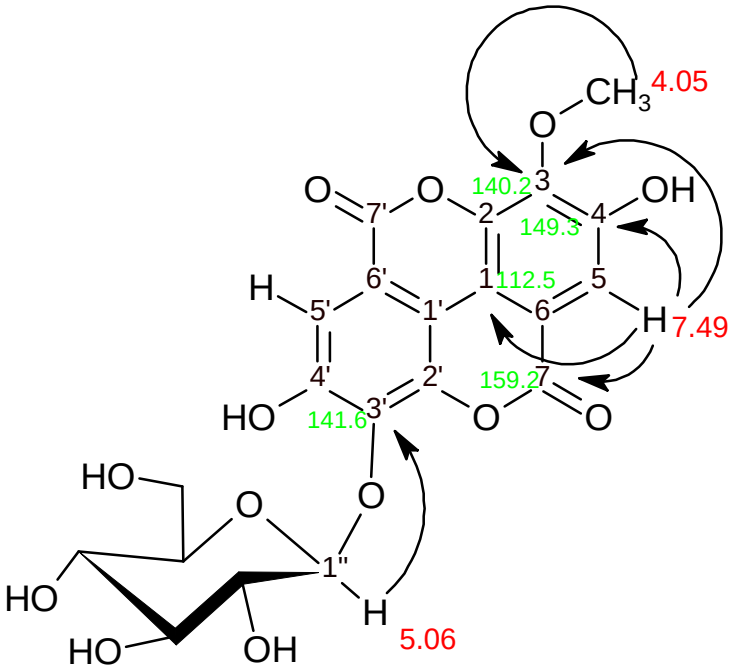

Figure 3.45. Structure and main HMBC correlations for **S4**. Chemical shifts are presented in ppm (green: ^{13}C, red: ^{1}H).

III.4.1.3. Structure determination of compound S5

Compound **S5** was isolated from MPLC fraction C_3 by semi-preparative HPLC as yellow needle-shaped crystals. The high resolution mass spectrum ESI-TOF-MS in negative mode provided a pseudo-molecular ion at *m/z* 300.9992 $[M-H]^-$ (Figure 3.46), calculated for $C_{14}H_5O_8$, 300.9984, which is consistent with the molecular formula $C_{14}H_6O_8$ of ellagic acid.

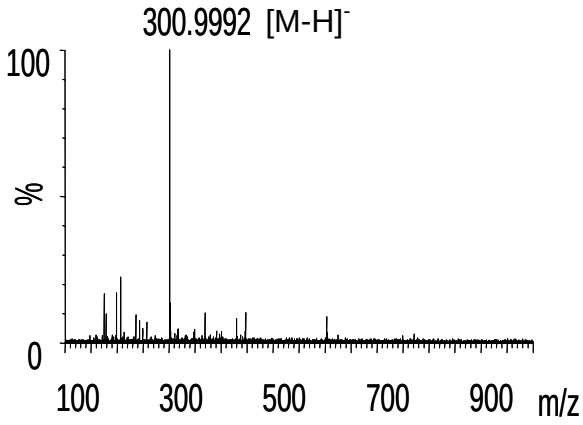

Figure 3.46. ESI-TOF-MS spectrum in negative mode of compound **S5**.

The [1]HNMR spectrum (Figure 3.47) of **S5** presented only one proton signal at δ_H 7.47 and the correlations observed in the HMBC spectrum (Appendix 8) and represented in Figure 3.48 confirmed the identification of ellagic acid in agreement with previously published values (Li *et al.*, 1999).

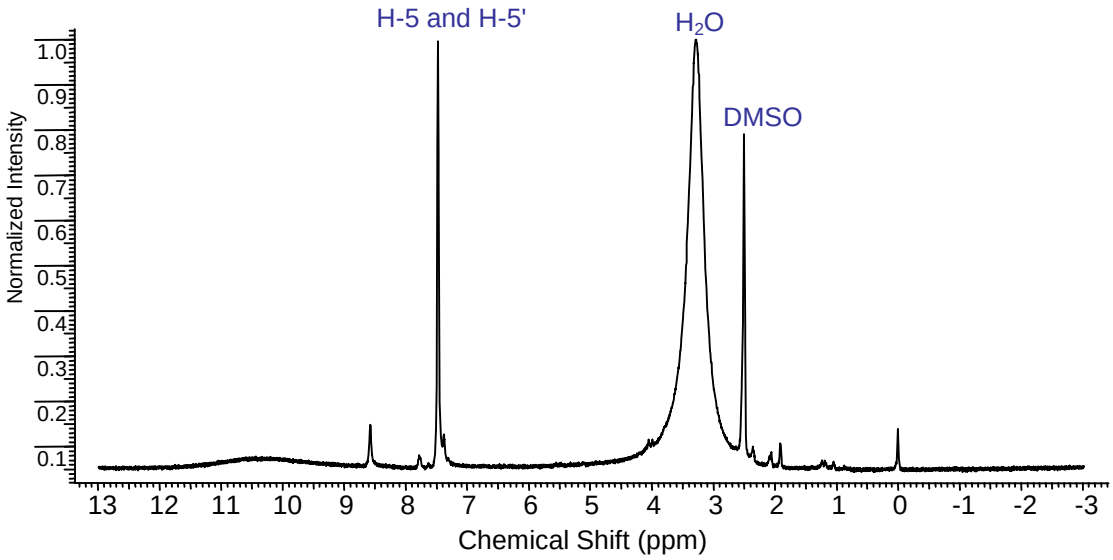

Figure 3.47. [1]H NMR spectrum of **S5**, 500 MHz, 35 °C, DMSO-d_6-D_2O (1:1).

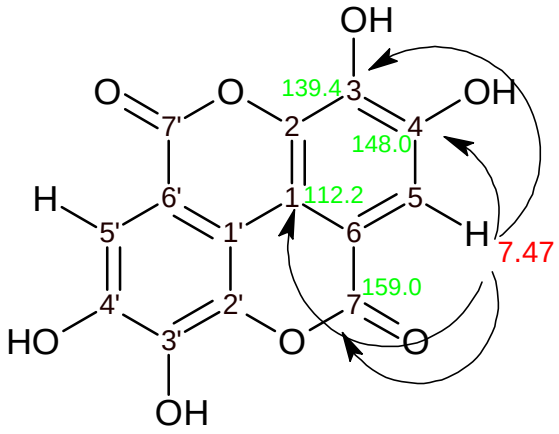

Figure 3.48. HMBC correlations and structure of **S5**. Chemical shifts are presented in ppm (green: ^{13}C, red: ^{1}H).

III.4.1.4. Structure determination of compound S7

Compound **S7** was isolated from fraction D by semi-preparative HPLC as a yellow brownish amorphous powder. The high resolution mass spectrum ESI-TOF-MS in negative mode provided a pseudo-molecular ion at *m/z* 461.0701 $[M-H]^-$ (Figure 3.49), calculated for $C_{21}H_{17}O_{12}$, 461.0720. The molecular formula was deduced to be $C_{21}H_{18}O_{12}$, which corresponds to that of at least three known ellagic acid derivatives (Table 3.16). The NMR analyses were thus necessary for the determination of the structure.

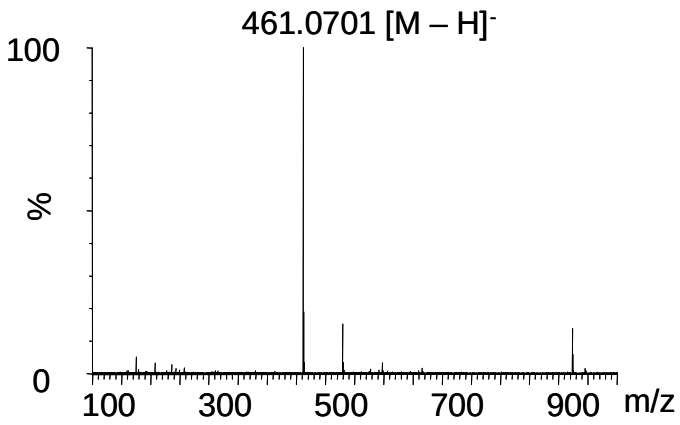

Figure 3.49. ESI-TOF-MS spectrum in negative mode of compound **S7**.

The ^{1}H NMR spectrum of **S7** (Figure 3.50) shows the presence of two aromatic protons at δ_H 7.75 and 7.51, indicating that the substitution of ellagic acid hydroxyl groups was not symmetric. A methoxyl group at δ_H 4.04, a sugar moiety with an anomeric proton at δ_H 5.46 and a methyl group at δ_H 1.14 were also observed. These data corroborate the hypothesis of a methylellagic acid rhamnoside. The ^{1}H NMR spectrum in the sugar regions exhibited five signals corresponding to methine protons and a methyl group. An additional methine proton was observed in the HSQC spectrum at δ_H 3.34 (coupling with a carbon at δ_C 71.3). This signal cannot be seen in the ^{1}H NMR spectrum due to overlap with the solvent signal. The connectivity between protons of the sugar moiety was established by the COSY spectrum, confirming the hypothesis of a rhamnoside. However, the resolution obtained in ^{1}H NMR spectrum did not allow the determination of the coupling constant for the anomeric proton. The HMBC and NOESY spectra were analyzed in order to determine the attachment position of the sugar moiety and the methoxyl group in the molecule. The main correlations observed in the HMBC spectrum (Appendix 9) are represented in Figure 3.51.

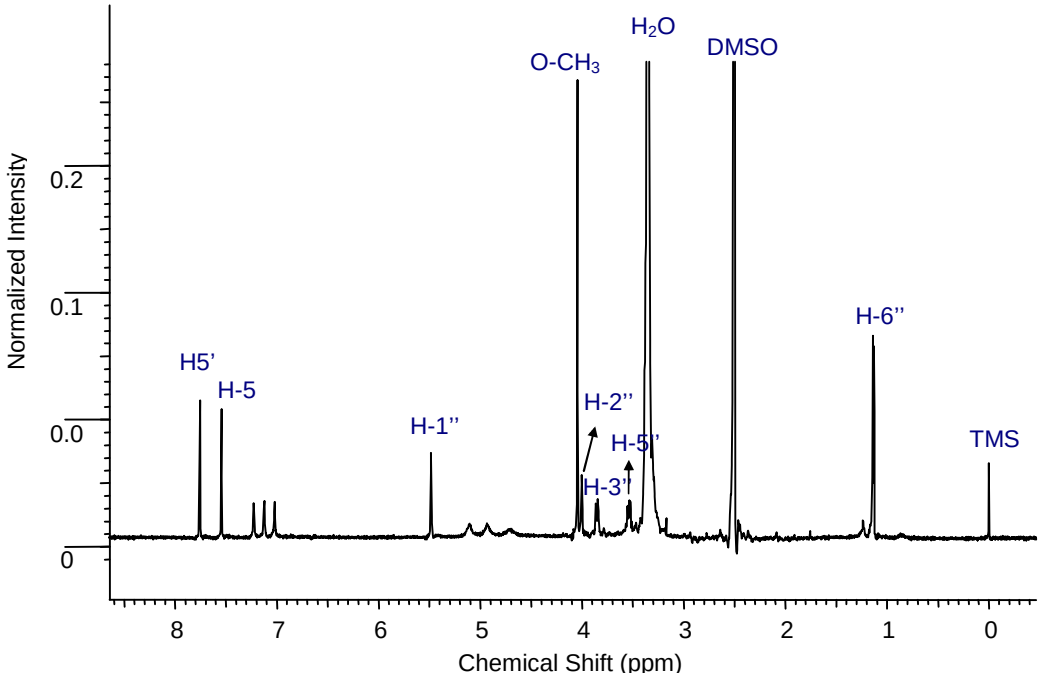

Figure 3.50. ^{1}H NMR spectrum of **S7** (500MHz, 35 °C, DMSO-d_6).

According to previous work (Elkhateeb *et al.*, 2005), a 4-*O*-methylellagic acid derivative presents a correlation between the methoxyl signal and H-5 in the NOESY spectrum. Such correlation could not be observed in the NOESY spectrum of **S7**. Moreover, both the methoxyl signal and H-5 presented a cross-peak with a carbon at δ_C 140.0 (C-3) in the HMBC spectrum, confirming that the methoxyl group was attached to position 3. Furthermore, the ^{13}C shift of 69.8 ppm (Table 3.18) was different from that of ca. 57 ppm, the typical value of an *O*-methyl substitution at C-4 of ellagic acid (Khallouki *et al.*, 2007). Finally, the evidence of an HMBC correlation between H-1'' and C-3' allowed the elucidation of **S7** as the ellagic acid derivative 3-*O*-methylellagic acid 3'-*O*-α-L-rhamnopyranoside.

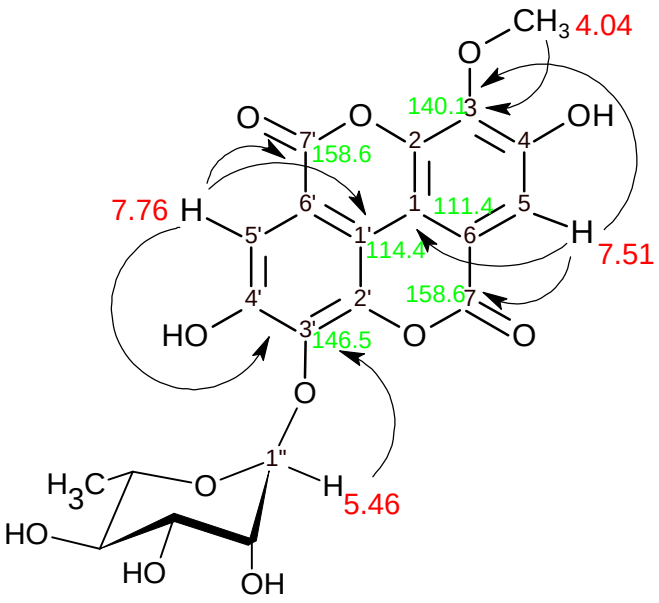

Figure 3.51. Structure and important HMBC correlations and structure of **S7**. Chemical shifts are presented in ppm (green: ^{13}C, red: ^{1}H).

III.4.1.5. Structure determination of compound S8

Compound **S8** was isolated form fraction D as a yellow amorphous powder. The high resolution mass spectrum HRESIMS in positive mode provided a pseudo-molecular ion at *m/z* 513.0652 $[M + Na]^+$, calculated for $C_{22}H_{18}O_{13}Na$, 513.0640. The deduced molecular formula of $C_{22}H_{18}O_{13}$ corresponds to the pseudo-molecular ion of compound **S8** in the HPLC/UV/ESIMS analysis of the aqueous extract, in negative mode (*m/z* 489.0 $[M-H]^-$, Figure 3.37). According to the literature, this molecular formula corresponds to that of several ellagic acid acetyl-rhamnopyranosides. Some examples are ellagic acid 2-*O*-α-L-2''-; 2-*O*-α-L-3''-; 2-*O*-α-L-4''-; 4-*O*-α-L-2''-; and 4-*O*-α-L-3''-*O*-acetyl-rhamnopyranoside, all of them isolated from the root bark of *Siphoneugena densiflora* Berg, another species from the family Myrtaceae (Gallo *et al.*, 2006).

The presence of an acetyl substituent could be confirmed by the analysis of the ^{1}H NMR spectrum (Figure 3.52) that presented a singlet integrating for three protons at δ_H 2.16, which presented a cross-peak with a carbon at δ_C 172.8 (C-7'') in the HMBC spectrum (Appendix 10). Moreover, the singlet at δ_H 1.29 ($-CH_3$) corroborates the hypothesis of a rhamnoside.

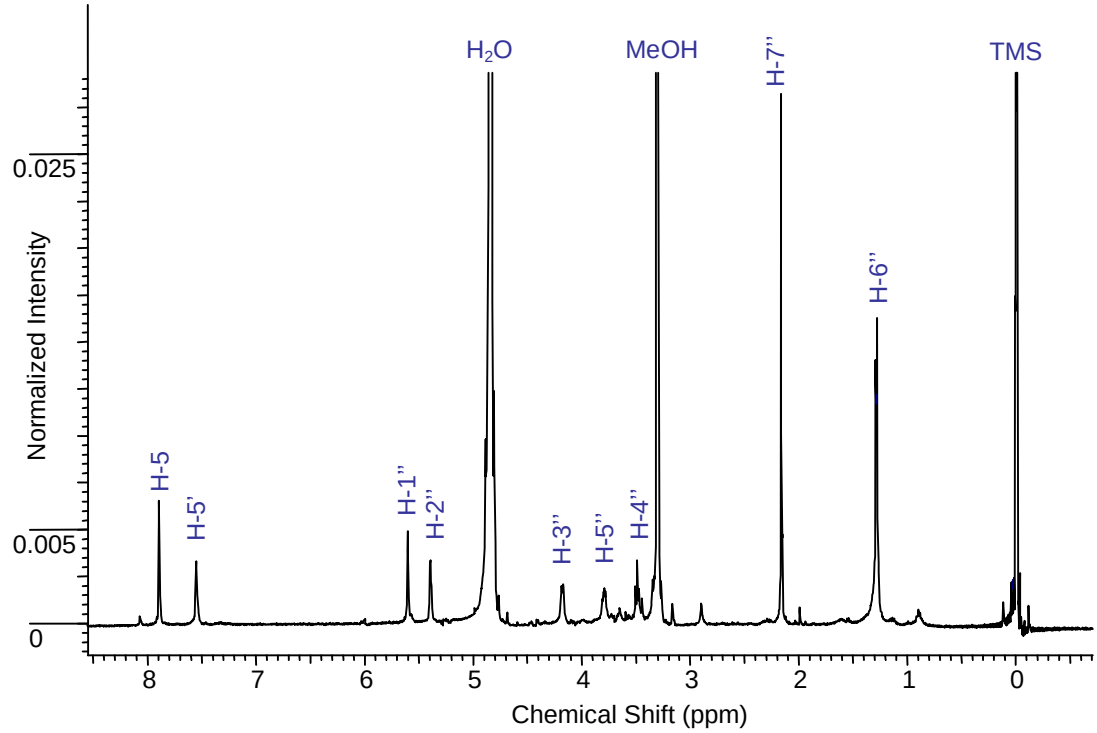

Figure 3.52. ^{1}H NMR spectrum (500MHz, 27 °C, CD_3OD) of **S8**.

The connectivity between protons of the sugar moiety was established by the analysis of the COSY, NOESY and HMBC correlations, confirming the hypothesis of an acetylated rhamnoside. The main NOESY and COSY correlations for the sugar moiety as well as the NOESY spectrum of **S8** are shown in Figure 3.53. The downfield shift of H-2'' (δ_H 5.39) in comparison to other ellagic acid rhamnosides (Table 3.17) allowed to determine the attachment of the acetyl group to C-2'' (δ_C 72.2).

Finally, the NOESY spectrum for compound **S8** presented a correlation between the anomeric proton (H-1'') and H-5, which is consistent with a sugar substitution at position 4 of ellagic acid. The compound was then identified as ellagic acid 4-*O*-α-L-2''-acetylrhamnopyranoside and its main HMBC and NOESY correlations are represented in Figure 3.54.

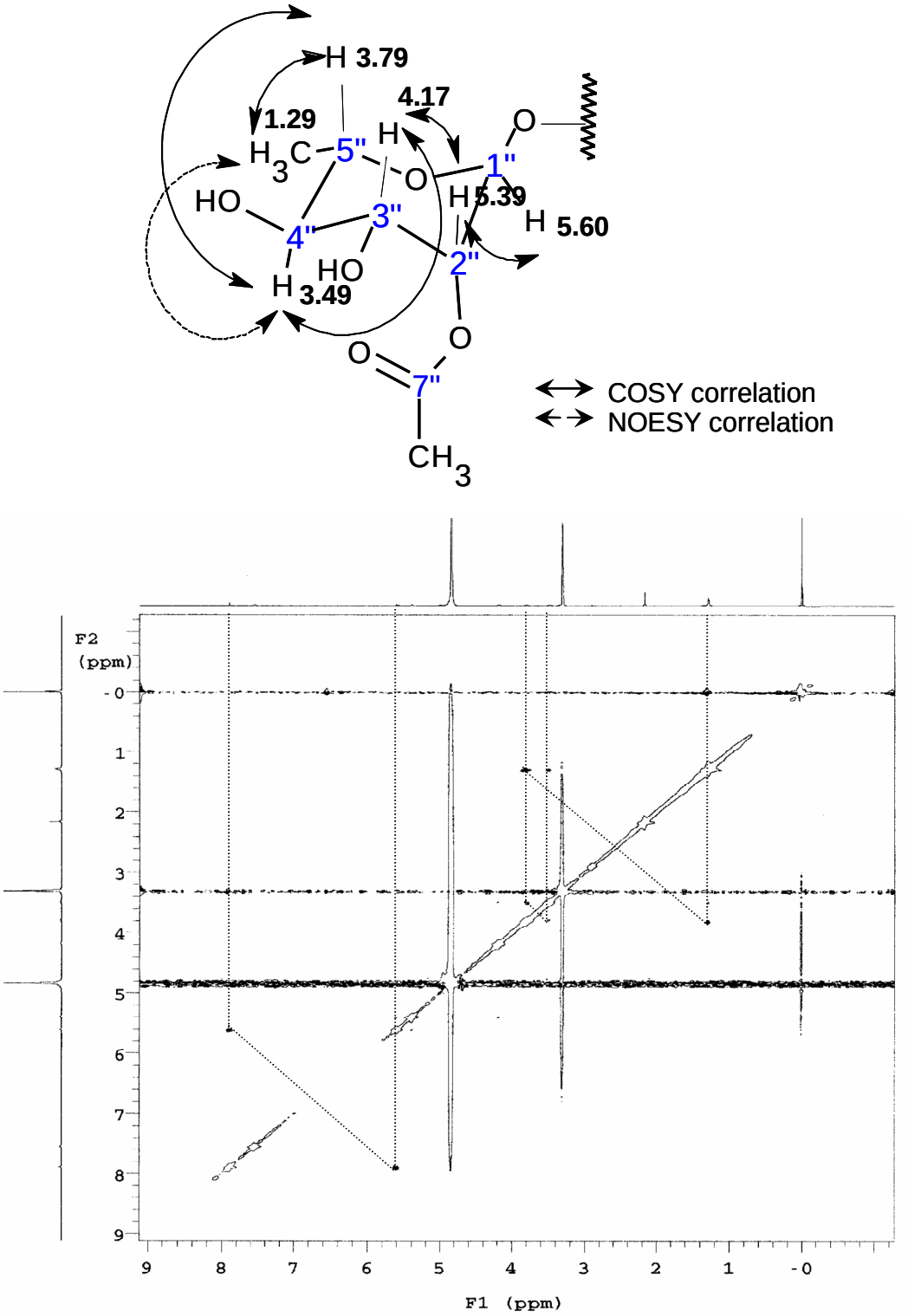

Figure 3.53. COSY and NOESY correlations observed for the acetylrhamnoside moiety of **S8**. NOESY spectrum (500 MHz, 27 °C, CD_3OD).

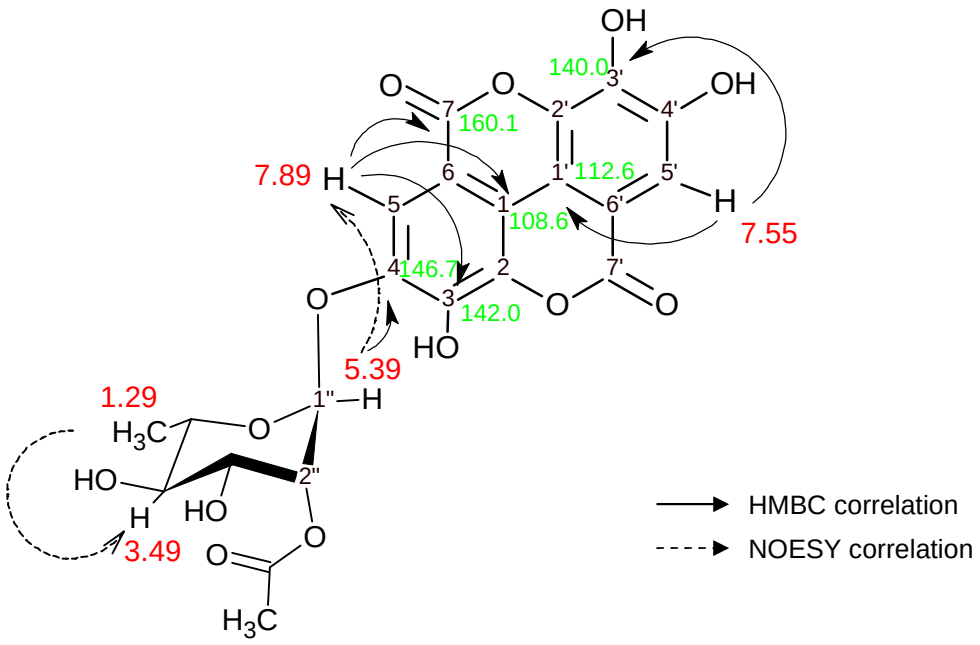

Figure 3.54. Structure, HMBC and NOESY correlations for compound **S8**. Chemical shifts are presented in ppm (green: ^{13}C, red: ^{1}H).

Table 3.17. 500 MHz ^{1}H NMR data of isolated ellagic acid derivatives*

Compound Position	S4[a]	S5[b]	S7[c]	S8[d]
5	7.49 (s)	7.47 (s)	7.51 (s)	7.89 (s)
3-OMe	4.05 (s)		4.04 (s)	
5’	7.71 (s)	7.47 (s)	7.76 (s)	7.55 (s)
1’’	5.06 (brs)		5.46 (brs)	5.60 (brs)
2’’	4.07 (brs)		4.00 (brs)	5.39 (brs)
3’’	3.52 (d, 9.8)		3.85 (dd, 3.3, 9.3)	4.17 (d, 6.3)
4’’	3.48 (brs)		3.34 (brs)	3.49 (t, 9.7)
5’’	3.73 (brs)		3.54 (dd, 6.2, 9.5)	3.79 (dd, 6.3, 9.3)
6’’	3.51[e]		1.14 (d, 6.0)	1.29 (d, 5.9)
8’’				2.16 (s)

*Chemical shifts relative to TMS (ppm) with multiplicity and important *J* couplings (Hz) in parentheses; [a]DMSO-*d6* at 40 °C; [b]DMSO-*d6* – D_2O (1 :1) at 35 °C, [c]DMSO-*d6* at 35 °C; [d]CD_3OD at 27 °C. [e] δ (ppm) obtained from the HSQC spectrum due to the overlap with solvent/water signal.

Table 3.18. ^{13}C NMR data of isolated ellagic acid derivatives*

Compound Position	S4[a]	S5[b]	S7[c]	S8[d]
1	112.5	112.2	111.4	108.6
2	nd	136.3	nd	nd
3	140.2	139.4	140.1	142.0
4	149.3	148.0	152.7	146.7
5	111.1	110.2	111.4	112.8
6	nd	149.5	113.0	nd
7	159.2	159.0	158.6	160.1
3-OMe	64.5		69.8	
1’	115.6	112.2	114.35	112.6
2’	nd	136.3	nd	nd
3’	141.6	139.4	146.5	140.0
4’	147.5	148.0	141.2	150.1
5’	112.2	110.2	111.2	111.1
6’	nd	149.5	107.2	nd
7’	159.5	159.0	158.6	160.8
1’’	nd		100.1	97.8
2’’	75.1		69.9	72.2
3’’	nd		70.0	69.1
4’’	74.2		71.7	72.8
5’’	nd		69.8	70.5
6’’	69.49		17.8	16.15
7’’				172.8
8’’				19.8

*Chemical shifts relative to TMS (in ppm). [a]DMSO-*d6* at 40 °C; [b]DMSO-*d6* – D_2O (1 :1) at 35 °C, [c]DMSO-*d6* at 35 °C; [d]CD_3OD at 27 °C.
nd=not detected.

III.4.2. Antiplasmodial activity of isolated compounds

The compounds isolated by semi-preparative HPLC were all tested *in vitro* against *P. falciparum*, and for their *in vitro* cytotoxicity on human fibroblasts or mice splenocytes. Samples were also screened against other parasites such as *Trypanosoma cruzi* and *T. b. brucei*. Results are presented in Table 3.19.

Table 3.19. Antiparasitic activity and cytotoxicity of compounds isolated from *S. cumini*.

Activity / Compound	Anti-*P. falciparum*[a,b]	Anti-*T. cruzi*[a,c]	Anti-*T. b. brucei*[a,d]	Cytotoxicity[a,e]
	IC_{50} (µM)			
S1	>32.00	7.29	6.00	29.41
S4	>32.00	>32.00	>32.00	>32.00
S5	2.78	>32.00	0.82	>32.00
S7	>32.00	>32.00	>32.00	>32.00
S8	>32.00	>32.00	>32.00	>32.00

[a]cf Experimental section V.6.2 for experimental assay description;
[b]IC_{50} >16 µM: inactive; IC_{50} between 2 and 16 µM: moderately active; IC_{50} <2 µM: highly active;
[c]IC_{50} >30 µM: inactive; IC_{50} between 2 and 30 µM: moderately active; IC_{50} <2 µM: highly active;
[d]IC_{50} >5 µM: inactive; IC_{50} between 1 and 5 µM: moderately active; IC_{50} <1 µM: highly active;
[e]tested on human fibroblasts (MRC-5 cell line); IC_{50} >30 µM: not toxic; IC_{50} between 10 and 30 µM: moderately toxic; IC_{50} <10 µM: highly toxic.

Ellagic acid (**S5**) presented a moderate activity against *P. falciparum* with an IC_{50} value of 2.78 µM. It was also considered highly active against *T. b. brucei* and presented no toxicity on human fibroblasts. When the isolated compounds were tested for the inhibition of β-hematin formation, only gallic acid (**S1**) and ellagic acid (**S5**) presented significant inhibition (Figure 3.55). Throughout the validation process of the in-house β-hematin assay, gallic acid was actually considered as an interfering compound, with no reduction of *in vitro* parasitaemia.

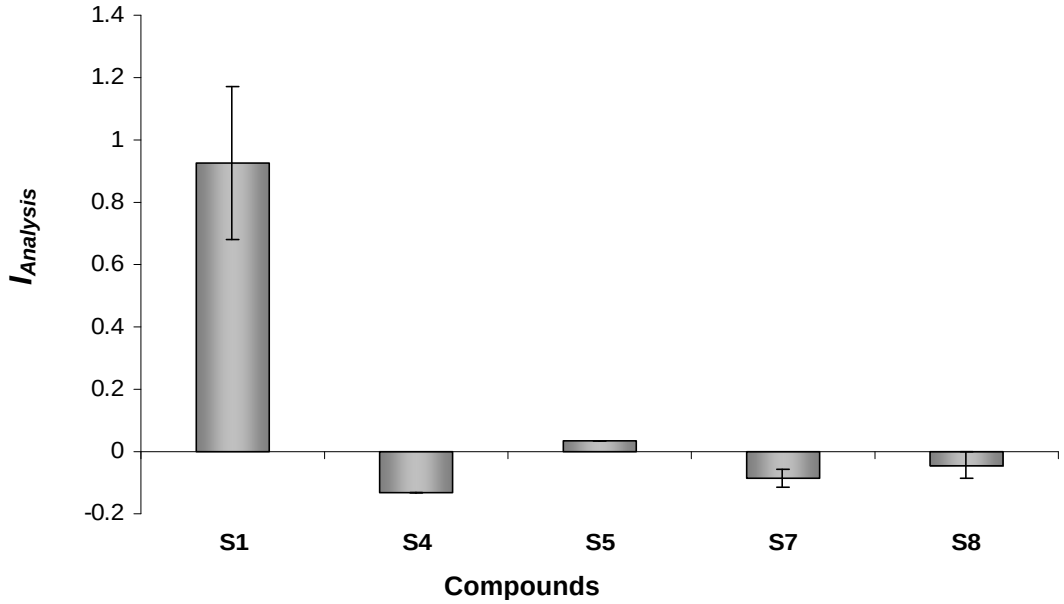

Figure 3.55. Inhibition of β-hematin formation by isolated compounds. Significant inhibition is denoted by positive values for $I_{Analysis}$.

On the other hand, ellagic acid has previously been studied for its activity against *P. falciparum in vitro* and it was identified as the active constituent of *Alchornea cordifolia* (Schumach. & Thonn.) Müll. Arg. (Euphorbiaceae), a plant recommended by traditional healers to treat malaria in Ivory Coast (Banzouzi *et al.*, 2002). Its mechanism of action was further studied *in vitro* based on two metabolic reactions necessary for the erythrocytic parasite form: the haemoglobin proteolysis by plasmepsin II and the detoxification of haematin into β-hematin. Ellagic acid and its derivative 3,4,5-trimethoxyphenyl (6'-*O*-galloyl)-β-D-glucopyranoside (TMPGG) were able to inhibit recombinant plasmepsin II with IC_{50} values of 4.02 and 8.74 µM, respectively. The authors considered these concentrations too high to account for the antiplasmodial activity. However, ellagic acid was able to inhibit β-haematin formation, which was then considered to explain the antiplasmodial *in vitro* activity (Dell'Agli *et al.*, 2003). In fact, ellagic acid has a flat molecular structure with a high electronic density, and thus would be able to form π-π interaction complexes with hematin monomers, inhibiting their association to form β-hematin. Another possible mechanism raised by Dell'Agli *et al.* (2003) to explain the

inhibition of β-hematin formation *in vitro* is the formation of coordination bonds between the Fe(III) of hematin and the aryl hydroxyl groups of ellagic acid, instead of the carboxylic acid group of another hematin monomer. In fact, in coordination complexes, a Lewis base donates its free pair of electrons to a metal cation, which acts as a Lewis acid. Ellagic acid is a weak Brønsted-Lowry acid, providing a conjugate base in aqueous solution, which is also considered as a Lewis base and could thus donate electrons to Fe(III) of hematin.

The *in vivo* properties of ellagic acid in malaria treatment have been already published on the rodent strain of the malaria parasite, *P. vinckei petteri* (Soh *et al.*, 2009). Interestingly, ellagic acid showed an ED_{50} lower than 1 mg/kg and 100% inhibition of parasite growth at 50 and 100 mg/kg when administered by intraperitoneal route. On the other hand, the oral administration showed very low inhibition of parasite growth.

One possible explanation for the lower effect of oral ellagic acid is the poor solubility of this compound, thus leading to poor oral absorption. According to the results presented in Table 3.18, ellagic acid heterosides isolated from *S. cumini* are not active *in vitro* compared to ellagic acid itself. However, in the case of oral administration, it is possible that they act as prodrugs. Thus, the *in vivo* antimalarial investigation of ellagic acid derivatives after oral administration is worthwhile.

Chapter IV

Conclusions and perspectives

The first part of this work, consisting of the screening of various plant extracts for antiparasitic activity, denoted that activity was difficult to detect in crude plant extracts without any pre-treatment of the samples. When the extracts were fractionated into major fractions, antiparasitic activity could be determined, allowing the selection of three plants for bio-guided fractionation and isolation steps: *Argemone mexicana* L. (Papaveraceae), *Licania octandra* (Hoffmanns. ex. Roem & Schult) Kuntze (Chrysobalanaceae), and *Syzygium cumini* (L.) Skeels (Myrtaceae). Conclusions and perspectives related to the results for each studied plant will be separately stated along this chapter.

IV.1. *Argemone mexicana*

A. mexicana was selected to be included in the screening tests due to the ethnopharmacological use of its traditional preparation as an antimalarial. The studied samples were clinical plant batches originating from a prospective, quasi-experimental clinical trial conducted together with a traditional healer in Mali (Willcox *et al.*, 2007). The study arose from a collaboration project between the non-governmental organization Antenna Technologies (Geneva, Switzerland) and the Department of Traditional Medicine of the Ministry of Health in Mali.

The first step in the study of *A. mexicana* decoctions was to analyze the HPLC/UV/MS profile of the extracts from different batches. This step allowed the on-line identification of the quaternary protoberberine alkaloid berberine. This alkaloid has previously demonstrated good antiplasmodial activity *in vitro* (Osorio *et al.*, 2008), but poor or no antimalarial activity in *Plasmodium* spp. infection in *in vivo* models (McCall *et al.*, 1994; Vennerstrom and Klayman, 1988). Considering the poor oral absorption of berberine (Bao *et al.*, 1997) and the amount of berberine previously found in *A. mexicana* non-clinical batches (20 mg/L) (Diop, 2006), it was important to pursue a bio-guided fractionation in order to check fractions of different polarities for the presence of active compounds that could contribute to the clinical efficacy of the traditional preparation. The bioassay guided fractionation was able to detect good antiplasmodial activity in an alkaloid-enriched CH_2Cl_2 fraction from the decoction.

Further fractionation procedures conducted with *A. mexicana* traditional preparation led to the isolation of three known alkaloids, allocryptopine, berberine and protopine, which have already been found in *A. mexicana* alkaloid extracts. However, this is the first report on the presence of these alkaloids in a traditional decoction to our knowledge. All isolated alkaloids could be tested *in vitro* against *P. falciparum*, as well as for their cytotoxicity and against other parasites, and presented good activity against a chloroquine-resistant strain of the malaria parasite. Nevertheless, it was noticed that the activity of berberine was non-specific. Similarly to the standard compound sanguinarine, a known toxic compound responsible for the toxicity of *Argemone* oil, berberine was active against other parasites and was highly cytotoxic on human fibroblasts. On the other hand, the two protopine-type isolated alkaloids allocryptopine and protopine were specifically active against *P. falciparum* and were not considered cytotoxic. When isolated compounds were tested for the inhibition of β-hematin formation, only allocryptopine showed significant inhibition.

Allocryptopine, berberine and protopine have a common feature with regards to their *in vivo* cardiac effects reported in the literature. Berberine itself has been used in Chinese medicine to treat arrhythmia and was denoted to prolong the duration of cardiac action potentials *in vitro* (Wang and Zheng, 1997). Similar effects were observed for allocryptopine and protopine (Li *et al.*, 2008; Yu *et al.*, 1999). Thus, the presence of these alkaloids in the traditional preparation could partially explain the adverse cardiac effects (increased QT intervals in ECG) observed in a few patients during the clinical assay conducted with *A. mexicana* decoction. Nevertheless, the exact mechanism of action of these alkaloids on the heart is still not clear, and different authors claim diverse mechanisms of action for each molecule (Li *et al.*, 2005; Li *et al.*, 2008; Rodriguez-Menchaca *et al.*, 2006). As a good perspective within the study of efficacy and safety of *A. mexicana* decoction, the mechanisms of action for the antiplasmodial activity and the cardiac effects of the active alkaloids should be investigated. A critical comparative study should also be designed in terms of isolated compounds with the aim of establishing the cardiotoxicity-antimalarial activity ratio. Moreover, the investigation of the protopine-type alkaloids together with berberine for the antimalarial activity using *in vivo* models is worthwhile.

A QNMR method could be successfully developed in order to rapidly determine the amount of active alkaloids in traditional preparations of the clinical batches. The obtained results revealed good concentrations of allocryptopine (from 110 to 180 mg/L), berberine (from 70 to 110 mg/L), and protopine (from 60 to 120 mg/L). The variation of the alkaloid content between the two analysed clinical batches could not be explained and several factors could contribute to this, such as differences in edafoclimatic conditions, period of collection, and differences in plant powder granulometry. Additionally, the concentration of berberine in clinical batches was, on average, 4 times the one previously established (20 mg/L) in non-clinical batches by semi-quantitative TLC and quantitative HPLC/UV methods (Diop, 2006). Since the extraction procedure was slightly different and batches were not exactly the same, the semi-quantitative TLC method was reproduced for the clinical batches using the same extraction procedures as the QNMR method. The amount of berberine found was once again of about 20 mg/L in all analysed clinical batches. In the TLC method, the recovery of berberine in spiked decoctions was very low (from 2.3 to 4.3 %). This probably means that the image of the TLC spots of berberine for the recovery sample solutions were saturated, and berberine could not be determined at concentrations higher than 20 mg/L. As a perspective in the research of suitable methods for assessing active compound concentration in *A. mexicana* decoction, some adaptations on the method could be proposed, such as establishing the superior limit of detection of the technique. Also, a semi-quantitative TLC method could be developed for the analysis of protopine, since this alkaloid presented some fluorescence and had an R_f value different from that of berberine. Even though semi-quantitative TLC methods seem the most suitable in the case of a low-cost quality control of an improved traditional medicine in Mali, the investigation of other methods, as photocolorimetric measurements, for instance, should be also taken into consideration in future research projects.

IV.2. *Licania octandra*

L. octandra presented a good antiplasmodial activity linked to the ethyl acetate fraction obtained from the hydroalcoholic extract of leaves. The HPLC/UV/MS analysis of the active fraction showed the presence of flavonoids, which could be concentrated into three major CPC fractions. When on-line dereplication was considered, six compounds

(**L2**-**7**) had their structure partially determined by means of MS and derivatization-UV analyses. Three compounds had their structure confirmed after isolation: (2R,3R)-taxifolin 3-*O*-β-D-xylopyranoside (**L2**), myricetin 3-*O*-α-L-rhamnopyranoside (**L4**) and quercetin 3-*O*-α-L-rhamnopyranoside (**L6**); while three other compounds had their structure inferred by dereplication techniques: taxifolin xyloside/arabinoside (**L3**), quercetine glucoside/galactoside (**L5**) and quercetin (**L7**).

Isolated compounds and their aglycones were tested against *P. falciparum* as well as other parasites, and their cytotoxicity was assessed on human fibroblasts. Among the tested compounds, quercetin was the most active with an IC_{50} value of 3.94 µg/mL. The 3-OH substitution of this flavonoid, as in **L6**, seemed to decrease toxicity and activity. However, **L6** was considered moderately active.

Myricetin and its 3-OH substituted derivative (**L4**) were also considered moderately active and, in this specific case, the 3-OH substitution did not seem to change the antiplasmodial activity.

Neither taxifolin nor its derivative **L2** presented any activity or toxicity. As a matter of fact, **L2** had the highest IC_{50} value on *P. falciparum* among studied flavonoids. Its main structural difference was the saturation between C-2 and C-3.

Some flavonoids have previously been studied for antimalarial activity *in vitro* and *in vivo*. While *in vitro* activity is well established and structure-activity relationships have been studied to some extent (Tasdemir *et al.*, 2006), the *in vivo* antimalarial activity of flavonoids is still controversial (Chen *et al.*, 1997; Portet *et al.*, 2007). The association of flavonoids with artemisinin seems to increase its activity and it was shown to play an important role in the interaction between artemisinin and hemin, especially methoxyflavones and chalcones (Bilia *et al.*, 2002). Thus, the mechanistic study of antiplasmodial flavonoids with diverse structures is indicated in the search for antiplasmodial and synergistic antimalarial activities.

IV.3. *Syzygium cumini*

S. cumini stem bark has previously been studied, denoting the presence of ellagic and gallic acid derivatives, and flavonoids. However, a series of ellagitannins has not been structurally elucidated (Bhatia and Bajaj, 1975; Sharma *et al.*, 2009). In the present thesis, a series of ellagic acid derivatives could be identified together with ellagic acid. Thus, gallic acid (**S1**), ellagic acid (**S5**), 3-*O*-methylellagic acid 3'-*O*-α-L-rhamnopyranoside (**S7**), ellagic acid 4-*O*-α-L-2''-acetylrhamnopyranoside (**S8**) and the new compound 3-*O*-methylellagic acid 3'-*O*-β-D-glucopyranoside (**S4**) were isolated during the bioguided fractionation of the stem bark decoction. The structural analysis of this class of compounds was difficult due to solubility problems, hygroscopic nature of compounds and broadening of NMR signals.

The most active fraction obtained from the decoction was the one containing ellagic acid. In fact, this compound had already been studied for its antiplasmodial activity *in vitro* and *in vivo* and its mechanism of action was associated with the inhibition of β-hematin formation (Banzouzi *et al.*, 2002). When the *in vitro* antiplasmodial activity of the isolated compounds was determined, only ellagic acid showed reduction of parasitaemia. The isolated compounds were also evaluated for the inhibition of β-hematin formation. Gallic and ellagic acids were able to significantly inhibit this physico-chemical reaction. However, gallic acid was considered as an interfering compound of this specific assay and this result could not be taken into consideration. The ellagic acid derivatives were not able to inhibit hematin dimerization, which was in accordance with the claim that the aryl hydroxyl groups of ellagic acid would be able to form coordination bonds with the Fe(III) of hematin (Sharma *et al.*, 2009). Nevertheless, given that the metabolization of these derivatives after oral administration is unknown, the *in vivo* study of these compounds for antiplasmodial activity would be worthwhile in testing their ability to act as prodrugs.

Chapter V

Experimental section

V.1. Plant material and extraction

Licania octandra hydroalcoholic extract was provided by Professor Marçal Queiroz Paulo from the Federal University of Paraíba, João Pessoa, Brazil.

Leaves of *L. octandra* were collected in the city of João Pessoa, state of Paraíba, Brazil, in July 2004. They were dried at 60°C, grounded, and extracted in Soxhlet with EtOH-H_2O (80:20) for 12 hours. The extract was filtered and evaporated to dryness under reduced pressure.

Syzygium cumini extract was provided by Professor Marçal Queiroz Paulo from the Federal University of Paraíba, João Pessoa, Brazil.

Stem bark was collected in the city of João Pessoa, state of Paraíba, Brazil, in July 2004. They were dried at 60°C, grounded, and extracted by decoction for 15 min. The resulting extract was filtered and freeze-dried.

Twelve batches of powdered dried leaves of *Argemone mexicana* were provided by Antenna Technologies (Geneva, Switzerland). Four out of them corresponded to batches employed in a successful clinical assay conducted during a collaboration project between Antenna Technologies and the Department of Traditional Medicine (DTM) in Mali (Willcox *et al.*, 2007). The origin of the batches is described in the next paragraph.

AM 1: DTM, Mali 2007; AM 2: Missidougou, Mali, 2005 ; AM 3: DTM, Bamako Mali, 2005 ; AM 4: DTM, Bamako Mali, 2005 ; AM 5: DTM, Bamako Mali, 2005 ; AM 6: DTM, Bamako Mali, 2005 ; AM 7: San José, Costa Rica 2006; AM 8: DTM, Missidougou, Mali, 2004 = clinical batch 2, patients 190-238 (Willcox *et al.*, 2007); AM 9: DTM, Missidougou, Mali, 2006 = clinical batch 1, patients 001-189 (Willcox *et al.*, 2007); AM 10: Mali 2005 ; AM 11: DTM, Sikasso, Mali, 2006 = clinical batch 3, patients 239-301 (Willcox *et al.*, 2007); AM 12: DTM, Sikasso, Mali, 2006 = clinical batch 3, patients 239-301 (Willcox *et al.*, 2007).

The extracts were prepared as described for the traditional preparation. For isolation purposes, 500 g of batch AM 8 was extracted by decoction in 2 L of boiling distilled water for 3 hours. The extract was freeze-dried and provided 115 g of extract.

V.2. Analytical chromatographic methods

V.2.1. Thin layer chromatography (TLC)

TLC was used as the method of choice for routine phytochemical analyses of crude extracts, fractions and pure compounds. This technique was also used as a support for chemical and biological screening of extracts and pure compounds and semi-quantitative determination of compounds in plant extracts.

Commercially available TLC plates were used: Silicagel 60 F_{254} pre-coated TLC aluminium sheets (Merck, Darmstadt). The TLC plates were developed in twin trough Camag chromatographic tanks saturated with the appropriate eluent. The solvent systems, often consisting of a binary or tertiary mixture, were adapted to the specific needs of an analysis. The quantity of material applied to the plate was usually 50-100 μg of extracts, 10-50 μg of fractions and 5-10 μg of pure compounds. After migration, the detection of the main, characteristic compounds of a drug was carried out by the observation of the extinguishing of fluorescence under UV at 254 nm, the appearance of fluorescence under UV at 366 nm and the observation of colours after revelation with appropriate chemical reagents. General TLC conditions for extracts and fractions obtained from the plants investigated in this thesis are summarized in Table 5.1.

Table 5.1. Main TLC conditions applied to extracts and fractions according to the investigated plant

Plant species	Solvent system	Detection
Argemone mexicana	formic acid-water-ethyl acetate (1:2:7) chloroform-ethyl acetate-methanol (2:2:1)	Dragendorff Godin's reagent
Licania octandra	Ethyl acetate-acetic acid-formic acid-water (100:11:11:10) ethyl acetate-methanol-water (25:7.5:2) Isopropanol-water (85:15)	Godin's reagent
Syzygium cumini	Ethyl acetate-acetic acid-formic acid-water (100:11:11:10)	Godin's reagent

V.2.2. Semi-quantitative thin layer chromatographic assay

A previously validated semi-quantitative thin layer chromatographic method was used to determine the amount of active alkaloids in two clinical batches of *A. mexicana* (Diop, 2006). A standard solution of berberine was prepared at 1 mg/mL in MeOH. For the calibration, dilutions were made to provide 5 concentrations (40, 60, 80, 100 and 120 µg/mL). TLC plates (10x20 cm) were pre-eluted with MeOH and allowed to dry. Calibration solutions were spotted on plates (5 µL spots). The extracts were spotted in triplicate on the same plate. The chromatographic system was formic acid-water-ethyl acetate (1:2:7). After elution, the plate was allowed to dry at room temperature and the plate was observed under a UV lamp (366 nm). A digital picture was taken for each plate and treated with the software ImageJ, where the image was selected in the 8 bit format. The parameter “mean grey value” was measured for each selected berberine spot. The mean grey values for calibration were used to provide a calibration curve. The generated equation was used to determine the concentration of berberine in the extracts.

Determination of berberine concentration in the traditional preparation: the decoction was prepared as described for the traditional preparation for three available clinical batches: batch AM 8 (29.4497 g of powdered extract), AM 9 (10.2503 g of powdered extract) and batch AM 11 (10.1023 g of powdered extract). The weighed samples were added with 300.00 mL (batch AM 8) and 100.00 mL (batches AM 9 and 11) distilled water in a 500 mL Erlenmeyer flask. Flasks were weighted and allowed to boil for 3 hours. After that, the flasks were weighed at room temperature in order to establish the loss of water. Batch AM 8 provided 42.31 mL of tea, while batch AM 11 provided 60.51 mL. The resulting tea was filtered and 3 aliquots of 10.00 mL of each batch were transferred to individual centrifuge tube. Each sample was added of 20 mL CH_2Cl_2, shaken for 5 min and centrifuged at 5000 rpm. The supernatant was transferred to another centrifuged tube and the operation was repeated 4 times. The CH_2Cl_2 layers of each sample were grouped in a 100 mL round flask and evaporated to dryness. Each sample was recovered in 1 mL methanol and spotted in triplicate for TLC analysis.

V.2.3. High performance liquid chromatography coupled with ultraviolet detection (HPLC/UV-DAD)

In this study, analytical high performance liquid chromatography coupled with a diode array UV detector (HPLC/UV-DAD) was used to analyze qualitatively the investigated extracts and fractions and provide information on the UV spectra of detected compounds. It was also used to guide the separation and isolation processes, optimize the conditions for MPLC and semi-preparative HPLC, and check the purity of the isolated compounds.

The HPLC systems used for the different analyses were: an HP-1100 system (Hewlett Packard, Palo Alto, CA, USA) equipped with a binary pump, with a DAD and an autosampler; an HP-1090 series II system (Hewlett Packard, Palo Alto, CA, USA) including a quaternary pump, DAD and an autosampler. The components of these two HPLC systems were controlled by Agilent ChemStation 8.01 software. The HPLC conditions used for the analysis of extracts and fractions are summarized in Table 5.2

Table 5.2. HPLC/UV-DAD conditions according to the investigated plant.

	Argemone mexicana	***Syzygium cumini*** ***Licania octandra***
Column	Symmetry C_{18} (Waters, Milford, USA)	Zorbax Extend C_{18} (Agilent, Germany)
Column size	250 x 4.6 mm i.d., 5 μm	250 x 4.0 mm i.d., 5 μm
Solvent system	MeCN (+0.1% formic acid)-water (+0.1% formic acid)	MeOH (+ 0.1% formic acid)-water (+0.1% formic acid)
Gradient	5:95 during 5 min to 60:40 in 30 min, to 100:0 in 5 min, and 100:0 during 5 min	2:98 to 100:0 in 40 min, 100: during 5 min
Flow rate	1.0 mL/min	1.0 mL/min
Detection (UV-DAD)	254, 336 and 280 nm	210, 254 and 366 nm

V.2.4. High performance liquid chromatography coupled with mass spectrometry (HPLC/MS)

HPLC/UV/MS was employed for a preliminary study of plant extracts and fractions and as a useful tool in the dereplication of compounds by the on-line spectroscopic information.

All HPLC/UV/MS analyses were made on a Finnigan MAT (San José, CA, USA) LCQ ion trap mass spectrometer using electrospray ionization (ESI) interface.

The MS methods are detailed in Table 5.3. MS^n experiments were performed by programming dependent scan events. The first event was a full MS scan in the region 150.0–1500.0 (MS^1); during the second event the main ion recorded was isolated and selectively fragmented in the ion trap (MS^2).

Table 5.3. ESI-MS conditions according to the investigated plant.

	Investigated plant	
	Argemone mexicana	*Licania octandra* *Syzygium cumini*
ESI source		
Capillary temperature	350 °C	200 °C
Source voltage	4 kV	5kV
Source current	80 µA	80 µA
Corona needle current	5 µA	5 µA
Ionization mode	positive	negative
Sheath gas pressure	60 psi	80 psi
Collision energy	15eV	15eV

V.2.5. High performance liquid chromatography/ultraviolet detector (HPLC/UV-DAD) with post-column addition of UV shift reagents

HPLC/UV-DAD analyses with post-column addition of UV shift reagents were used as a useful dereplication tool for the analysis of flavonoid-enriched fractions. The method used for post-column addition of UV shift reagents was based on previously reported protocols (Simoes-Pires *et al.*, 2005; Wolfender and Hostettmann, 1993). For flavonoid analysis the following reagents were used: at room temperature: sodium acetate (weak base), potassium hydroxide (strong base) and sodium acetate/boric acid. The following solvents were used at 90°C (to ensure full complexation): aluminium chloride in acidic and non-acidic conditions.

The extracts were analysed by HPLC using an Agilent Zorbax Extend C_{18} column (250 x 4.0 mm i.d., 5 μm) eluted with a linear gradient of methanol–water containing 0.05% trifluoroacetic acid from 2:98 to 100:0 in 60 min). The flow rate was 0.6 mL/min; UV detection was at 210, 254 and 366 nm, and UV spectra (DAD) were recorded between 200 and 500 nm. For HPLC/UV-DAD analysis under weak base conditions, a first pump was used for the addition of sodium acetate (0.5 M, 0.2 mL/min) and a second for sodium hydroxide (0.01 M, 0.2 mL/min). The resulting pH in the eluent was 7. For strong base addition, the first pump was used to carry potassium hydroxide (0.3 M, 0.3 mL/min), resulting in a solution of pH 14. For the analysis with sodium acetate/boric acid, the first pump carried a mixture of 0.1 M sodium acetate and 0.7 M boric acid (1:1, 0.2 mL/min) and the second pump carried sodium hydroxide (0.01 M, 0.2 mL/min) giving a solution of pH 5. For the analysis with aluminium chloride under acidic conditions, only one pump delivered aluminium chloride (0.3 M, 0.2 mL/min) to final pH 3.5; whilst for non acidic conditions, a second pump was used to carry sodium hydroxide (0.01 M, 0.2 mL/min) to final pH 6. All reagent solutions were filtered through a Millipore 0.50 µm filter before use. Prior to analyzing the fraction, quercetin was used to test the effect of the UV shift reagents. Post-column addition of shift reagents and adjuvant bases was achieved by two Waters M-6000 pumps. Neutralization of the mobile phase was performed in an Upchurch mixer (Oak Harbor, WA, USA), while reaction with the shifts reagent was carried out in a 10 µL visco mixer from Lee (Westbrook, CO, USA) followed by a reaction coil. The reaction coil was placed in a column oven when temperature control was necessary. UV

spectra were recorded on a Hewlett Packard (Palo Alto, CA, USA) model HP-1050 PAD and data were processed using a HP Chemstation from Hewlett Packard

V.2.6. Ultra performance liquid chromatography coupled with high resolution mass spectrometry (UPLC/HR-TOF-MS)

UHPLC/HR-TOF-MS analyses were performed on a Micromass-LCT Premier Time of Flight mass spectrometer from Waters (Milford, MA, USA) with an electrospray (ESI) interface coupled with an Acquity UPLC system from Waters. Detection was performed in positive and negative ion modes during the same analysis in the range m/z 100-1000 in centered mode with a scan time of 0.2 s and an interscan delay of 0.3 s for polarity switching. ESI conditions in positive and negative modes were capillary voltage 2800 V, cone voltage 40 V, source temperature 120 °C, desolvation temperature 250 °C, cone gas flow 20 L/h, and desolvation gas flow 800 L/h. For internal calibration, a solution of leucine-enkephalin from Sigma-Aldrich (Steinheim, Germany) at 5 µg/mL was infused through the lockmass probe at a flow rate of 5 µL/min, using a second Shimadzu LC-10ADvp LC pump (Duisburg, Germany). The separation was performed on a 150 mm × 2.1 mm i.d., 1.7 µm, Acquity BEH C18 UPLC column (Waters) in the gradient mode at a flow rate of 0.3 mL/ min with the following solvent system: A) 0.1 % formic acid-water, B) 0.1 % formic acid-acetonitrile; 2-98% B in 7.0 min. The temperature was set at 30 °C. The injected volume was 5 µl.

V.3. Preparative and semi-preparative chromatographic methods

V.3.1. Vacuum liquid chromatography (VLC)

A VLC was conducted by filling a 250 mL support with the stationary C_{18} phase LiChroprep® 40-63 µm, (Merck, Darmstadt, Germany). The support was connected to a vacuum system. The stationary phase was first eluted with MeOH (5 x 250 mL) for conditioning followed by water (for equilibrating). The sample was diluted in 100 mL water and introduced into the support. The elution of the sample was first conducted with 600 mL water, followed by 600 mL MeOH.

V.3.2. Centrifugal partition chromatography (CPC)

CPC fractionations were conducted on a counter-current chromatograph CCC-1000 (Pharma-Tech Research Corp.) equipped with dynamic coils of 650 mL total volume. The rotation speed was set at 1000 rpm. Two LC-300 pumps (Scientific Systems Inc.) were used in order to pump the same volume of each of both liquid phases into the coils at a flow rate of 3.0 mL/min for each phase. Once the coils were filled, the chosen mobile phase was pumped alone and the CCC module was adjusted for the desired elution mode: 1) head to tail, if the lower phase was the mobile phase or 2) tail to head, if the upper phase was the mobile phase. The sample was diluted in 30 mL of a mixture of upper and lower phases (1:1) and injected through the injection coil. A UV-visible Knauer detector was coupled with chromatographic system followed by a Tarkan 600 recorder and an automatic sample collector LKB Bromma 2070 Ultrorac® II. By the end of the initial elution, an inversion of elution mode was conducted (phase inversion).

V.3.3. Size exclusion liquid chromatography

Size exclusion liquid chromatography was conducted using Sephadex LH-20 gel (G.E. Healthcare) as stationary phase and MeOH as the mobile phase. Samples were diluted in up to 1 mL MeOH to be applied onto the column and eluted with MeOH.

V.3.4. Medium pressure liquid chromatography (MPLC)

The equipment used consisted of a Büchi B-681 pump, a Büchi B-687 gradient device, a Knauer K 2001 UV detector, a Pharmacia LKB Rec 1 recorder and an automatic Büchi B-684 fraction collector. A Lichroprep® C_{18} stationary phase (15-25 µm, Merck) was used for all separations and it was packed in a pressure-resistant column of variable size, depending on the sample amount. The choice of the solvent system was performed by analytical HPLC/UV and transposed directly to MPLC. A stepwise gradient of MeOH-water was employed as mobile phase, starting at 5:95 and gradually increased to 100:0, according to the on-line UV chromatogram profile. The maximal pressure was set to 20 bars and the samples were placed in an introduction cartridge after being mixed with 3 times its weight of stationary phase.

V.3.5. Semi-preparative high performance liquid chromatography (SPHPLC)

SPHPLC was used in order to purify the compounds from pre-purified fractions. The equipment was a Shimadzu LC-8A binary pump equipped with a SPD-10A VP Shimadzu UV-Vis detector (Kyoto, Japan). The flow rate was set to 10 mL/min. For *A. mexicana* fractions, an Xterra Prep MS C_{18} OBD™ column (150 x 19 mm i.d., 5 *µ*m) was employed for the separations and the solvent system was A) Water and B) MeOH. An isocratic mode at 5% B was applied for fraction AM 8_A_2, while an isocratic mode at 42% was chosen for fractions AM 8_D_1, AM 8_D_2. In the case of *Licania octandra*, a µBondapak® C_{18} pre-packed column (100 x 25 mm i.d, 10 µm) placed in a radial compression module (Milford, MA, USA) was employed. The solvent system was A) water + 0,05% TFA and B) MeOH + 0,05% TFA, at 30% B in isocratic mode. In the case of *Syzygium cumini*, the same solvent system as *L. octandra* was used, and a Symmetry Prep™ C_{18} column (150 x 19 mm i.d., 7 µm) was employed. The isocratic mode at 30% B was chosen for fraction C_3, while, 35% B was chosen for fraction D.

V.4. Physico-chemical methods

V.4.1. Optical rotation ($[\alpha]_D$)

The optical rotation of the pure compounds was measured on a Perkin-Elmer 241 polarimeter (Wellesley, MA, USA) with the sodium D line (589.3 nm) as the source of light. The measurements were made at 20 °C in a 10 cm cell. The results were calculated with the following formula:

$$[\alpha]_D^{20°C} = \frac{1000 \cdot \alpha}{l \cdot c}$$

α = observed rotation

l = cell length in dm

c = concentration in g/100 mL

V.4.2. Infrared spectrophotometry (IR)

The IR spectra of the pure compounds were obtained on a Perkin-Elmer 1600 FTIR instrument (Wellesley, MA, USA). The technique used for the preparation of the solid sample was the formation of KBr pellets. Generally 1 mg of the isolated compound was mixed with 200 mg of dry KBr. This mixture was finely ground using a ball mill, and pressed to a transparent disk. The spectra of the disks were recorded versus the empty reference beam (4 scans, 2.0 cm^{-1}, 500-4000 cm^{-1}).

V.4.3. Ultraviolet spectrophotometry (UV)

The UV spectra of the isolated compounds were recorded in methanol on a Perkin-Elmer Lambda 20 spectrophotometer (Wellesley, MA, USA). Quartz cells were used for samples and blanks. The results were reported in nm as the wavelength of the maxima.

V.4.4. High resolution mass spectrometry (HRMS)

High resolution mass spectra were obtained on a Micromass-LCT Premier Time of Flight (TOF) mass spectrometer (Waters, MA, USA) with an electrospray interface and coupled with an Acquity UPLC system (Waters, MA, USA). ESI conditions: capillary voltage 2800V, cone voltage 40V, MCP detector voltage 2650 V, source temperature 120 °C, desolvation temperature 250 °C, cone gas flow 10 L/h, desolvation gas flow of 550 L/h. Detection was performed in positive and negative ion modes in the m/z range 100–1000 with a scan time of 0.25 s in centroid mode. For the dynamic range enhancement (DRE) lockmass, a solution of leucine–enkephalin (Sigma–Aldrich, Steinheim, Germany) at 5 µg/mL was infused through the lockmass probe at a flow rate of 20 µL/min with the help of a second LC pump (Shimadzu LC-10ADvp, Duisburg, Germany). The separations were carried out on Waters Acquity UPLC columns at 30 °C (BEH C18: 50 mm x 1.0mm, 1.7 µm) with the following solvent system: A) 0.1% formic acid–water, B) 0.1% formic acid–acetonitrile. The gradient elution was performed at a flow rate of 300 µL/min using: 5% B for 0.3 min, 5–98% B in 4 min and holding at 98% B for 2 min.

V.4.5. Nuclear magnetic resonance spectrometry (NMR)

Nuclear magnetic resonance spectrometry (NMR) was used as the main analytical method for the structural elucidation of the isolated compounds. The ^{1}H and ^{13}C NMR spectra were recorded on a Varian Inova 500 MHz spectrometer (Palo Alto, CA, USA) at 500 and 125 MHz, respectively. The instrument was controlled by Varian VNMR software installed on a Sun workstation (Santa Clara, CA, USA). All NMR measurements were performed in deuterated solvents (Dr Glaser AG, Basel, Switzerland) at 25 °C, except for compounds with a different temperature cited in section 3 of this thesis. In the case of ellagic acid derivatives, the mixture of two or three deuterated solvents was sometimes necessary. The shifts are indicated in ppm relative to tetramethylsilane (TMS) as an internal standard for ^{1}H spectra, and the deuterated solvent shift as reference for ^{13}C spectra.

In order to observe homo- and heteronuclear correlations between proton and carbon atoms of the analyte, complementary two dimentional (2D) experiments were performed. For advanced and 2D spectra including COSY, HSQC, HMBC and NOESY, standard pulse sequences provided in the original VNMR software were employed.

V.4.6. Quantitative nuclear magnetic resonance (NMR) method

Linearity and accuracy assay: for assessing linearity and accuracy of the method, a calibration curve was established in triplicate for allocryptopine. A standard solution was first prepared with 9.0 mg of isolated allocryptopine and 9.0 mg of anthracene, used as internal standard, in 1800 µL of pyridine-d_5. Successive dilutions of the standard solution were conducted to get triplicates of five concentrations for allocryptopine (5.5, 2.5, 1.7, 0.85 and 0.6 mg/mL) and anthracene (5.3, 2.4, 1.6, 0.8, 0.5 mg/mL), according to the exactly weighed mass of standards. ^{1}H NMR spectra were obtained using 600 µL of each diluted solution. Concentrations were calculated with the following formula:

$$Conc_{calc} = \frac{I_A}{I_{IS}} \times \frac{N_{IS}}{N_A} \times \frac{MW_A}{MW_{IS}} \times Conc_{IS}$$

Where:

Conc $_{calc}$ = calculated concentration;

I_A = absolute integral value for the analyte selected peak;

I_{IS} = absolute integral value for the internal standard selected peak;

N_{IS} = number of protons integrated in the internal standard selected peak;

N_A = number of protons integrated in the analyte selected peak;

MW_A = molecular weight of the analyte;

MW_{IS} = molecular weight of the internal standard;

Conc $_{IS}$ = internal standard concentration.

Determination of alkaloid concentration in the traditional preparation: the decoction was prepared as described for the traditional preparation for two available clinical batches: batch AM 8 (10.0403 g of powdered extract) and batch AM 11 (10.0640 g of powdered extract). The weighed samples were added with 100.00 mL distilled water in a 500 mL Erlenmeyer flask. Flasks were weighted and allowed to boil for 3 hours. After that, the flasks were weighed at room temperature in order to establish the loss of water. Batch AM 8 provided 42.31 mL of tea, while batch AM 11 provided 60.51 mL. The resulting tea was filtered and 3 aliquots of 10.00 mL of each batch are transferred to individual centrifuge tube. Each sample was added of 20 mL CH_2Cl_2, shaken for 5 min and centrifuged at 5000 rpm. The supernatant was transferred to another centrifuged tube and the operation was repeated 4 times. The CH_2Cl_2 layers of each sample were grouped in a 100 mL round flask and evaporated to dryness. Each sample was recovered in 600 µL pyridine-d_5 for NMR analysis. The concentration in the analyzed sample was determined using the formula described above.

^{1}H NMR parameters: spectra were recorded in the Varian Inova 500 MHz spectrometer previously described, at 42 °C. Each sample was recorded with the following parameters: 100 scans per sample 0.20 Hz/point, pulse width (PW) = 8.0 µs, and relaxation delay (RD) = 1.0 s. FID files were Fourier transformed with the 1D NMR processor of ACDlabs® 8.0. Sweep width = 6000.60 Hz, LB= 0.3 Hz. Signal to noise (S/N)

ratio was higher than 20. Peak areas were expressed as absolute integrals and the start and end point of the integration of each peak were selected manually.

V.5. Chemical methods

V.5.1. Reagents for TLC detection

After development and mobile-phase solvent evaporation, zones were detected by various means. Colored substances may be viewed without any treatment. Colorless substances were first detected if they showed self-absorption in the short-wave UV region (254 nm) or if they could be excited to produce fluorescence by UV radiation (366 nm). Otherwise, detection was achieved by means of chemical reagents producing colored zones. Three main chemical reagents were used to detect compounds on TLC plates:

Godin's general reagent: first, the plate was sprayed with a solution of equivalent volumes of 1% vanillin in ethanol and 3% perchloric acid in water. Then, the dried layer was sprayed with a solution of 10% sulfuric acid in ethanol and heated to ca. 100 °C for 5 min. Colored zones were produced on a pale background.

Dragendorff specific reagent (alkaloid detection): (a) 0.85 g of bismuth subnitrate and 10 g of tartaric acid were dissolved in 40 mL of water. (b) 16 g KI were dissolved in 40 mL of water. Color reagent: 5 mL of (a), 5 mL of (b), 20 g of tartaric acid and 100 mL of water were mixed and then sprayed on the plate to give orange zones on a yellow background.

DPPH specific reagent (radical scavenger detection): a solution of 0.2% 2,2-diphenyl-1-picrylhydrazyl radical in methanol was sprayed on TLC plates. Compounds showing radical scavenging activity appeared as yellow spots against a purple background.

V.5.2. Acidic hydrolysis

Heterosides were submitted to hydrolysis with 20 mL of HCl 0.05 N at 65°C for 24h. Sugars were extracted by partition with *n*-BuOH and had their R_f compared to that of standard sugars on TLC eluted plates.

V.5.3. Enzymatic hydrolysis

Heterosides were treated with β-D-glucosidase in 1 mL NaOAc buffer (pH 5.0) for three days at 40 °C. The aglycones were extracted by partition with ethyl acetate and submitted to HPLC/UV-DAD analysis in order to confirm hydrolysis.

V.6. Bioassays

V.6.1. Preliminary activity screening

Anti-*P. falciparum* assay: *Plasmodium falciparum* (strain W2, chloroquine-resistant, mefloquine-sensitive) was maintained in human A+ erythrocytes in RPMI 1640 (GIBCO-BRL) supplemented with 10% human plasma at 37ºC in a 5% CO_2-air mixture. Antiplasmodial effect of extracts was measured by the [^{3}H]-hypoxanthine incorporation assay. Trophozoite stages at 1% to 2% parasitaemia and 2.5% haematocrit were incubated with or without extracts, in non-toxic concentrations to mouse spleen cells, in culture medium without hypoxanthine; a mefloquine control (as a reference antimalarial drug) was used. Parasites were harvested using Packard Filtermate 196 cell harvester and the radioactivity in dried filters was counted using a β-counter. Mean values of the triplicates expressed in counts per minute (CPM) were calculated and growth inhibition was given as the percentage of control values (Zalis *et al.*, 1998).

Anti-*T. cruzi* and antileishmanial assays: *Trypanosoma cruzi* (epimastigote form of Y strain) and *Leishmania amazonensis* (promastigote form of MHOM/BR88/BA-125 Leila strain) were maintained at 25 ºC in liver infusion tryptose medium (Difco, Detroit, MI, USA) supplemented with 10% FBS, 1% hemin (Sigma, St. Louis, MO, USA), 1% R9

medium (Hyclone) and 5% sterile human urine. Epimastigotes of *T. cruzi* and promastigotes of *L. amazonensis* were plated in 96-well plates at 1 x 107 and 5 x 106 parasites/well, respectively, with or without plant extracts, in non-toxic concentrations to mouse spleen cells. After incubation at 25 °C for 24 h, the number of viable parasites was evaluated by counting in Neubauer chamber using a light microscope. Mean values of the triplicates were calculated and growth inhibition was given as the percentage of control values.

Cytotoxicity assay: BALB/c spleen cells obtained from normal mice were used in this assay. Cells were added at 5 x 106 cells/well to 96-well plates with or without plant extracts, and in the presence of concanavalin A (2 µg/mL, Sigma). Plates were incubated for 48 h at 37ºC and 5% CO_2. One µCi of [^{3}H]-thymidine was added to each well, and plates were incubated for additional 18 h. Uptake of [^{3}H]-thymidine was determined by the measuring of radioactivity using a β-counter as described above. Mean values of the triplicates expressed in CPM were calculated, and lymphoproliferation inhibition was given as the percentage of control values. Concentrations causing an inhibition greater than 30% were arbitrarily considered cytotoxic (Soares *et al.*, 2006).

V.6.2. Secondary activity screening of extracts, fractions and pure compounds

Anti-*P. falciparum* assay: The chloroquine-resistant strains of *P.falciparum* (*Pf* K1) was used: The strain was maintained in RPMI-1640 medium supplemented with 0.37 mM hypoxanthine, 25 mM Hepes, 25 mM $NaHCO_3$, and 0.5% Albumax® with 2-4% washed human O^+ erythrocytes. All cultures and assays were conducted at 37 °C under an atmosphere of 4% CO_2, 3% O_2 and 93% N_2. Extract/compound stock solutions were prepared in 100% DMSO at 20 mg/mL or mM. The samples were serially pre-diluted (2-fold or 4-fold) in DMSO followed by a further (intermediate) dilution in demineralized water to assure a final in-test DMSO concentration of <1%. Assays were performed in 96-well microtiter plates, each well containing 10 µL of the compound watery dilutions together with 190 µL of the malaria parasite inoculum (1% parasitaemia, 2% HCT). Parasite growth was compared to untreated-infected (100% growth) and uninfected-controls (0% growth). After 72 h incubation at 37°C, plates were frozen at –20 °C. After thawing, 20 µL of each well was transferred into another plate together with 100 µL Malstat™ reagent and 20 µl of

a 1/1 mixture of PES (phenazine ethosulfate, 0.1 mg/mL) and NBT (Nitro Blue Tetrazolium Grade III, 2 mg/mL). The plates were kept out of light for 2 hours and change in color was measured spectrophotometrically at 655 nm. The results were expressed as % reduction in parasitaemia compared to control wells and IC_{50}-values were calculated. Compounds/extracts were tested at 5 concentrations (64, 16, 4, 1 and 0.25 µM or µg/mL). Chloroquine was included as reference drug. The compound was classified as inactive when the IC_{50} was higher than 16 µM. When IC_{50} lay between 16 and 2 µM, the compound was regarded as being moderately active. When the IC_{50} is lower than 2 µM, the compound was classified as highly active on the condition that it also demonstrated selective action (absence of cytotoxicity).

Anti-*T. cruzi* assay: *Trypanosoma cruzi*, Tulahuen CL2, β-galactosidase strain (nifurtimox-sensitive) was used. The strain was maintained on MRC-5 SV2 (human lung fibroblast) cells in MEM medium, supplemented with 200 mM L-glutamine, 16.5 mM $NaHCO_3$, and 5% inactivated fetal calf serum. All cultures and assays were conducted at 37 °C under an atmosphere of 5% CO_2. Compound/extract stock solutions were prepared in 100% DMSO at 20 mM or mg/mL. The samples were serially pre-diluted (2-fold or 4-fold) in DMSO followed by a further (intermediate) dilution in demineralized water to assure a final in-test DMSO concentration of <1%. Assays were performed in sterile 96-well microtiter plates, each well containing 10 µL of the compound watery dilutions together with 190 µL of MRC-5 cell/parasite inoculum (4.103 cells/well + 4.104 parasites/well). Parasite growth was compared to untreated-infected controls (100% growth) and non-infected controls (0% growth) after 7 days incubation at 37 °C and 5% CO_2. Parasite burdens were assessed after adding the substrate CPRG (chlorophenol red β-D-galactopyranoside): 50 µL/well of a stock solution containing 15.2 mg CPRG + 250 µL Nonidet in 100 mL PBS. The change in color was measured spectrophotometrically at 540 nm after 4 hours incubation at 37 °C. The results were expressed as % reduction in parasite burdens compared to control wells and an IC_{50} (50% inhibitory concentration) was calculated. Compounds were tested at 5 concentrations (64, 16, 4, 1 and 0.25 µM or mg/mL). Nifurtimox or benznidazole were included as the reference drugs. The test compound was classified as inactive when the IC_{50} was higher than 30 µg/mL or µM. When IC_{50} lay between 30 and 2 µg/mL or µM, the compound was regarded as being moderately active. When the IC_{50} was lower than 2 µg/mL or µM, the compound was

classified as highly active on the condition that it also demonstrated selective action (absence of cytotoxicity).

Anti-*T. b. brucei* assay: The *Trypanosoma brucei brucei* Squib 427 strain (suramin-sensitive) was used in this study. The strain was maintained in Hirumi (HMI-9) medium, supplemented with 10% inactivated fetal calf serum. All cultures and assays were conducted at 37 °C under an atmosphere of 5% CO_2. Compound/extract stock solutions were prepared in 100% DMSO at 20 mM or mg/mL. The samples were serially pre-diluted (2-fold or 4-fold) in DMSO followed by a further (intermediate) dilution in demineralized water to assure a final in-test DMSO concentration of <1%. Assays were performed in sterile 96-well microtiter plates, each well containing 10 µL of the compound dilutions together with 190 µL of the parasite suspension (1.5x104 parasites/well). Parasite growth was compared to untreated-infected (100% parasite growth) and uninfected controls (0% growth). After 3 days incubation, parasite growth was assessed fluorimetrically after addition of 50 µL resazurin per well. After 24 hours at 37 °C, fluorescence was measured (λ_{ex} 550 nm, λ_{em} 590 nm). The results were expressed as % reduction in parasite growth/viability compared to control wells and an IC_{50} (50% inhibitory concentration) was calculated. Compounds/extracts were tested at 5 concentrations (64, 16, 4, 1 and 0.25 µM or µg/mL). Suramin or melarsoprol were included as the reference drugs. The compound was classified as inactive when the IC_{50} was higher than 5 µg/mL or µM. When IC_{50} lay between 5 and 1 µg/mL or µM, the compound was regarded as being moderately active. When the IC_{50} was lower than 1 µg/mL or µM, the compound was classified as highly active on the condition that it also demonstrated selective action (absence of cytotoxicity).

Cytotoxicity assay: Human fibroblasts MRC-5 SV2 cells were cultured in MEM + Earl's salts-medium, supplemented with L-glutamine, $NaHCO_3$ and 5% inactivated fetal calf serum. All cultures and assays were conducted at 37 °C under an atmosphere of 5% CO_2. Compound/extract stock solutions were prepared in 100% DMSO at 20 mM or mg/mL. The samples were serially pre-diluted (2-fold or 4-fold) in DMSO followed by a further (intermediate) dilution in demineralized water to assure a final in-test DMSO concentration of <1%. Assays were performed in sterile 96-well microtiter plates, each well containing 10 µL of the compound watery dilutions together with 190 µL of MRC-5 SV2 inoculum (3x104 cells/mL). Cell growth was compared to untreated-control wells (100% cell growth) and medium-control wells (0% cell growth). After 3 days incubation, cell

viability was assessed fluorimetrically after addition of 50 µL resazurin per well. After 4 hours at 37°C, fluorescence was measured (λ_{ex} 550 nm, λ_{em} 590 nm). The results were expressed as % reduction in cell growth/viability compared to control wells and IC_{50} (50% inhibitory concentration) was determined. The compounds/extracts were tested at 5 concentrations (64, 16, 4, 1 and 0.25 µM or µg/mL). The compound is classified non-toxic when the IC_{50} was higher than 30 µg/mL or µM. Between 30 and 10 µg/mL or µM, the compound was regarded as moderately toxic. When the IC_{50} was lower than 10 µg/mL or µM, the compound is classified as highly toxic. Cytotoxic reference compounds included tamoxifen or niclosamide.

β-hematin formation inhibition assay: solutions at 50 mM of pure compounds were prepared in 1.0 M HCL/MeOH/DMSO (5:3:2). Samples were distributed in a 96-well plate. A previously established Phiβ-assay (Ncokazi and Egan, 2005) was used to develop the in-house inhibition assay, based on β-hematin photocolorimetric determination. Colorimetric measurements were performed at 405 nm in an EL-808 apparatus (Bio-Tek Instruments, Inc.) and qualitative results were statistically obtained by $I_{Analysis}$.

V.7. Physical constants and spectral data for the isolated compounds

Compound A1

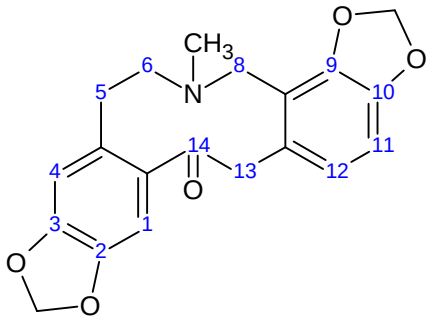

protopine

CA index name	Bis[1,3]benzodioxolo[4,5-c:5',6'-g]azecin-13(5H)-one, 4,6,7,14-tetrahydro-5-methyl-
Formula	$C_{20}H_{19}NO_5$
Exact mass	353.1263 Da
Molecular Weight	353.3368 Da
Aspect	amorphous white solid
UV ($MeOH_{aq}$) λ_{max}	217.7, 276.3 nm
IR ν_{max} (KBr)	1656 cm^{-1}
^{1}H NMR 500 MHz pyridine-d_5, 70 °C	δ 1.94 (3H, s, N-CH_3), 2.46 (2H, bs, H-6), 2.89 (2H, bs, H-5), 3.63 (s, 2H, H-8), 3.96 (2H, s, H-13), 5.86 (2H, s, O-CH_2-O), 5.90 (2H, s, O-CH_2-O), 6.71 (1H, s, H-4), 6.75 (1H, d, J= 8.0 Hz, H-11), 6.77 (1H, d, J= 8.0 Hz, H-12), 7.12 (1H, s, H-1)
^{13}C NMR 125 MHz pyridine-d_5, 70 °C	δ 31.7 (C-5), 41.7 (N-CH_3), 47.2 (C-13), 51.7 (C-8), 58.7 (C-6), 101.6 (O-CH_2-O), 102.1 (O-CH_2-O), 107.1 (C-11), 108.4 (C-1), 111.2 (C-4), 119.5 (C-8a), 126.2 (C-12), 130.4 (C-12a), 133.5 (C-4a), 137.5 (C-14a), 146.9 (C-2), 147.3 (C-9), 147.3 (C-10), 148.7 (C-3), 194.8 (C-14)
HRESIMS *m/z*	354.1360 $[M+H]^+$ (calculated for $C_{20}H_{20}NO_5$, 354.1341)

Compound A2	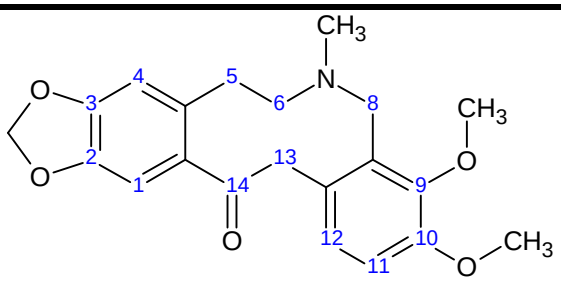 **allocryptopine**
CA index name	[1,3]Benzodioxolo[5,6-e][2]benzazecin-14(6H)-one, 5,7,8,15-tetrahydro-3,4-dimethoxy-6-methyl-
Formula	$C_{21}H_{23}NO_5$
Exact Mass	369.1576 Da
Molecular Weight	369.4110 Da
Aspect	amorphous white solid
UV ($MeOH_{aq}$) λ_{max}	285.9, 219.1 nm
IR ν_{max} (KBr)	1655 cm^{-1}
^{1}H NMR 500 MHz pyridine-d_5, 70 °C	See Table 3.3
^{13}C NMR 125 MHz pyridine-d_5, 70 °C	δ 32.6 (C-5), 41.9 (N-CH_3), 47.3 (C-13), 51.6 (C-8), 56.3 (O-CH_3), 58.6 (C-6), 61.0 (O-CH_3), 102.1 (O-CH_2-O), 109.3 (C-1), 111.3 (C-4), 112.1 (C-11), 126.2 (C-12), 129.3 (C-8a), 130.1 (C-12a), 133.8 (C-14a), 137.5 (C-4a), 146.9 (C-2), 148.7 (C-9), 148.8 (C-3), 152.6 (C-10), 192.9 (C-14)
HRESIMS *m/z*	370.1635 $[M+H]^+$ (calculated for $C_{21}H_{24}NO_5$, 370.1654)

Compound A3	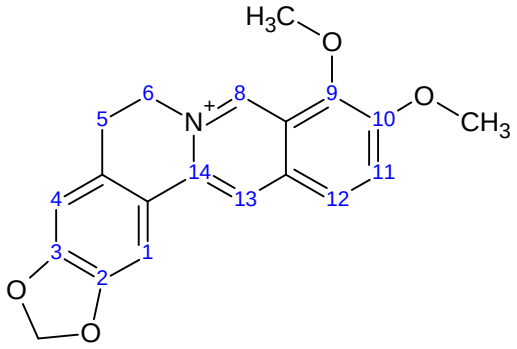 **berberine**
CA index name	Benzo[g]-1,3-benzodioxolo[5,6-a]quinolizinium, 5,6-dihydro-9,10-dimethoxy-
Formula	$C_{20}H_{18}NO_4^+$
Exact Mass	336.1230 Da
Molecular Weight	336.3606 Da
Aspect	amorphous yellow solid
UV ($MeOH_{aq}$) λ_{max}	
^{1}H NMR 500 MHz DMSO-d_6	δ 3.21 (2H, bs, H-5), 4.07 (3H, s, O-CH_3), 4.10 (3H, s, O-CH_3), 4.95 (2H, bs, H-6), 6.17 (2H, s, O-CH_2-O), 7.08 (1H, s, H-4), 7.80 (1H, s, H-1O), 8.02 (1H, d, J=9.2 Hz, H-12), 8.21 (1H, d, J= 9.2 Hz, H-11), 8.96 (1H, s, H-13), 9.90 (1H, s, H-8)
^{13}C NMR 125 MHz DMSO-d_6	δ 26.8 (C-5), 56.0 (C-6), 57.8 (O-CH_3), 63.2 (O-CH_3), 102.7 (O-CH_2-O), 106.5 (C-1), 106.5 (C-8), 109.3 (C-4), 121.0 (C-13), 121.0 (C-14a), 124.4 (C-12), 127.7 (C-11), 131.4 (C-4a), 133.8 (C-12a), 138.2 (C-14), 144.5 (C-9), 146.6 (C-8a), 148.5 (C-2), 150.6 (C-3), 151.2 (C-10)
HRESIMS *m/z*	336.1222 $[M]^+$ (calculated for $C_{20}H_{18}NO_4$, 336.1236)

Compound A5	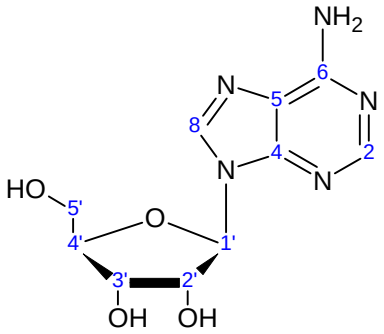
	adenosine
CA index name	adenosine
Formula	$C_{10}H_{13}N_5O_4$
Exact Mass	267.0967 Da
Molecular Weight	267.2413 Da
Aspect	amorphous white solid
UV ($MeOH_{aq}$) λ_{max}	262 nm
^{1}H NMR 500 MHz DMSO-d_6	δ 3.56 (1H, d, J=12.1, H-5'b), 3.68 (1H, d, J=12.1, H-5'a), 3.99 (1H, bs, H-4'), 4.17 (1H, bs, H-3'), 4.62 (1H, bs, H-2'), 5.89 (1H, d, J=6.3, H-1'), 7.34 (2H, s, NH_2), 8.36 (1H, s, H-8), 8.16 (1H, s, H-2)
HRESIMS *m/z*	268.1009 $[M+H]^+$ (calculated for $C_{10}H_{14}N_5O_4$, 268.1046)

Compound L2	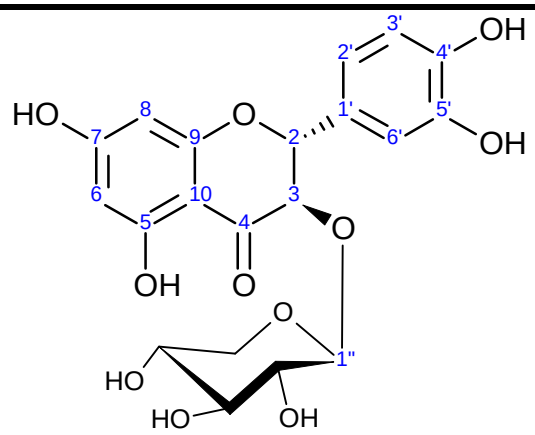
	(2R, 3R)-taxifolin 3-*O*-β-D-xylopyranoside
CA index name	4H-1-Benzopyran-4-one, 2-(3,4-dihydroxyphenyl)-2,3-dihydro-5,7-dihydroxy-3-(D-xylopyranosyloxy)-, (2R-trans)- (9CI)
Formula	$C_{20}H_{20}O_{11}$
Exact Mass	436.1005 Da
Molecular Weight	436.3662 Da
Aspect	amorphous green solid
$[\alpha]_D^{20\,°C}$ aglycone	+11.55° (*c* 0.57, EtOH)
UV (MeOH) λ_{max}	290 nm
^{1}H NMR data	see Table 3.8
^{13}C NMR data	see Table 3.8
HRESIMS *m/z*	435.0914 $[M-H]^-$ (calculated for $C_{20}H_{19}O_{11}$, 435.0927)

Compound L4

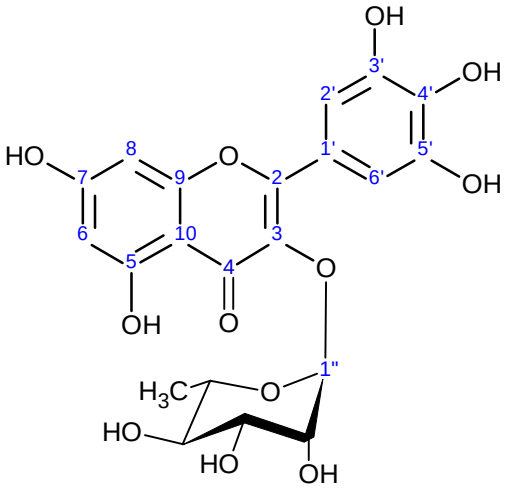

myricetin 3-*O*-α-L-rhamnopyranoside

CA index name	4H-1-Benzopyran-4-one, 3-[(6-deoxy-α-L-mannopyranosyl)oxy]-5,7-dihydroxy-2-(3,4,5-trihydroxyphenyl)-
Formula	$C_{21}H_{20}O_{12}$
Exact Mass	464.0954 Da
Molecular Weight	464.9763 Da
Aspect	amorphous yellow solid
UV (MeOH) λ_{max}	260, 355 nm
^{1}H NMR data	See Table 3.8
^{13}C NMR data	see Table 3.8
HRESIMS *m/z*	463.0852 $[M-H]^-$ (calculated for $C_{21}H_{19}O_{12}$, 463.0877)

Compound L6

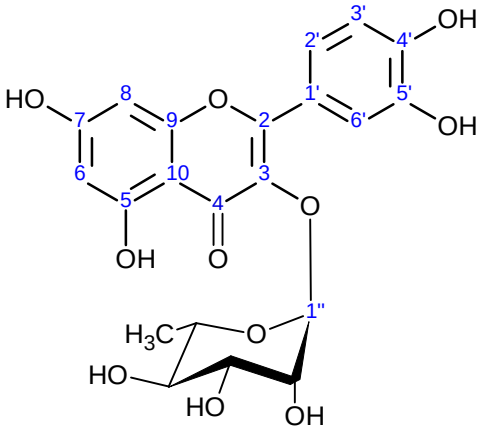

quercetin 3-*O*-α-L-rhamnopyranoside

CA index name	4H-1-Benzopyran-4-one, 3-[(6-deoxy-α-L-mannopyranosyl)oxy]-2-(3,4-dihydroxyphenyl)-5,7-dihydroxy-
Formula	$C_{21}H_{20}O_{11}$
Exact Mass	448.1005 Da
Molecular Weight	448.3769 Da
Aspect	amorphous pale yellow solid
UV (MeOH) λ_{max}	260, 350 nm
^{1}H NMR data	See Table 3.8
^{13}C NMR data	see Table 3.8
HRESIMS *m/z*	477.0929 $[M-H]^-$ (calculated for $C_{21}H_{19}O_{11}$, 447.0927)

Compound S1	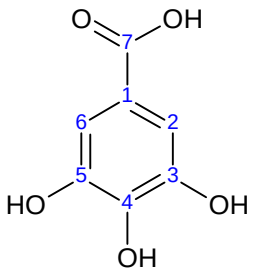
	gallic acid
CA index name	Benzoic acid, 3,4,5-trihydroxy-
Formula	$C_{14}H_{20}N_2O_3$
Exact Mass	170.0215 Da
Molecular Weight	170.1195 Da
Aspect	Amorphous yellowish-white solid
UV ($MeOH_{aq}$) λ_{max}	215, 271 nm
^{1}H NMR 500 MHz CD_3OD	δ 7.08 (2H, s, H-2 and H-6)
^{13}C NMR 500 MHz CD_3OD	δ 110.3 (C-2 and C-6), 139.5 (C-4), 146.3 (C-3 and C-5), 170.4 (C-7)
ESI-MS *m/z*	168.92 $[M - H]^-$

Compound S4

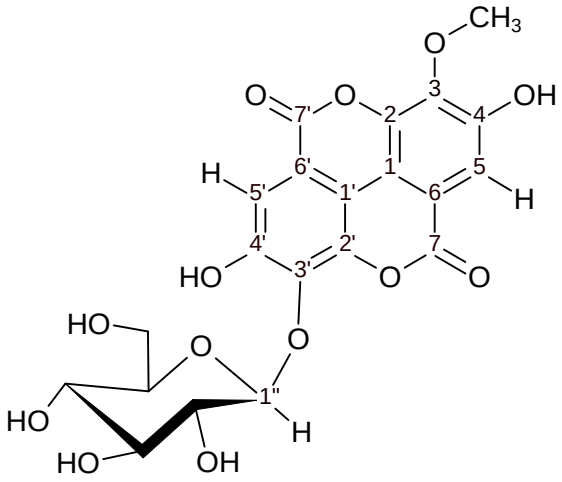

3-*O*-methylellagic acid 3'-*O*-β-D-glucopyranoside

Formula	$C_{21}H_{18}O_{13}$
Exact Mass	478.0747 Da
Molecular Weight	478.3598 Da
Aspect	amorphous brownish-yellow solid
UV ($MeOH_{aq}$) λ_{max}	254, 329 (sh), 360 nm
^{1}H NMR data	see Table 3.15
^{13}C NMR data	see Table 3.16
HRESIMS *m/z*	477.0633 $[M-H]^-$ (calculated for $C_{21}H_{17}O_{13}$, 477.0669)

Compound S5	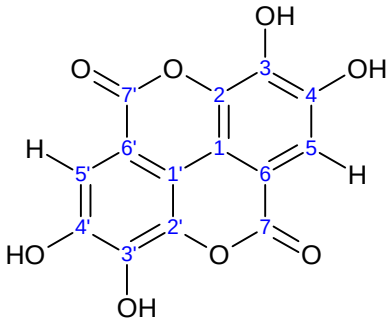
	ellagic acid
CA index name	[1]Benzopyrano[5,4,3-cde][1]benzopyran-5,10-dione, 2,3,7,8 tetrahydroxy-
Formula	$C_{14}H_6O_8$
Exact Mass	302.0062 Da
Molecular Weight	302.1926 Da
Aspect	Yellow needle-shaped crystals
UV ($MeOH_{aq}$) λ_{max}	255, 369 nm
^{1}H NMR data	See Table 3.15
^{13}C NMR data	See Table 3.16
HRESIMS *m/z*	300.9992 $[M-H]^-$ (calculated for $C_{14}H_5O_8$, 300.9984)

Compound S7

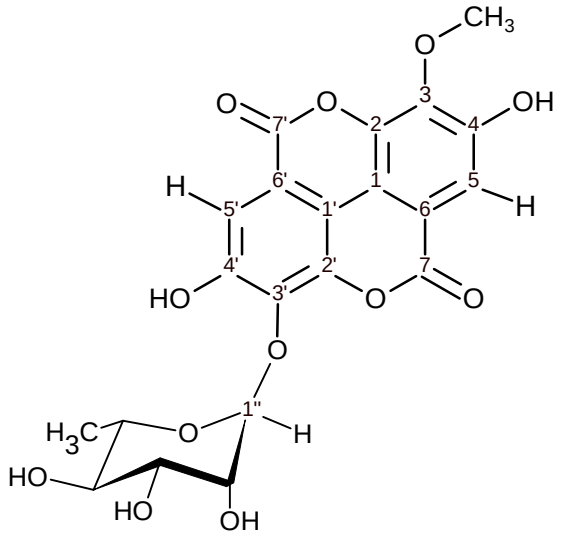

3-*O*-methylellagic acid 3'-*O*-α-L-rhamnopyranoside

Formula	$C_{21}H_{18}O_{12}$
Exact Mass	264.1474 Da
Molecular Weight	264.3203 Da
Aspect	amorphous brownish yellow solid
UV ($MeOH_{aq}$) λ_{max}	250, 300(sh), 350(sh), 366 nm
^{1}H NMR data	see Table 3.15
^{13}C NMR data	see Table 3.16
HRESIMS *m/z*	461.0701 $[M-H]^-$ (calculated for $C_{21}H_{17}O_{12}$, 461.0720)

Compound S8

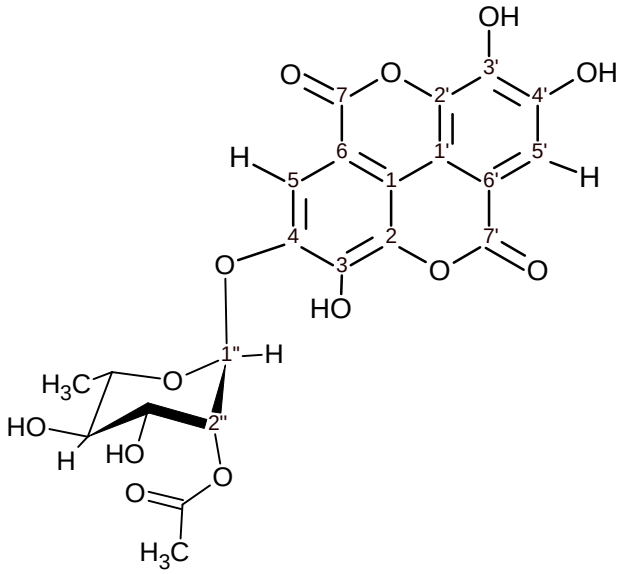

ellagic acid 4-O-α-L-2''-acetylrhamnopyranoside

CA index name	[1]Benzopyrano[5,4,3-cde][1]benzopyran-5,10-dione, 2-[(2-O-acetyl-6-deoxy-α-L-mannopyranosyl)oxy]-3,7,8-trihydroxy-
Formula	$C_{22}H_{18}O_{13}$
Exact Mass	490.0747 Da
Molecular Weight	490.3705 Da
Aspect	amorphous yellow solid
UV ($MeOH_{aq}$) λ_{max}	256, 302(sh), 344(sh), 362 nm
^{1}H NMR data	see Table 3.15
^{13}C NMR data	see Table 3.16
HRESMS *m/z*	513.0652 $[M+Na]^+$ (calculated for $C_{22}H_{18}O_{13}Na$, 513.0640)

Chapter VI

References

- B -

Badisa R. B., Chaudhuri S. K., Pilarinou E., Rutkoski N. J., Hare J., Levenson C. W. 2000. *Licania michauxii* Prance root extract induces hsp 70 mRNA and necrotic cell death in cultured human hepatoma and colon carcinoma cell lines. *Cancer Letters* **149**: 61-68.

Banzouzi J. T., Prado R., Menan H., Valentin A., Roumestan C., Mallie M., Pelissier Y., Blache Y. 2002. *In vitro* antiplasmodial activity of extracts of *Alchornea cordifolia* and identification of an active constituent: ellagic acid. *Journal of Ethnopharmacology* **81**: 399-401.

Bao L., Li B., Yang B., Wang H., He X., Wu S., Li W. 1997. A research of metabolism kinetics of berberine chloride after oral administration. *Chinese Pharmacological Bulletin* **13**: 95.

Benthe H. F. 1956. Antifibrillary action of quinidine and similar substances. *Naunyn-Schmiedeberg's Archives of Pharmacology* **229**: 82-91.

Bentley K. W. 1998. *The isoquinoline alkaloids*. CRC Press: London.

Bhargava K. K., Dayal R., Seshadri T. R. 1974. Chemical components of *Eugenia jambolana* stem bark. *Current Science* **43**: 645-646.

Bhatia I. S., Bajaj K. L. 1975. Chemical Constituents of seeds and bark of *Syzygium cumini*. *Planta Medica* **28**: 346-352.

Bilia A. R., Lazari D., Messori L., Taglioli V., Temperini C., Vincieri F. F. 2002. Simple and rapid physicochemical methods to examine action of antimalarial drugs with hemin. Its application to *Artemisia annua* constituents. *Life Sciences* **70**: 769-778.

Bourdy G., Willcox M. L., Ginsburg H., Rasoanaivo P., Graz B., Deharo E. 2008. Ethnopharmacology and malaria: new hypothetical leads or old efficient antimalarials? *International Journal for Parasitology* **38**: 33-41.

Braca A., Bilia A. R., Mendez J., Morelli I. 1999a. Three flavonoids from *Licania densiflora*. *Phytochemistry* **51**: 1125-1128.

Braca A., De Tommasi N., Mendez J., Morelli I. 1999b. Flavonoids and triterpenoids from *Licania heteromorpha* (Chrysobalanaceae). *Biochemical Systematics Ecology* **27**: 527-530.

Braca A., Morelli I., Mendez J., Battinelli L., Braghiroli L., Mazzanti G. 2000. Antimicrobial triterpenoids from *Licania heteromorpha*. *Planta Medica* **66**: 768-769.

Braca A., Bilia A. R., Mendez J., Morelli I. 2001a. Myricetin glycosides from *Licania densiflora*. *Fitoterapia* **72**: 182-185.

Braca A., Sortino C., Mendez J., Morelli I. 2001b. Triterpenes from *Licania licaniaeflora*. *Fitoterapia* **72**: 585-587.

Braca A., Luna D., Mendez J., Morelli I. 2002a. Flavonoids from *Licania apetala* and *Licania licaniaeflora*. *Biochemical Systematics and Ecology* **30**: 271-273.

Braca A., Sortino C., Politi M., Morelli I., Mendez J. 2002b. Antioxidant activity of flavonoids from *Licania licaniaeflora*. *Journal of Ethnopharmacology* **79**: 379-381.

Braga F. G., Bouzada M. L. M., Fabri R. L., Matos M. O., Moreira F. O., Scio E., Coimbra E. S. 2007. Antileishmanial and antifungal activity of plants used in traditional medicine in Brazil. *Journal of Ethnopharmacology* **111**: 396-402.

Breasted J. H. 1930. *The Edwin Smith surgical papyrus*. University of Chicago Press: Chicago.

Brito F. A., Lima L. A., Ramos M. F. S., Nakamura M. J., Cavalher-Machado S. C., Siani A. C., Henriques M. G. M. O., Sampaio A. L. F. 2007. Pharmacological study of anti-allergic activity of *Syzygium cumini* (L.) skeels. *Brazilian Journal of Medical and Biological Research* **40**: 105-115.

Bringmann G., Gulder T. A. M., Reichert M., Gulder T. 2008. The online assignment of the absolute configuration of natural products: HPLC-CD in combination with quantum chemical CD calculations. *Chirality* **20**: 628-642.

- C -

Carballeira N. M. 2008. New advances in fatty acids as antimalarial, antimycobacterial and antifungal agents. *Progress in Lipid Research* **47**: 50-61.

Castilho R. O., de Oliveira R. R., Kaplan M. A. C. 2005. Licanolide, a new triterpene lactone from *Licania tomentosa*. *Fitoterapia* **76**: 562-566.

Castilho R. O., Kaplan M. A. C. 2008. Chemical constituents of *Licania tomentosa* Benth. (Chrysobalanaceae). *Química Nova* **31**: 66-69.

Cavin A., Dyatmyko W., Hostettmann K. 1999. Screening of Indonesian plants for antifungal and free radical scavenging activities. *Pharmaceutical Biology* **37**: 260-268.

Chang Y. C., Chang F. R., Khalil A. T., Hsieh P. W., Wu Y. C. 2003a. Cytotoxic benzophenanthridine and benzylisoquinoline alkaloids from *Argemone mexicana*. *Zeitschrift fuer Naturforschung, C: Journal of Biosciences* **58**: 521-526.

Chang Y. C., Hsieh P. W., Chang F. R., Wu R. R., Liaw C. C., Lee K. H., Wu Y. C. 2003b. Two new protopines argemexicaines A and B and the anti-HIV alkaloid 6-

acetonyldihydrochelerythrine from formosan *Argemone mexicana*. *Planta Medica* **69**: 148-152.

Chaudhuri S. K., Badisa R. B., Pilarinou E., Walker E. H. 2002. Licamichauxiioic-A and -B acids - two ent-kaurene diterpenoids from *Licania michauxii*. *Natural Product Letters* **16**: 39-45.

Chen M., Christensen S. B., Zhai L., Rasmussen M. H., Theander T. G., Frokjaer S., Steffansen B., Davidsen J., Kharazmi A. 1997. The novel oxygenated chalcone, 2,4-dimethoxy-4'-butoxychalcone, exhibits potent activity against human malaria parasite *Plasmodium falciparum in vitro* and rodent parasites *Plasmodium berghei* and *Plasmodium yoelii in vivo*. *Journal of Infectious Diseases* **176**: 1327-1333.

Choy C. S., Cheah K. P., Chiou H. Y., Li J. S., Liu Y. H., Yong S. F., Chiu W. T., Liao J. W., Hu C. M. 2008. Induction of hepatotoxicity by sanguinarine is associated with oxidation of protein thiols and disturbance of mitochondrial respiration. *Journal of Applied Toxicology* **28**: 945-956.

Cordell G. A. 1981. *Introduction to Alkaloids. A Biogenetic Approach*. John Wiley & Sons: New York.

CRC. 2009. CRC Dictionary of Natural Products on DVD 1982 - 2009. Version 17:2. 1982-2009 CRC Press, 2009 Hampden Data Services Ltd. Accessed on April 24, 2009.

- D -

Damasceno D. C., Lima P. H. O., Galhiane M. S., Volpato G. T., Rudge M. V. C. 2002. Evaluation of the hypoglycemic effect of sapogenin extracted from *Eugenia jambolana* seeds. *Revista Brasileira de Plantas Medicinais* **4**: 46-54.

Dell'Agli M., Parapini S., Basilico N., Verotta L., Taramelli D., Berry C., Bosisio E. 2003. *In vitro* studies on the mechanism of action of two compounds with antiplasmodial activity: ellagic acid and 3,4,5-trimethoxyphenyl (6'-O-galloyl)-beta -D-glucopyranoside. *Planta Medica* **69**: 162-164.

Diallo D., Graz B., Falquet J., Traoré A. K., Giani S., Mounkoro P. P., Berthé A., Sacko M., Diakité C. 2006. Malaria treatment in remote areas of Mali: use of modern and traditional medicines, patient outcome. *Transactions of the Royal Society of Tropical Medicine and Hygiene* **100**: 515-520.

Diop E. H. A. 2006. Mise au point d'une méthode de contrôle de qualité des préparations traditionelles à base d'*Argemone mexicana* L. (Papaveraceae), une plante utilisée dans le traitement du paludisme au Mali. Travail de Diplôme. Section des Sciences Pharmaceutiques. Ecole de Pharmacie Genève-Lausanne. Genève: Université de Genève.

- E -

Egan T. J. 2008. Recent advances in understanding the mechanism of hemozoin (malaria pigment) formation. *Journal of Inorganic Biochemistry* **102**: 1288-1299.

Eichler A. W. 1865. Papaveraceae. *In*: Martius C. F., editor. *Flora Brasiliensis: enumeratio plantarum*. J. Cramer: Weinhem; 313-316.

Elford B. C. 1986. L-Glutamine influx in malaria-infected erythrocytes: a target for antimalarials? *Parasitology Today* **2**: 309-312.

Elkhateeb A., Subeki, Takahashi K., Matsuura H., Yamasaki M., Yamato O., Maede Y., Katakura K., Yoshihara T., Nabeta K. 2005. Anti-babesial ellagic acid rhamnosides from the bark of *Elaeocarpus parvifolius*. *Phytochemistry* **66**: 2577-2580.

- F -

Fogliani B., Raharivelomanana P., Bianchini J.-P., BouraIma-Madjèbi S., Hnawia E. 2005. Bioactive ellagitannins from *Cunonia macrophylla*, an endemic Cunoniaceae from New Caledonia. *Phytochemistry* **66**: 241-247.

- G -

Gallo M. B. C., da Silva F. C., Vieira P. C., Fernandes J. B., da Silva M. F. d. G. F. 2006. New natural products from *Siphoneugena densiflora* Berg (Myrtaceae) and their chemotaxonomic significance. *Journal of the Brazilian Chemical Society* **17**: 279-288.

Gao F., Wang H., Mabry T. J., Kinghorn A. D. 1990. Dihydroflavonol sweeteners and other constituents from *Hymenoxys turneri*. *Phytochemistry* **29**: 2865-2869.

Gillespie S. H., Pearson R. D. 2001. *Principles and practice of clinical parasitology*. Wiley: New York.

Ginsburg H., Krugliak M. 1999. Chloroquine - some open questions on its antimalarial mode of action and resistance. *Drug Resistance Updates* **2**: 180-187.

Grabley S., Thiericke R. 1999. The impact of natural products on drug discovery. *In*: Grabley S., Thiericke R., editors. *Drug Discovery from Nature*. Springer-Verlag: Berlin; 3-37.

Grycova L., Dostal J., Marek R. 2007. Quaternary protoberberine alkaloids. *Phytochemistry* **68**: 150-175.

- H -

Haisova K., Slavik J. 1975. Minor alkaloids from *Argemone mexicana*. *Collection of Czechoslovak Chemical Communications* **40**: 1576-1578.

Heller W., Forkmann G. 1994. Biosynthesis of flavonoids. *In*: Harborne J. B., editor. *The Flavonoids. Advances in research since 1986*. Chapman & Hall: New York; 676.

Heywood V. H. 1993. *Flowering plants of the world*. Oxford University Press: Oxford.

Hostettmann K., Marston A., Hostettmann M. 1998. *Preparative chromatography techniques*. Springer-Verlag: Berlin.

Hyde J. E. 2007. Drug-resistant malaria - an insight. *Febs Journal* **274**: 4688-4698.

- I -

Israilov A., Yunusov M. S. 1986. Alkaloids of four species of *Argemone*. *Chemistry of Natural Compounds* **22**: 189-192.

Iwasa K., Kim H. S., Wataya Y., Lee D. U. 1998. Antimalarial activity and structure-activity relationships of protoberberine alkaloids. *European Journal of Medicinal Chemistry* **33**: 65-69.

Iwasa K., Nishiyama Y., Ichimaru M., Moriyasu M., Kim H. S., Wataya Y., Yamori T., Takashi T., Lee D. U. 1999. Structure-activity relationships of quaternary protoberberine alkaloids having an antimalarial activity. *European Journal of Medicinal Chemistry* **34**: 1077-1083.

- J -

Jagetia G. C., Baliga M. S. 2002. *Syzygium cumini* (Jamun) reduces the radiation-induced DNA damage in the cultured human peripheral blood lymphocytes: a preliminary study. *Toxicology Letters* **132**: 19-25.

Jamine R., Daisy P., Selvakumarb B. N. 2007. *In vitro* efficacy of flavonoids from *Eugenia jambolana* seeds against ESβL-producing multidrug-resistant enteric bacteria. *Research Journal of Microbiology* **2**: 369-374.

- K -

Karthic K., Kirthiram K. S., Sadasivam S., Thayumanavan B. 2008. Identification of α-amylase inhibitors from *Syzygium cumini* Linn seeds. *Indian Journal of Experimental Biology* **46**: 677-680.

Khallouki F., Haubner R., Hull W. E., Erben G., Spiegelhalder B., Bartsch H., Owen R. W. 2007. Isolation, purification and identification of ellagic acid derivatives, catechins, and procyanidins from the root bark of *Anisophyllea dichostyla* R. Br. *Food and Chemical Toxicology* **45**: 472-485.

Kopanski L., Schnelle G. 1988. Isolation of bergenin from barks of *Syzygium cumini*. *Planta Medica* **54**: 572.

Kosalge S. B., Fursule R. A. 2009. Investigation of ethnomedicinal claims of some plants used by tribals of Satpuda Hills in India. *Journal of Ethnopharmacology* **121**: 456-461.

Kraft C., Jenett-Siems K., Siems K., Solis P. N., Gupta M. P., Bienzle U., Eich E. 2001. Andinermals A-C, antiplasmodial constituents from *Andira inermis*. *Phytochemistry* **58**: 769-774.

Kraft C., Jenett-Siems K., Siems K., Jakupovic J., Mavi S., Bienzle U., Eich E. 2003. *In vitro* antiplasmodial evaluation of medicinal plants from Zimbabwe. *Phytotherapy Research* **17**: 123-128.

Kreier J. P. 1980. *Malaria. Epidemiology, chemotherapy, morphology, and metabolism*. Academic Press: New York.

- L -

Lee J. H., Johnson J. V., Talcott S. T. 2005. Identification of ellagic acid conjugates and other polyphenolics in muscadine grapes by HPLC-ESI-MS. *Journal of Agricultural and Food Chemistry* **53**: 6003-6010.

Letouzey R., White F. 1978. *Flore du Cameroun. Chrysobalanacées*. Muséum National d'Histoire Naturelle: Paris.

Lewis K., Ausubel F. M. 2006. Prospects for plant-derived antibacterials. *Nature Biotechnology* **24**: 1504-1507.

Li B., Wu Q., Shi J., Sun A., Huang X. 2005. Effects of protopine on intracellular calcium and the PKC activity of rat aorta smooth muscle. *Shengli Xuebao* **57**: 240-246.

Li X. C., Hala N., Elsohly C. D., Hufford A. M. C. 1999. NMR assignments of ellagic acid derivatives. *Magnetic Resonance in Chemistry* **37**: 856-859.

Li Y., Wang S., Liu Y., Li Z., Yang X., Wang H., Wen Y., Chen Y. 2008. Effect of α-allocryptopine on transient outward potassium current in rabbit ventricular myocytes. *Cardiology* **111**: 229-236.

Lima L. A., Siani A. C., Brito F. A., Sampaio A. L. F., Henriques M. d. G. M. O., Riehl C. A. d. S. 2007. Correlation of anti-inflammatory activity with phenolic content in the leaves of *Syzygium cumini* (L.) Skeels (Myrtaceae). *Química Nova* **30**: 860-864.

- M -

Mandal S., Barik B., Mallick C., De D., Ghosh D. 2008. Therapeutic effect of ferulic acid, an ethereal fraction of ethanolic extract of seed of *Syzygium cumini* against streptozotocin-induced diabetes in male rat. *Methods and Findings in Experimental and Clinical Pharmacology* **30**: 121-128.

Maniara G., Rajamoorthi K., Rajan S., Stockton G. W. 1998. Method performance and validation for quantitative analysis by ^{1}H and ^{31}P NMR spectroscopy. Applications to analytical standards and agricultural chemicals. *Analytical Chemistry* **70**: 4921-4928.

Markham K. R. 1982. *Techniques of flavonoid identification*. Treherne J. E., Rubery P. H., editors. Academic Press: London.

MBG. 2009. Missouri Botanical Garden Tropicos Database. Accessed on May 19, 2009 (http://www.tropicos.org).

McCall D. L. C., Alexander J., Barber J., Jaouhari R. G., Satoskar A., Waigh R. D. 1994. The first protoberberine alkaloid analog with *in vivo* antimalarial activity. *Bioorganic and Medicinal Chemistry Letters* **4**: 1663-1666.

Miranda M. M. F. S., Goncalves J. L. S., Romanos M. T. V., Silva F. P., Pinto L., Silva M. H., Ejzemberg R., Granja L. F. Z., Wigg M. D. 2002. Anti-herpes simplex virus effect of a seed extract from the tropical plant *Licania tomentosa* (Benth.) Fritsch (Chrysobalanaceae). *Phytomedicine* **9**: 641-645.

- N -

Ncokazi K. K., Egan T. J. 2005. A colorimetric high-throughput β-hematin inhibition screening assay for use in the search for antimalarial compounds. *Analytical Biochemistry* **338**: 306-319.

Newman D. J., Cragg G. M. 2007. Natural products as sources of new drugs over the last 25 years. *Journal of Natural Products* **70**: 461-477.

Niemetz R., Gross G. G. 2005. Enzymology of gallotannin and ellagitannin biosynthesis. *Phytochemistry* **66**: 2001-2011.

- O -

Osorio E. J., Robeldo S. M., Bastida J. 2008. Alkaloids with antiprotozoal activity. *In*: Cordell G. A., editor. *The Alkaloids. Chemistry and Biology*. Academic Press: London; 113-179.

- P -

Phillipson J. D., Zhu M., Cai Y. 1998. Biological testing of plant extracts - should polyphenols be removed? *Polyphenols Actualities* **18**: 22-25.

Poonam K., Singh G. S. 2009. Ethnobotanical study of medicinal plants used by the Taungya community in Terai Arc Landscape, India. *Journal of Ethnopharmacology* **123**: 167-176.

Portet B., Fabre N., Roumy V., Gornitzka H., Bourdy G., Chevalley S., Sauvain M., Valentin A., Moulis C. 2007. Activity-guided isolation of antiplasmodial

dihydrochalcones and flavanones from *Piper hostmannianum* var. *berbicense*. *Phytochemistry* **68**: 1312-1320.

Prance G. 1972a. Ethnobotanical notes from Amazonian Brazil. *Economic Botany* **26**: 221-237.

Prance G. T. 1972b. Chrysobalanaceae. *Flora Neotropica* **9**: 1-410.

Pushpalatha E., Muthukrishnan J. 1995. Larvicidal activity of a few plant extracts against *Culex quinquefasciatus* and *Anopheles stephensi*. *Indian Journal of Malariology* **32**: 14-23.

- R -

Ralph S. A., van Dooren G. G., Waller R. F., Crawford M. J., Fraunholz M. J., Foth B. J., Tonkin C. J., Roos D. S., McFadden G. I. 2004. Tropical infectious diseases: metabolic maps and functions of the *Plasmodium falciparum* apicoplast. *Nature Reviews Microbiology* **2**: 203-216.

Ramirez R. O., Roa C. C., Jr. 2003. The gastroprotective effect of tannins extracted from duhat (*Syzygium cumini* Skeels) bark on HCl/ethanol induced gastric mucosal injury in Sprague-Dawley rats. *Clinical Hemorheology and Microcirculation* **29**: 253-261.

Ramos M. F. S., Siani A. C., Souza M. C., Rosas E. C., Henriques M. G. M. O. 2006. Evaluation of the antiinflammatory activity of essential oils from five Myrtaceae species. *Revista Fitos* **2**: 58-66.

Robert A., Bonduelle C., Laurent S. A. L., Meunier B. Heme alkylation by artemisinin and trioxaquines. 2006. *Journal of Physical Organic Chemistry* **19**: 562-569.

Rodriguez-Menchaca A., Ferrer-Villada T., Lara J., Fernandez D., Navarro-Polanco R. A., Sanchez-Chapula J. A. 2006. Block of hERG channels by berberine: mechanisms of voltage and state-dependence probed with site-directed mutant channels. *Journal of Cardiovascular Pharmacology* **47**: 21-29.

Ross I. A. 2003. *Medicinal plants of the world*. Humana Press: New York.

Ruan Z. P., Zhang L. L., Lin Y. M. 2008. Evaluation of the antioxidant activity of *Syzygium cumini* leaves. *Molecules* **13**: 2545-2556.

- S -

Sagrawat H., Mann A. S., Kharya M. D. 2006. Pharmacological potential of *Eugenia jambolana*: a review. *Pharmacognosy Magazine* **2**: 96-105.

Sahu N. K., Sahu S., Kohli D. V. 2008. Novel molecular targets for antimalarial drug development. *Chemical Biology and Drug Design* **71**: 287-297.

Sanwal P. C., Sen A. K., Pal A. K. 1973. Histochemical studies on alkaline phosphatase activity in uterus of mice on injection of plant estrogens. *Indian Journal of Animal Sciences* **43**: 352-354.

Schmidt E., Lötter M., Mc Cleaned W., Burrows S., Burrows J. E. 2002. *Trees and shrubs of Mpumalanga and Kruger National Park*. Jacania Media: Johannesburg.

Scott T. 1996. *Concise Encyclopedia. Biology*. Walter de Gruyter: New York.

Shafi P. M., Rosamma M. K., Jamil K., Reddy P. S. 2002. Antibacterial activity of *Syzygium cumini* and *Syzygium travancoricum* leaf essential oils. *Fitoterapia* **73**: 414-416.

Shankar M. B., Parikh J. R., Geetha M., Mehta R. S., Saluja A. K. 2007. Anti-diabetic activity of novel androstane derivatives from *Syzygium cumini* Linn. *Journal of Natural Remedies* **7**: 214-219.

Sharma A., Patel V. K., Ramteke P. 2009. Identification of vibriocidal compounds from medicinal plants using chromatographic fingerprinting. *World Journal of Microbiology and Biotechnology* **25**: 19-25.

Sharma B., Viswanath G., Salunke R., Roy P. 2008. Effects of flavonoid-rich extract from seeds of *Eugenia jambolana* (L.) on carbohydrate and lipid metabolism in diabetic mice. *Food Chemistry* **110**: 697-705.

Shinde J., Taldone T., Barletta M., Kunaparaju N., Hu B., Kumar S., Placido J., Zito S. W. 2008. α-Glucosidase inhibitory activity of *Syzygium cumini* (Linn.) Skeels seed kernel *in vitro* and in Goto-Kakizaki (GK) rats. *Carbohydrate Research* **343**: 1278-1281.

Simoes-Pires C. A., Queiroz E. F., Henriques A. T., Hostettmann K. 2005. Isolation and on-line identification of antioxidant compounds from three *Baccharis* species by HPLC-UV-MS/MS with post-column derivatisation. *Phytochemical Analysis* **16**: 307-314.

Snow R. W., Guerra C. A., Noor A. M., Myint H. Y., Hay S. I. 2005. The global distribution of clinical episodes of *Plasmodium falciparum* malaria. *Nature* **434**: 214-217.

Soares M. B. P., Brustolim D., Santos L. A., Bellintani M. C., Paiva F. P., Ribeiro Y. M., Tomassini T. C. B., Ribeiro dos Santos R. 2006. Physalins B, F and G, seco-

steroids purified from *Physalis angulata* L., inhibit lymphocyte function and allogeneic transplant rejection. *International Immunopharmacology* **6**: 408-414.

Soh P. N., Witkowski B., Olagnier D., Nicolau M. L., Garcia-Alvarez M. C., Berry A., Benoit-Vical F. 2009. *In vitro* and *in vivo* properties of ellagic acid in malaria treatment. *Antimicrobial Agents and Chemotherapy* **53**: 1100-1106.

Sultana B., Anwar F., Przybylski R. 2007. Antioxidant activity of phenolic components present in barks of *Azadirachta indica*, *Terminalia arjuna*, *Acacia nilotica*, and *Eugenia jambolana* Lam. trees. *Food Chemistry* **104**: 1106-1114.

- T -

Tabopda T. K., Ngoupayo J., Liu J., Ali M. S., Khan S. N., Ngadjui B. T., Luu B. 2008. α-glucosidase inhibitors ellagic acid derivatives with immunoinhibitory properties from *Terminalia superba*. *Chemical and Pharmaceutical Bulletin* **56**: 847-850.

Tanaka N., Tanaka T., Fujioka T., Fujii H., Mihashi K., Shimomura K., Ishimaru K. 2001. An ellagic compound and iridoids from *Cornus capitata* root cultures. *Phytochemistry* **57**: 1287-1291.

Tripathi P. N., Tripathi M., Pandey V. B., Singh D. 1999. Alkaloids of *Argemone mexicana*. *Oriental Journal of Chemistry* **15**: 185-186.

Tasdemir D., Lack G., Brun R., Ruedi P., Scapozza L., Perozzo R. 2006. Inhibition of *Plasmodium falciparum* fatty acid biosynthesis: Evaluation of FabG, FabZ, and FabI as drug targets for flavonoids. *Journal of Medicinal Chemistry* **49**: 3345-3353.

- V -

Veigas J. M., Narayan M. S., Laxman P. M., Neelwarne B. 2007. Chemical nature, stability and bioefficacies of anthocyanins from fruit peel of *Syzygium cumini* Skeels. *Food Chemistry* **105**: 619-627.

Veigas J. M., Shrivasthava R., Neelwarne B. 2008. Efficient amelioration of carbon tetrachloride induced toxicity in isolated rat hepatocytes by *Syzygium cumini* Skeels extract. *Toxicology in vitro* **22**: 1440-1446.

Vennerstrom J. L., Klayman D. L. 1988. Protoberberine alkaloids as antimalarials. *Journal of Medicinal Chemistry* **31**: 1084-1087.

Verma S. K., Dev G., Tyagi A. K., Goomber S., Jain G. V. 2001. *Argemone mexicana* poisoning: autopsy findings of two cases. *Forensic Science International* **115**: 135-141.

- W -

Wall M. E., Wani M. C., Brown D. M., Fullas F., Olwald J. B., Josephson F. F., Thornton N. M., Pezzuto J. M., Beecher C. W. W., Farnsworth N. R. and others. 1996. Effect of tannins on screening of plant extracts for enzyme inhibitory activity and techniques for their removal. *Phytomedicine* **3**: 281-285.

Wang Y. X., Zheng Y. M., Zhou X. B. 1996. Inhibitory effects of berberine on ATP-sensitive K^+ channel in cardiac myocytes. *European Journal of Pharmacology* **316**: 307-315.

Wang Y. X., Zheng Y. M. 1997. Ionic mechanism responsible for prolongation of cardiac action-potential duration by berberine. *Journal of Cardiovascular Pharmacology* **30**: 214-222.

Wernsdorfer W. H. 1980. The importance of malaria in the world. *In*: Kreier J. P., editor. *Malaria: Epidemology, chemotherapy, morphology, and metabolism*. Academic Press: New York; 1-93.

WHO. 2006. *Guidelines for the treatment of malaria*. WHO Press: Geneva.

WHO. 2008. *World Malaria Report 2008*. WHO Press: Geneva.

Willcox M. L., Graz B., Falquet J., Sidibe O., Forster M., Diallo D. 2007. *Argemone mexicana* decoction for the treatment of uncomplicated *falciparum* malaria. *Transactions of the Royal Society of Tropical Medicine and Hygiene* **101**: 1190-1198.

Wolfender J. L., Hostettmann K. 1993. Liquid-chromatographic UV detection and liquid-chromatographic thermospray mass-spectrometric analysis of *Chironia* (Gentianaceae) species - a rapid method for the screening of polyphenols in crude plant-extracts. *Journal of Chromatography A* **647**:191-202.

Wright C. W., Marshall S. J., Russell P. F., Anderson M. M., Phillipson J. D., Kirby G. C., Warhurst D. C., Schiff P. L., Jr. 2000. *In vitro* antiplasmodial, antiamoebic, and cytotoxic activities of some monomeric isoquinoline alkaloids. *Journal of Natural Products* **63**: 1638-1640.

Wu S. H., Chen Y. W., Yang L. Y., Li S. L., Li Z. Y. 2008. A new ellagic acid glycoside from *Paeonia delavayi*. *Fitoterapia* **79**: 474-475.

- Y -

Yan X. H., Guo Y. W. 2004. Two new ellagic acid glycosides from leaves of *Diplopanax stachyanthus*. *Journal of Asian Natural Product Research* **6**: 271-276.

Yang S. W., Zhou B. N., Wisse J. H., Evans R., van der Werff H., Miller J. S., Kingston D. G. I. 1998. Three new ellagic acid derivatives from the bark of *Eschweilera coriacea* from the Suriname rainforest. *Journal of Natural Products* **61**: 901-906.

Ye L., Yang J. 1996. Ellagic glycosides and triterpenoids from *Duchesnea indica* Focke. *Yaoxue Xuebao* **31**: 844-848.

Yu L., Sun A., Wu Q., Huang X. 1999. Effects of protopine on physiological characteristics of isolated guinea pig atrium. *Zhongguo Yaolixue Tongbao* **15**: 432-434.

Yunes R. A., Cechinel-Filho V. 2001. Breve análise histórica da química de plantas medicinais: sua importância na atual concepção de fármaco segundo os paradigmas ocidental e oriental. *In*: Yunes R. A., Calixto J. B., editors. *Plantas medicinais sob a ótica da química medicinal moderna*. Argos: Chapecó; 356.

- Z -

Zalis M. G., Pang L., Silveira M. S., Milhous W. K., Wirth D. F. 1998. Characterization of *Plasmodium falciparum* isolated from the Amazon region of Brazil: evidence for quinine resistance. *American Journal of Tropical Medicine and Hygiene* **58**:630-637.

Appendices

TABLE OF APPENDICES

Appendix 1. HPLC/UV analyses at 254 nm of different batches of *A. mexicana* decoction (cf Experimental section for HPLC conditions).

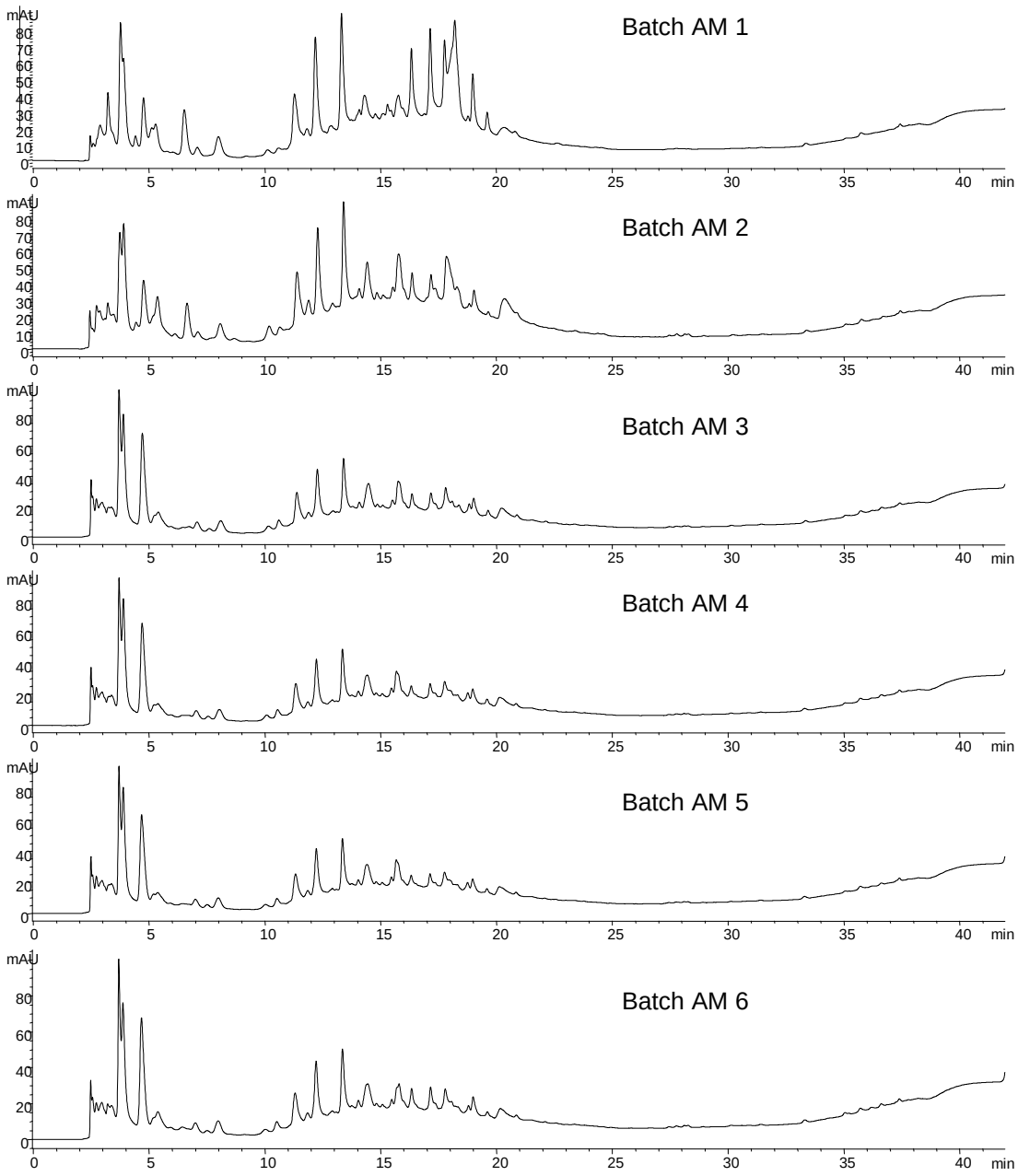

HPLC/UV analyses at 254 nm of different batches of *A. mexicana* decoction (cf Experimental section for HPLC conditions).

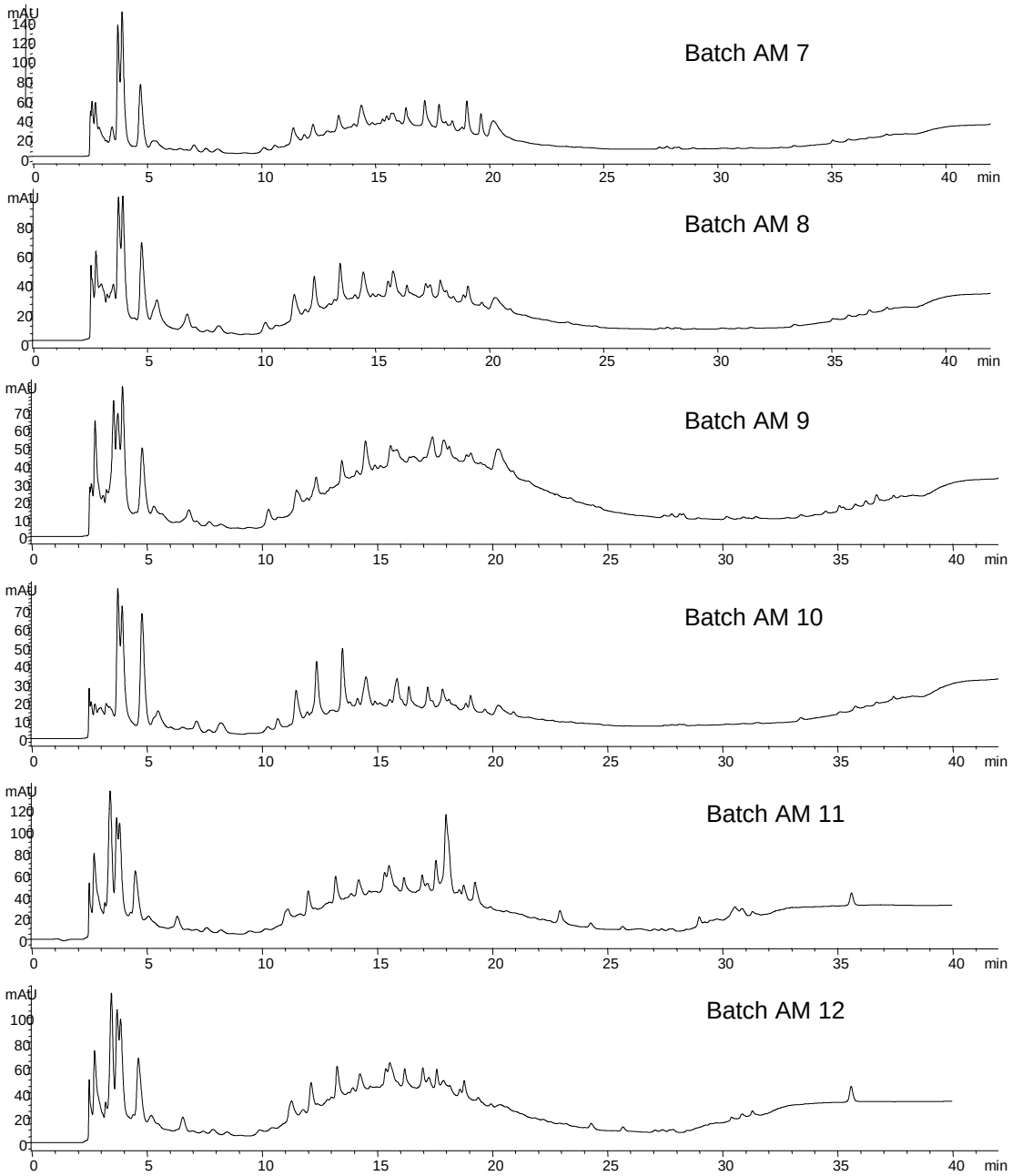

Appendix 2. HMBC spectrum of **A1** (500 MHz, 70 °C, pyridine-d_5). F1=^{13}C and F2=^{1}H.

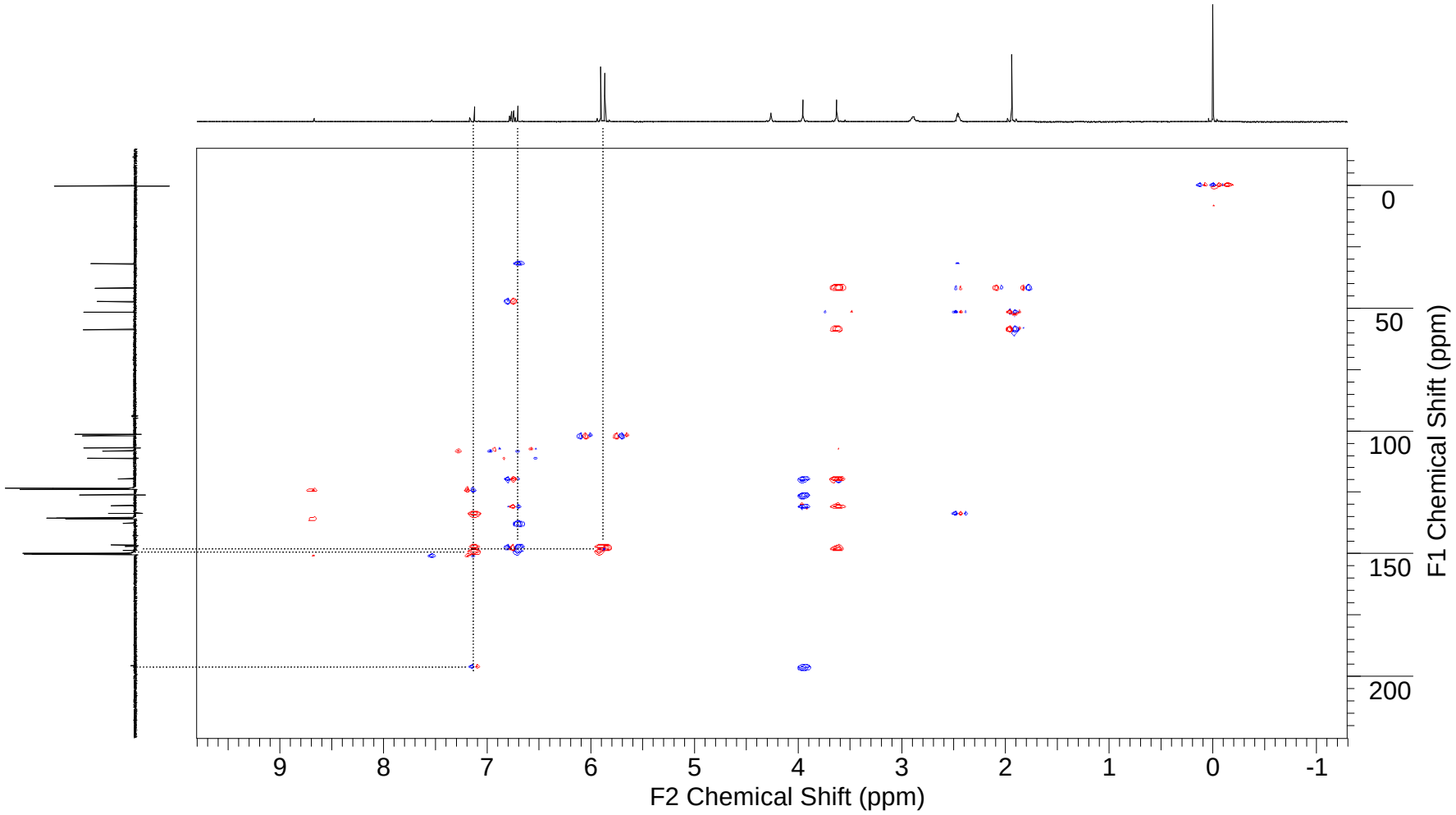

Appendix 3. HMBC spectrum of **A2** (500 MHz, 70 °C, pyridine-d_5). F1=^{13}C and F2=^{1}H.

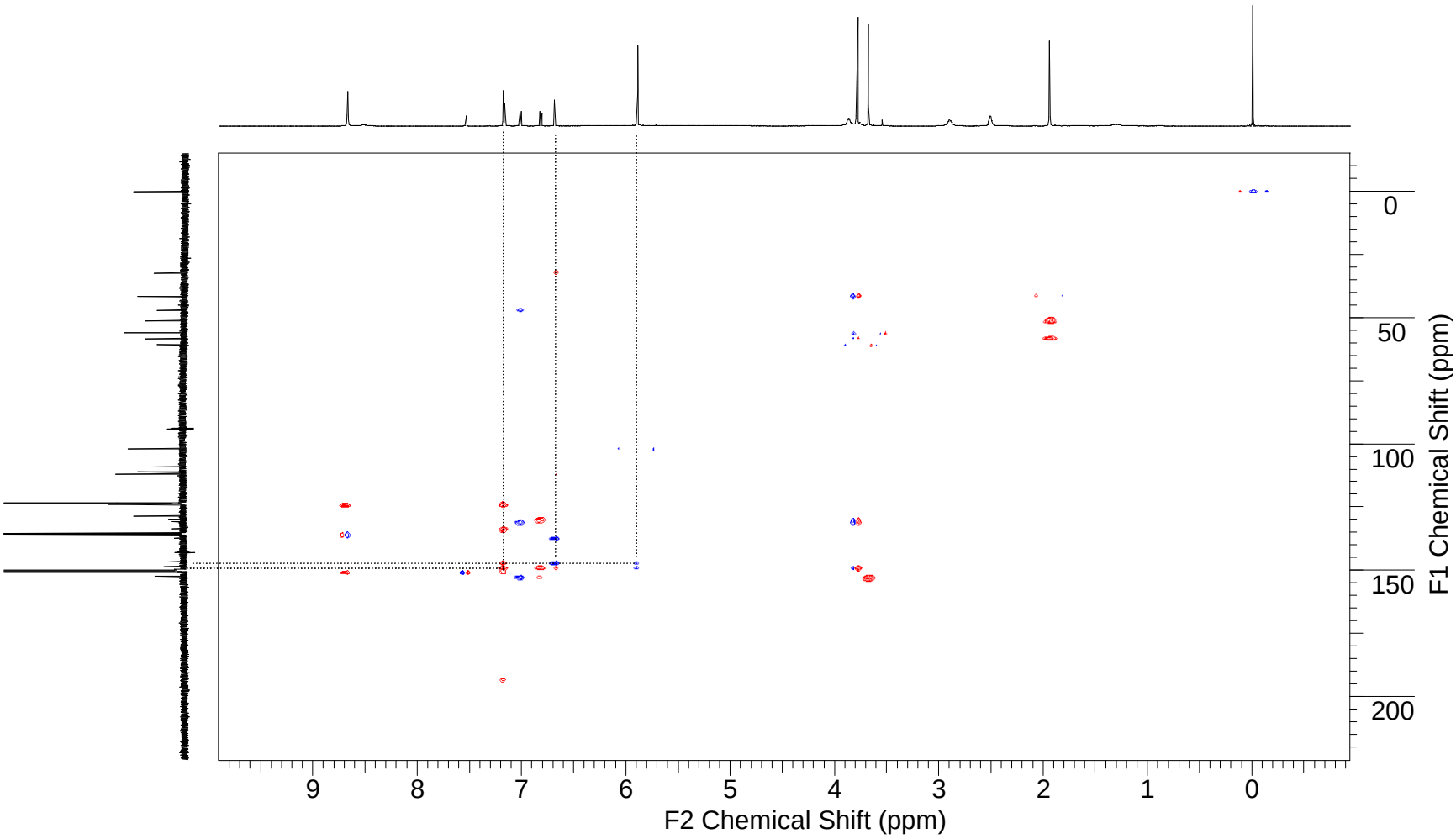

Appendix 4. HMBC spectrum of **A3** (500 MHz, 70 °C, DMSO-d_6).

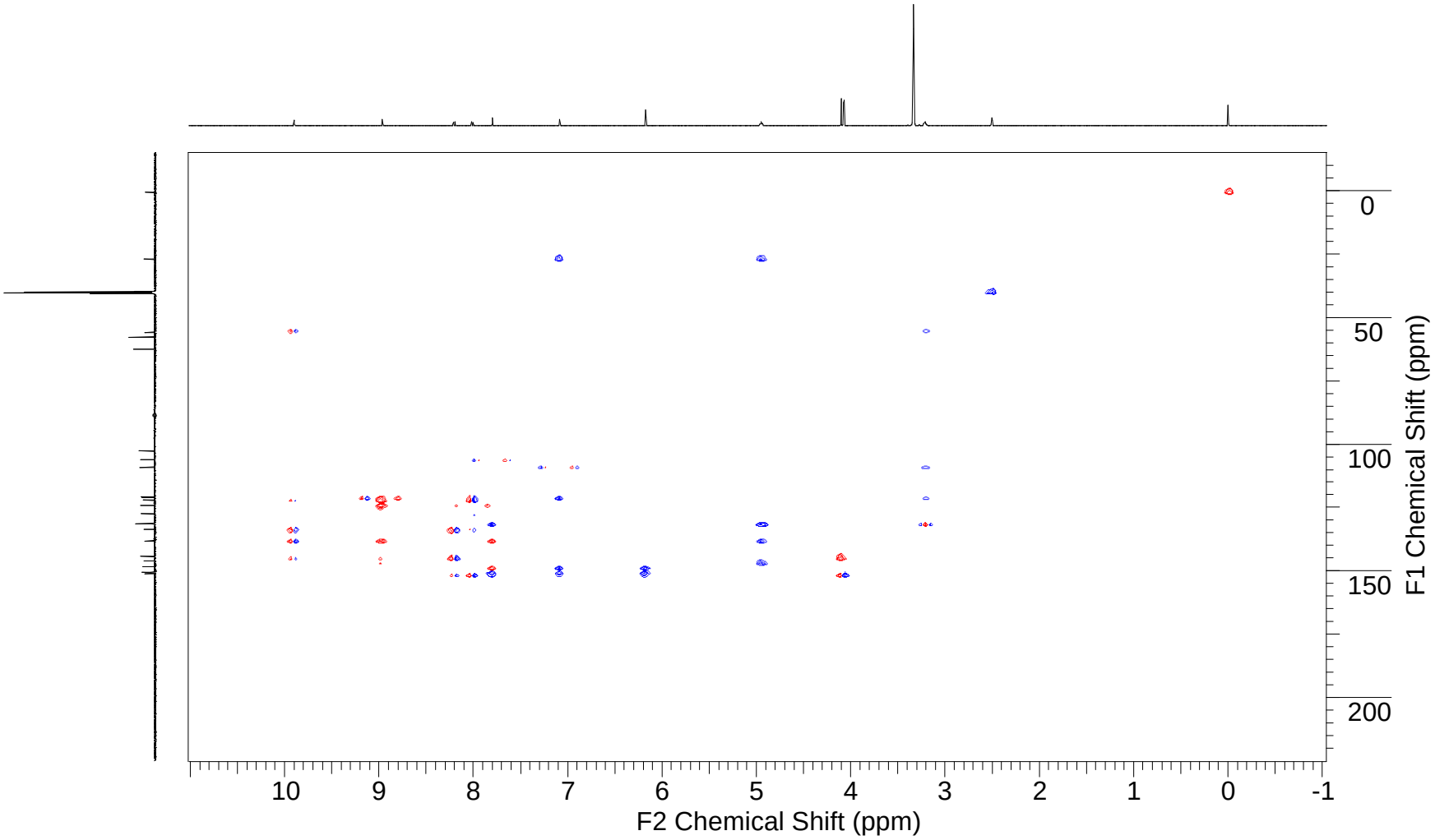

Appendix 5. HMBC spectrum of **L4** (500 MHz, 25 °C, CD_3OD, F1= ^{13}C shift, F2= ^{1}H shift).

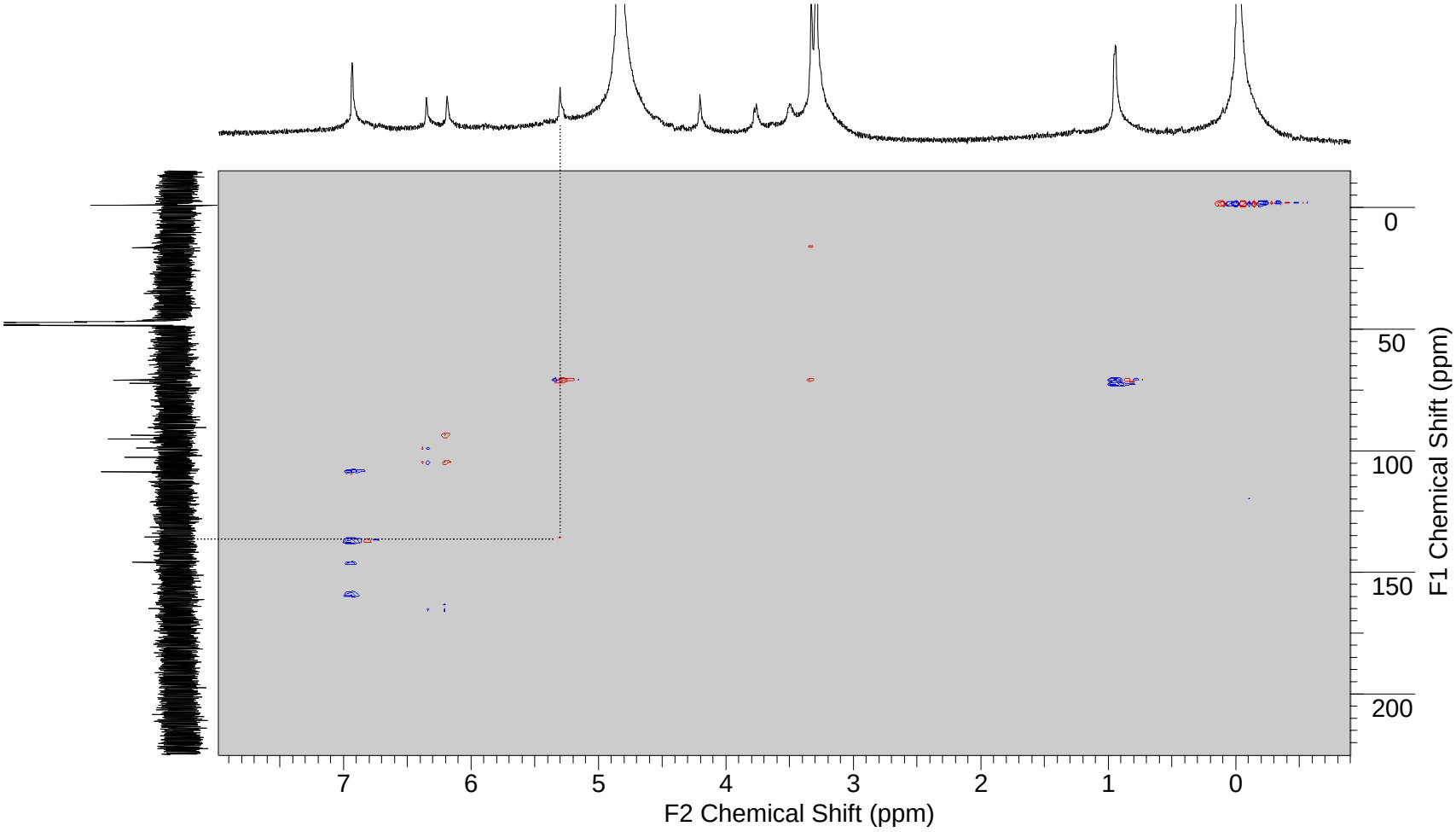

Appendix 6. HMBC spectrum of **S1** (500 MHz, 27 °C, CD_3OD).

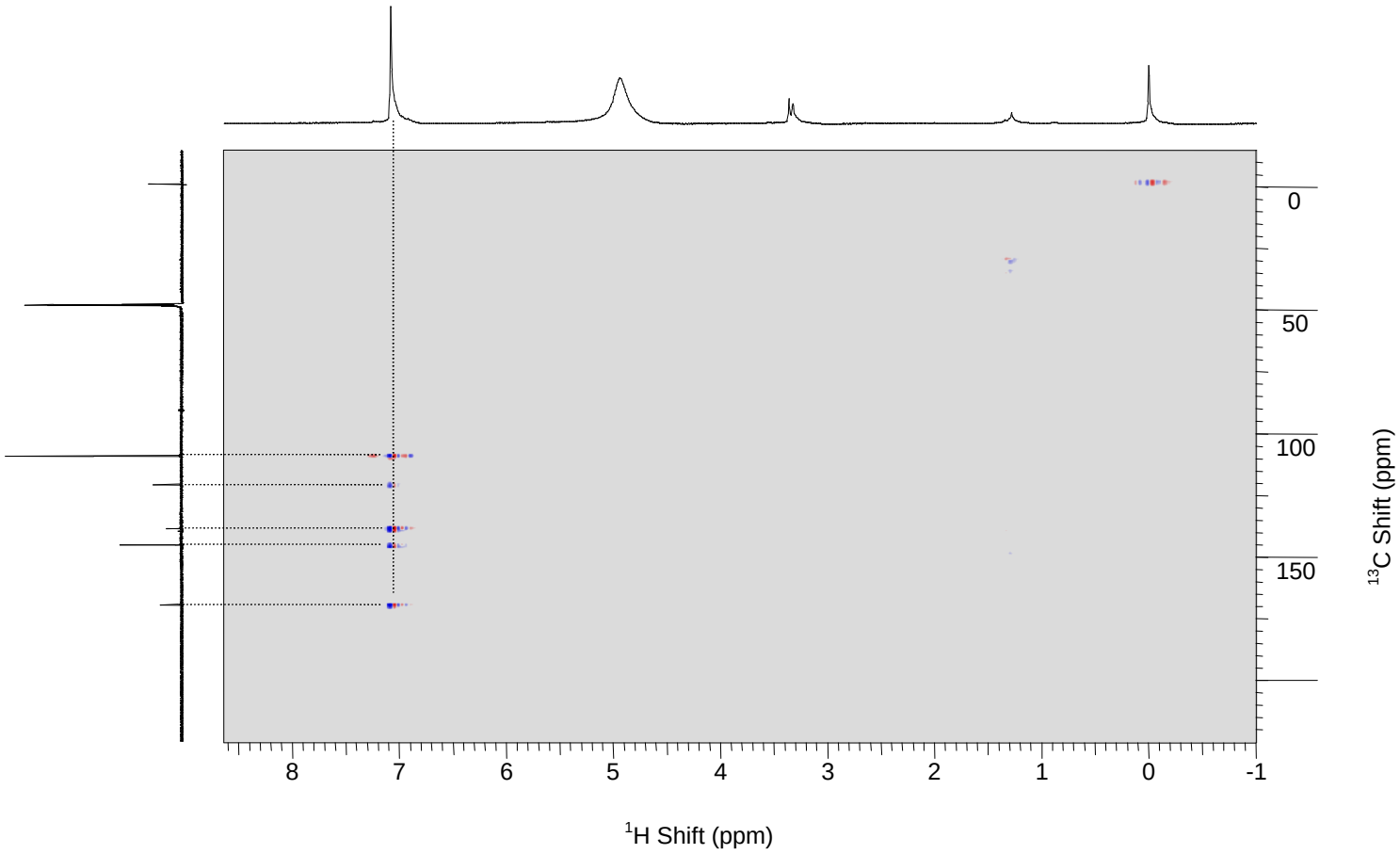

Appendix 7. HMBC spectrum of **S4** (500 MHz, 40 °C, DMSO-d_6; F1= ^{13}C shift with zoom from 35 to 220 ppm, F2= ^{1}H shift).

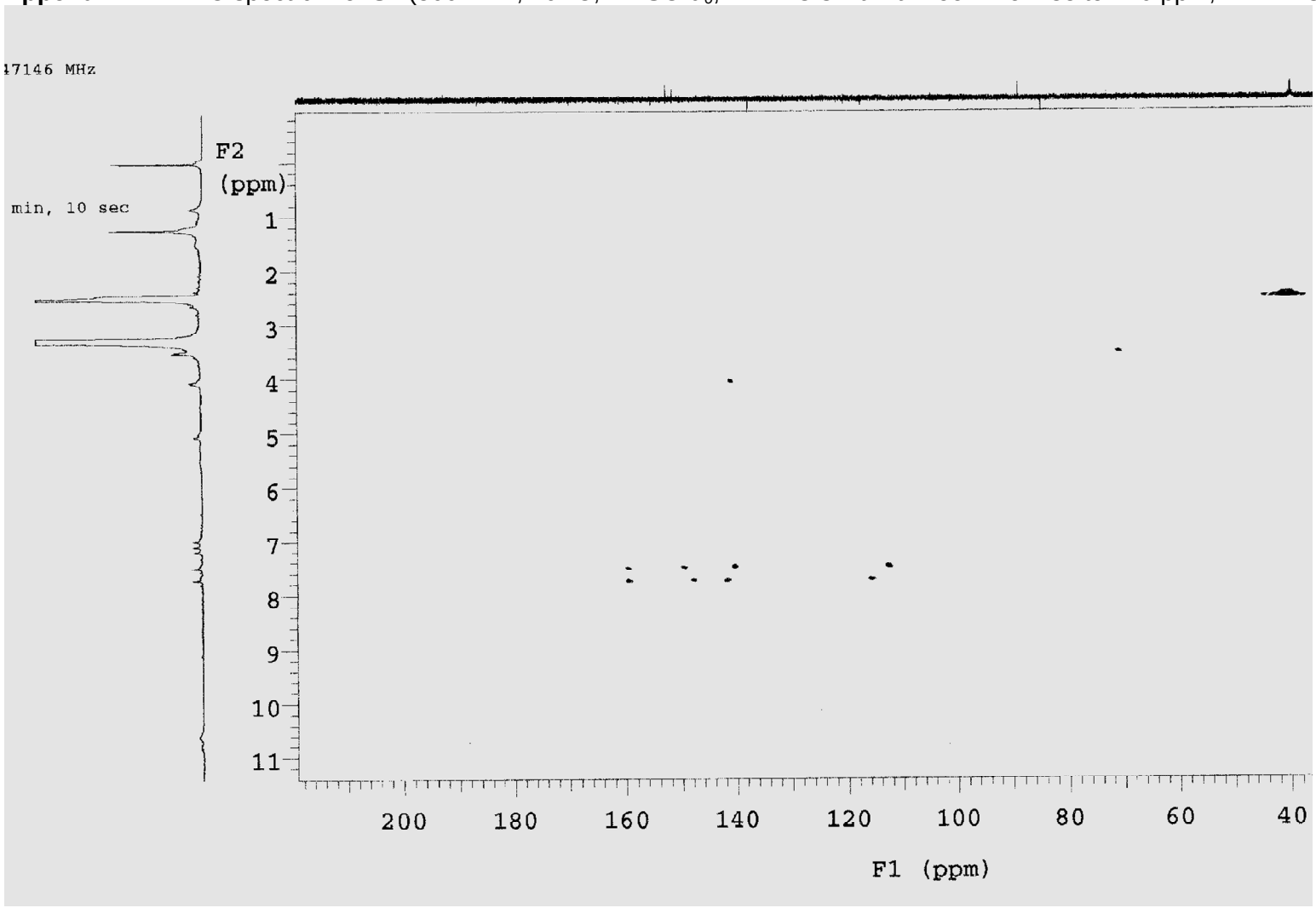

Appendix 8. HMBC spectrum of **S5**, 500 MHz, 35 °C, DMSO-d_6 – D_2O (1:1).

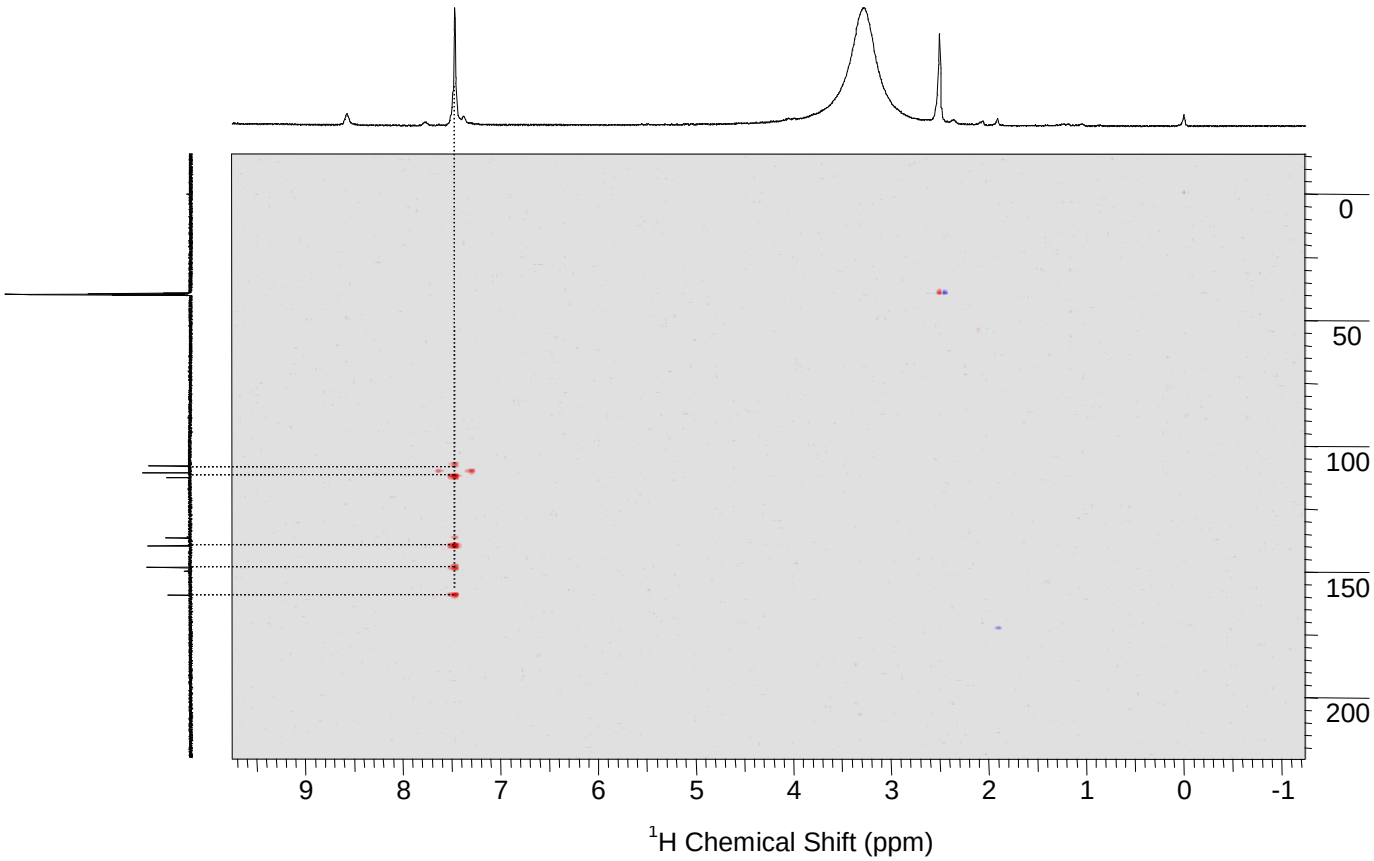

Appendix 9. HMBC spectrum of **S7** (500MHz, 35 °C, DMSO-d_6; F1= ^{13}C shift, F2= ^{1}H shift).

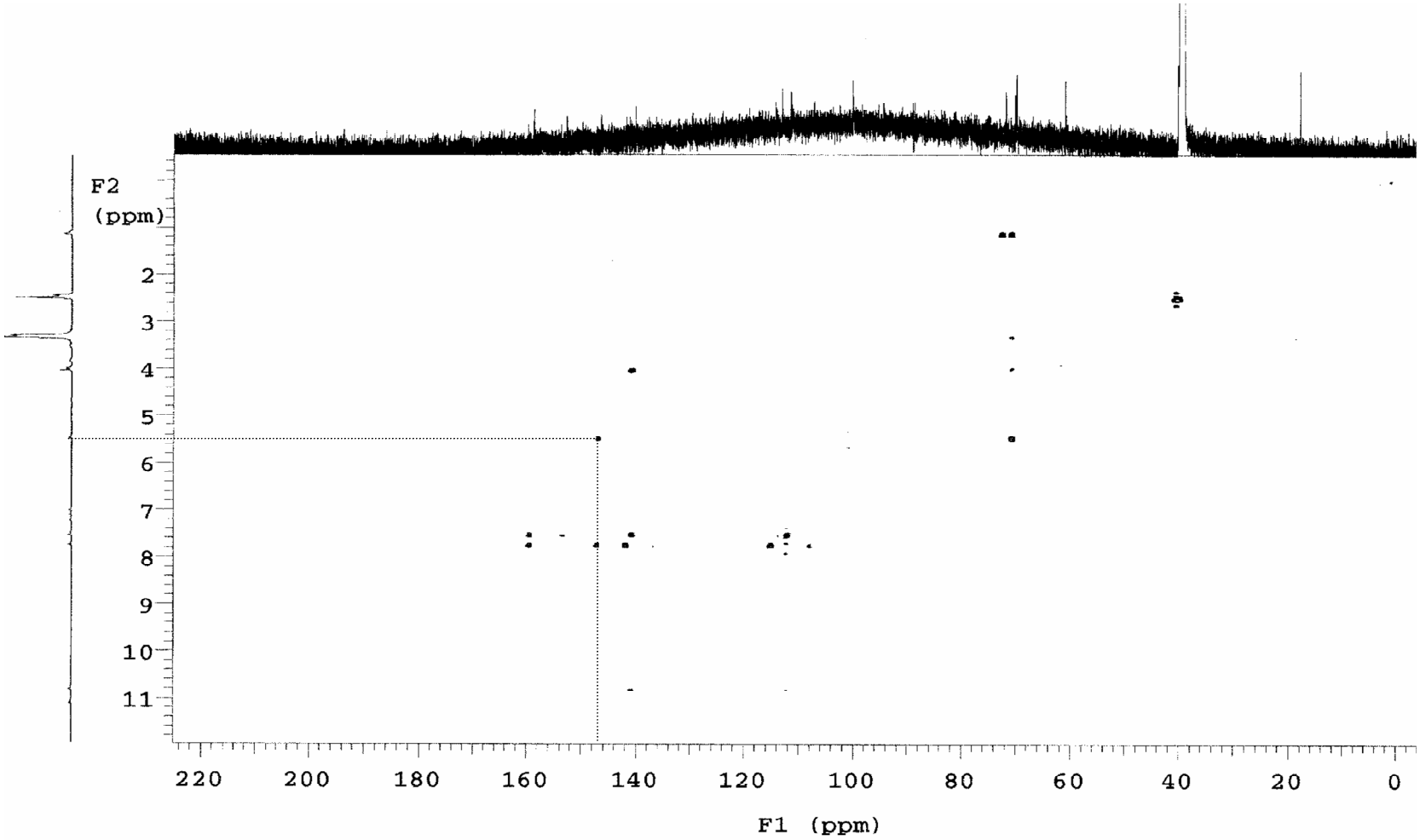

Appendix 10. HMBC spectrum of **S8** (500MHz, 35 °C, DMSO-d_6; F1= ^{13}C shift, F2= ^{1}H shift).

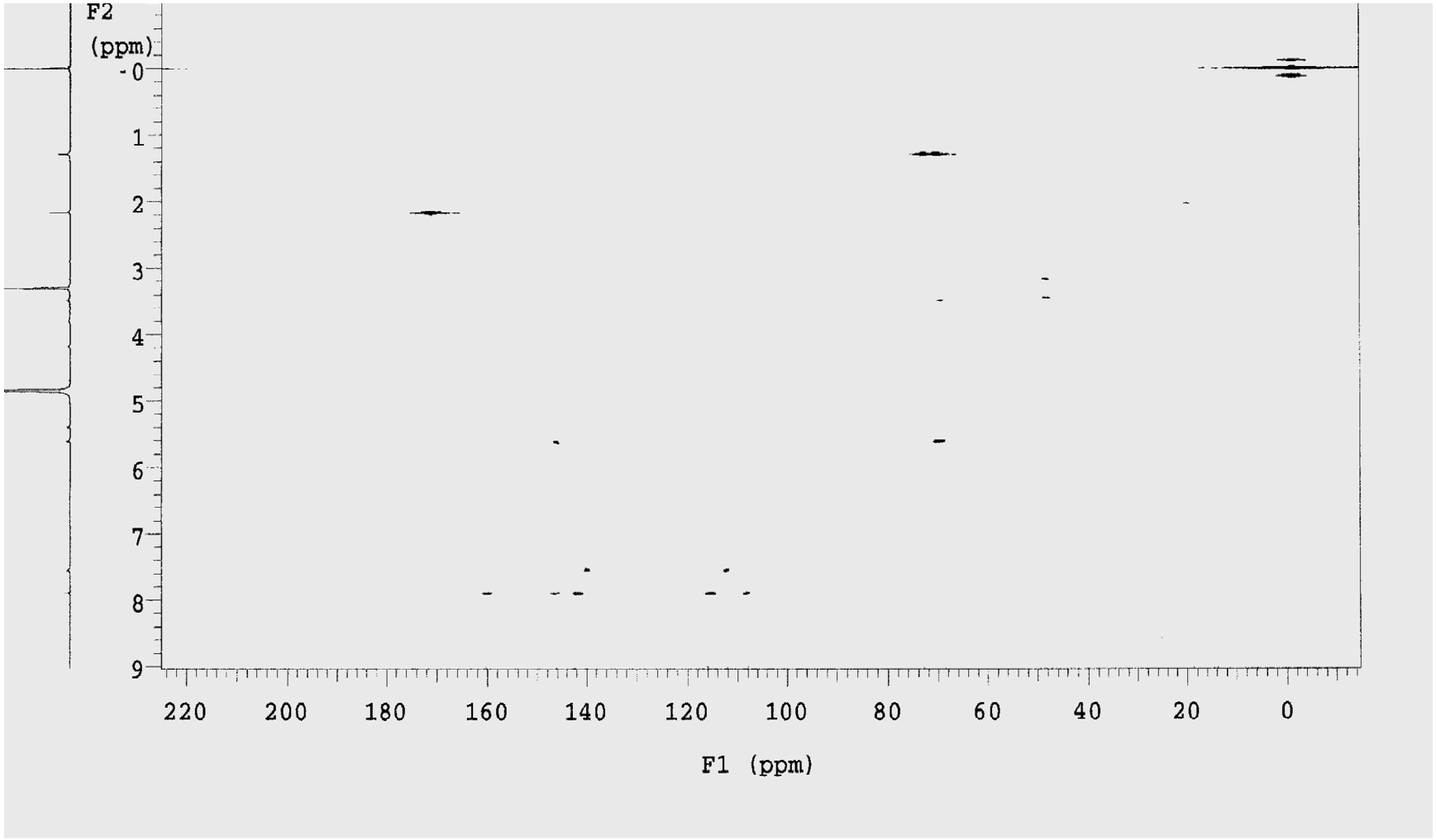

Appendix 11. TLC plates and calibration curves for the semi-quantitative determination of berberine in different clinical batches.

Batch AM 8

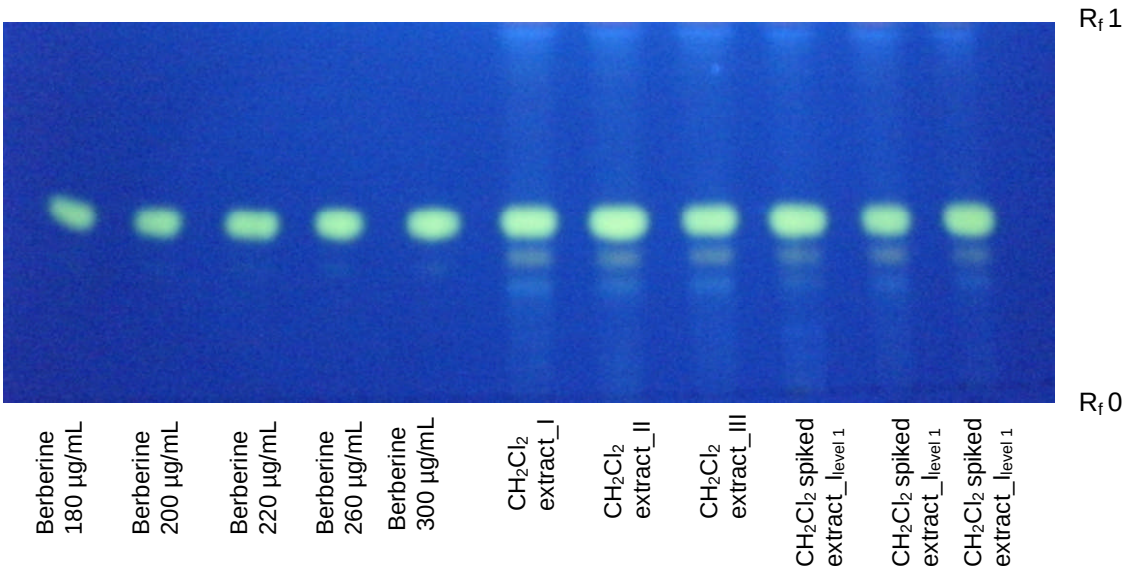

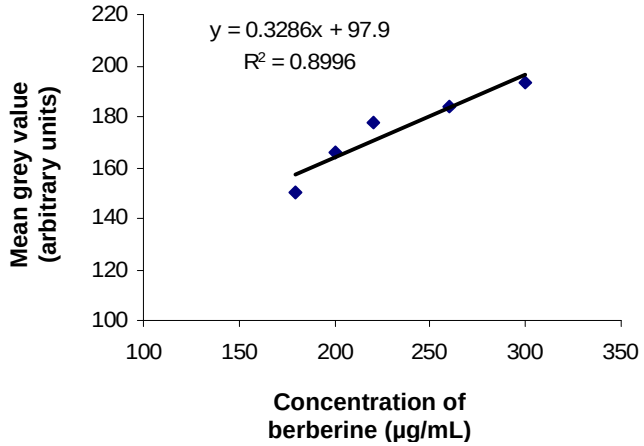

TLC plates and calibration curves for the semi-quantitative determination of berberine in different clinical batches.

Batch AM 8

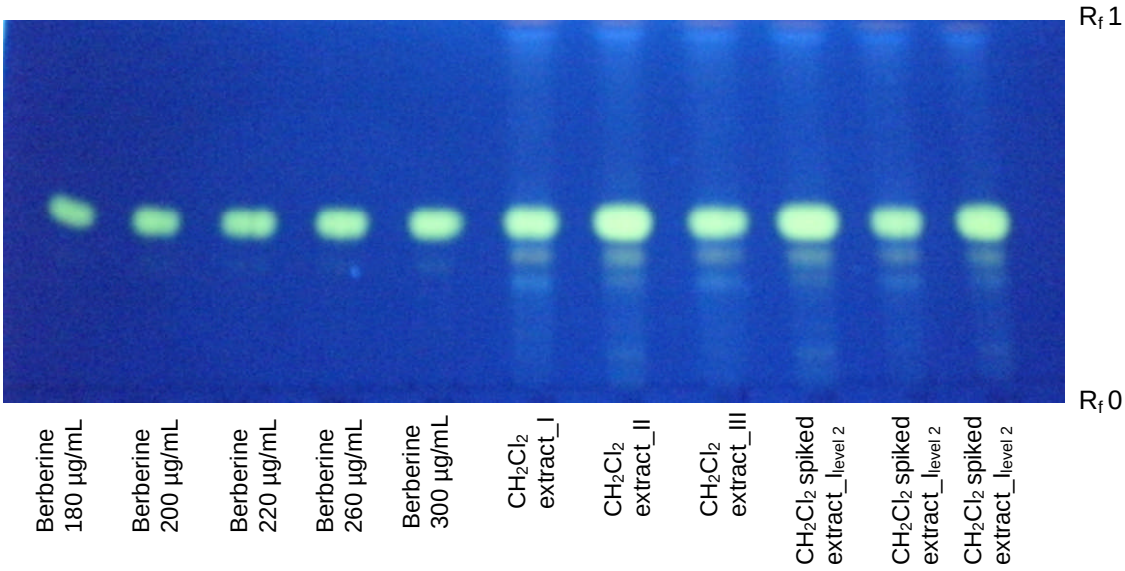

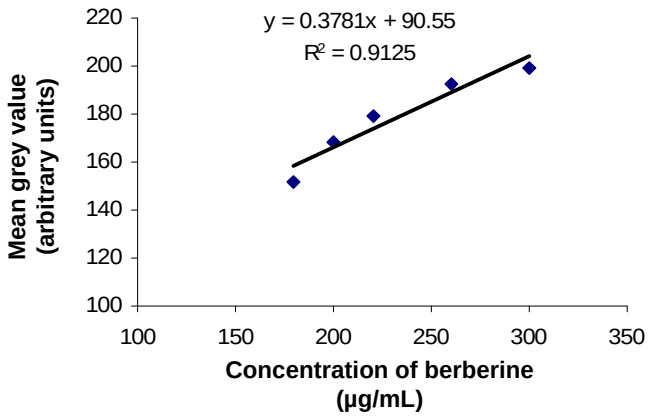

TLC plates and calibration curves for the semi-quantitative determination of berberine in different clinical batches.

Batch AM 8

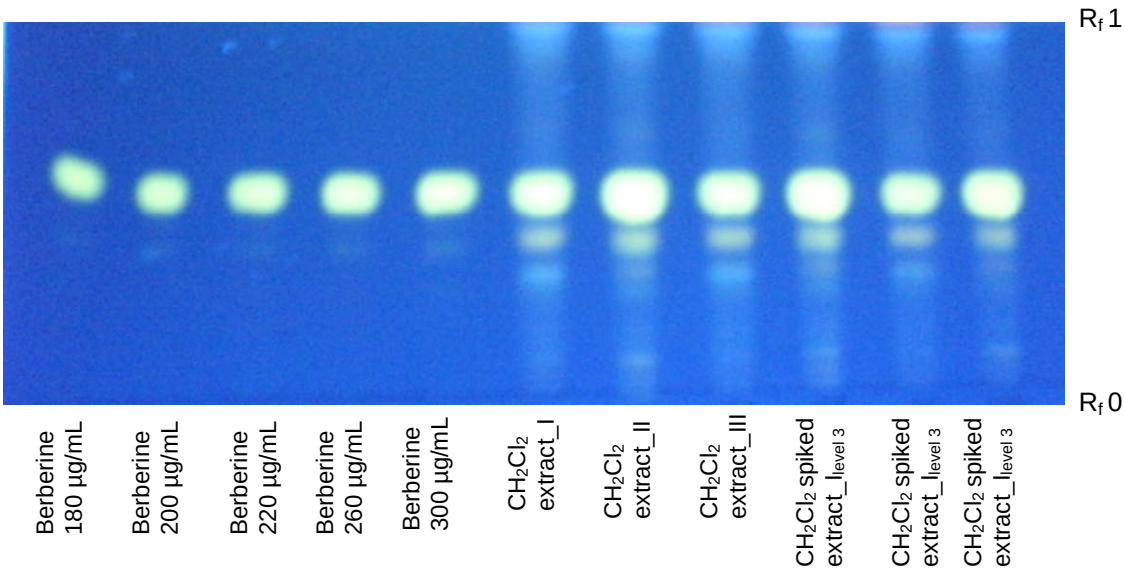

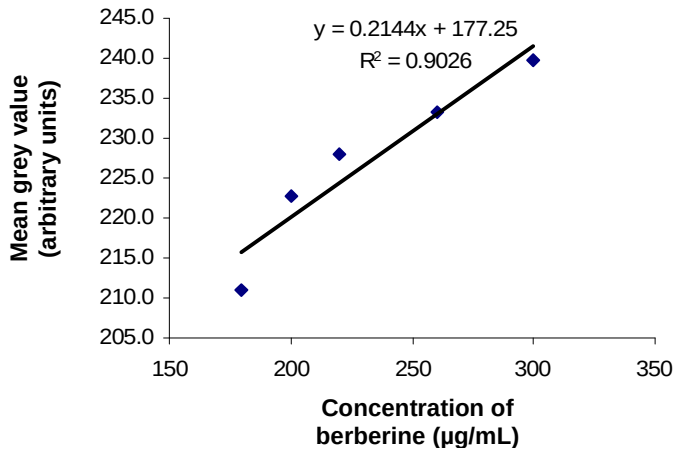

TLC plates and calibration curves for the semi-quantitative determination of berberine in different clinical batches.

Batch AM 9

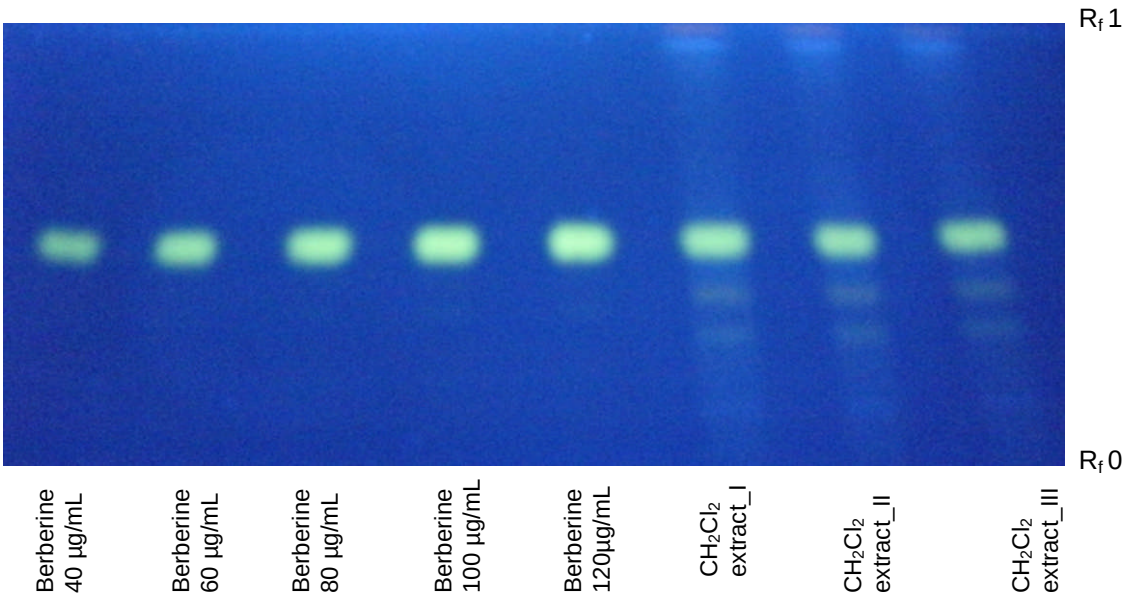

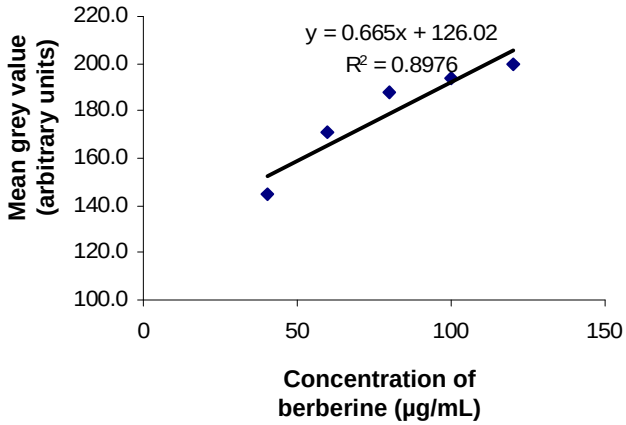

TLC plates and calibration curves for the semi-quantitative determination of berberine in different clinical batches.

Batch AM 11